National University of Science and Technology
POLITEHNICA Bucharest

Faculty of Industrial Engineering and Robotics

Journal of Industrial Engineering and Robotics

2025, Volume 9, Issue 2

CONTROL SYSTEM OF A ROBOTIC ARM USING EEG SIGNALS

CONSTANTIN Darius-Costin[1], DINU Cristian[1], GHINULESCU Alexandra[1], SAVU Tom (Conducător științific)

[1]Faculty of Industrial Engineering and Robotics, Specialization: Applied Informatics in Industrial Engineering,, Year of Study: I , e-mail: ghinulescu.alexandra@gmail.com

ABSTRACT: Electroencephalography (EEG) is a method for recording the brain's electrical activity, with a long-standing history in neuroscience and forming the foundation of modern brain-computer interface (BCI) technologies. This project explores the use of brain signals captured through an 8-electrode EEG headset for the real-time control of a robotic arm. The study highlights the integration of EEG technologies with the OpenBCI platform, detailing the essential hardware and software components: electrodes, microprocessor, signal interpretation algorithms, and the interface with the robotic device. The applications of this system are diverse, ranging from medical prosthetics to industrial automation, demonstrating its adaptive potential and impact on future technologies. This project contributes to the development of brain-computer interfaces by optimizing critical parameters and creating a platform that facilitates automation and personalization of robotic control.

KEYWORDS: EEG, brain-computer control, brain signals, automation, OpenBCI

1. Introduction

This paper aims to design and implement a Brain-Computer Interface (BCI) system using EEG (electroencephalographic) signals to control a robotic arm. BCI technology enables direct communication between the human brain and an external device without relying on physical movements or traditional interfaces. This approach opens new perspectives in fields such as robotics, healthcare, and human-machine interaction.

The main objective of this work is to implement a functional system that allows real-time command transmission to a robotic arm by interpreting brain activity. Additionally, the project seeks to validate the proposed method's effectiveness and explore its potential application in other areas, such as controlling electric wheelchairs, interacting with games or software without traditional peripherals, and aiding in the diagnosis of neurological or psychological disorders (e.g., depression, schizophrenia, Alzheimer's).

To achieve these objectives, the project followed several essential steps: EEG signal acquisition and preprocessing, feature selection, classification using machine learning methods, and finally, system integration with a robotic interface. The entire process was focused on achieving accurate and intuitive control of the robotic device, demonstrating the feasibility of such a solution in a real-world context.

Fig. 1 EEG system for robotic arm control [1]

2. System structure and Operating Principles

The experimental model consists of three main components: the EEG signal acquisition system, the data processing and interpretation unit, and the controlled robotic arm. Together, they form a functional input-processing-output chain, typical of BCI systems.

The EEG acquisition system includes a set of electrodes mounted on the user's scalp and connected to a portable EEG device. This device captures real-time brain activity and transmits it to the processing unit. The EEG signals are processed in a specialized software environment (e.g., MATLAB or Python) through several steps: filtering, artifact removal, relevant feature extraction, and classification. Machine learning algorithms (e.g., SVM or neural networks) are used for classification, trained to recognize patterns associated with motor intentions (e.g., movement to the left or right). After classification, the commands are sent to a microcontroller that operates the robotic arm, executing corresponding actions such as moving in specific directions or lifting objects.

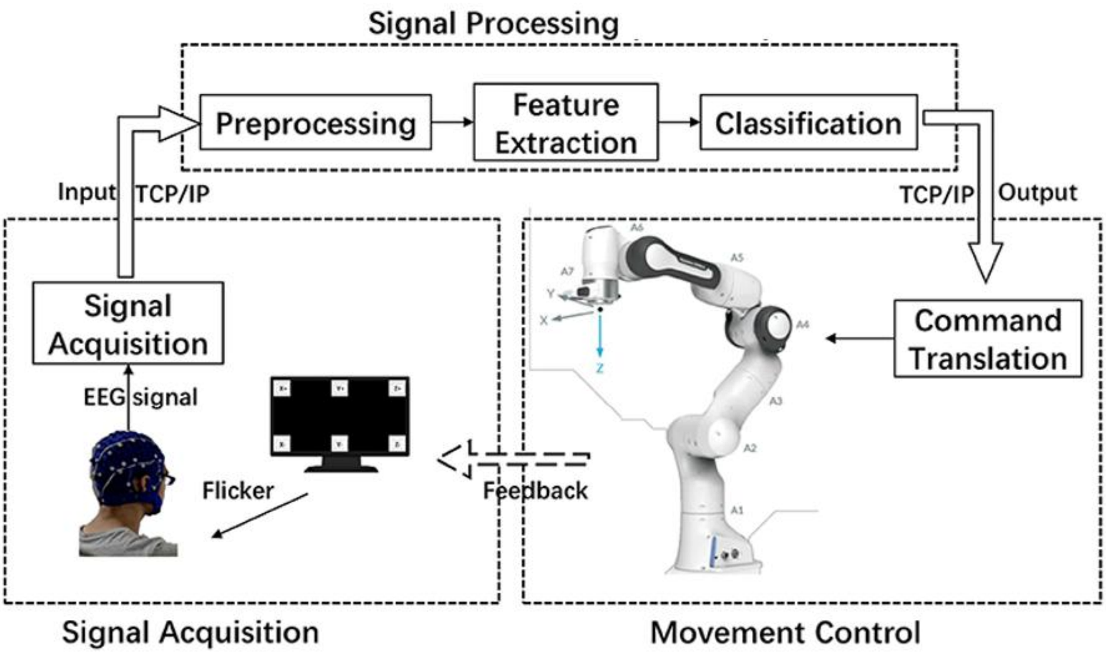

Fig. 2 System operation diagram [2]

The entire process occurs in real time, offering the user intuitive and non-invasive control over the robotic system. The modular system structure allows adaptation to other applications by modifying the output component or adjusting the recognized signal classes. Thus, the principles used in this experimental model can be easily extended to other assistive devices or software applications.

Initial experimental tests collected EEG signals from eight electrodes placed according to the international 10-20 system in areas associated with the primary motor cortex and premotor cortex—regions involved in planning and executing voluntary movements. These areas were strategically chosen because the neuronal activity generated here directly reflects the user’s motor intentions.

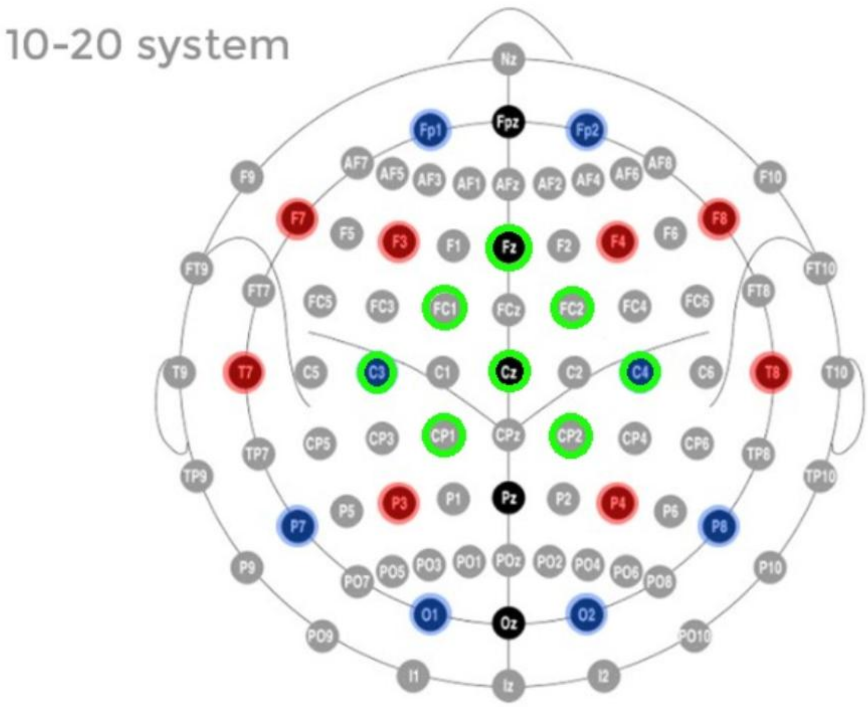

Fig. 3 EEG sensor layout [3]

To obtain relevant signals, participants were instructed to perform simple movements (e.g., hand clenching) or to mentally simulate these movements without physically executing them (motor imagery). This type of brain activation produces detectable responses in brain waves, particularly in frequency bands such as mu (8–12 Hz) and beta (13–30 Hz), which are characteristic of motor activity.

Signals were collected and visualized in real time using the OpenBCI GUI platform, which allows continuous monitoring of EEG activity across channels. After acquisition, raw data were exported and processed in MATLAB using a specialized EEG analysis library. Processing included signal filtering to reduce noise (including ocular and muscular artifacts), significant feature extraction, and classification based on the user’s expressed motor intentions.

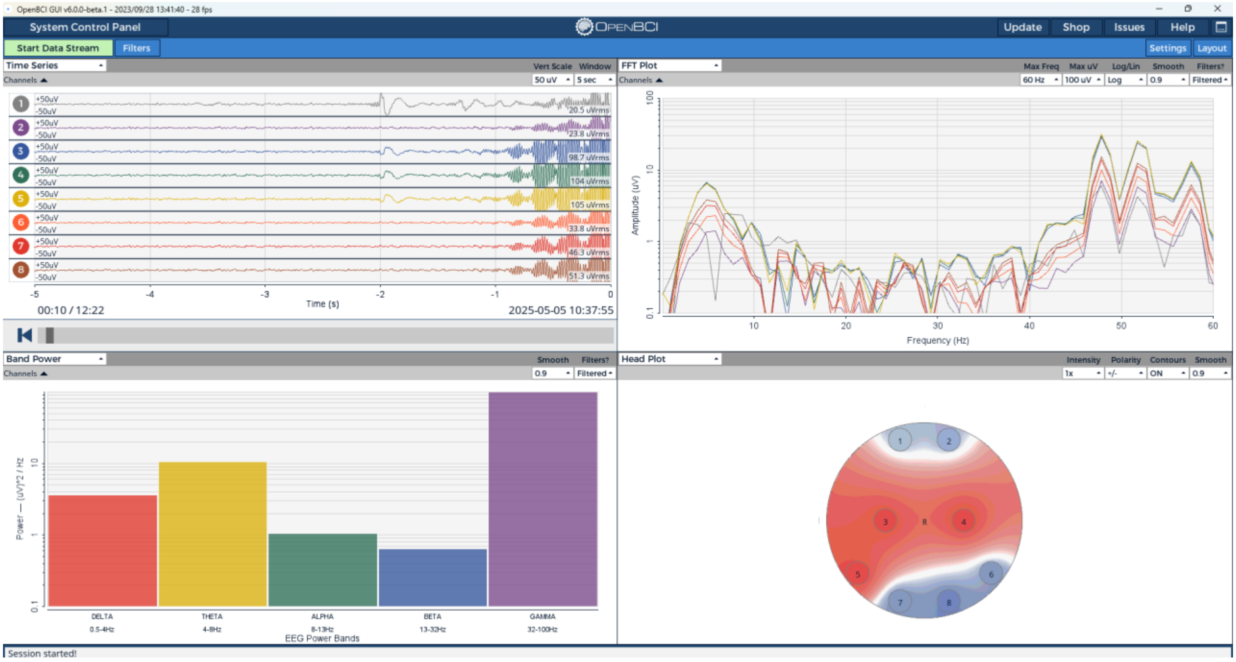

Fig. 4 OpenBCI software interface

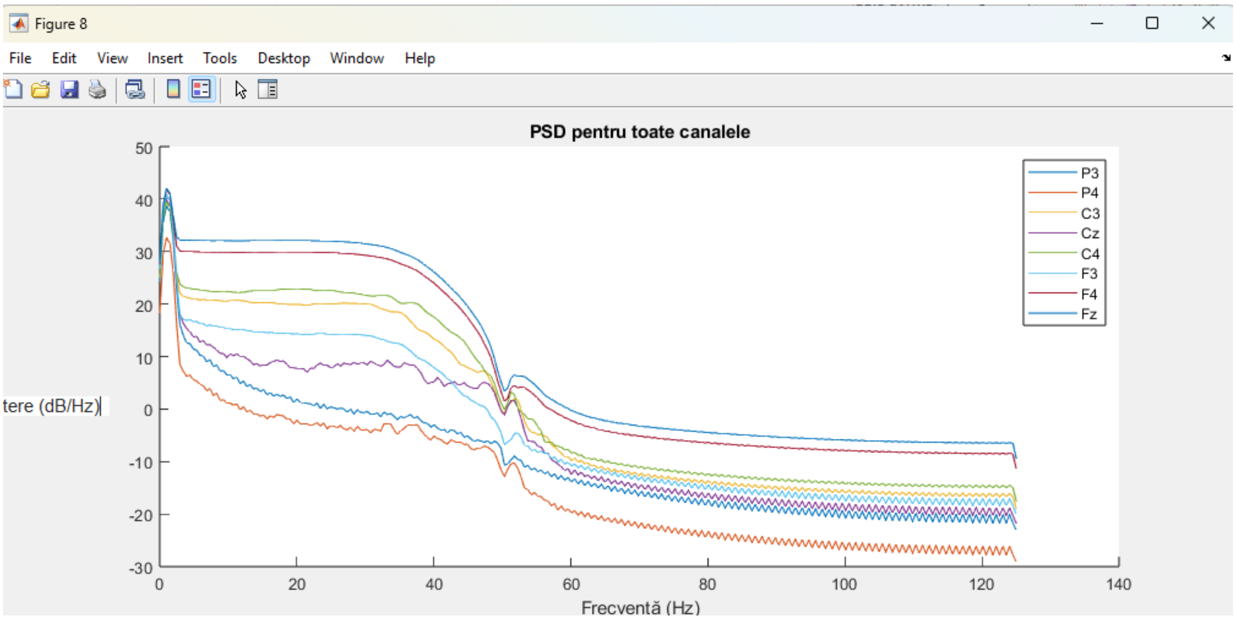

Fig. 5 Signal filtering in MATLAB

At this stage, initial datasets have been obtained, providing a promising foundation for further development. Upcoming phases include additional testing to expand the dataset and improve the signal processing algorithms, aiming for more accurate classification and, consequently, finer control of the robotic arm’s movements. These steps are essential to define a clear and robust command set that can be accurately interpreted by the system in real time.

For a better understanding of how EEG data were collected, the figure below shows the experimental setup used in testing. The system includes a 3D-printed modular structure with eight electrodes fixed in locations corresponding to the motor cortex. The acquisition board is directly connected to the electrodes via colored wires, facilitating signal transmission to the

OpenBCI GUI software interface. This setup allows for stable positioning on the scalp and correct electrode placement, ensuring the signal quality required for EEG signal processing and classification.

Fig. 6 EEG headset

3. The 10-20 System

The 10-20 system is an international standard that divides the skull into 10–20% segments for electrode placement, ensuring consistent EEG study results despite differences in head size and shape

Each electrode is identified using letters and numbers. The letter indicates a brain region: F – frontal, T – temporal, P – parietal, O – occipital. The only exception is F7 and F8, which are actually in the anterior temporal region, not the frontal region as the name may suggest. Numbers refer to the hemisphere: even numbers for the right side and odd numbers for the left. For the central region, the number is replaced with a “z”. [4]

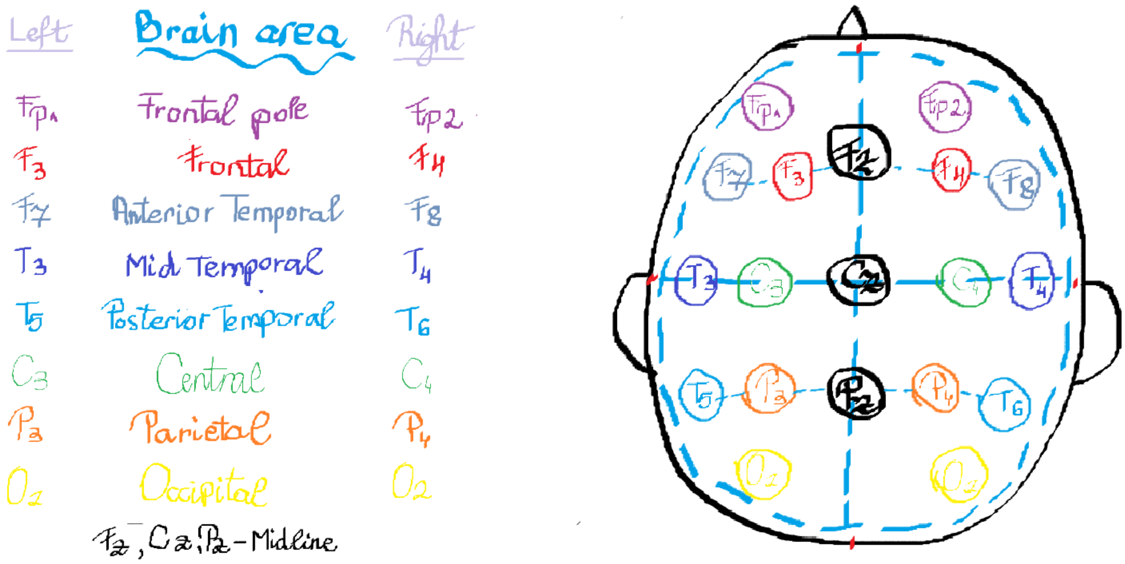

Fig. 7 The 10-20 system diagram

4. Conclusions

This project explored the possibility of controlling a robotic arm using EEG signals, demonstrating how BCI technology can revolutionize how people with disabilities regain independence. EEG-based robotic arm control relies on brain activity captured by electrodes, which is then interpreted and translated into precise commands that generate the desired robotic movements. Machine learning and EEG signal processing technologies enable intuitive and adaptive interaction, and by integrating sensory feedback, users can adjust movements in real time, enhancing the user experience.

Ultimately, this project represents a significant step toward a future where technology becomes an ally of humanity, supporting individuals with special needs in their recovery and social integration while also offering innovative solutions in robotics and brain-computer interface development.

5. Bibliography

[1] https://www.sciencefocus.com/news/this-robot-arm-can-be-controlled-by-the-power-of-your-brain (Accessed on 10.10.2024)
[2]https://www.frontiersin.org/journals/neurorobotics/articles/10.3389/fnbot.2022.855825/full (Accessed on 20.10.2024)
[3] https://shop.openbci.com/products/ultracortex-mark-iv?srsltid=AfmBOopfb-9rwGtIguZankrNVJUR1iD7_PzMGRtM7-IhkJ_6Jm2lDF7z (Accessed on 05.01.2025)
[4] https://www.doccheck.com/de/detail/photos/42650-10-20-system (Accessed on 10.01.2025)

STRATEGIC MARKETING RESEARCH FOR THE DEVELOPMENT OF A HEIGHT-ADJUSTABLE DESK

NĂSTASE Marian-Sebastian[1], CIOBĂNESCU Codruț-Decebal[1], GIURGI Darius-Mihai[1] ,DUMITRESCU Andrei (Conducător științific)

[1]Faculty of Industrial Engineering and Robotics, Programme: Industrial Design and Innovative Products, Master degree year I, e-mail: nastase_sebastian@yahoo.com

ABSTRACT: The aim of the scientific paper is to analyse the current market situation and the real need to develop a height adjustable desk. The current issue of sedentary behaviour and its impact on health was analysed, highlighting the growing need for ergonomic solutions such as height-adjustable desks. The same analysis was applied to the market by analysing competitors, design trends, and the main features of existing products. Subsequently, market opportunities were identified, the project mission was formulated, and the 5W1H method was applied to select the target audience. Data collected through a questionnaire helped outline a table of user requirements and competitor product characteristics. In conclusion, the findings support the development of a competitive product tailored to real market needs.

KEY WORDS: Height-adjustable desk, market research, productivity, employee health, muscle discomfort

1. Introduction

Given the fact that the number of people working in fields that involve office work, and a sedentary lifestyle is constantly increasing, there are more frequent health problems related to body posture, fatigue, and decreased productivity. In this context, height-adjustable desks represent an innovative solution that meets modern ergonomics and flexibility needs. The paper aims to investigate the opportunities for implementing this product on the market based on research into the fundamental problem it is designed to solve, the current market trend, and the competitive offer in order to identify the real development potential of this product.

2. Current status of the product related topics

Given the context outlined in the previous chapter, it has been concluded that people have begun reporting health issues as a consequence of a sedentary lifestyle. Sedentarism is associated with obesity, type 2 diabetes, cardiovascular diseases, and musculoskeletal problems. A thorough investigation into this issue revealed that in the 18th and 19th centuries, the use of standing desks was linked to productivity and was regarded as a sign of prestige and wealth. Notable figures such as Napoleon Bonaparte and Winston Churchill reportedly used such desks for strategic planning [1].

Alternating between sitting and standing positions helps reduce muscular discomfort, improves blood circulation, and boosts productivity. This statement is supported by a 2023 study, which concluded that participants chose to stand for an average of 47 minutes per day and showed a 6.5% increase in productivity compared to those using traditional desks [2]. Another study found that young people spend approximately 68% of their day sitting, with only 30% standing up once every hour, and an average of three sitting breaks per hour [3].

There is a well-established relationship between job satisfaction and productivity, with individuals who work while standing reporting higher job satisfaction [4, 5]. Another comprehensive study analysing 8,497 scientific articles on the subject concluded that there is sufficient evidence to demonstrate that alternating between sitting and standing leads to positive health outcomes and increased productivity [6].

The height-adjustable desk market is experiencing rapid growth, driven by structural changes in work practices (remote and hybrid work), increased health awareness, and technological advancements in ergonomic solutions.

A market research report by "Grand View Research" states that the market was valued at 7.75 billion dollars in 2023 and is expected to grow at a compound annual growth rate (CAGR) of approximately 5.20% by 2030. This trend is supported by growing awareness of the negative impacts of sedentary behaviour on physical and mental health. Employers and individual workers are increasingly investing in ergonomic solutions, with adjustable desks being among the most popular options due to their benefits in improving posture, reducing back pain, and enhancing comfort during long work hours. Another key factor is the shift towards hybrid and remote work, accelerated by the COVID-19 pandemic, which has increased demand for flexible and health-oriented furniture adaptable to various workspaces. Adjustable desks are increasingly integrated into modern office spaces and residential setups, contributing to higher employee productivity some studies report productivity gains of 10–20%.

Furthermore, the industry is shifting toward sustainability, with many manufacturers opting for recyclable or eco-friendly materials (such as bamboo) and energy-efficient technologies. The dominant market segment is represented by convertible desks (with electric or manual adjustment features), which allow easy transitions between sitting and standing. This global trend highlights not only the need for comfort but also a paradigm shift regarding occupational health, prevention, and modern workspace design. The same study also points to a market growth of approximately 6.5% for smart desks with integrated technologies [7, 8].

3. Analysis of similar products, competitors and product features

In order to identify the trends among existing products on the market, 30 models were analysed and in Figure 1 there are highlighted ten of the most notable ones that stands out due to their features and design.

Fig. 1. Analysed models of adjustable-height desks

The current trend for height-adjustable desks emphasizes minimalism, functionality, and ergonomics. Products increasingly integrate silent electric systems with position memory, sustainable materials (such as bamboo), and smart accessories like USB ports, cable management solutions, and mobile app controls. Additionally, there is a growing interest in integrating desk design into modern environments, both residential and corporate [9]. The most encountered technical features include:

1. Electric lifting system – with 1, 2, or 3 motors for increased stability and higher weight capacity.
2. Digital control – control panel with preset height buttons.
3. Lifting capacity – typically ranges from 50 kg to 150 kg.
4. Adjustment speed – generally between 2–5 cm/second.

5. Noise level – modern systems operate at low noise levels (< 50 dB).
6. Safety systems – automatic stop and child-lock features.
7. Bluetooth connectivity – some models can connect to other devices or mobile applications.

The most used materials for these products are solid oak, walnut, or maple wood (for a premium appearance), bamboo, laminated MDF for the desktop surface, and metal for the support frame. Some models incorporate glass elements to enhance elegance.

The major manufacturers of such products are Uplift Desk, FlexiSpot, Herman Miller, and Ikea. The first two offer extensive customization options, including material selection, desk shape, and control panel placement. They have also taken a creative approach by introducing innovative models, such as height-adjustable desks with an integrated hammock or a built-in treadmill. Those models are illustrated in Figure 2.

Fig. 2. Unusual designs of desks

4. Identification of the market opportunities

To develop such a product, it is essential to understand market demand and identify existing opportunities. Achieving this requires insight into people's lifestyles within a complex social context. Through detailed research on the social environment and the market, it can be concluded that the greatest opportunity for this product lies in companies that have started prioritizing employee health and comfort in response of growing awareness of the negative effects of sedentarism among those who spend long hours seated. In a world where office work is increasingly dominant and a part of the daily professional life for a large portion of people, a height-adjustable desk is becoming a necessity rather than a luxury. Therefore, companies that adopt this measure to protect their employees will generate significant demand.

Additional market opportunities identified through research include:

1. Studies have shown an increase in the height-adjustable desk market, making it an ideal time to launch a product with strong sales potential.
2. Large corporations and start-ups aim to create employee-friendly environments and focusing on employee well-being and increased productivity.
3. The product's development has not yet reached market saturation, meaning there are numerous possibilities for improvement and the implementation of new features.
4. As presented earlier, studies confirm the multiple health benefits of using a height-adjustable desk, suggesting that many users will be motivated by a desire to invest in their health.
5. Growth in industries that involve prolonged desk work, such as IT, design, engineering, graphic design, and architecture where professionals spend many hours at a computer and require a customizable workspace that supports multiple monitors and specialized technologies (e.g., 3D mouse), which can be seamlessly integrated into the desk design.

To successfully launch a product on the market, it is essential to understand and identify consumer needs. These needs form the foundation of a buyer's decision-making process. A height-adjustable desk must meet specific requirements related to health, ergonomics, efficiency, and flexibility. Based on market opportunity analysis, these consumer needs can be summarized as follows:

1. The need to prevent back pain by alternating between sitting and standing up in work positions.
2. The need for a specially designed workspace to enhance productivity and comfort through customizable features.
3. The need for a high-quality, durable product at a competitive price.
4. The need for an intuitive and easy-to-use device that accommodates a wide range of users.
5. The need for a futuristic-looking desk that aligns with technological progress and blends seamlessly into modern interiors.

At the same time, opportunities do not come without challenges. Some of the identified challenges include:

1. Higher price compared to a standard desk.
2. Lack of awareness regarding the negative health effects of sedentarism.
3. Long product lifespan (most companies offer a 15-year warranty), potentially leading to a decline in sales once the market reaches saturation.

The target market segment includes individuals aged 20 to 65 (professionally active), regardless of marital or family status, living in urban areas (particularly large cities where corporations are present), and working in predominantly desk-based jobs. These individuals are typically professionals such as design engineers, IT specialists and so on with higher education or postgraduate degrees—and have above-average incomes. They tend to lead health-conscious lifestyles focused on prevention and well-being. This product may also be purchased by companies employing individuals in this area of specialty. Those users are active on social media, possess well-developed critical thinking skills, and are good at filtering information.

5. Mission of the development team

The mission of the development team is to redefine office work experience through an ergonomic, modular, and customizable product that promotes user health, comfort, and efficiency. We aim to deliver a smart, sustainable, and adaptable solution tailored to the needs of modern professionals and companies investing in the well-being of their employees—offered at a competitive price.

The targeted market will be:

1.Corporations or medium to large-sized companies investing in office space planning.

2. Creative start-ups interested in personalized workspaces.

3. Public or educational institutions focused on employee wellness.

4. Self-employed individuals working long hours at the computer, particularly in fields such as IT, design, architecture, and engineering.

5. General consumers that want to optimize their home workspace.

The business will pursue the following core objectives:

1. Official market launch by the end of 2026.
2. Achieve a minimum of 500 pre-orders before launch.
3. Manufacture at least 1,000 units within the initial launch phase.
4. Attain a minimum 75% monthly sales rate of the produced inventory.
5. Secure a 10% market share within the first six months after launch.
6. Establish at least 10 commercial partnerships with large companies seeking to improve workplace environments.

The fundamental features forming the basis for the desk's development include the presence of an electric motor connected to a power source, the ability to save preset height positions, and a highly efficient design. Building upon these core elements, customer opinion research will be conducted to introduce innovative features and enhance the product in order to appeal to a broad segment of users.

6. Identifying potential clients using the 5W1H method

The 5W1H method is an investigation technique used to fully understand a situation, problem, or strategy by answering six essential questions (Who, What, When, Where, Why, and How).

Who? – Who are the potential customers?

• Individual consumers: Active professionals aged 20–65 who work from home or in hybrid mode, in fields like IT, design, architecture, marketing, consulting, etc.

• Companies and corporations: Interested in improving their workspaces and employee well-being (e.g., IT firms, start-ups, creative agencies, multinationals).

• Health and wellness enthusiasts: Concerned about posture and preventing back pain.

What? – What are their needs?

• The desire to prevent back pain and other sedentary-related issues.
• The need for flexibility and comfort in their workspace.
• The search for a modern, smart, and customizable desk.
• Interest in sustainability and high-quality, long-lasting products.

When? – When might they need the product?

• When working long hours from home or at the office.
• When setting up or renovating their workspace.
•After experiencing physical discomfort, back pain, or receiving medical recommendations.

Where? – Where are these customers located?

• In large cities (Bucharest, Cluj-Napoca, Iași, Brașov, etc.) – urban environments.
• In corporate office spaces.
• In personal homes for those working remotely.

Why? – Why would they buy this product?

• As a solution to combat sedentary lifestyles and improve physical health.
• To increase productivity and personal well-being.
• Because it matches their lifestyle and personal preferences.
• Because it's a long-term investment, not just a piece of furniture.

How? – How can they be convinced to purchase?

• Through testimonials and product demonstrations (e.g., videos, unboxing experiences).
• By offering user-friendly online configuration and customization tools.
• With company-specific offers, early bird discounts, and extended warranties.

7. Analysed data from potential clients

To correlate the previously identified information with the actual needs of users, a questionnaire containing 15 questions was conducted, with 44 respondents. Figures 3 and 4 highlight four of the most important questions from the survey.

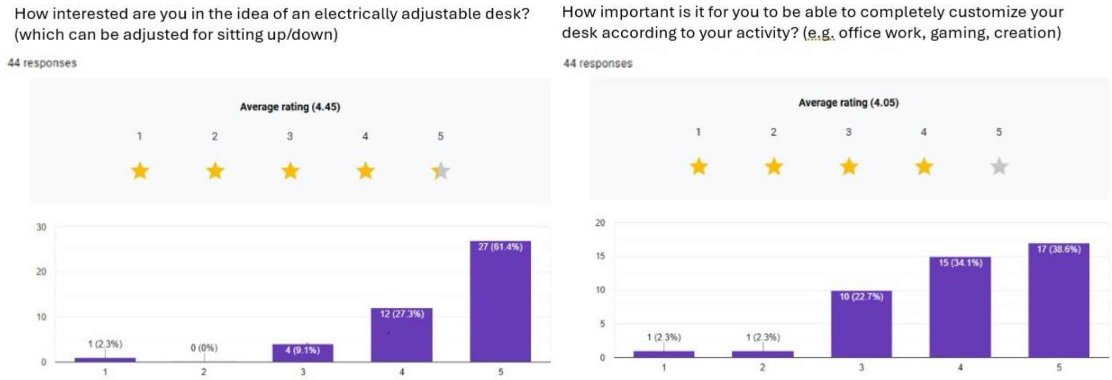

Fig. 3. Level of interest in height-adjustable desks

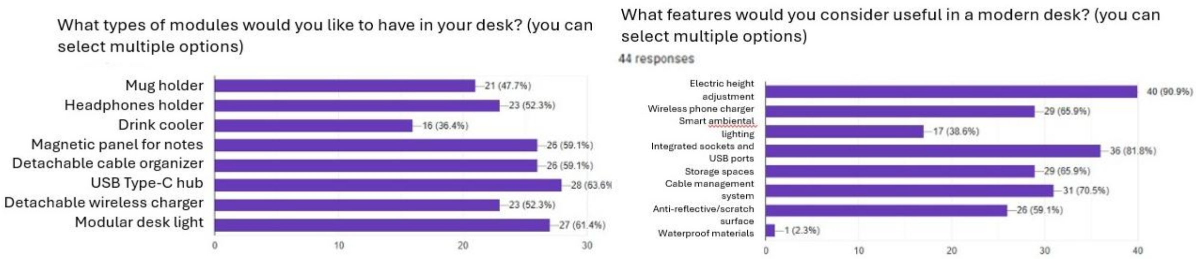

Fig. 4. Desired product features

The charts show that a large majority of respondents would consider purchasing a height-adjustable desk and believe it is important to fully customize their workstation based on their professional activity. The two graphs presented in figure 4 highlight several features that could be further developed, such as a modular lamp, cable management system, USB hub connection ports, or a headphone stand.

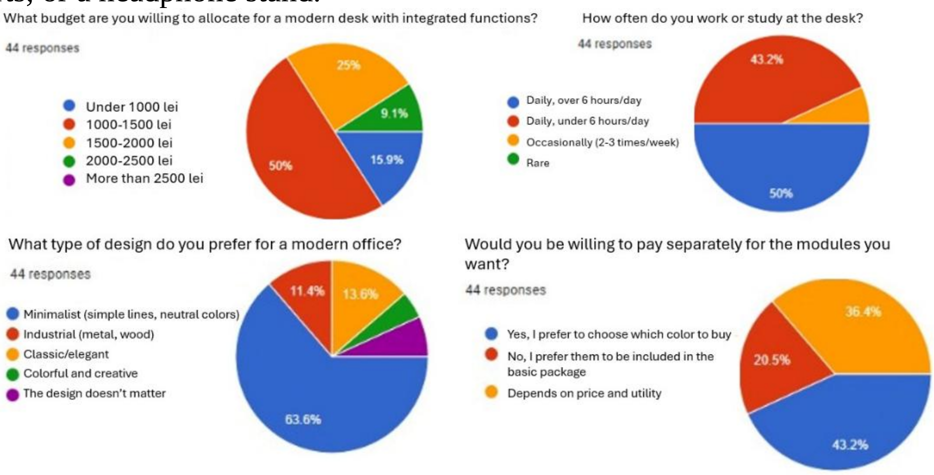

Fig. 5. Statistics about people needs

The four questions whose responses are presented in Figure 5 aim to gather data related to the price consumers are willing to pay for this product, the preferred design style (with a majority of respondents indicating a preference for minimalist design), and the possibility of purchasing different modules for the electric desk separately.

As a conclusion from the survey, we can state that people express clear interest in such a product, and the concept of modularity and separate module purchasing is perceived positively, as it allows each person to choose only the features they need. Another potential advantage lies in the fact that this concept is not yet widely developed in our country .

8. Analysis of competitive products on the market

In order to form a clear understanding of the functional features and the competitive market, an analysis was carried out on products that are already popular on the market. The information on those products has been compiled in Table 1.

Table 1. Competitive products analysis

Product name	Imagine	Price [RON]	Public success	Functional characteristics	Market share
FlexiSpot E7		1400	8	Management cable system bought separately 15 years warranty	Premium product
Fezibo electric standing desk		450	6	Management cable system bought separately 5 years warranty	Low-cost product
Branch duo		2800	7	Management cable system bought separately 10 years warranty	Premium product
Secretlab MAGNUS Pro		3900	6	Management cable system included 5 years warranty	Premium product
FlexiSpot EG8 Comhar		1500	7	Management cable system bought separately 15 years warranty	Low-cost product

Table 2. Comparison of the most important characteristics

	Measure unit	Product 1	Product 1	Product 1	Product 1	Product 1
Dimension	cm x cm	210x80	127x60	147x69	170x80	140x71
Number of motors	No.	2	1	1	2	1
Mass lifted	Kg	161	120	125	120	50
Height adjustment range	cm	123	118	118	125	121

In Table 2 there are summarized all technical specifications of the five selected desks. We can observe that the desks currently available on the market have limited functions—most offer only vertical lifting capability and do not include additional features in the base price. For most models, the cable management system must be purchased separately.

9. Conclusion

Based on all the data analysed and the information gathered, the idea of developing an electric height-adjustable desk to accommodate users in both sitting and standing positions shows strong potential for success. A basic need has been identified, and market data indicates that this sector is growing. The identified opportunities have been validated through market research.

The innovative aspect of this project is the goal of promoting a healthy lifestyle by adapting to the needs of modern society and developing a modular customization system for the desk, allowing users to work in an environment that meets all their needs.

Further research will be conducted to develop a functional prototype and identify the most in-demand modules for adding extra features. Some of these modules could include: a desk lamp, flexible monitor arm, holders for headphones or cups, PC peripherals, device connection modules, cable organizers, drawers or storage boxes for office supplies, or a footrest.

10. Bibliography

[1]. Jeffrey K. "History of Standing Desks" [Available: https://notsitting.com/history/] [Accessed 26 April 2025].

[2]. Wang, H., et al. (2025), “Quantifying the impacts of posture changes on office worker productivity: an exploratory study using effective computer interactions as a real-time indicator.” BMC Public Health, vol. 23, no. 2198.

[3]. Arundell L, Salmon J, et al. (2019), “Exploring when and how adolescents sit: Cross-sectional analysis of activPAL-measured patterns of daily sitting time, bouts and breaks.” BMC Public Health;19:653. doi:10.1186/s12889-019-6960-5.

[4]. Arnold, A.E.; Coffeng, J.K. et al. (2016), “The relationship between job satisfaction and productivity-related costs: A longitudinal analysis.”, J. Occup. Environ. Med., 58, 874–879.

[5]. Grunseit, A.C., et al. (2013), „Thinking on your feet”: A qualitative evaluation of sit-stand desks in an Australian workplace.” BMC Public Health, vol. 13, no. 365.

[6]. Tew, G.A., et al. (2015), „Systematic review: height-adjustable workstations to reduce sedentary behaviour in office-based workers.” Occupational Medicine, vol. 65, no. 5, pp. 357–366.

[7]. "Standing Desks Market Size, Share & Trends Analysis Report." *Grand View Research*, 2024, [Available:www.grandviewresearch.com/industry-analysis/standing-desks-market-report] [Accessed 26 April 2025].

[8]. "Contemporary Height Adjustable Desk Market – Industry Analysis." Technavio, 2024, [Available: www.technavio.com/report/contemporary-height-adjustable-desk-market-industry-analysis] [Accessed 26 April 2025].

[9]. "Best Standing Desk of 2025: Over 40 Models Reviewed for the Home and Office." TechRadar, 19 Oct. 2022, [Available: www.techradar.com/news/best-standing-desk] [Accessed 26 April 2025].

RESEARCH ON THE DEVELOPMENT OF A DEVICE FOR ASSISTING EYEGLASSES SELECTION

CERNEA Victor[1], SAS Loredana-Maria[2], MÁRTON Csilla[3], TARBĂ Ioan-Cristian(Conducător științific)

[1,2]Faculty of Industrial Engineering and Robotics, Specialization: Computer Applications in Industrial Engineering, Year of study: 1, e-mail: cerneavictor0@gmail.com
[3]Faculty of Industrial Engineering and Robotics, Specialization: Industrial Design and Innovative Products, Year of study: 1

ABSTRACT: This paper presents the development of an innovative Virtual Try-On (VTO) device aimed at enhancing the eyeglass purchasing experience. The proposed system integrates augmented reality (AR), computer vision, and 3D rendering technologies to enable users to virtually try on various eyeglass models in real-time using a touchscreen kiosk. By combining MediaPipe FaceMesh for facial landmark detection with Three.js for realistic 3D model rendering, the solution delivers an interactive, accurate, and user-friendly experience. Key technical challenges — such as precise alignment, dynamic scaling, and head movement tracking — are addressed to ensure high-fidelity rendering and real-time responsiveness. The paper also analyzes current market solutions, identifies key technological challenges, and discusses future research directions, highlighting AR's role in bridging online and in-store shopping experiences.

KEYWORDS: Augmented Reality, glasses, facial recognition

1. Introduction

Selecting the right glasses—whether for vision correction or sun protection—requires aesthetic, functional, and ergonomic evaluation of the wearer. Key challenges include ensuring proper fit to facial features, comfort for long-term wear (ergonomics), or optical functionality (type of lenses, thickness, visual distortion effects). In parallel with these obstacles, another important aspect is customer satisfaction, which is influenced by the time spent, reliability, and the variety of models available for selection. In fast-paced retail environments (e.g., stores, malls, airports), consumers need a solution that combines speed, visual precision, and psychological comfort in the selection process. The experience in medical offices is slightly different, as the medical consultation experience is added, amplifying the need for an as intuitive experience as possible.

2. Problem Statement and Research Goals

The main issue addressed is the improvement of the experience of trying on and purchasing glasses through a touch-based system integrated into kiosks. Virtual eyewear testing systems aim to solve this problem by realistically simulating the wearing of glasses, allowing users to visualize different models without physically trying them on, thus eliminating the need for the actual pair and eliminating the need for physical try-ons assisted by store consultants.

This paper presents a kiosk-based device that allows users to visualize and simulate wearing different models of glasses in real-time, as faithfully as possible to real life.

3. State of the Art and Current Approaches

The integration of touch-based systems in kiosks for virtual eyewear fitting, Figure 1, represents a significant advancement in retail technology, combining augmented reality (AR), artificial intelligence (AI), and haptic feedback to create enhanced interactive shopping experiences. The development of interactive kiosks with multi-touch capabilities has been a cornerstone in enhancing user engagement. The system uses computer vision and motion detection technologies to provide smooth interactions, allowing users to explore products in a more intuitive way. The integration of touch-based interfaces with AR technology allows users to interact with virtual glasses in a more natural and engaging way, merging physical and digital retail [1].

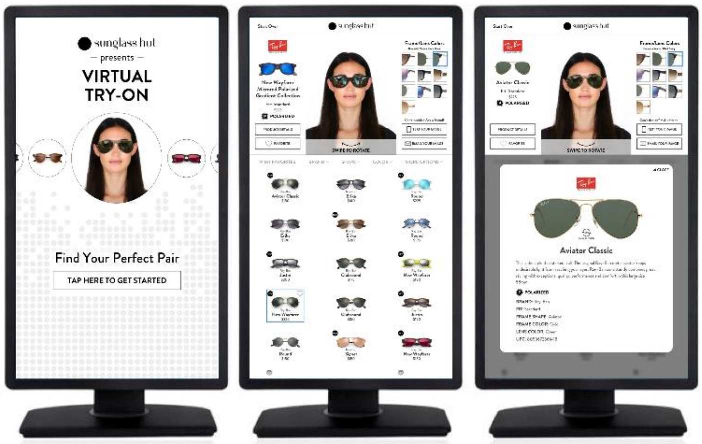

Figure 1. Eyewear Virtual Testing Platform as a Kiosk Solution [2]

Augmented reality (AR) is a technology that overlays digital information onto the real world, enhancing the user experience by combining virtual elements with physical environments. The concept of AR dates back to the 1960s, with the development by Ivan Sutherland of the first head-mounted displays (HMDs), initially used for telepresence and later evolving into virtual reality (VR) applications. Over the decades, AR has been improved and applied in various fields, starting with the military, medical, marketing, and others. The adoption of virtual fitting technologies based on augmented reality (AR) influences consumer behavior, especially among younger generations, such as millennials and Generation Z. These technologies enhance the shopping experience by providing a tool that facilitates the transition from in-store purchases to online shopping. The integration of interactive kiosks in retail environments further amplifies this effect, creating a hybrid shopping experience that combines the best of online and offline commerce [3] [4]. Virtual Try-On systems also use advanced computer vision and deep learning techniques to create realistic 3D models of glasses on users' faces. However, this article focuses on developing a solution that allows the fitting of real 3D-scanned glasses, with the ultimate goal of enhancing the fitting and purchasing experience of existing glasses models. Systems in this industry often use RGB-D cameras (RGB + depth sensor) or facial landmark detection to ensure a precise fit and realistic rendering [5] [6]. Achieving an experience as close as possible to the classic one in VTO is essential for user satisfaction. Camera calibration plays an essential role in ensuring the alignment of virtual glasses with the real proportions of the user's face. This is achieved through mobile web interfaces that acquire the camera parameters and apply coordinate transformations to align virtual objects with real-world measurements. Such calibration ensures a realistic representation, enhancing the overall experience [7].

Modern VTO systems often operate without the need for significant human intervention, relying instead on automated processes for facial feature detection and the application of virtual glasses models. These systems are particularly beneficial for users who prefer to avoid human interaction—a phenomenon that has not been extensively analyzed but is present in some studies. One such study suggests that up to 70% of shoppers prefer not to interact with other people while shopping [8]. The automation of these processes reduces complexity and makes the technology more accessible to a wider audience. VTO systems have proven to reduce product return rates by offering users a more accurate experience of the appearance and fit of the glasses before making a purchase. This not only saves retailers the costs associated with returns but also increases customer satisfaction, leading to greater loyalty and repeat purchases from retailers who benefit from this technology. At the same time, autonomous systems succeed in minimizing the need for skilled personnel in the optical industry [9]. Usability studies have consistently shown that VTO applications receive above-average satisfaction scores, especially when optimized for both desktop and mobile devices [10]. For major retailers, implementing VTO technologies can serve as a competitive advantage, attracting tech-savvy consumers who value immersive and interactive shopping experiences [3].

The acceptance of AR technologies is influenced by consumers' attitudes, education, and perceptions. In regions where consumers are more open to new technologies, the adoption of VTO systems is higher, leading to increased purchase intentions and greater brand engagement. In contrast, in regions with more conservative attitudes toward technology, the adoption of such systems may be slower, highlighting the need for targeted marketing and education efforts [11].

4. Theoretical Foundations and Research Challenges

The virtual try-on system integrated into a kiosk is an innovative technology designed to enhance the shopping experience by allowing users to virtually try on pairs of glasses. Its main functionality revolves around its ability to overlay digital images of products onto a user's real-time image or video. The VTO kiosk typically consists of several key components. First, it requires a high-resolution camera or imaging unit to capture the user's image or video. Second, it needs advanced software capable of processing and overlaying digital images of products onto the user's face. Finally, it must have an intuitive interface that allows customers to navigate through different options, select products, and view the virtual image.

A key feature of the VTO kiosk is its ability to preserve user privacy. Unlike cloud-based solutions, on-device processing ensures user data never leaves the kiosk. This is particularly important in environments where data privacy is a concern, such as retail stores, public spaces, or medical offices.

In addition to the main function, they may also offer style suggestions, product recommendations, and virtual presentations. These features not only enhance the user experience but also provide valuable insights for business owners, helping them understand customer preferences and optimize their inventory.

The kiosk’s hardware is equally critical. High-resolution cameras and displays are required to provide a clear and detailed image, while touchscreens or voice-activated controls make the system easy to use. Some advanced kiosks may include features such as gesture recognition, allowing users to interact with the system in a more natural and intuitive way. The hardware component also contributes to the inclusion of people with disabilities through these alternative methods of interaction [12]. Despite the numerous benefits of VTO kiosks, there are several challenges associated with their implementation. One of the main challenges is the high cost of development and deployment. The advanced technologies required for VTO kiosks, such as high-resolution cameras and sophisticated software, can be expensive to implement and maintain.

In addition to hardware challenges, the software implementation of a VTO system raises a series of significant technical difficulties, particularly when aiming for a realistic, smooth, and portable experience across as many devices as possible. Although Python is an extremely popular language for rapid prototyping and algorithm development in fields such as image processing and machine learning, it has not proven to be an optimal solution in this context.

Due to Python's limitations in real-time performance, cross-platform compatibility, and integration challenges with high-performance 3D rendering engines, we opted for a web-based approach. Thus, the Three.js framework was chosen, which enables 3D rendering in the browser via WebGL and provides granular control over the positioning and texturing of 3D objects, making it ideal for a cross-platform application that runs entirely on the client side.

Implementing such an application requires solving a series of software challenges, starting with detecting and tracking the user's face. Algorithms such as MediaPipe Face Mesh (developed by Google) can be used for this purpose, generating over 400 facial landmarks in real-time. These algorithms form the foundation for correctly positioning virtual glasses. However, integrating them into a web environment introduces challenges related to performance and latency, especially on resource-limited devices such as older tablets or smartphones.

Another critical aspect is the precise positioning of the 3D glasses model based on data from the facial detection algorithm. This process requires complex transformations and the alignment of key facial points (such as the temples, nose bridge, or eyebrow line) with anchor points in the virtual model. Even minor deviations in these transformations can compromise the realism of the experience. For a convincing result, calibration based on the user’s actual facial dimensions is also necessary, adding another layer of difficulty in the absence of an exact measurement system.

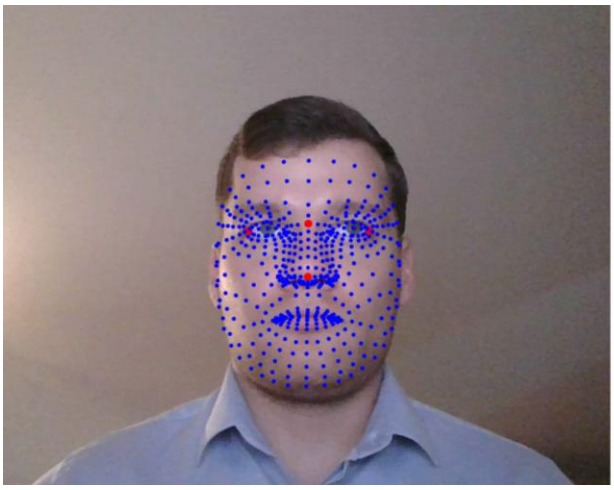
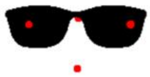

Figure 2. Alignment of facial landmarks (red) with the virtual model's anchor points

In addition to these challenges, a major obstacle in development was the use of realistic 3D models of glasses. These are typically obtained through 3D scanning using photogrammetric scanners or multi-angle image-based reconstruction. However, this process is costly and difficult to standardize.

The resulting models require significant optimization to be loaded and rendered quickly in a browser, involving retopology (restructuring of the 3D mesh), polygon reduction, and texture compression. The integration of materials from .MTL or GLTF files must also be handled carefully to maintain a realistic appearance without compromising performance.

Furthermore, there is the challenge of real-time head movement tracking. To maintain proper alignment between the user's face and the 3D model, robust head pose estimation methods must be implemented. In this context, techniques such as Pose Estimation and the use of rotation matrices (yaw, pitch, roll) are essential. These must be updated every frame while maintaining the application's performance at least 30 FPS for a smooth experience.

The user experience must be refined through a responsive and intuitive interface, allowing users to quickly switch between models, rotate, zoom, or compare products without requiring technical support. As a web application, testing across multiple browsers and screen sizes adds an extra layer of complexity—particularly when maintaining graphical fidelity and the stability of facial tracking algorithms.

5. Implemented Approach: Methods, Technologies, and Testing

By using MediaPipe and Three.js libraries, we developed an interactive application capable of real-time 3D glasses positioning on the user's face, captured via webcam. Additionally, the solution includes adjustment mechanisms for the position, size, and orientation of the glasses, as well as the ability to choose between multiple models.

The application is browser-based and relies on four main components:

1. Real-time video capture from the user's camera;
2. Facial feature detection via MediaPipe FaceMesh;
3. 3D rendering of GLB models using Three.js;
4. The user interface (including relevant tools).

The workflow: the webcam captures the user's face, followed by the MediaPipe model which identifies 468 facial landmarks. The key points needed for glasses positioning are then extracted, after which the 3D model is positioned and rotated based on these points, with the final result being rendered in WebGL over the video feed.

Facial feature detection uses Google's FaceMesh model, which enables fast and accurate detection of a detailed set of facial landmarks (468 in total). From these, we only used a few considered essential for proper glasses positioning and orientation:

- The top of the nose (landmark[168]);
- The bottom of the nose (landmark[1]);
- The corners of the eyes (landmark[33] and landmark[263]);
- The forehead and chin (landmark[10] and landmark[152]);
- The eyebrow corners (landmark[70] and landmark[300]).

Figure 3. The facial landmarks listed above

We set the glasses position using 3D coordinates relative to facial landmarks. First, we transform the normalized coordinates [0, 1] provided by MediaPipe. Then, we transpose these values into the Three.js coordinate system, which uses an inverted X-axis and negative Z-depth to maintain natural perspective:

```
const noseX = (noseBridge.x - 0.5) * 2;
const noseY = -(noseBridge.y - 0.5) * 2;
const noseZ = -noseBridge.z * 3;
glasses.position.set(noseX, noseY, noseZ);
```

To achieve a realistic orientation of the 3D model, we constructed a rotation matrix based on three orthogonal vectors:

- The **"forward" vector** – the direction between the nose bridge and the nose tip;
- The **"right" vector** – between the eye corners;
- The **"up" vector** – obtained as the cross product of the other two.

This orthogonal vector approach provides stable orientation tracking, eliminating uncontrolled rotations and jitter that commonly occur with simpler tracking methods.

Figure 4. Color customization

Figure 5. Size and vertical axis position adjustment

Figure 6. Automatic head movement adaptation

Figure 7. Horizontal axis position adjustment

A recurring challenge in augmented reality systems is accurately representing head tilt. To address head tilt, we implemented a correction algorithm that calculates the angle between forehead and chin landmarks and applies a rotation quaternion around the X-axis. Quaternions are a robust mathematical method for representing rotations in 3D space, avoiding issues associated with Euler rotations—such as *gimbal lock* (i.e., the loss of a degree of freedom in a multi-axis mechanism at certain alignments). In our implementation, the quaternion is derived from an angle calculated between two facial key points (forehead and chin) and applied as an additional rotation to the 3D glasses model to reflect vertical head tilt. This approach ensures the glasses remain naturally aligned with facial features, even when the user tilts or raises their head.

Glasses scaling is performed dynamically based on the distance between eyebrow corners, providing a more stable estimate of face width than measuring between ears (which are often partially obscured). This ensures proportional sizing for each user. Beyond automatic scaling, users can manually adjust the 3D model's size and position via an interactive control panel exposing four parameters:

- **Scale**
- **X-axis position** (left/right)
- **Y-axis position** (up/down)
- **Z-axis position** (forward/backward)

The interface was designed to be minimalist yet functional. Sliders offer real-time control over each adjustment dimension, instantly reflecting changes on the model. This allows fine-tuning for individual models, compensating for detection errors or morphological differences between users. Additionally, all parameters are globally exposed (via window) for saving or reuse.

The solution was built modularly to support dynamic loading of multiple glasses models (.glb format) via the GLTFLoader mechanism. While the current version uses a single model, extending it to a multi-model selector is trivial: each model can be added to the scene using the same algorithm, managed through a list and navigation system.

Testing was conducted on multiple devices (desktop and laptop, with different operating systems) under various lighting conditions. The results showed:

- Real-time performance: Very low latency (<100 ms);
- Good stability: Glasses positioning remains accurate during slow and moderate movements;
- Visual precision: Natural alignment with facial features, without distortions;
- Minimal positioning errors only in cases of partial facial occlusion (hand, prescription glasses);
- High usability thanks to the simple interface and adjustment options.

6. Conclusion

This study presents the development of an innovative virtual glasses try-on system, combining modern technologies such as augmented reality and computer vision to deliver a realistic and interactive user experience. The proposed solution employs advanced algorithms for facial feature detection and 3D model rendering, ensuring precise positioning and dynamic real-time adjustments. Testing confirmed the system's effectiveness, and demonstrated strong performance in speed, stability, and ease of use.

The original contributions of this work include:

1. Implementation of a cross-platform web application, accessible on multiple devices without requiring advanced hardware resources.
2. Integration of manual adjustment for adapting to individual facial structures.
3. Optimization of 3D models and processing pipeline to ensure smooth performance even on resource-limited devices.

Future research will focus primarily on improving automated glasses positioning accuracy, enhancing facial tracking algorithms under variable lighting conditions, expanding the glasses model database, and implementing additional features such as personalized recommendations based on facial analysis. The study also explores potential applications in other domains like fashion and wearable accessories. This project demonstrates how augmented reality technology can transform traditional shopping experiences by offering an effective virtual alternative to physical try-on methods.

7. Bibliography

[1] N. Gourier, J. Letessier, J. Maisonnasse and S. Borkowski, *IHM '09: Proceedings of the 21st International Conference on Association Francophone d'Interaction Homme-Machine,* 2009.

[2] "JEFFREY KUO" [Online]. Available: https://www.jeffreykuodesign.com/. [Accessed 05 2025].

[3] B. Konarzewski and M. Reiner, "Augmented Shopping: Virtual Try-On Applications in Eyewear E-retail", 2023.

[4] T. Trivedi, "Generation Z Inclined Toward Immersive Shopping Experiences: AR Virtual Try-On in Online Retail in India" in *Immersive Technology and Experiences*, 2023.

[5] P. Azevedo and T. Oliveira-Santos, "An Augmented Reality Virtual Glasses Try-On System", 2016.

[6] G.-L. Lin and T. H. Chan, "The 3D Glasses Try-On System of Augmented Reality Using Intel RealSense", 2019.

[7] W.-C. C. C. A. D. H.-W. C. FuChe Wu, "Real-Size Experience for Virtual Try-On", 2024.

[8] J. M. Germain, "Many Shoppers Now Want Zero In-Store Human Interaction", 2020. [Online]. Available: https://www.ecommercetimes.com/story/many-shoppers-now-want-zero-in-store-human-interaction-86913.html. [Accessed 5 2025].

[9] T. Kobayashi, Y. Sugiura, H. Saito and Y. Uema, "Automatic Eyeglasses Replacement for a 3D Virtual Try-on System", 2019.

[10] D. Marelli, S. Bianco and G. Ciocca, "Faithful Fit, Markerless, 3D Eyeglasses Virtual Try-On" in *Pattern Recognition. ICPR International Workshops and Challenges*, 2021.

[11] N. A. B. Ibrahim, T. Y. Chen, N. H. Ahmad and P. M. Antara, "The Acceptance of Augmented Reality's Role in Elevating Customer Attitude within Malaysia's Local Fashion Merchandising", *Advances in Social Sciences Research Journal,* 2024.

[12] O. Georgiouț, H. Limerick, L. Corenthy and M. Perry, "Mid-Air Haptic Interfaces for Interactive Digital Signage and Kiosks", 2019.

RESEARCH ON THE DEVELOPMENT OF A TECHNICAL SOLUTION FOR EFFECTIVE ENFORCEMENT OF ROAD MARKINGS

ROTARU Rareș-Andrei[1], MARINESCU Marius-Gabriel[1], DRĂGHICI Dănuț-Alexandru[1], DURLAN Robert-Andrei[1], TARBĂ Ioan-Cristian

[1]Faculty of Industrial Engineering and Robotics, Specialization: Applied Informatics in Industrial Engineering, Year of study: I, e-mail: draghici.alexandru2001@gmail.com

Abstract: The paper called "Research on the development of a technical solution for efficient road markings application" focuses on the realization of a robotized system capable of applying road markings on asphalt surfaces. The system is built on a modular structure of aluminum v-slot profiles and integrates several subsystems: axle movement (with stepper motors and linear guides), wheel movement (with DC motors), paint application (with automatic electric spray gun). Orientation on the lane is provided by a Pixy2 camera, which allows automatic trajectory correction.

Keywords: System, marking, paint, trajectory.

1. Introduction

Road markings are an essential element in ensuring traffic safety, as they guide and assist drivers in making their journeys in optimal conditions. These markings must be clear and give drivers sufficient reaction time to prevent undesirable incidents for themselves and other road users.

Global interest in road markings increased significantly with the introduction of the first center line to separate oncoming traffic, an idea originally proposed by Edward Hines, a commissioner from Michigan, USA. This idea was first put into practice in 1921 by Frederick Basley on a street in Madison, Wisconsin. As paved road networks expanded and traffic volumes increased, it became necessary to develop high-performance equipment for applying and drying paint quickly, especially during periods of inclement weather. Thus, the first specialized vehicles with capacities of up to 4,500 gallons of paint were developed. [1]

At the same time, the composition of paint used for road markings has undergone major developments over the last eight decades, moving from plain paint to thermoplastic paint and then to night-visible reflective paint. The latter is based on the use of glass microbeads, which, when applied to the surface of freshly traced paint, reflect the light of vehicle headlights. Reflective technology was patented by Edwin R. Gill in 1933. [2]

2. Current state of the robotic system

The robotic road marking system is currently at an advanced stage of development, with some of the subsystems already completed and integrated. The choice of the components of each subsystem has been made considering the required accuracy, structural strength and reliability under real operating conditions.

The chassis constitutes the structural basis of the robot and was built using v-slot aluminum profiles (Fig.1). These profiles were selected for their strength and flexibility in assembly, thus allowing modular construction and easy to adapt to the project needs. Specific connectors and fasteners ensure the structural integrity and stability required to carry out the activities. The main components chosen are the aluminum v-slot profiles (20x40 mm and 20x20 mm), thanks to the optimal ratio between mechanical strength and light weight, the T-slot connectors and fasteners, which allow quick and efficient adjustments, and the joint plates for stiffening the structure.

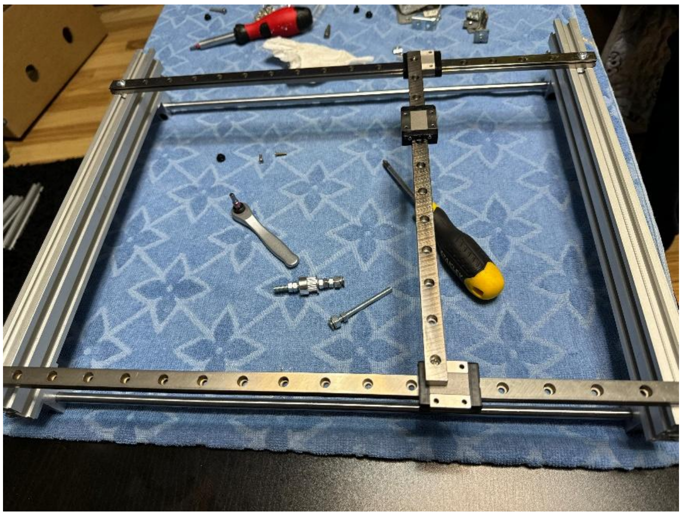

Fig. 1 - Chassis

The axis motion subsystem ensures the precise movement of paint application equipment and is essential for clear and accurate marking. MGN12 linear guides were used for this subsystem, chosen for their high accuracy, ability to withstand moderate loads and low friction resistance. Nema 17 stepper motors were selected for their precise positioning control. The GT2 transmission belts were chosen for efficient and quiet transmission of the motors' power to the axles, and the mechanical travel limiters are designed to protect the system against exceeding travel limits and prevent damage to the equipment (Fig. 2).

Fig. 2 – Axis motion

The wheeled travel subsystem allows the entire robotic system to move, providing the necessary mobility for sequential road marking. The JGA25-370 geared DC motors have been chosen for the torque and travel speed suitable for controlled movement on the road surface. Power supplies, including batteries and electronic distribution systems, ensure autonomy and reliable system operation.

3. Robotic system development

Currently, the system is being developed in directions aiming at automatic and accurate robot orientation in the middle of the road lane. We propose to integrate a Pixy2 smart camera (Fig. 3). It has built-in algorithms for fast image processing, identifying objects by color and shape in an efficient and reliable way. The Pixy2 camera can be connected to an Arduino or Raspberry Pi microcontroller, providing the ability to track the centerline of the lane in real time and automatically adjust the robot's position. [3] This method allows automatic deviation correction, increasing accuracy and reducing the need for manual intervention.

Fig. 3 – Camera Pixy2 [3]

The real-time image analysis performed by Pixy2 involves continuously capturing video frames, automatically identifying the marker line and providing precise information about the relative position of the robot with respect to this line. This keeps the robot always centered on the lane, improving the safety and accuracy of the markings (Fig. 4).

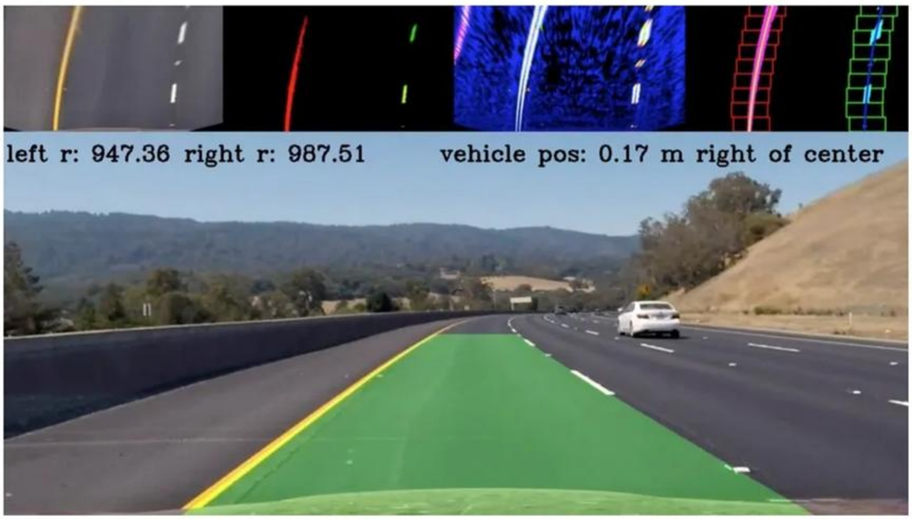

Fig. 4 – Image analysis [4]

For the precise and uniform creation of road markings, we propose the use of an automatic electric paint spray gun. This type of device allows precise electronic regulation of the paint flow and distribution, ensuring a constant and uniform application on the asphalt surface. (Fig. 5)

Fig. 5 – Paint spray gun [5]

The major advantage of using an electric spray gun is its ability to be precisely controlled, with quick adjustments according to the type and thickness of marking desired. The electric gun thus contributes significantly to process efficiency, reducing paint consumption and minimizing waste. Its use also ensures optimum coverage and a uniform finish, essential for clear and durable markings.

To improve maneuverability and precision in positioning the robot on the road surface, we propose the use of special wheels with knobs, known as “Omni wheels”. These wheels allow the robot to move in all directions without the need for wide turns, thereby increasing the flexibility and control of the movement.

Omni wheels are equipped with small rollers arranged around their circumference, facilitating quick and precise direction changes. This type of wheel is ideal for applications where precise steering and high maneuverability are required, such as road marking applications.

Fig. 6 – Omniwheel [6]

4. Testing the current system

An Arduino development board and DC & Nema 17 motors with the corresponding drivers were used to verify the components and the functionality of the system; the motors were connected, the power supply was connected, and a test program was run. (Fig. 7)

Fig. 7 – Testing the DC motors

5. Summary

The robotic system has real-life applicability and offers a modern solution, making the human user's work easier and increasing process safety.

Currently, the first 2 subsystems, namely the wheeled and the axle driven subsystems are finalized and have passed including the testing part, with favorable results. For the belt guidance part, further research is still ongoing. During testing, it was found that certain metal components can be replaced with 3D-printed parts, reducing the weight of the assembly without compromising rigidity or functionality.

6. Bibliography

[1]. Brian Bowman (2001), *Estimating the Effective Live of Pavement Marking Based of Crash History* - https://www.eng.auburn.edu/files/centers/hrc/IR-01-02.pdf - accessed on 07.05.2025

[2]. Pavement traffic marking, https://onlinepubs.trb.org/Onlinepubs/nchrp/nchrp_syn_17.pdf - accessed on 07.05.2025

[3]. Pixy2 CAM, https://www.sparkfun.com/pixy2-cmucam5.html - accessed on 07.05.2025

[4]. Line tracking for line-following, https://www.researchgate.net/figure/Detected-Vehicle-boundaries-by-the-RT-VDT-algorithm_fig2_343263011 - accessed on 07.05.2025

[5]. Paint gun, https://www.bricodepot.ro/unelte/unelte-electrice/erb-pistol-vopsit-800w.html - accessed on 07.05.2025

[6]. EasyMech Omni wheel, https://www.optimusdigital.ro/ro/mecanica-roti/11435-roata-dubla-de-aluminu-easymech-omni-127-mm-bearing-roller.html - accessed on 07.05.2025

RESEARCH ON THE DESIGN OF AN AUTOMATED UNIT FOR MEDICINE DOSE DISTRIBUTION

STOIAN Ioana-Andreea, NAIPEANU Delia, RADU Daniel, POPÎRLAN Robert-Florin, PRELIPCEAN Claudiu Ștefan, TARBĂ Ioan Cristian (Conducător științific)

Faculty: Industrial Engineering and Robotics, Specialization: AII, DIPI, IEMA, Year of study: I,
e-mail: delianaipeanu0505@gmail.com

Abstract: This paper proposes the design of an automated unit for distributing medicine doses in medical facilities. The system consists of a dispenser that prepares the treatment based on each patient's prescription and a mobile robot that handles delivery. The goal is to reduce human errors and support the medical staff by automating repetitive tasks. Key functions of the system are defined and linked to the technical principles behind them. The paper also includes the functional modeling of the product and sets a clear SMART objective for future implementation.

Keywords : dispenser, automation, automated distribution, drug delivery

1. Introduction

In recent years, hospitals and care centers have begun to adopt automated solutions to reduce human error and make the work of medical staff more efficient. One area where automation can have a significant impact is treatment administration, especially in the context of overcrowding and staff shortages.

This paper proposes the development of an automated drug distribution system, composed of a dispenser that prepares doses according to each patient's treatment and a programmable mobile robot that transports the container to the appropriate room. This aims to develop a practical solution, easy to implement in medical units, that would contribute to a safer administration of treatments and to the efficiency of staff activity.

2. Current status

Today's dispensers have evolved significantly, becoming much more efficient and intelligent than their predecessors. Omnicell has become one of the global leaders in the development of automated medical dispensers, used in hospitals for controlled drug distribution, such as the Omnicell XT. At the same time, BD has revolutionized this field with its Pyxis MedStation ES system, which optimizes medication management and increases patient safety.

Among the applications relevant to this research is the Dispensing Robot at the University Hospital of Cuenca, Spain.

The University Hospital of Cuenca has adopted an advanced system for dispensing medicines in the pharmacy, managed entirely by a robot. The robot receives medicines delivered by pharmaceutical companies without human intervention, recording essential parameters such as expiry date and batch number. The system categorizes and stores medicines efficiently, ensuring quick and organized access to each product. At the patient’s request, the robot identifies and delivers the appropriate dose of medicine, transporting it to an automated collection point, available 24/7. This means that patients can collect their medicines at any time, thanks to the continuous operation of the system. [1]

One advantage is that automating the process reduces the risk of human error in managing and dispensing medications, and pharmaceutical staff can devote more time to consulting and other clinical activities, due to the reduction of repetitive tasks. [1]

Fig. 1 The dispensing robot at the University Hospital of Cuenca, Spain [2]

Also, another relevant application for this research is the “Apparatus” medicine dispenser [AU20230231401]. The invention (Fig. 3) describes an innovative apparatus intended for the automatic dispensing of medicines according to a prescribed regimen. This device offers functionalities such as storage, controlled distribution and user notification.

The device addresses the shortcomings of existing devices, such as the difficulty of refilling containers, limitations in compatibility with different blister types, and the inability to reuse medication containers. It also facilitates patient medication handling by automating dispensing processes.

The product is configured with multiple pockets for storing medication, made of flexible materials such as silicone for easy loading and unloading. Includes a pusher head for releasing medication from the pockets. A positioning system with guides and gantry allows precise alignment of the pusher mechanism with the appropriate pocket. Touch screen display and/or mobile app for programming medication regimens. Visual and audio notifications for timely medication administration. Containers can be refilled by users through specially designed slots or flaps. [3]

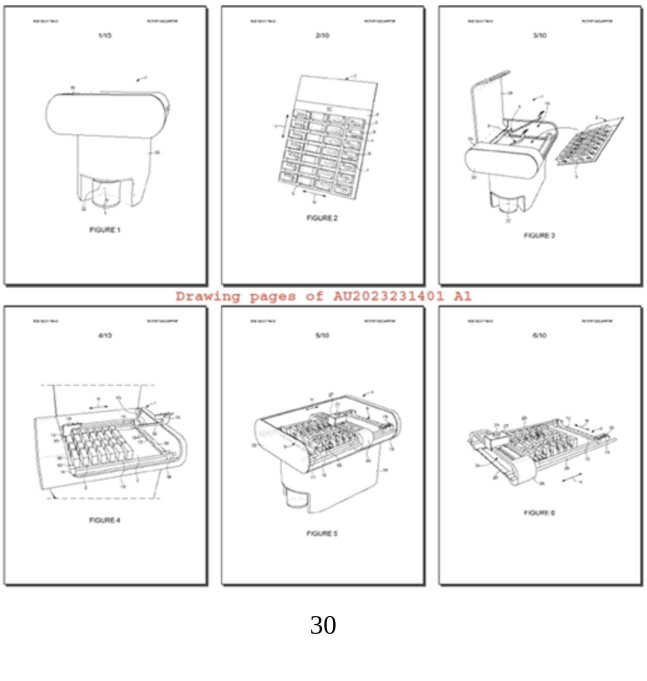

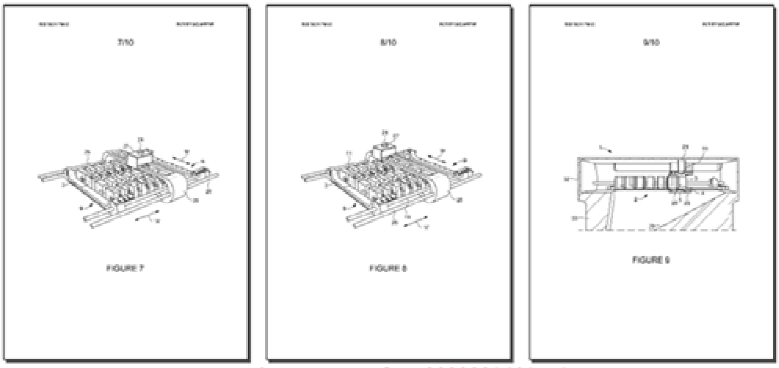

Drawing pages of AU2023231401 A1

Fig. 3. Medicine dispenser "Apparatus" [3]

3. Phenomena underlying product functions

The design of a device such as an automated medication dispenser (AMD) requires a clear understanding of the functions it must perform and the technical phenomena associated with each function. To ensure correct, safe and efficient operation, it is important that these functions are analyzed from the early stage of product development. This section presents the system functions and the technical principles underlying their realization.

The main function of the dispenser is the automatic distribution of drugs, according to a pre-established program for each patient. This is achieved through electronically controlled mechanical drives, coordinated by a microcontroller. The system may include sensors for checking the position or container. A correct and timely dosage is essential for the safety of the treatment.

For a clearer presentation of the functions defined in the project, they have been summarized in the following table (Table 1). Each function is identified by a symbol and briefly described, along with mentions of its role in the overall functioning of the automatic medicine dispenser.

Table 1. Product features

FUNCTION SYMBOL	DEFINITION OF FUNCTION (verb + noun)	Function type						
		Objective	subject	generous	Main	Auxiliary	On duty	For sale
F	DAM allows for the automatic distribution of medications according to a pre-established schedule	X		X	X			
F1	DAM allows user notification at the time of distribution	X			X	X		
F2	DAM has a locking system to prevent unauthorized access	X		X	X			
F3	DAM is compatible with several types of drugs	X		X	X			
F4	DAM has dual power supply (plug and battery)	X				X	X	
F5	DAM has a simple and intuitive user interface		X			X	X	
F6	DAM can be controlled via a mobile application	X		X	X			
F7	DAM features ergonomic design and compact dimensions		X			X	X	
F8	DAM has a low noise level	X				X	X	
F9	DAM is made from recyclable materials and in accordance with medical standards	X					X	
F10	DAM is protected against environmental factors	X				X	X	
F11	DAM allows the pre-establishment of drug categories based on the medical prescription for each patient	X			X			X
F12	DAM provides a septic space for medicines	X		X	X			

To develop the main and secondary functions of the automatic medicine dispenser, a series of physical and technological phenomena underlying the operation of each subsystem were identified. These phenomena are essential to ensure correct operation and to meet user requirements. For example, automatic medicine dispensing is based on mechanical dosing movements and electronic control via microcontroller, while the user interface involves digital display, intuitive buttons and visual or auditory feedback. Other important functions, such as dual power supply, silent operation, ergonomic design or the use of materials compliant with medical standards, are supported by phenomena such as automatic switching of the power source, vibration isolation or the choice of biocompatible materials. Also, functions such as organizing medicines according to prescription and ensuring a septic space involve phenomena related to software control, tightness and sanitation. Overall, the correct identification of these phenomena contributes both to the technical performance of the system and to its reliability and safety in use.

4. Functional modeling of the system

To more clearly understand how the proposed system works, an activity diagram (Fig. 5), a system diagram (Fig. 6), and also the 3D model of the product (Fig. 7-10) were created.

The activity diagram highlights the steps taken from the moment the dispenser receives patient information to the delivery of treatment. This visual representation allows tracking the interaction between the main subsystems (dispenser, controller, and patient) and highlights the sequential logic of operations.

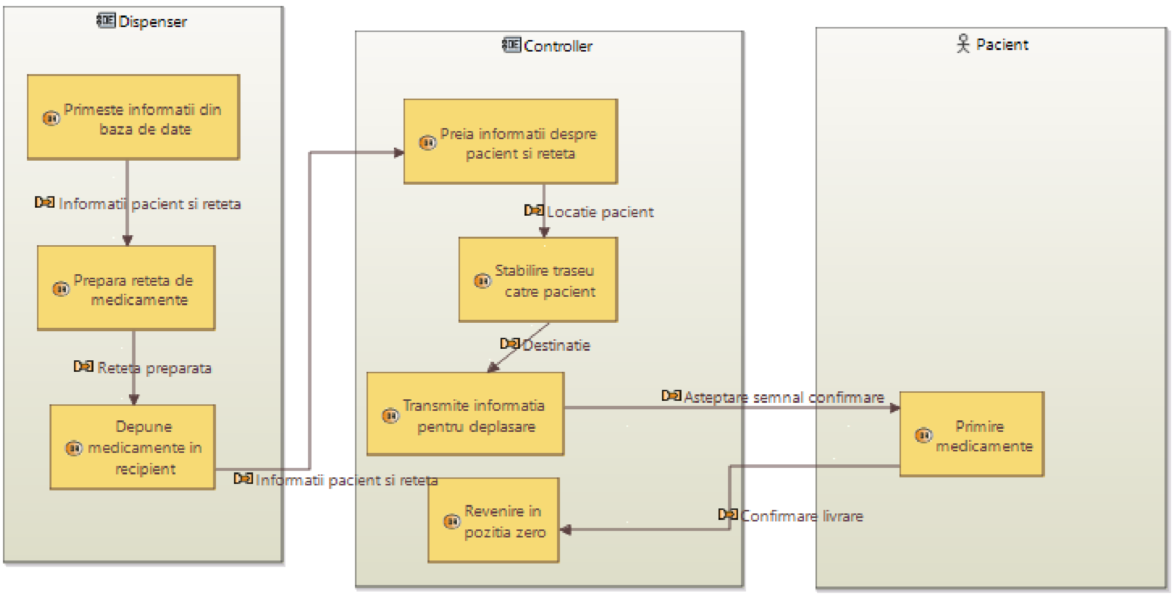

Fig. 5. System activity diagram

The diagram shows the following steps:

- The dispenser receives patient and prescription information from a database.
- Prepare the prescription and place the medications in a container.
- The controller takes the information and determines the patient's location.
- The route is established and the movement command is sent to the robot.
- After delivery, the patient confirms receipt, and the system returns to its starting position.

This scheme helps validate the system logic and can form the basis for future software or automation implementations.

The following figure shows the system and subsystem diagram that make up the automatic medicine dispenser. Through it we can see the main subsystems.

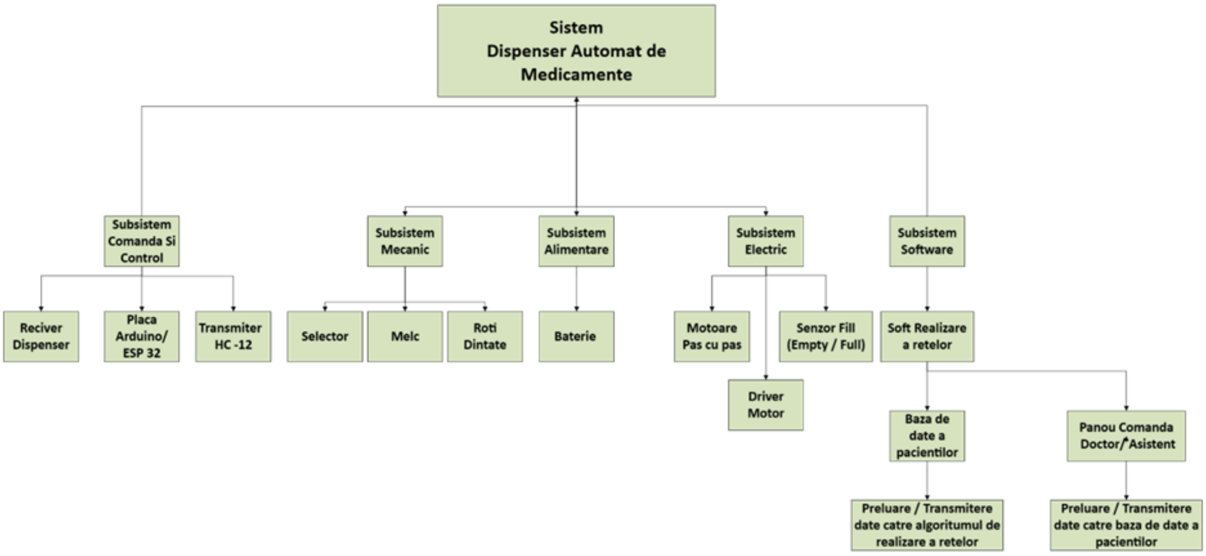

Fig. 6. System diagram

From the previous figure we can see how the device will be controlled, it is based on an arduino/esp32 board that will receive its information through an HC-12 radio transmitter (It has the role of both receiving and transmitting data from the Dispenser to a computer or a server.)

The mechanical subsystem represents the moving parts of the entire assembly. Their main role is to transmit the movement of the motors to the medicine tubs to distribute them into each vial for each patient.

The entire system will operate on battery power, benefiting from considerable storage capacity to ensure optimal performance and reduce the risk of unexpected shutdown due to battery discharge.

For the electrical subsystem, they will consider stepper motors with the ability to rotate considerable amounts. And the sensors will confirm the filling level of the container so that you never run out of medicine.

The software subsystem will consider an interface that can be used by both doctors and assistants to complete each patient's data with their prescription and other important data. This data will help in preparing the prescription that will later be taken over by the automatic dispenser.

The storage and selection assembly consists of a cylindrical container, a lid, a rotating disk, 2 gears and a stepper motor. The motor engages the rotating disk through two gears to allow the dosage of the medicine stored in the container. The containers have an opening, aligned with that of the disks so that the medicines can reach the funnel and then into the robot container. These can be removed from inside the unit for maintenance or supply.

Fig. 7. Storage and dosing assembly

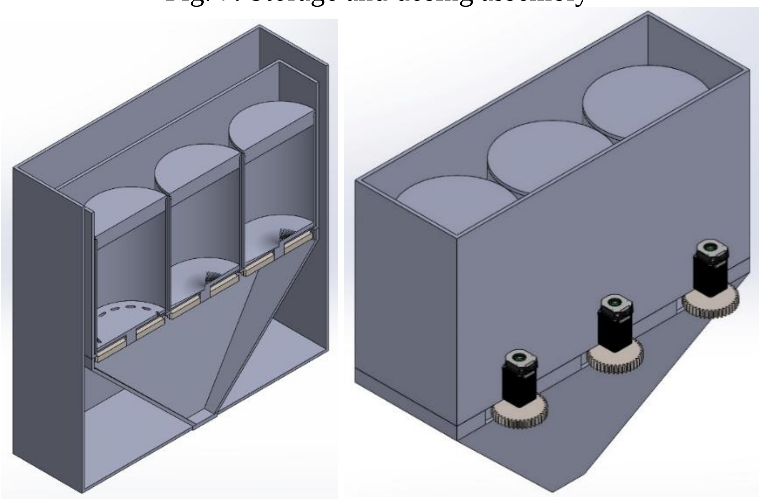

Fig. 8. Drug distribution unit

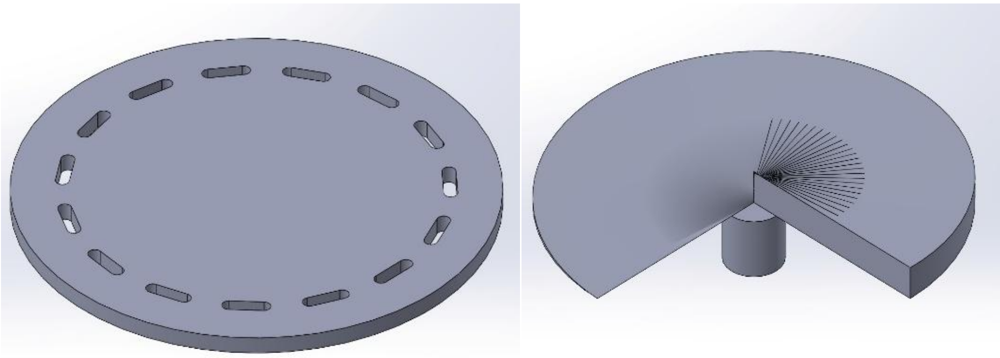

Fig. 9. Versions of the rotating disk for drug dosing

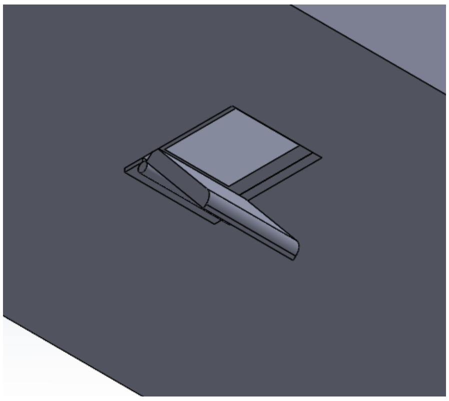

Fig. 10. Hatch for dispensing medication

5. Defining sales objectives

To transform the developed project into a functional product, with real impact in the medical system, a SMART objective can be formulated, as follows:

"Development and implementation of an automated system for distributing drug doses, installed in at least two hospitals in Romania by the end of 2027 , with the aim of reducing treatment administration errors by at least 30 % and improving the efficiency of medical staff by at least 35 %."

- Specific (Specific), by clearly defining the purpose (automating the medication distribution process);
- Measurable (Measurable), by establishing performance indicators (number of units installed, reduction of errors, increase in efficiency);
- Achievable, considering the technological level of the prototype and the potentially available resources;
- Relevant, because it responds to an essential need in Romanian hospitals and supports digitalization in healthcare;
- Time-Bound, proposing a total duration of 30 months for development, testing and implementation.

Implementing a SMART goal is the basis of a business plan or an applied research initiative with clear results in the medical field. [7]

6. Conclusions

The paper aims to design an automated system consisting of a medicine dispenser and a mobile robot that delivers treatment to patients according to established prescriptions. The system is designed to reduce administration errors and support the work of medical staff in conditions where hospitals are facing staff shortages and overcrowding. Existing solutions on the market, such as Omnicell or Pyxis MedStation, are analyzed, and a concrete example of application is presented – the robot in the Cuenca University Hospital, which automatically manages the entire process of dispensing medicines.

From a technical point of view, the paper identifies the main functions of the system, such as dose distribution, user notification, compatibility with multiple types of drugs and control via the application. The phenomena underlying each function are also explained, and through functional modeling and the presentation of hardware and software components (controller, sensors, interface, mechanical assembly), the project acquires a clear structure. Finally, a SMART objective is formulated, aiming to implement the system in hospitals by 2027, with the aim of reducing errors by 30% and increasing staff efficiency by 35%.

7. Bibliography

[1].https://ro.espacenet.com/publicationDetails/biblio?CC=AU&NR=2023231401A1&KC=A1&FT=D&ND=3&date=20241003&DB=EPODOC&locale=ro_RO [accessed on 08.05.2025]
[2].https://ro.espacenet.com/publicationDetails/biblio?CC=CN&NR=212218457U&KC=U&FT=D&ND=3&date=20201225&DB=EPODOC&locale=ro_RO [accessed on 08.05.2025]
[3]. Drăghici, G. (1999). Integrated Product Engineering. Eurobit Publishing House, ISBN 973-96065-7-1, Timişoara;
[4]. *** COSMOS/M – Finite Element System, User Guide, 1995.
[5]. Roxana PUIU. "Sales Management" Course Notes, UPB, 2024-2025

EQUIPMENT FOR HYBRID TECHNOLOGY EDM-ECM+US

[1]BOGOSLOV V. Vasile Ionuț, [2]CRISTINA D. Ioana Mădălina, [3]DUCA M. Anca-Valentina, [2]IONESCU N. Roxana Silvia Elena, [1]RĂSCOL S. Viorica, [4]Liviu Daniel GHICULESCU(Conducător științific)

Facultatea de Inginerie Industrială și Robotică, Specializarea: [1]INPN, [2]IEMA, [3]IPFP, [4]Conducător ştiinţific, Anul de studii: II, e-mail: ancavalentina2202@gmail.com

ABSTRACT: This paper presents the design concept of equipment for a hybrid technology that combines electrical discharge machining (EDM) and electrochemical machining (ECM) in an ultrasonic field (US). To this end, an analysis of competing products was carried out, playing a key role in both the conceptual and detailed design of the equipment. Potential buyers were identified, and an economic analysis model was also applied.

KEYWORDS: Hybrid technology, EDM, ECM, US.

1. Introduction

Unconventional technologies are increasingly used in industry due to their advantages. Processes such as EDM, WEDM, and ECM are applied for machining conductive, hard, wear-resistant, and corrosion-resistant materials [1], [2]. EDM and WEDM fall under thermal erosion machining, where material is removed by melting and vaporization, but they have the disadvantage of low productivity [1]. ECM operates through anodic dissolution in an electrolytic cell, with limited control over surface precision [3]. The integration of ultrasonic vibrations (above 20 kHz) into these processes brings significant benefits: increased productivity, improved precision, and reduced wear. In EDM, vibrations aid in removing the molten material, while in ECM they enhance the dissolution process [3]. This paper focuses on the development of a hybrid EDM-WEDM-ECM equipment with ultrasonic assistance, composed of distinct but functionally integrated subsystems.

2. **Analysis of Competing Products**

Fig. 1 Holmarc ECDM, model HO-ECDM-0 [5]

Fig. 2 Sodick A-Series (AC600GH) [4]

Hybrid EDM-ECM machining products are rare and typically used in highly specialized applications, such as processing hard materials or parts with complex shapes. Some examples of machines and equipment that integrate both EDM and ECM machining processes include those produced by Sodick, Holmarc, KRC, Stratasys, Electronica, Oerlikon, Schunk, Kennametal, GF Machining Solutions, Voxel Innovation, and Mitsubishi Electric.The Holmarc model HO-ECDM-0 is a research system that combines EDM and ECM for machining non-conductive materials. It features CNC control, an XYZ platform, and a 300V power source for controlled discharges [5].Sodick provides an example of hybrid technology with its A-Series (AC600GH), which combines water jet technology with wire EDM for more efficient machining—especially in terms of heat management and the removal of molten particles [4].

3. Conceptual Design of Hybrid EDM+US, WEDM+US and ECM+US Equipment:

3.1. Defining the General Function

An equipment that combines EDM, ECM, and WEDM technologies with ultrasonic vibrations aims to efficiently process materials by merging the principles of these conventional methods with the advantages of ultrasound, such as gas bubble removal, increased productivity, and improved surface quality.

3.2 Highlighting Critical Issues

There are several conditions for optimizing working parameters in order to achieve specific technological performance [6]:

1. Process Stability: The tool oscillation amplitude (Ay) must be smaller than the front gap (sF) to avoid short circuits and excessive wear.

$$A_y < s_F \quad [\mu m] \tag{1}$$

where: Ay is the maximum longitudinal ultrasonic oscillation amplitude of the tool.

2. Maximizing the gap: A higher ignition voltage (u_0) allows discharges in wider gaps, which improves particle evacuation.

3. Minimizing discharge energy: In finishing EDM modes, low-energy pulses (We) are recommended.

4. Maximizing pulses per oscillation: A higher number of commanded pulses (nic) during one oscillation period (Tus) increases efficiency through cumulative microjet effects.

5. Effective cavitation: The ultrasonic power (PcUS) must ensure the acoustic pressure exceeds the cavitation threshold in the dielectric fluid.

6. Minimizing acoustic pressure: In finishing processes, the acoustic pressure should be optimized to reduce roughness without compromising cavitation conditions.

7. Acoustic chain resonance: The natural frequency of the system (f_0) should match the ultrasonic frequency range (fUS) generated by the system to ensure vibration efficiency.

8. Tool-electrode wear reduction: Long-duration pulses (ti) promote the deposition of a protective carbon layer, thereby reducing electrode wear.

3.3 Highlighting Applicable Natural Phenomena

a) Natural Phenomena in (W)EDM+US

The pressure inside gas bubbles formed around the plasma channel limits its cross-section and influences current density (J), improving EDM efficiency. The bubble dynamics follow four phases: high internal pressure, gradual pressure drop, sudden collapse, and sharp pressure rise [7]. These phases correspond to variations in volumetric wear, influenced by pulse polarity. Deposition of a carbon layer on the electrode—characteristic of hydrocarbon-based dielectrics—initially protects the tool, but wear increases over time depending on process parameters. In short-duration finishing modes (10–15 min), even negative volumetric wear was observed. Ultrasonic vibrations affect this process: the oscillation period (TUS) contains two half-periods with distinct cavitation effects on wear (Figs. 3 and 4). In the first half-period (0–25 µs at 20 kHz), compression of the dielectric occurs, with capillary phenomena influencing material transfer.

b) Natural Phenomena in ECM+US

In classic ECM, the working gap variation (dx/dt) is determined by the difference between the tool feed rate (s) and the anodic dissolution rate (vp). This gap is influenced by the type of electrolyte, the workpiece material, and the potential difference (ΔU), which is typically under 24 V for highly conductive electrolytes, resulting in current densities below 1 A/cm² [7]. The ECM deburring process is static, based on Tipton's model (Fig. 5), which assumes constant conductivity along the OX axis, electrodes at the same potential, and application of Ohm's law. ECM assisted by ultrasound (ECM+US) provides a significant advantage by transmitting vibrations into the electrolyte, preventing the formation of passive layers on the workpiece and enhancing material removal efficiency.materialului.

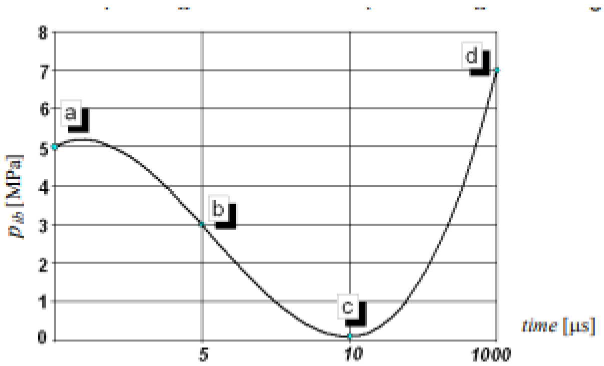

Fig. 3 Variation of pressure inside the gas bubble for a pulse time of 10 µs, EDM finishing [7]

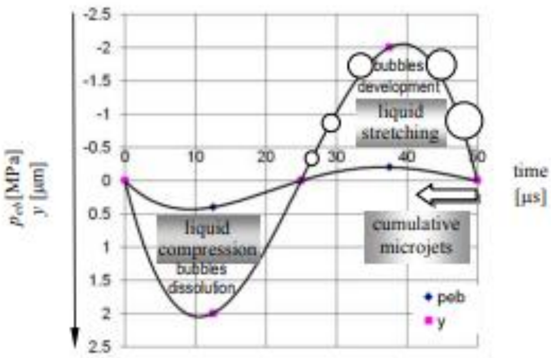

Fig. 4 Ultrasonically induced cavitation phenomena in EDM+US [7]

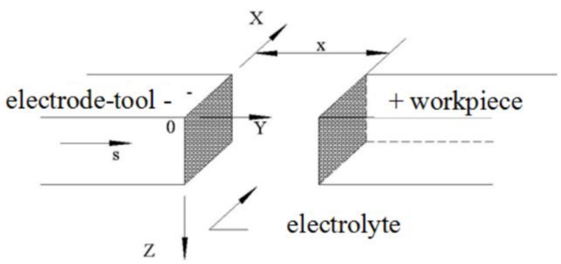

Fig. 5 Tipton's Model [7]

Ultrasonic frequencies can induce cavitation in the electrolyte, surpassing the necessary pressure threshold [8]. Tool vibrations cause a pumping effect due to the incompressibility of the electrolyte: during vertical oscillations of the electrode, the liquid is periodically drawn in and expelled from the machining zone, refreshing the active area and increasing process efficiency.

c) Simultaneous EDM-ECM+US Processing

Besides classic ECM at voltages under 24 V, it is also possible to perform machining at high voltages above 80 V. This allows the use of low-concentration, cost-effective, eco-friendly, and easily prepared electrolytes like NaCl solution. The processing mechanism features a stable vapor and gas envelope on the workpiece surface, separating it from the electrolyte and enabling intense chemical and electrochemical reactions between the workpiece material (anode) and the electrolyte vapors—known as the Wien effect [9]. Faraday's electrolysis laws no longer apply as in classic ECM processes [10].

4. Detailed Design of the EDM+US, ECM+US, and WEDM+US Equipment

Figure 6 shows the preliminary model of the hybrid machining equipment for EDM+US, ECM+US, and WEDM+US processes. On the machine table 1, equipped with T-slots, are mounted the dielectric liquid tank 2 for EDM+US and WEDM+US and the electrolyte tank 3 for ECM+US. The dielectric liquid used has low viscosity, suitable for WEDM. The machining fluids in both tanks are filtered in a continuous cycle: particles are evacuated through tubes 4, filtered through two sieves (Fig. 7-1,2)—one with 0.2 mm holes and the other with 0.02 mm holes. For WEDM, the fluid also passes through a resin frame for water deionization (Fig. 7-3). For finishing and superfinishing operations, a third, finer filtration system (0.002 mm) can be added. The filtered liquid is transferred from the mobile tanks 5 back into the working tanks using pumps 6 through pipes 7. Flow is controlled by valves 8, and fluid pressure is monitored with pressure gauges 9.

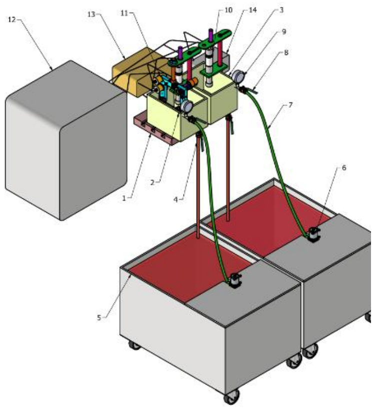

Fig. 6 Hybrid technology equipment assembly (W)EDM-ECM+US

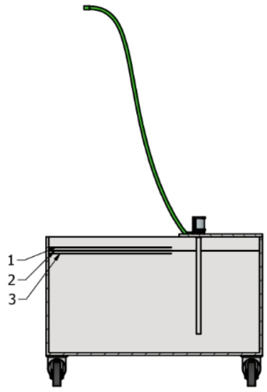

Fig. 7 Mobile tank subassembly

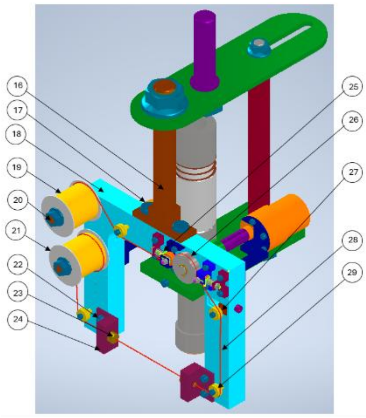

Fig.8 WEDM+US equipment assembly, isometric view

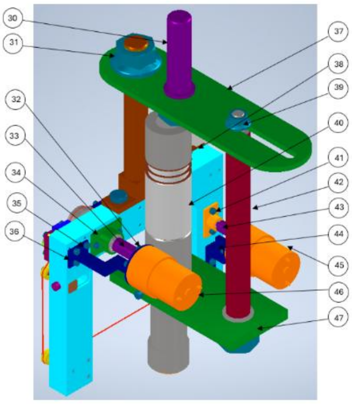

Fig.9 WEDM+US equipment assembly, isometric view

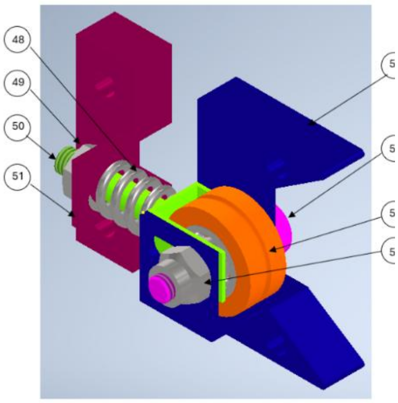

Fig.10 Wire electrode pressing system

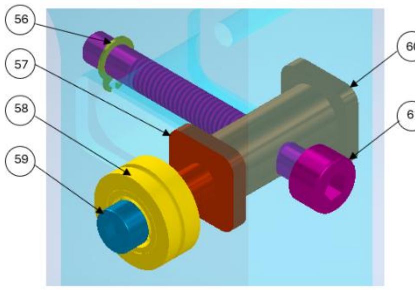

Fig.11 Wire electrode tensioning assembly

Machining in the ultrasonic field is performed via the ultrasonic chain 10, which includes a reflective bushing, piezoceramic plates, nodal flange, radiating bushing, all assembled with a hexagonal screw, and a concentrator that holds the copper electrode at the end. The US chain is mounted on the EDM machine's working head using a rod. The EDM generator 12 provides voltage pulses, producing successive discharges (current pulses), the ECM generator 13 is a DC power supply and the US generator 14 delivers voltage oscillations >1000V at frequencies >20,000 Hz.

Figures 8 and 9 illustrate the WEDM+US cutting equipment with a wire electrode integrated into an ultrasonic chain. The electroerosive and ultrasonic components are mounted on the support plate 37 using columns 42 and 16 and flanged hex nuts M20, part 31. The ultrasonic chain can move along a groove in the support plate and is mounted on the EDM machine's head via the Ø20 column part 30.

Other components of the WEDM system are attached to the main support frame 18. The wire electrode is unspooled from the supply reel 19 and guided into the machining zone by a braking roller 26, driven by a braking motor 46 with a coupling sleeve 33. The wire is pressed onto the brake roller via the pressing system 25.

Tensioning the wire electrode (0.1–0.5 mm in diameter) is done with the tensioning system 27. Its path is defined by deviation rollers 29. Two support bodies 24, mounted at the open end of the frame, allow threading of the guides 23, which have holes for the erosion wire. The guide construction enables flexible selection of wire sizes.

The collection reel 21 retrieves the used wire 28, driven by motor 45 through a direct-drive shaft 43 mounted in the support housing 41.

Fig. 10 shows the pressing system, composed of: a stop block 51, a glide channel support 52 for the roller support with parallel arms 50, the pressing roller 54, a threaded sliding block 53, and a self-locking nut 55. The pressing force from the spring 48 is adjusted using a hex nut 49.

Fig. 11 illustrates a screw-adjusted mechanical wire tensioner composed of: a sliding guide body 60, a mobile block with axle 57 and a tensioning roller 58, all fastened with a locking screw 59. Te nsion force is adjusted by the screw 61, which threads into the guide body and is locked in place by a retaining ring 56 in the support frame 18.

5. Identifying Customer Requirements

To determine the requirements of potential clients for the development of a hybrid industrial electrochemical and electro-discharge machining system—with or without ultrasonic assistance—a dedicated questionnaire was administered to experts from relevant organizations.One of the main aspects analyzed was the experts' willingness to invest in modern, including unconventional, technologies. According to Figure 12, half of the respondents consider such an investment necessary or appropriate, while the other half do not see it as a priority, citing budget constraints or other priorities.Although 57.1% of respondents believe that current equipment is insufficient, only 50% plan to purchase new systems—highlighting a gap between needs and real investment capacity. Furthermore, only 21.4% currently use hybrid unconventional machining technologies (e.g., EDM+US, EDM+ECM) as shown in Figure 13, indicating low adoption.

Fig. 12. Intention to acquire new equipment in the future

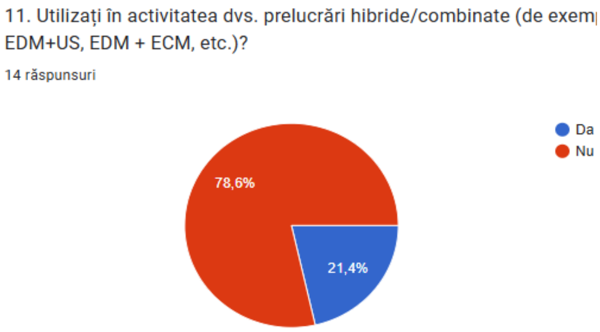

Fig. 13. Use of hybrid machining in current operations

When evaluating the current technical infrastructure for unconventional machining processes, 42.9% of the experts found it to be adequate for their institutional needs, while the remaining 57.1% considered it insufficient. This indicates a clear demand for more advanced or additional equipment. Regarding the acceptable budget for purchasing a hybrid system, most experts—specifically 85.8%—indicated a preference for a price range between 10,000 and 20,000 RON. This defines a realistic and clearly targeted price point for such a system. Overall, the responses reflect a consistently favorable perception toward a modular and adaptable hybrid machining system. Respondents highlighted several key benefits, such as reducing both acquisition and production costs, diversifying the range of producible items, increasing productivity, supporting educational activities, and enhancing research capabilities. The academic and research applications of such a system were emphasized as particularly important, with many respondents seeing strong potential for implementation in universities, innovation centers, and small to medium-sized enterprises. There is a clear and well-justified interest in the development of such a hybrid system, which is perceived as highly useful and versatile across industrial, educational, and scientific domains.

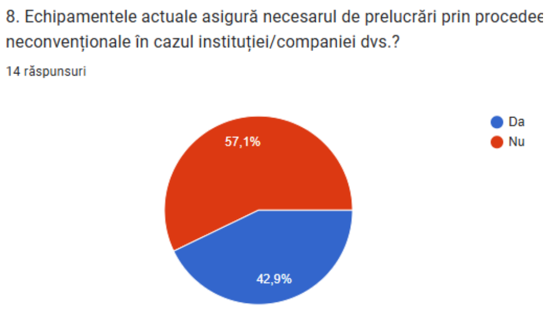

Fig. 14. Ensuring the required machining through unconventional methods

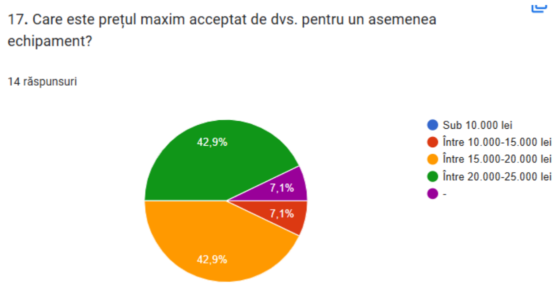

Fig. 15. Price accepted by respondents

6. Commercialization of the Product

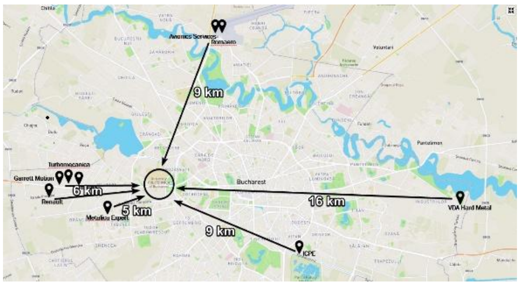

Fig. 16 Map of Bucharest and potential buyers

The placement of the product will be done only on a made-to-order basis, depending on the buyer's needs [11]. The request for a quote will be addressed directly to the manufacturer, and the offer will be made according to the customer's needs. In this way, the buyer has access to three types of electro-discharge machining: EDM, WEDM, and ECM. Potential buyers from the Bucharest area are shown in Figure 16.

7. Intellectual Property Rights Utilization

Fig. 17. Proposed brand

Intellectual property rights, especially industrial property rights, are very important for protecting the designed solution, increasing the value of the company that will commercialize the product, strengthening the brand, and gaining a competitive advantage through exclusivity, licensing, and attracting investment.Among the most important are patenting and trademark registration. The trademark proposed by the development team is presented in Figure 17.

8. Pricing and Break-Even Profit Determination Using Non-Cooperative Game Theory

For determining the final selling price under competitive conditions, Non-Cooperative Game Theory can be applied, which models strategic interactions between firms [12]. This theory assumes rational players who base their decisions on anticipating others' behavior, without the possibility of legally binding contracts between parties, with cooperation emerging only as a strategic equilibrium (Aguirre, 2021). The application of this theory is justified by the oligopolistic market structure targeted, with a small number of firms significantly influencing the market, and the company's optimal strategic response can be determined based on the Cournot–Nash equilibrium [12], a plausible scenario given the company's evolution in the unconventional machining market, particularly for injection molds.To apply this theory, the production cost and price were calculated for a single piece and, respectively, for the simultaneous delivery of 4 pieces, as follows: 1 piece: manufacturing cost 9,700 RON/piece, 15% profit, resulting in price p_1 = 11,155 RON/piece; 4 pieces: production cost 5,207.9 RON/piece, 100% profit, resulting in price p_2 = 10,416 RON. Based on these data, using the coordinates (1; 11,155) and (4; 10,416), with the help of a specific application [13], the inverse demand function was determined as:

$$p(x) = -246{,}33\,x + 11401{,}33 \quad (2)$$

For determining the equilibrium price, the following conditions are considered:

1. Context: a. Market served by n firms; b. Homogeneous products – from the consumers' perspective, goods produced by all firms are perfect substitutes; c. Competition by quantity; d. Simultaneous choice – the n firms must choose their outputs simultaneously, without knowing the choices of competitors.

2. *Normal form of the game:* *i = 1, 2,..., n* (Firms); The output of each firm $x_i \geq 0$, that is $x_i \in [0, \infty)$, *i = 1,2,...,., n;* The profit of firm i (our firm) corresponding to the combination of strategies (x_i, x_{-i}) is:

$$\Pi_i(x_i, x_{-i}) = p(x_i + x_{-i}) \cdot x_i - C_i(x_i) \quad (3)$$

where c is the variable cost.

Given the strategy profile $(x_1, x_2, \ldots, x_n)$ which can also be written (x_i, x_{-i}), we note $\Pi_i(x_i, x_{-i})$ the profit of our company associated with any combination of strategies in which our company produces x_i units and other firms produce together x_{-i}, units, being irrelevant for our firm how x_{-i} is distributed among the other *n–1* firms. In Cournot oligopoly games, it is said [12] that $\left(x_1^*, x_2^*, \ldots, x_n^*\right) \equiv (x_i^*, x_{-i}^*)$ is a Cournot-Nash equilibrium if: $x_i^* = f_i(x_{-i}^*)$, $(\forall)i$, $i = 1, 2, \ldots, n$, where $f(x_{-i}^*)$ is the best response function to all strategies of other firms producing total output x_{-i}. Using relation (2) and the relation:

$$\Pi_i(x_i, x_{-i}) = [a - b \cdot (x_i + x_{-i})] \cdot x_i - (d + c \cdot x_i)$$

(4)

we obtain:

$$\Pi_i(x_i, x_{-i}) =$$
$$[-246,33 (x_i + x_{-i}) + 11401,33]\, x_i - 5207,9\, x_i = -246,33\, x_i^2 - 246,33\, x_i x_{-i} + 6193,43\, x_i$$

(5)

Based on relation (3), the problem is profit maximization, namely:

$$\frac{\partial \Pi_i (x_i, x_{-i})}{\partial x_i} = a - c - 2b\, x_i - b\, x_{-i} = 0$$

(6)

$$\frac{\partial \Pi_i (x_i, x_{-i})}{\partial x_i} = -492,66\, x_i - 246,33\, x_{-i} + 6193,43 = 0$$

(7)

From the Cournot-Nash equilibrium condition, it follows:

$$x_i = f_i(x_{-i}) = \frac{a - c - b x_{-i}}{2b}$$

(8)

$$x_i = f_i(x_{-i}) = \frac{6193,43 - 246,3 x_{-i}}{492,66}$$

(9)

In symmetric equilibrium $x_i^* = \overline{x^*}$ și $x_{-i}^* = (n-1)\overline{x^*}$, $i = 1, 2, \ldots, n$, so the equilibrium condition becomes:

$$\overline{x^*} = f_i((n-1)\overline{x^*}) = \frac{a - c - b(n-1)\overline{x^*}}{2b}$$

(10)

$$\overline{x^*} = f_i(3\overline{x^*}) = \frac{6193,43 - 246,3 \cdot 3 \cdot \overline{x^*}}{492,66}$$

(11)

from which we deduce the symmetric Cournot-Nash equilibrium production of each firm:

$\overline{x^*} = 5,02 \cong 5$ units.

The total equilibrium output for all 4 firms will be:

$x^* = n\overline{x^*} = 4 \cdot 5 = 20$ units

and using relation (2), the ***Cournot*** equilibrium price will be:

$p^* = p(x^*) = -246,33 \cdot 20 + 11401,33 = 6474,73$ lei/piece

The equilibrium profit per piece will be::

$\Pi_i = p^* - c_i = 6474,73 - 5207,9 = 1266,83$ lei/piece

Using relation (4), the total equilibrium profit for firm i (our company) is:

$$\Pi_i(x_i, x_{-i}) = [-246,33 \cdot 20 + 11401] \cdot 5 - 5207,9 \cdot 5 = \mathbf{6334,15\ lei}$$

(sau $\Pi_i(x_i, x_{-i}) = 1266,83 \cdot 5 = 6334,15$ lei)

which corresponds to a profit of 6474,73/5207,9 = 1,24 (24%)

9. Conclusions

The contributions of this paper to the research topic include: the development of a hybrid machining equipment EDM-WEDM-ECM + US, consisting of subsystems with different machining mechanisms. This allowed identification of competing products with corresponding performance, development of conceptual design elements for the hybrid technology equipment (general and secondary functions), and description of natural phenomena applicable to hybrid processes (both successive and simultaneous). A preliminary version of the hybrid technology equipment was designed, which can be implemented on a classic EDM machine. Several potential clients were identified in the automotive, aerospace, mold manufacturing, electronics, and medical fields.

For calculating the manufacturing cost of the hybrid EDM-ECM-US system, based on the activities necessary for producing the three subsystems, the ABC (Activity Based Costing) method was chosen, which relies on determining the cost of each group of activities. For determining the cost of each subsystem, the direct cost method was used, which is based on identifying cost components (materials, labor, overheads, depreciation, etc.).

To set the final selling price under competitive conditions, Non-Cooperative Game Theory was applied, according to which, under oligopoly conditions, a selling price of 6,474.73 RON per unit was established, at a manufacturing cost of 5,207.9 RON per unit, with a profit of 1,266.83 RON per unit, corresponding to a 24% profit.

10. Bibliografie

[1]. Abu Zeid, O.A. (1997). On the effect of electro-discharge machining parameters on the fatigue life of AISI D6 tool steel. J. Mater. Process. Technol., vol. 68, p. 27-32

[2]. Merdan, M.A.E.R., Arnell, R.D. (1991). The surface integrity of a die steel after electro-discharge machining, 2. residual stress distribution. Surf. Eng., vol. 7, p. 154-158

[3]. Balan, A.S.S.; Giridharan, A. ”A progress review in wire electrical discharge machining process.” Int. J. Autom. Mech. Eng. 2017, 14, 4097–4124

[4] *** Sodick pag available at , https://sodick.eu/products/wire-edm/alc600gh accessed at: 04.05.2025

[5] *** Holmarc Available at https://www.holmarc.com/electrochemical_discharge_machining_system.php, accessed at: 04.05.2025

[6]. Ghiculescu, D. (2021), ”Computer-assisted engineering and manufacturing in the field of unconventional machining.”, Course in Romanian, Production Engineering Dept., University Politehnica Bucharest, Romania.

[7]. Ghiculescu, D. (2016), “Contributions to Development and Innovation of Ultrasonically Aided Nonconventional Machining”, Habilitation Thesis, Production Engineering Dept., University Politehnica from Bucharest, Romania.

[8]. Shen, Z. Y., Tsui, H. P., (2021), “An Investigation of Ultrasonic-Assisted Electrochemical Machining of Micro-Hole Array”, Dep. of Mechanical Engineering, National Central University, Taoyuan 32001, Taiwan.

[9]. Ghiculescu, D. (2021), „Advanced Electrochemical Discharge Machinning Methods”, Course in Romanian, Production Engineering Dept., University Politehnica from Bucharest, Romania.

[10]. Elman C. Jameson. (2001). ”Electrical Discharge Machining”. Edo Society of Manufacturing Engineers Dearborn, Michigan

[11] *** ONA for aeronautics & turbine industries, Available at ONA EDM: EDM Machines for aeronautics and turbine sector, accessed at: 10.05.2024

[12]. *** Aguirre Iñaki, Notes on Market Power and Strategy, Department of Economic Analysis, University of the Basque Country, 2020 – 2021, Available at https://www.ehu.eus/iaguirre/, accessed 05.09.2024

[13] *** Desmos. Scientific calculator*** https://www.desmos.com/calculator/md6buy4efz, accesat Februarie 2025

DEVELOPMENT OF PRODUCT SPECIFICATION FOR AN INNOVATIVE ORTHOSIS

DINU Ana-Maria, FLORESCU Mircea-Alexandru, NĂSTASE Andreea Cristina, ROȘCULEȚ, Elena-Teodora, SAFTA Roxana-Elena, Andrei DUMITRESCU(Conducător științific)

ABSTRACT: This paper presents the design and development of a customized foot orthosis with integrated vibration and heating. It begins by outlining the project's objectives and context. The strategic marketing section explores market opportunities, defines the product mission, and analyzes data from potential users and competitors. Specifications are established through requirement matrices and competitive analysis. The conceptual design aligns product functions with user needs. Detailed design defines the product's geometry, and materials.

KEYWORDS: orthosis, vibrations, heat, development, customization.

1. Introduction

The aim of the project is to develop an innovative foot orthosis, using 3D printing technology and equipped with a vibration and heating system, which will improve patient recovery, reduce pain and optimize blood circulation, thus providing a modern and effective solution for rehabilitation. The main objective is to investigate, design and implement this orthosis to improve patient mobility. The justification of the need for this project is based on the current necessity for innovative and effective solutions in mobility recovery for people affected by musculoskeletal disorders. The integration of vibrations and heat into the proposed orthosis can bring significant benefits in accelerating the healing process and improving the life quality of patients.

2. Strategic Product Marketing

The targeted market segments include patients in post-operative or traumatic recovery, people with chronic conditions, elderly people with circulatory problems, people with reduced mobility and athletes looking for effective solutions for recovery, pain reduction and prevention of injuries.

The main need chosen for product development is **Relief of Chronic Pain**. This aspect is essential for a large segment of patients and offers a solid market opportunity, thus justifying development of the innovative orthosis with vibration and heating system.

2.1. Current state of the project theme

Similar products are:

- There are orthoses on the market with basic functions, such as mechanical foot support, but very few integrate both vibrations and heating systems.
- Examples of existing solutions include carbon fiber heated orthotics, vibration orthotics without advanced digital control, and custom 3D printing devices, which are in the early stages of adoption.

The phenomenon underlying the operation of the product:

- Mechanical vibrations are widely used in medical recovery due to their beneficial effects on the muscular and joint system.
- Applying heat locally is a technique recognized for its beneficial effects in relieving pain and improving mobility.

2.2. Data collected from potential customers

In order to develop a product adapted to real needs, a questionnaire was applied to potential users of the 3D orthosis with vibration and heat, targeting orthopedic patients, athletes, the elderly and people with circulatory problems. The questionnaire was distributed online and offline, and the final sample included 50 participants, selected so that it best reflects the diversity of potential users.

Table 1. Main Product Requirements

Requirement	Importance	Motivation
Warm-up for muscle relaxation	Crucial (5)	50% of users consider it essential.
Vibrations to stimulate circulation	Required (4)	54% have circulatory problems.
Minimum autonomy of 4 hours	Required (4)	55% prefer a battery life of more than 4 hours.
Shoe compatibility	Required (4)	60% consider this aspect very important.
Comfort and customizable fit	Crucial (5)	68% have chronic pain, so comfort is essential.
Price between 200-500 RON	Desired (3)	40% are willing to pay this amount.

2.3. Competitor Product Data

Competitor product data is presented in Table 2.

Table 2. Competing Products

Product name	Image	Price (lei)	Commercial success (1... 9)	Functional features	Market Segment
Push Sports 8 Orthosis		150	5	- support - stability - lightweight material - comfort	Daily use
Walker Rom Orthosis		442	8	- support - stability - adjustable size - adaptability - durability	Medical rehabilitation
Orthosis Triamed		70	6	- lightweight material - comfort - support - adaptability	Daily use
Turbomed orthosis		1660	8	- support - stability - durability - posture correction	Medical rehabilitation
Orthosis Drop Foot		300	5	- support - stability - comfort - lightweight material	Daily use

Product name	Image	Price (lei)	Commercial success (1... 9)	Functional features	Market Segment
Orthosis MzcrJosv		60	6	- lightweight material - comfort - support - adaptability	Daily use
Orthosis Donjoy Actylight		250	7	- lightweight material - comfort - support - adaptability	Daily use

Table 3. Technical specifications of competing products

Features	Unit of measure-ment	Push Sports 8 Orthosis	Walker Rom Orthosis	Orthosis Triamed	Turbomed orthosis	Orthosis Drop Foot	Orthosis MzcrJosv	Orthosis Donjoy Actylight
Weight	g	200	1050	280	400	220	180	300
Dimensions (length/circum-ference)	cm	22.5 / 23	31.5 / 24	25 / 21	32 / 22	22 / 23	24 / 26	25 / 30
Rigidity	N/m	500	1400	600	1700	400	350	800
Durability	(1… 5)	2	4	2	5	2	2	3

3. Setting specifications

3.1. Requirements Matrix – Quality Characteristics

To ensure that the foot orthosis meets the requirements of users, the process of defining measurable technical specifications was based on the transformation of primary requirements into quality characteristics. These features allow for accurate product evaluation and the creation of an effective differentiation strategy from the competition.

The table 4 details the degree to which user requirements are translated into measurable characteristics. The score (from 1 to 5) indicates the relevance of each characteristic in meeting the respective requirement.

Table 4. Correlation of requirements with quality characteristics

User requirements	Importance	Weight (g)	Vibration (Hz)	Heating (°C)	3D flexible material	Degree of customization
C1: Comfort in use	5	3	2	4	4	5
C2: Muscle relaxation/recovery	4	1	5	5	2	2
C3: Light weight/portability	3	5	2	1	3	2
C4: Anatomical customization	4	2	1	1	4	5

The most important quality characteristics to be optimized are:

- The degree of customization and the material used, as they have a strong correlation with the priority requirements regarding comfort and anatomical adaptation;
- Heating and vibration parameters, for therapeutic efficiency;
- Weight, to maintain portability and comfort during use.

These results inform subsequent technical decisions regarding the design of the prototype and the choice of hardware and material components.

3.2. Objective and limit values – Acceptable for quality characteristics

For each characteristic, objective values (ideal) and limit values (realistic, but satisfactory) have been defined.

Table 5. Target - limit values

Feature	Objective value (ideal)	Limit value (realistic)	Feature Type (STB/GTN/NTM)
Total Weight	≤ 0.8 kg	≤ 0.9 kg	Smaller the better (STB)
Lifespan	5 years	4 years	Greater than necessary (GTN)
Warm-up time	≤ 30 seconds	≤ 60 seconds	Smaller the better (STB)
Controllable temperature range	30–45°C	30–50°C	Neither too much nor too little (NTM)
Vibration engine noise level	≤ 15 dB	≤ 20 dB	Smaller the better (STB)
Degree of 3D customization	100% adjustable	100% adjustable	Neither too much nor too little (NTM)
Total Production Cost	≤ 500 RON	≤ 600 RON	Greater than necessary (GTN)

Identifying Product Value in Use (VUP) dimensions:

- Therapeutic effectiveness: The product must support recovery, stimulating circulation and reducing muscle pain.
- Comfort and customization: Adjustability and quality materials are essential for comfort in the long term.
- Affordability: The price should be affordable, without compromising quality, to attract a range wide range of consumers.
- Durability and reliability: The durability and reliability of the product will increase trust and value perceived by users.

4. Conceptual design

4.1. General function and component functions

General function of the product: Providing support, rehabilitation and comfort to the user by correcting the position of the foot, stimulating blood circulation, reducing pain and promoting relaxation, through vibration and heating.

Component functions:

Main functions:

- Biomechanical support: Providing stability to the foot by correcting position and reducing pressure on the joints.

- Circulatory stimulation: Improving blood circulation in the leg through controlled vibrations.
- Thermotherapy: Generating heat to relax the muscles and relieve pain.

Secondary functions:

- Customization: Adjust the vibration intensity and temperature according to the user's preferences.
- Electronic control: Manage settings through a control panel.
- Safety: Prevention of overheating through integrated temperature sensors.

Support functions:

- Comfort: Use of ergonomic and anti-allergic materials.
- Ease of use: Integration of an adjustable clamping system and intuitive design.
- Portability: Light weight and energy autonomy if needed.

Critical problems that may occur are possible areas of the foot that do not receive adequate stimulation, the risk of insufficient or uneven heating, constant vibrations can affect the longevity of the mechanism, avoiding burns or discomfort caused by overheating, in the case of a portable product, the duration of use may be limited.

The natural phenomena applicable to the foot orthosis frame the thermoregulation of animals, mammals using fur or fat to retain heat, similar to the insulating materials in the orthosis; blood flow in mammals, the efficient circulation of blood through rhythmic contractions, inspiring the design of vibrations used in orthotics to stimulate microcirculation; heat conservation in birds, which use feathers to reduce heat loss, for the orthosis using thermal insulating materials that imitate this process; and the thermal conductivity of the soil that maintains constant temperatures through heat transfer, the orthosis being designed to distribute heat evenly over the entire surface of the foot.

Table 6. Natural phenomena associated with critical functions

Critical function	Associated natural phenomenon
Biomechanical support	Adaptation of natural shapes to pressure: e.g. animal foot pads for weight distribution.
Stimulation of blood circulation	Vibrations produced by insects (e.g. bees) to generate rhythmic movements that stimulate flows.
Heat generation and maintenance	Thermoregulation of mammals by fur or fat to preserve heat.
Uniform vibration distribution	The natural vibrations of insect wings to cover a large area evenly.
Keeping the temperature constant	Heat preservation in birds through the structure of the plumage that effectively insulates.

4.2. In-house research for new construction solutions

Analysis and identification of specific needs

For the development of a vibration and heating foot orthosis, it is crucial to understand the needs of the users. Users' needs:

- Relief of muscle and joint pain;
- Stimulation of peripheral circulation;
- Ergonomic comfort for long-term use;
- Easing the post-trauma recovery process;
- Improved mobility and flexibility of the joints.

These requirements are essential to ensure the efficiency and functionality of the product in everyday life.

Proposed innovations

In order to meet the identified requirements, the following innovations are proposed:

- Integration of smart technology: The devices will include sensors that monitor muscle activity and adjust vibrations and temperature based on the user's movements.
- Advanced materials: The use of heat-resistant and ergonomic materials that provide comfort and durability.
- Control via mobile app: Allows customization of settings directly from the phone, providing a user-friendly interface.
- Safety devices: Self-protection functions against overheating and other risks related to long-term use.

Development of constructive solutions

In order to implement the proposed innovations, a prototype will be built that will combine the following components:

- Vibration modules used for muscle stimulation and circulation
- Electronically controlled heating elements that provide localized thermotherapy
- Sensor systems that monitor pressure, temperature and movements for automatic adjustment
- Ergonomic case made of hypoallergenic and wear-resistant materials.

Individual/Group Generated Concepts

Some concepts include:

- Concept A: Orthosis with sensors that automatically adjust vibrations and temperature according to the user's activity.
- Concept B: Smart orthosis that can be controlled by voice or app for precise customization of settings.
- Concept C: Orthosis with active fabric that improves mobility and keeps heat evenly distributed.
- Concept D: TPU orthosis with Voronoi architecture, controlled heating and localized vibrations.

The concepts are presented in Figures 1-4. Concept 1 is rounded and durable (a traditional structure). Concept 2 is functional and simple (mesh triangular) – the design retains clear lines without too much detail with a smooth surface. Concept 3 is slim and elegant (model lattice) – the shape is slim with slightly arched straight lines that provide a modern look but no intricate details. Concept 4 is resistant and airy (Voronoi architecture) - it ensures a balanced weight distribution, avoiding areas of excessive pressure on the joints.

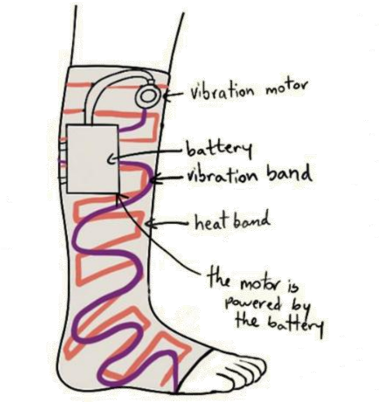

Fig. 1. Concept 1 uses the traditional medical orthosis model

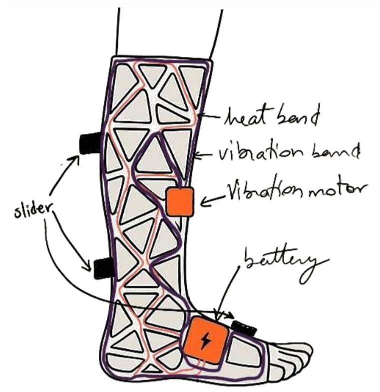

Fig. 2. Concept 2 uses the Triangular Mesh pattern

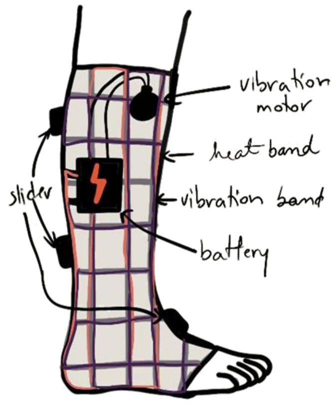

Fig. 3. Concept 3 uses the Lattice model

Fig. 4. Concept 4 uses the Voronoi architecture

Table 7. Pro/Cons argumentation on architectures

Architecture	Pro	Against
Traditional	Uniform weight and pressure distribution	Complexity requires advanced techniques
	Durability and adjustable stand	Requires precise methods for manufacturing
	High stress resistance	Reduced flexibility
Mesh Triangular	Easy to shape and manufacture	Insufficient rigidity in some cases
	Lightweight	Loss of resistance in some areas
	Decent flexibility	Requires precise geometry for efficiency
Lattice	Light weight and flexibility	Variable durability
	Easy to customize	Requires perfect geometry for efficiency
	Open structure allows ventilation	Possible loss of strength in some cases
Voronoi	Optimal weight distribution	Possible complexity in manufacturing
	Unique and aesthetic design	Requires precision to avoid deformation
	High resistance depending on the configuration	Possible limitation of applicability in some cases

4.3. Systematic exploration

Generation of partial conceptual solutions for critical functions

The critical functions identified are biomechanical support, circulatory stimulation and thermotherapy for relaxation and recovery.

Partial conceptual solutions include separate vibration and heating modules, in which each part is integrated into a modular system that can be individually adjusted; design combined with TPU with Voronoi architecture, which provides the optimal combination of flexibility, distributed pressure and localized thermotherapy; multi-parameter electronic control, through intelligent settings for adjusting vibration and heat according to the user's needs.

Generation of integral concepts for critical functions

The integral concepts formulated for the critical functions of the orthosis are: smart orthosis, i.e. a combination of electronic technology, TPU materials and Voronoi architecture that provides biomechanical support and adaptive thermotherapy; hybrid vibration and heating system, integrated into a single device, which offers precise adjustments through mobile application and feedback sensors and customizable architecture with thermotherapy and vibrations, the optimal combination of TPU material flexibility and thermal efficiency, having localized vibrations for recovery.

Establishment of selection criteria

Selection criteria will be established to assess which concepts best perform the critical functions between functionality and adaptability, user comfort, thermal and vibration safety, thermal performance, vibration efficiency and durability of the TPU material.

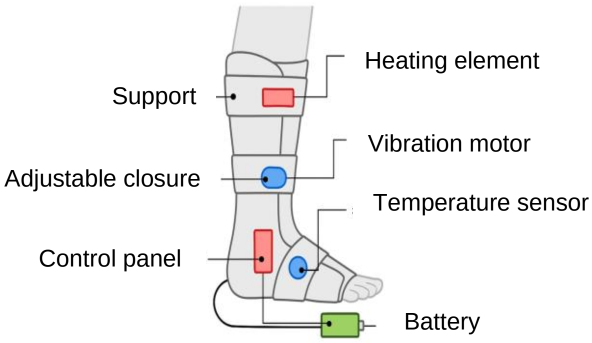

Fig. 5. General structure of the orthosis

Detailed design

5.1. Proportionality, shapes, dimensions and tolerances

- Shapes: The orthosis has an ergonomically shape adapted to the contours of the foot.
- Dimensions: Length: 25-30 cm, width: 10-15 cm, height: 2-4 cm (tibia), 5 mm-1 cm (sole).
- Tolerances: Vibration mounting: ±0.2 mm, temperature: ±1°C, fixing: ±0.5 mm.

5.2. Ergonomic conditions

- Safety: Sensors to prevent overheating and heat-resistant materials; rounded edges to prevent injury.
- Anthropometry: Adjustable orthosis for different foot sizes.
- Physical limits: Weight: 300-500 g, thickness: 2-4 cm.

5.3. Aesthetic Design

Desired visual attributes:

- Sustainability: Durable and flexible materials, ergonomic shape.
- Clear functionality: Visually suggested functions without loading the product.
- Ergonomics: Shape inspired by biomimetic models.
- Modernity: Minimalist style with neutral colors and subtle accents.

Visual attributes to be avoided:

- Brutality: Solid appearance, but not painful.
- Complexity: Avoidance of over-design.
- Bulkiness: Harmonious dimensions for ease of portability.

5. Conclusions

The study on strategic marketing and specifications for the vibration and heat foot orthosis highlights the need for a well-founded approach in the development and commercialization of this innovative product. Detailed analysis of the market and user needs guided the creation of an effective and competitive orthosis, integrating vibrations for the significant benefits brought to users. The application of strategic marketing concepts and market research facilitates the adaptation of the product to consumer requirements, strengthening the position and ensuring success in a competitive environment. The conceptual design gives a clear idea of the characteristics that the orthosis must meet in order to achieve its purpose, the detailed design included defining the shape, dimensions, materials and treatments, making the necessary calculations and drawing up the technical drawings, subsequently addressing the homologation, use, marketing and recycling of the product.

References

Cummings, S. R., & Melton, L. J., 2002, *Epidemiology and outcomes of osteoporotic fractures*, The Lancet, vol. 359, nr. 9319, pp. 1761–1767. [Online].At: Epidemiology and outcomes of osteoporotic fractures - The Lancet [Accessed on 12 February 2025].

Eurostat, 2024, *Healthcare resource statistics – hospital discharges and length of stay*. [Online]. At: Home - Eurostat [Accessed on 7 April 2025].
Institutul Național de Statistică, 2023, *Anuarul Statistic al României*. [Online]. At: Bun venit la Institutul Naţional de Statistică | Institutul Naţional de Statistică [Accessed on 20 January 2025].
International Osteoporosis Foundation, 2021, Osteoporosis in Europe: A compendium of country-specific reports. [Online]. At: International Osteoporosis Foundation | IOF [Accessed on 5 March 2025].
Kanis, J. A. et al., 2019, SCOPE 2021: "A new scorecard for osteoporosis in Europe", *Archives of Osteoporosis*, vol. 14, art. 58. [Online]. At: SCOPE 2021: a new scorecard for osteoporosis in Europe - PubMed 6 [Accessed on 15 February 2025].
Popescu, M., Ionescu, A., & Radu, F., 2020, "Fracture management and rehabilitation practices in Romania: A national review", *Romanian Journal of Orthopaedic Surgery*, vol. 34, nr. 2. [Online]. At: Systematic review of clinical practice guidelines for adults with fractures: identification of best evidence for rehabilitation to develop the WHO's Package of Interventions for Rehabilitation | Journal of Orthopaedics and Traumatology | Full Text[Accessed on 9 March 2025].
The Burden of Musculoskeletal Diseases in the United States, 2023, Orthopedic injury incidence and economic burden.]. Beste Online Casino Zonder CRUKS 2025 [Accessed on 28 April 2025].
https://aulive.com/ [Accessed on 28 April 2025].

MICROWAVE PASTEURIZATION INSTALLATION

ENE Elena[1], PALOȘI Andrei-Florin[2], UNGUROIU Maria-Miruna[1] ,GHICULESCU Liviu-Daniel[3]
(Conducător științific)

Faculty of Industrial Engineering and Robotics, Study program: [1]INPN, [2]IPFP, Year of study: I, e-mail: ene_elena123@yahoo.com
[3]Faculty of Industrial Engineering and Robotics, Manufacturing Engineering Department, University POLITEHNICA of Bucharest

ABSTRACT: The paper deals with the numerical simulation by the finite element method of the microwave pasteurization process. Information is presented on the state of the pasteurization process and the facilities dedicated to it. The results obtained from the numerical simulation are consistent with the experimental results, based on this fact, but also duet o the needs of the customers, a microwave pasteurization installation was 3D modeled in the work. The microwave pasteurization process is very effective in removing pathogenic components from food in a short time.

KEYWORDS: installion, microwave, pasteurization, numerical simulation, customers.

1. Introduction

Pasteurization is the process by which the growth of microorganisms in food is slowed down.The process is named its creator, the chemist and microbiologist Louis Pasteur.The first pasteurization test was performed by Louis Pasteur and Claude Bernard on April 20, 1862.The process was originally conceived as a way to prevent the acidification of wine and bear.[1]

Microwaves are thought to inactivate enzymes and kill microbes mostly through conventional thermal mechanisms.[2] For long-term preservation, the products are subjected to the thermal process in a pressurized chamber.[3] The thermal treatments to which the products are subjected are: thermalization, low pasteurization of milk LTLT, high pasteurization of milk HTST, ultrapasteurization, sterilization, sterilization in containers.[4]

2. Strategic Marketing

The segmentation of the product market is based on the specific requirements regarding the quality and structure of the offer, the affirmation and manifestation of the demand from buyers, the frequency, and the average size of the purchase, etc. In any type of enterprise, the role of marketing is to contribute to a better understanding of its audience in order to adapt to the external environment and achieve maximum efficiency. [5]

2.1. Identifying Market Opportunities

a. *Portfolio of Customer Needs*

Three primary needs are identified, numbered N1, N2, and N3:

- N1: The need to ensure food safety.
- N2: The need to extend the shelf life of food products.
- N3: The need to reduce processing time and costs.

b. *Opportunities / Products*

"Today's competition is more than ever based on product development capabilities." [5]

The products that fully or partially satisfy these needs are represented by microwave pasteurization installations (MPI). These are specialized products designed to provide efficient and rapid pasteurization of food using microwave technology.

Market opportunities for the developed microwave pasteurization installation are represented by the increasing demand for safe and healthy food products.

c. *Customers for Product Distribution*

Selecting customers involves identifying actual and potential customers who could benefit from the microwave pasteurization installation.

The equipment is aimed at the following types of customers:

1. Food industry enterprises, especially SMEs that process and produce various types of food.
2. Research and educational institutions:
   - ➢ Students – occasional use
   - ➢ Professors – occasional use
   - ➢ Laboratories – relatively frequent use

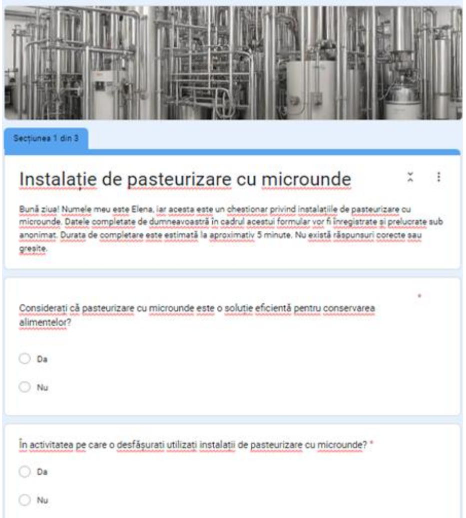

Fig. 2. Online Questionnaire [6]

2.2.Formulating the Mission for the Selected Product Development

- Customer Selection Matrix

The customer selection matrix is presented in Table 1.

Table 1. Customer Selection Matrix

	Top Users	Average Users	Occasional Users	Centers
Category 1	7	2	2	1
Category 2	1	6	2	
Category 3	2	2	5	

The guide for conducting interviews to identify customer needs for the microwave pasteurization installation is presented in Table 2.

Table 2. Guide for Conducting the Interview to Identify Customer Needs for the IPM Product

<table>
<tr><td>Client:
Address:
Phone:
Would you like to collaborate? Yes No</td><td colspan="2">Interviewers:
Date:
Current Uses:
User's Occupation:</td></tr>
<tr><td>Question</td><td>Client's Statement</td><td>Interpreted Need</td></tr>
<tr><td>1. Do you consider microwave pasteurization an effective solution for food preservation?</td><td>a) Yes
b) No</td><td></td></tr>
<tr><td>2. In your current activity, do you use microwave pasteurization installations?</td><td>a) Yes
b) No</td><td></td></tr>
<tr><td>3. How often do you use the microwave pasteurization installation in a week?</td><td>a) Daily
b) Several times a week
c) Occasionally
d) Rarely</td><td></td></tr>
<tr><td>4. What are the main reasons you use the microwave pasteurization installation? (multiple answers possible)</td><td>a) Speed of the process
b) Nutrient preservation in food
c) Food freshness maintenance
d) Reduced contamination risk
e) Others</td><td></td></tr>
<tr><td>5. Are you satisfied with the performance of the microwave pasteurization installation?</td><td>a) Completely satisfied
b) Mostly satisfied
c) Not very satisfied
d) Not satisfied</td><td></td></tr>
</table>

6. Do you believe a microwave pasteurization installation can help maintain hygiene standards in food processing?	Da, într-o mare măsură 1 ○ 2 ○ 3 ○ 4 ○ 5 ○ Nu, deloc	
7. What are the main criteria you consider when choosing a microwave pasteurization installation? (multiple answers possible)	a) Process efficiency b) Installation capacity and size c) Food safety d) Product reliability and durability e) Installation cost f) Others	
8. Are you willing to pay a higher price for a microwave pasteurization installation that offers advanced features or superior performance?	a) Yes b) No	
9. Do you think a microwave pasteurization installation can help reduce the microbiological contamination risk of food and extend its shelf life?	a) Yes b) No	

3. Setting specifications

The main characteristics of a microwave pasteurization installation (MPI) are its power, its operating frequency and the volume of the enclosure. The optimal operation of the plant directly depends on the proper correlation of these technical parameters.

3.1. Technical characteristics of a microwave installation

The useful power of a pasteurization installation indicates the efficiency of the process: a higher value means faster pasteurization, being directly proportional to the volume of the enclosure. The maximum power consumed reflects the electricity consumption required for operation. The operating frequency influences the uniformity of heating; unsuitable frequencies can cause uneven heating, damage to the equipment or interference with other devices. For safety, the plants are equipped with protections such as resonant cavity shielding and magnetron locking systems when the door is opened, preventing exposure to microwaves. A larger enclosure volume allows for a more uniform distribution of microwaves, improving pasteurization results.

3.2. Matrices used to determine technical characteristics

In order to identify the optimal parameters of the installations operation, several products already on the market were compared. The matrix of competing products is presented in table 3.1.

Table 3.1. Competing products matrix

Size/feature	Unity	Products					
		Myria MM720 [7]	MGB 25332 [8]	SMW 6021 [9]	MOC201 [10]	LHMS [11]	MLHS [12]
Oven power	W	700	900	800	700	2000-15000	75000-200000
Rated power	W	1050	1450	1200	1100	3000-20000	90000-240000
Dimensions (L x h x l)	mm	44x33x25,8	40x38,8x59	45x38x26	24x47x34	83x30x97	84x61x249
Mass	kg	10,7	18,5	12	9,4	-	-
Operating frequency	MHz	2450	2450	2450	2450	2450	915
Volume	L	20	25	20	20	-	-
Type	Integrable / freestanding	freestanding	integrable	freestanding	freestanding	freestanding	freestanding

Control type	Mechanical / digital	mechanical	mechanical	digital	digital	digital	digital
Use	Household / industrial	household	household	household	household	industrial	industrial

Subsequently, the requirements matrix was created in order to determine the objective characteristics.

The matrix of required quantities is presented in Table 3.2 below. Analyzing table 3.2, the target parameters of the pasteurization installation are established, presented in table 3.3.

Table 3.2 Requirements size matrix

Requirement		Importance of the requirement	Size/feature												
			Oven power	Noise level	Rated power	Dimensions (L x h x l)	Mass	Operating frequency	Volume	Type	Control type	Material	Energy efficiency	Reliability	Ease of maintenance
			1	2	3	4	5	6	7	9	10	11	12	13	14
1	MPI[1] can be used on an industrial scale	4	●		●				●						
2	MPI does not overheat	5	●		●			●				●	●	●	
3	MPI has a large volume	3				●			●						
4	MPI does not consume energy	4			●								●		
5	MPI presents safety	5			●			●			●			●	
6	MPI is stable in operation	3	●		●			●							
7	MPI resists mechanical action	3				●	●					●		●	●
8	MPI it is not noisy	2		●											
9	MPI poses minimal danger pentru	5	●		●			●							
10	MPI heats food evenly	5	●					●							
11	MPI can be transported	2				●	●			●					●
12	MPI is made of durable material	4					●					●		●	●
13	MPI it is easy to clean	3							●			●			●

Table 3.3 Objective specifications

NNo.	*The size*	Feature type	Relative importance	*Unity*	*Limit values*	*Target values*
1	Enclosure volume	GTB	5	L	>20	25
2	Type of processed food		5	Liquid/solid	Liquid+solid	Liquid+solid
3	Installation power	GTB	5	W	>700	800
4	Pasteurization quality	GTB	5	-	Upper	Upper
5	Ensures operator safety		4	Yes/No	Yes	Yes
6	Overall dimensions	GTB	4	mmxmmxmm		
7	Special tools for maintenance		3	Yes/No	No	No

[1] MPI – Microwave Pasteurization Installation

8	Power consumed	STB	5	W	<2000	1200
9	Total weight	STB	4	kg	<20	10
10	Operating noise level	STB	3	dB	<70	60
11	Maintenance manual		4	Yes/No	Yes	Yes
12	Cleaning time	STB	4	min	<20	10

*GTB = Greater The Best
*STB = Smaller The Best

4. Conceptual design

The general function of a microwave pasteurization installation (MPI) is to heat food/liquids to a temperature where they no longer present a danger to human health due to the elimination or inactivation of microorganisms, bacteria and viruses from the chemical composition through the process of pasteurization.

In table 4.1. general function, component function, main functions and critical functions of MPI are presented.

Table 4.1. MPI functions

No.crt	The function type	Function description
1	General function	Inactivation of microorganisms in the composition of food products by microwave pasteurization.
2	Component function	Recovery of energy accumulated from microwaves during pasteurization to be used to preheat the next liquid to be pasteurized.
3	Main function	a. Introduction of the food/liquid for pasteurization b. Introduction of microwaves for pasteurization c. Carrying out the pasteurization process of the products d. Collection of pasteurized food/liquids
4	Critical function	The introduction of microwaves for pasteurization, the heating time and the temperature from which the process starts; Realization of the food/liquid pasteurization process

4.1. External research to identify new constructive solutions

In order to be able to identify new constructive solutions, we have analyzed several invention patents on this topic.The main patents we have studied are the following:

- *Process and installation for thermal processing of milk– Patent No. RO 125073 B1*[3]
- *Method and apparatus for microwave processing of planar materials – Patent No. US 6546646 B1*[13]
- *Post package pasteurization for meat products – Patent No. US 2007/0065551 A1*[14]
- *Microwave sterilization or pasteurization transport carriers – Patent No. US 10681923 B2*[15]
- *Microwave-assisted sterilization and pasteurization system using synergistic packaging, carrier and laucher configurations – Patent No. US 10966293 B2*[16]
- *Installation for thermal processing of sour cream and production process – Patent No. RO 125652 A2*[17]
- *Mobile installation for obtaining juice from fruits and vegetables – Patent No. RO 2015 00039 U1*[18]
- *Pasteurization installation – Patent No. RO 113800 B1*[19]
- *Egg pasteurization process – Patent No. RO 90641 B*[20]
- *Soft drink – Patent No. RO 132904 A0*[21]
- *Process and plant for the manufacture of probiotic, fortified dairy products – Patent No. RO 131605 A2*[22]

4.2. Constructive solutions

The constructive solutions that have been identified are presented in table 4.2.

Table 4.2. Constructive solutions

No. crt.	The constructive solution	Execution
1	Modular and flexible design	Use of standardized modules
2	Precise control of temperature and processing time	Using temperature sensors and an advanced control algorithm
3	Automation and digital control	Implementation of automation and digital control systems
4	Easy cleaning and maintenance	Use of corrosion-resistant materials and ease of access to components for maintenance and repair

4.3. Block diagram of the microwave pasteurization installation

The block diagram of the microwave pasteurization installation is represented in figure 2.

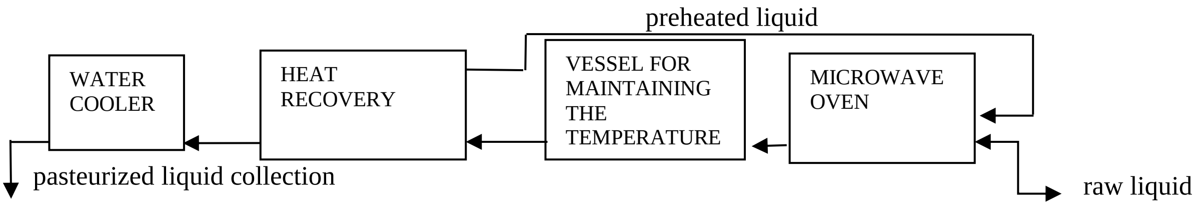

Fig.2 MPI Block diagram

4.4. Modeling-simulation of the microwave pasteurization installation

In order for this MPI to be physically realized, a simple modeling and simulation (finite element method) was carried out in the Comsol Multiphyisics 5.5. program. From this modeling-simulation it emerged that the MPI can be physically realized as it will meet the required conditions.
The numerical simulation of the microwave pasteurization process was carried out for the food liquid – milk. The steps of the numerical simulation were as follows:

1. Choosing the calculation module– Microwave Heating Frequency-Transient;
2. Parameterization of the model presented in figure 3;

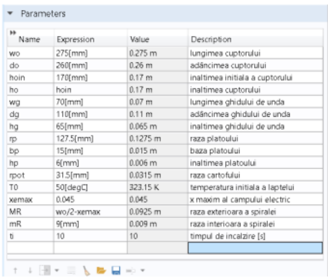

Fig.3 Parameterization of the model [23]

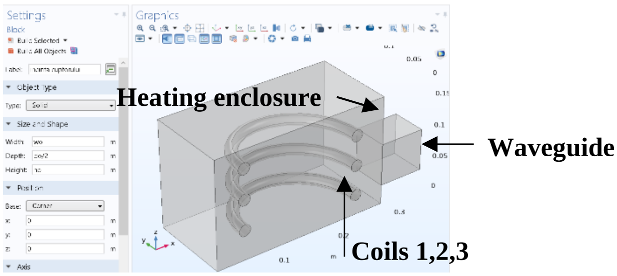

Fig.4 Creating geometry [23]

3. Geometry of the model – the microwave heating enclosure will be made. It is composed of the following elements: the heating enclosure, the waveguide and the 3 coils, shown in figure 4.
4. Allocation of materials for the furnace, waveguide and coils 1,2,3 as follows: air for the interior of the furnace and the waveguide, milk for the walls of the furnace and silicon for the walls of the coils.These materials have properties specific to the chosen calculation model.
5. Boundary conditions – these refer to the initial milk temperature T0=50[°C], the condition of electromagnetic wave propagation without the usual heat transfer inside the oven, the wave emission port, the impedance condition, the conductor condition perfectly magnetic. Some of these conditions are represented in figures 5,6,7,8 și 9.
6. Discretization of the model – for discretization, free tetrahedral elements with fine discretization are used inside the heated material, figure 10.

7. Running the model and evaluating the results – the maximum and minimum values of the temperature on the surface of the coils are 74.5[°C] and 50.005[°C], respectively. The results obtained are presented in the figures 11, 12.[23]

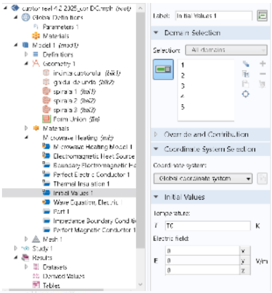

Fig. 5 Setting the initial temperature[23]

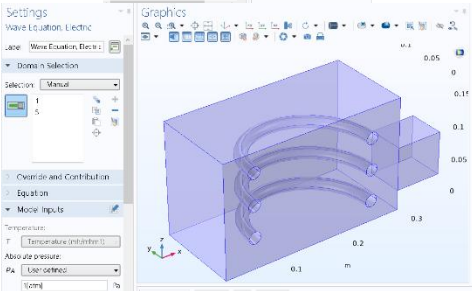

Fig. 6 The condition of propagation of electromagnetic waves[23]

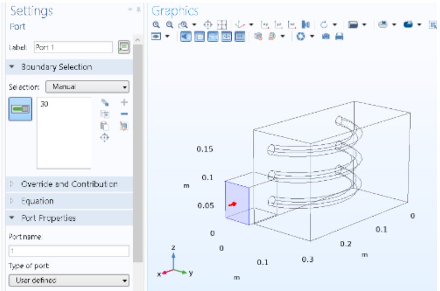

Fig. 7 Wave emitting port [23]

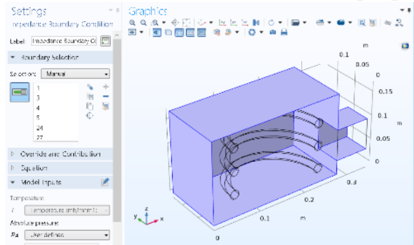

Fig. 8 The impedance condition [23]

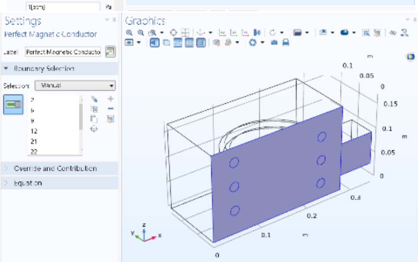

Fig. 9 The condition of a perfect magnetic conductor [23]

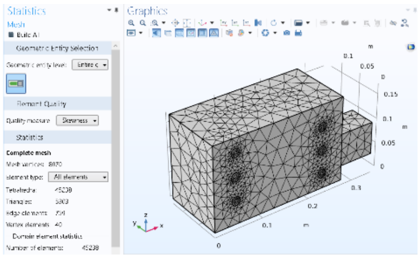

Fig. 10 Discretization, statistics and model quality [23]

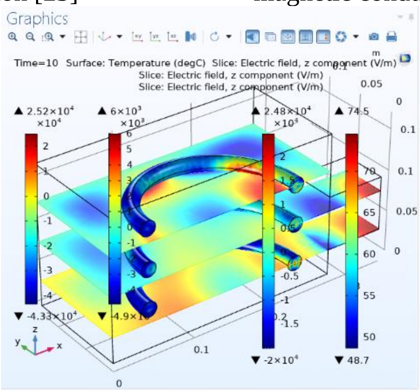

Fig. 11 Simulation results [23]

Timp	Temperatura [degC]
0	50
1	53
2	55,7
3	58,3
4	60,7
5	63
6	65,3
7	67,5
8	69,9
9	72,2
10	74,5

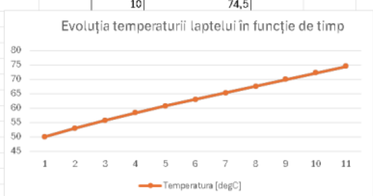

Fig. 12 Maximum temperatures at different time periods [23]

5. Detailed design

In this chapter, the microwave pasteurization plant will be presented at a conceptual level. It is represented in the figure 13.

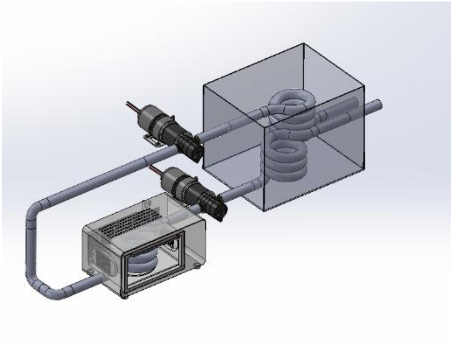

Fig. 13 Microwave pasteurization plant assembly – concept level

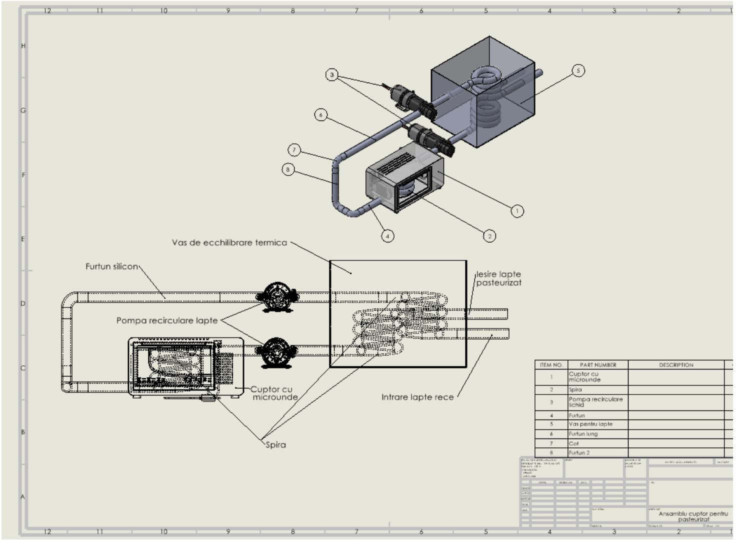

Fig. 14 Preliminary assembly drawing of the microwave pasteurization installation

Process description: Raw (cold) milk is introduced inside the thermal balance vessel using a liquid transfer pump, which then circulates through the coil where the heat is absorbed from inside the vessel, and then reaches the coil in the microwave oven. Inside the microwave oven, the actual pasteurization process is carried out, and then the pasteurized (warm) milk reaches the thermal balance vessel using the transfer pump where it gives off heat, and is then stored.For this stage of the microwave pasteurization installation, we also made a preliminary assembly drawing, so that we know most of the components needed to be able to build the installation. The preliminary assembly drawing of the installation is shown in the figure 14.

6. Product Commercialization

The product developed by this project is a microwave pasteurization installation. One category of potential customers for this product is enterprises in the food industry, typically micro-enterprises. Based on this, we have selected several such SMEs around Bucharest that produce milk, juices, and other food products.

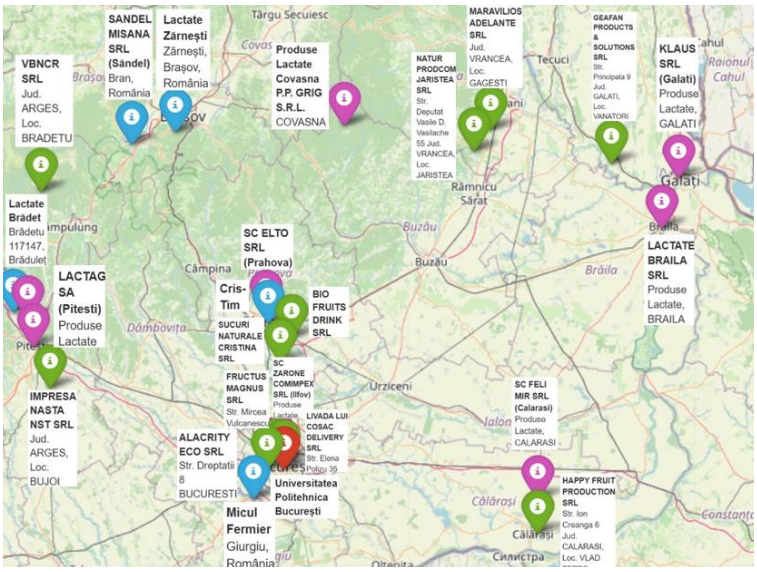

Fig.17 Map of SMEs around Bucharest producing milk, juices, and other food products

7. Conclusions

The contributions of the work consist of the following elements regarding the research topic addressed: identifying market opportunities related to needs, grouping customers by category, developing a questionnaire to identify market needs, creating a map with potential customers around Bucharest; establishing product specifications using the matrix of competing products, size-requirements based on which the objective specifications were established; conceptual design elements, general function, component, main and critical, were developed, external research was conducted analyzing a series of patents, some constructive solutions were developed, a block diagram of the installation based on the results of finite element modeling of the heating process of some liquids in the food industry (milk); a preliminary model of the microwave pasteurization installation was designed, and an overall drawing of the preliminary pasteurization installation was also made.

8. Bibliography

[1] Constantin, A. M. and Csaltos, C. (2011), "Research on the Use of Microwaves for the Antibacterial Treatment of Milk", Brașov;

[2] Tajchakavit, S. (1997), "Microwave Heating of Fruit Juices: Kinetics of Enzyme Inactivation/Microbial Destruction and Evaluation of Enhanced Thermal Effects", Vol.1, pp.86–110, ISSN 0-612-44605-0;

[3] ICPE S.A., Ica Research & Development S.R.L., et al., Process and Equipment for Thermal Processing of Milk, Romania, RO-1250731-B1, 2010;

[4] Gavrilut, Cristina, Alternative Methods for Milk Treatment: The Journal of Specialists in the Meat and Dairy Industries. Available at: https://www.meat-milk.ro/tetra-pak-metode-alternative-de-tratare-laptelui/ (Accessed: May 2, 2023);

[5] Ghiculescu, L.D, Ionescu, N., *Creativity and Intellectual Property*, Moodle Platform, Bucharest, 2024. Available at: https://curs.upb.ro/2023/my/courses.php (Accessed: 15.04.2024);

[6] *** https://forms.gle/WcrmWbww3d1prfDX9 (Accessed: 23.04.2024);

[7] *** Myria Microwave Oven MM720W, Available at: http://myria.ro/ro/cuptoare-cu-microunde/1095/cuptor-cu-microunde-myria-mm720w-700w-20l-alb.html (Accessed: 20.03.2024);

[8] *** Microwave Oven User Manual MGB25332BG, Available at: https://www.beko.ro/cuptor-cu-microunde-mgb25332bg (Accessed: 20.03.2024);

[9] *** Sencor SMW 6021 Microwave Oven User Manual, Available at: http://www.sencor.ro/cuptor-microunde/smw-6021 (Accessed: 20.03.2024);

[10] *** Microwave Oven User Manual MOC201102W, Available at: https://www.beko.ro/cuptor-cu-microunde-beko-moc201102w (Accessed: 20.03.2024);

[11] *** 6kW Liquid Heating Microwave System, Available at: https://industrialmicrowave.com/microwave-systems-liquids-fluids-heating/6kw-microwave-system/ (Accessed: 20.03.2024);

[12] *** 915MHz Liquid Heating Industrial Microwave System Brochure, Available at: https://industrialmicrowave.com/resources/915-mhz-liquid-heating/ (Accessed: 20.03.2024);

[13] Thomas, S. D., Method and Apparatus for Microwave Processing of Flat Materials, United States of America, US-6546646 B1, 2003;

[14] Alton, W. J., Post-Packaging Pasteurization for Meat Products, United States of America, US-2007/0065551 A1, 2007;

[15] Tang, J., Liu, F., Transport Carriers for Microwave Sterilization or Pasteurization, United States of America, US-10681923 B2, 2020;

[16] Raider, M., Behringer, D., et al., Microwave-Assisted Sterilization and Pasteurization System Using Synergistic Packaging, Carrier and Launcher Configurations, United States of America, US-10966293 B2, 2021;

[17] Turcin, V., Pencioiu, P., Thermal Processing Installation for Cream and Process for Its Production, Romania, RO 125652 A2, 2009;

[18] Naguly, S.L., Mobile Installation for Extracting Juice from Fruits and Vegetables, Romania, RO 2015 00039 U1, 2015;

[19] Antohi, C.M., Nițescu, E., Mitroi, A., Pasteurization Installation, Romania, RO 113800 B1, 1998;
[20] Padly, Y., Borgeaud, R., Egg Pasteurization Process, Romania, RO 90641 B, 1987;
[21] Buturugă, D.A., Refreshing Beverage, Romania, RO 132904 A0, 2018;
[22] Lungulescu, G., Process and Equipment for the Production of Fortified Probiotic Dairy Products, Romania, RO 131605 A2, 2017;
[23] Alexa, L.V., Unguroiu, M.M., Numerical Simulation of the Microwave Pasteurization Process, Scientific Session, May 2023, Faculty of Industrial Engineering and Robotics;
[24] https://www.listafirme.ro/1032/d9.htm, accessed on 15.01.2025;
[25] https://www.afacerist.ro/lista-firme/produse_lactate/, accessed on 15.01.2025.

ECO-FRIENDLY HYBRID SYSTEM FOR ELECTRICAL ENERGY GENERATION

MATEI Tudor-Aurelian, CIORTESCU Cătălin,ALEXA Luca-Valentin

OPRAN Constantin Gheorghe, PEȚA Luigi Mădălin(Conducători științifici)

Faculty of Industrial Engineering and Robotics, Year of study: 2, e-mail: thuddor@gmail.com

ABSTRACT: This research presents an innovative hybrid system for environmentally friendly electrical energy generation, combining solar and wind power sources. The paper outlines the current state of the field, fundamental principles, and the key advantages of such systems, emphasizing the potential of the proposed product and idea while highlighting the project's feasibility and future development prospects. The system's design concept is approached with the aim of maximizing energy efficiency and ensuring resilience in diverse weather conditions. Calculation formulas for both photovoltaic panel output and wind turbine power are applied to determine the specifications of the conceptual product. A robust structure that integrates both solar panels and wind turbines is essential for the system's optimal operation. The feasibility study and economic analysis provide insight into the long-term costs and profitability of the system.

KEY WORDS: energy, hybrid, ecological, efficient, economical.

1. Introduction

Solar energy systems have become a common presence in today's world, with both the photovoltaic market and research labs showing signs of stagnation in terms of truly innovative ideas. Recently, most research has focused on improving the materials used in solar panels, aiming to enhance their efficiency, durability, and long-term performance.

In the past few years, there has been a strong push to develop and apply photovoltaic systems in as many fields as possible — from automotive and aerospace to telecommunications. This rapid expansion has brought the industry to a turning point, where fresh, creative solutions are needed to take green energy technologies to the next level.

One common limitation found in most recent studies and real-world applications is that these systems are usually designed for urban areas, while rural and mountainous regions are often left behind in terms of innovation and access to sustainable energy.

In this context, the current paper proposes and analyses the feasibility of a hybrid system that combines two renewable sources — solar and wind — to produce clean electrical energy. The goal is to offer a practical and scalable solution for areas that are often overlooked in the green energy transition.

2. Identifying market opportunities

To better identify market opportunities, a preliminary portfolio of customer needs was developed in order to clearly define the main requirement that the proposed product must fulfil.

This portfolio initially included five primary needs, from which the key need was selected as follows:

N: The need for a green energy generation system capable of supplying power to the grid throughout the entire year.

Based on this need assessment, the following market opportunity was identified:

For need N: The lack of an advanced and reliable hybrid system that combines multiple renewable energy technologies for stable electricity generation.

Following a detailed analysis and the application of a Product Decision Matrix, the chosen concept for development was the "Hybrid System for Environmentally-Friendly Electrical Energy Generation", designed specifically to address need N.

3. Current state of research

The main objective of this project is the development of an integrated hybrid system for environmentally friendly electricity generation, using renewable energy from both the sun and the wind. This system supports and contributes to the transition toward sustainable energy sources by reducing dependence on fossil fuels and minimizing environmental impact. By combining solar and wind technologies, the project aims to ensure a continuous and stable energy supply regardless of weather conditions, thereby maximizing both efficiency and reliability.

Operating a hybrid electrical system involves high complexity due to the intermittent and seasonal nature of wind and solar energy. These characteristics highlight the need for energy storage to manage variability, as well as fast-acting protection systems that can respond to unexpected power interruptions.

The paper titled "**ECO-FRIENDLY HYBRID SYSTEM FOR ELECTRICAL ENERGY GENERATION**" investigates, in an applied manner, the reliability, efficiency, and both economic and energetic benefits of the system developed as part of a master's research project.

The proposed system can be divided into three main components:

1) renewable energy sources based on solar and wind energy, supported by a battery storage system and corresponding converters connected to a DC bus,

2) a load-side inverter and a single-phase load,

3) a real-time controller that manages the energy system. [1]

The hybrid power supply system consists of two integrated photovoltaic (PV) modules and a wind turbine. A second PV module was used to extend battery storage capacity and allow longer operation, while the wind turbine helped increase battery charging during periods with wind but no sun, especially in winter and at night. Results showed that the hybrid system successfully powered a 30-watt LED streetlight. A wind power output of 113 W was achieved at a maximum wind speed of 12.10 m/s recorded in 2021, with a wind turbine efficiency of 56.64%. Additionally, based on a HOMER optimization analysis comparing three scenarios—using a solar PV system, a standalone wind turbine, or a combined hybrid solar-wind system—the hybrid option clearly proved to be the optimal solution. [2]

Fig. 1. Hybrid Power Supply System for Street Lighting [2]

As previously mentioned, operating such an electrical system becomes challenging due to the intermittent and seasonal nature of wind and solar energy. To manage this variability, a complementary solution is needed alongside the two energy harvesting technologies — specifically, a method for storing and later using the surplus energy generated during periods of favourable weather, when wind and solar production exceeds the demand from the grid.

Considering these key aspects in the development of an innovative product that hybridizes the two renewable energy generation methods, a conceptual diagram was created using a hydropower-inspired system to store excess energy. This schematic is shown in Figure 2.

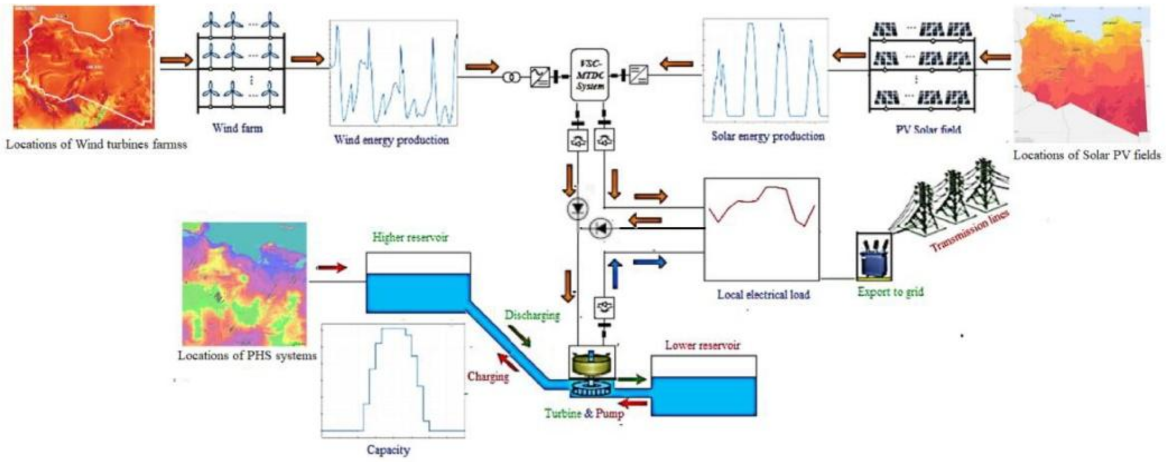

Fig. 2. Conceptual Diagram of the Hybrid Eco-Friendly Power Generation System [3]

The system studied and developed is composed of three main parts, as illustrated in the diagram: the power supply system, which includes wind turbine farms and photovoltaic (PV) solar panel fields; the energy storage system, represented by Pumped Hydro Storage (PHS); and the consumer side, represented by the public power grid.

To address the issue of grid stability under conditions of renewable energy oversupply, the hybrid system uses hydropower stations to stabilize the network by creating a buffering layer. When wind and solar production exceeds grid demand, the excess energy is directed toward pumping operations, storing potential energy for later use. During periods of low renewable energy production, the stored hydroelectric energy is used to maintain grid balance.

Control devices play a crucial role in maintaining voltage and frequency stability in the grid — two of the biggest challenges when integrating a growing share of renewable energy sources into the public power network. [3]

4. Overview of Existing Competing Solutions

Table 1. Data on competing products

Competing products	Product specifications
 Fig.3. GES-500 Wind and Solar Hybrid System [4]	The GES-500 System (Hybrid Solar and Wind Energy System) consists of a solar panel, a battery bank module, an MPPT-type solar charge controller, a grid-tie inverter module, a wind power generation unit, a wind energy monitoring module, a three-phase rectifier module, a combined solar and wind control module, and a charge measurement unit. By integrating all these components, a comprehensive learning platform was created for implementing both wind and solar energy within a hybrid system. This platform helps students better understand the theory behind on-grid and off-grid solar energy systems, wind energy generation, hybrid systems, and various related applications. [4]

Competing products	Product specifications
 Fig.4. Wind and Solar off-grid 5KW system[5]	The 5 kW off-grid wind–photovoltaic system is a hybrid solution capable of operating under all environmental conditions, thanks to the combination of two alternative energy sources: solar and wind. Due to the high quality of its components, the hybrid system benefits from a long operational lifespan. The electricity generation process is highly stable, which justifies the investment through a relatively short payback period. This 5 kW off-grid wind–photovoltaic system is recommended for locations without grid access, such as guesthouses, mountain cabins, beekeeping or livestock farms. It is also suitable for users already connected to the grid who wish to achieve energy independence or significantly reduce their electricity bills. The system provides an average daily production of 8–10 kWh during winter and 10–15 kWh during summer from the photovoltaic panels, while the wind turbine delivers 600 Wh at a wind speed of 11 m/s. The total energy storage capacity of the battery bank is 7.2 kW. [5]
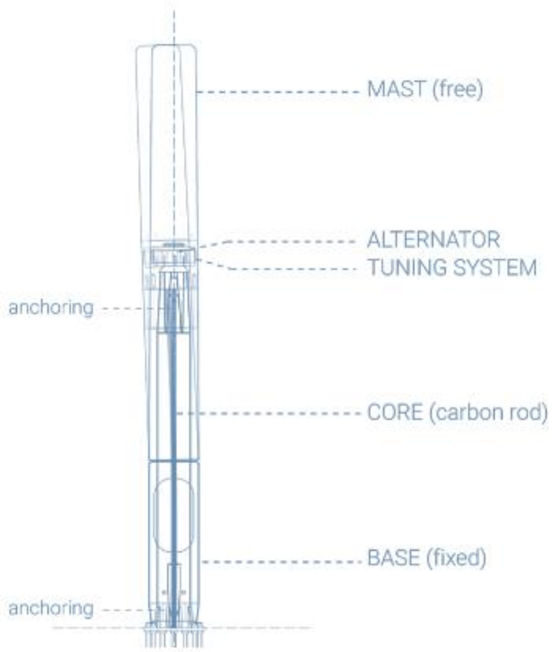 Fig.4. VIV generators through resonance [6]	Vortex devices represent a simple concept that allows for easy construction, installation, and operation. They consist of a fixed base and a mast that oscillates freely, perpendicular to the wind direction. The internal components never come into direct contact, but they interact with one another to generate electrical energy. When wind flows around the structure, pressure vortices are created. The frequency of these vortices depends on the wind speed, and if the structure has a natural resonance frequency, it begins to oscillate and produce energy. This aeroelastic resonance phenomenon is known as Vortex Shedding and occurs frequently in nature. Similar to traditional alternators, the device enables interaction between coils and magnetic fields, generating electricity through electromagnetic induction—without the need for a rotating shaft. The magnets serve as a tuning mechanism, modifying the apparent elastic constant of the mast, thereby increasing the range of wind speeds at which oscillations occur. [6]

5. Preliminary Financial Analysis

The preliminary financial analysis begins with the creation of a price list based on the average purchase prices or approximate values of all components contributing to both direct and indirect costs. As a result, the following list of estimated prices has been compiled:

Material costs:

- Solar panels: assumed cost per photovoltaic panel – 500 RON
- FDM filaments: approximately 100–200 RON/kg
- Servomotors: approximately 75–100 RON/unit
- Photoluminescent sensors: 40–120 RON/unit
- Arduino boards: 100 RON/unit
- Cabling: 2–8 RON/meter

Labor costs:

- Energy cost for 3D printers: estimated at 0.4–0.8 RON/kWh
- Labor hour cost: 50–120 RON/hour for technicians and engineers

Transport costs:

Transportation costs will vary significantly depending on distance and volume, but an average cost of 800 RON per shipment will be considered.

Management Costs:

A percentage of 10–15% of the total direct costs will be allocated for project management.

Marketing Costs:

Total marketing expenses are estimated to represent approximately 5–10% of the overall costs, including advertising and online management.

Table 2. Project costs

Category	**Estimated Unit Cost (RON)**	**Quantity / Percentage**	**Total Cost (RON)**
Solar panels	500 RON	6 units	3000 RON
FDM filaments	150 RON	10 kg	1500 RON
Servomotors	75 RON	4 units	300 RON
Photoluminescent sensors	80 RON	6 units	480 RON
Arduino boards	100 RON	6 units	600 RON
Cables	6 RON	50 meters	300 RON
3D printer energy consumption	0.6 RON	1000 kWh	600 RON
Labor	80 RON	25 hours	2000 RON
Transportation	800 RON	1 delivery	800 RON
Management (12.5% of direct costs)	–	12.5%	1197.5 RON
Marketing (7.5% of total costs)	–	7.5%	718.5 RON
Estimated Total	–	–	11,496 RON

Total direct costs: 9580 RON

Total indirect costs: 1916 RON

Estimated total project cost: 11,496 RON

The next step in the preliminary financial analysis is to determine a selling price for the product, in order to ensure profitability.

Selling price:

$$PV = C_T \times (1 + M_P)$$

Where:

C_T = Total Cost
M_P = Profit Margin (considered 20% for this project)

Once these two aspects have been established, we can apply the following formula for the product under development:

$$PV = 11496 \times (1 + 0{,}2) = 13795{,}2 \text{ LEI} + \text{TVA}$$

The established price must cover all costs and generate sufficient profit to justify the initial investment.

6. Conceptual design

The conceptual design process begins with the development of an innovative solution that aims to hybridize the two methods of generating green energy. The complexity of this design phase lies in creating a product that can be harmoniously integrated into the natural landscape of the installation site, while also maintaining a high level of functionality and usefulness. Thus, the inspiration for the solar energy generation system was drawn from floral design.

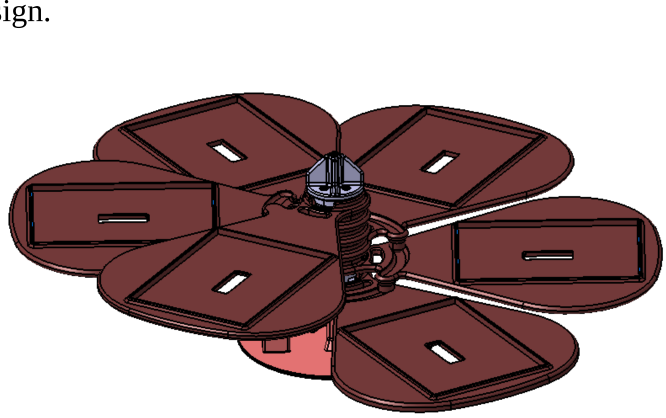

Fig.5. Conceptual Design of the Integrated Photovoltaic Panels

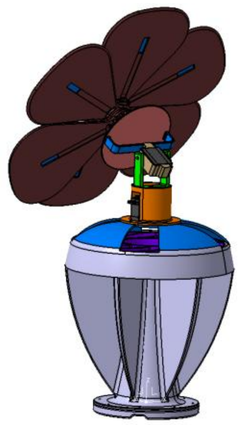

Fig.6. Integration of the Protection and Solar Tracking Mechanism into the Device

The general function of the photovoltaic system is: "Tracking the point of maximum solar intensity, capturing solar energy, and converting it into electrical energy." The component functions ensure that the product operates within its designated parameters. These functions include: capturing and converting sunlight into electricity (performed by six photovoltaic panels measuring 80 mm × 110 mm); tracking the position of the light source (through photoluminescent sensors connected to MG90S and MG995 servomotor-driven rotation systems); and folding and protecting the solar panels (achieved by rotating a central shaft connected to the main petal and rotational mechanisms, as shown in Figure 7).

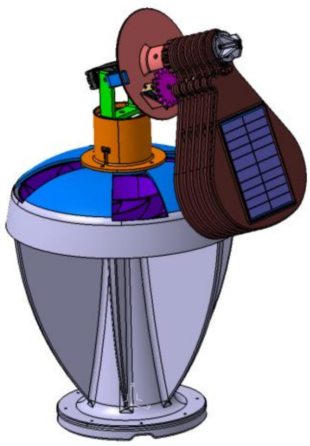

Fig.7. Protection of the Photovoltaic System through Solar Panel Folding

The general function of the integrated horizontal-axis wind turbine is: "Capturing wind energy and converting it into electrical energy." The conceptual design of the wind system is based on fulfilling the following criteria: maximum efficiency at moderate wind speeds, use of durable and cost-effective materials, and ease of manufacturing (via 3D printing). The chosen turbine type for the conceptual design is HAWT (Horizontal-Axis Wind Turbine), due to its easy integration into the system's central shaft and its high rotational speed output, which is characteristic of this turbine configuration.

Necessary data for designing the wind turbine:

Table 3. Established Values and Parameters for the Wind Turbine

Parameter	**Value**
Rotor diameter (R)	0.15 m
Wind speed (v)	20 m/s
Air density (ρ)	1.225 kg/m³
Power coefficient (C_p)	0.45
Tip Speed Ratio (TSR)	6
Number of blades (N)	9
Selected air foil profile	Selig S1223 (small size, high lift)
Lift coefficient (C^L)	~1.2 (for S1223 at optimal angle of attack)

Rotation Speed Calculation:

Using the TSR formula, the angular velocity is determined and then converted into revolutions per minute (RPM):

$$TSR = \frac{wR}{v} => w = \frac{TSR \times v}{R} = \frac{6 \times 20}{0{,}15} = 800\ rad/s$$

$$RPM = w \times \frac{60}{2\pi} = 800 \times \frac{60}{6{,}283} \approx 7640\ RPM$$

Table 4. Discretization of the Blade for Sectional Calculations

Section Number	**Position from Center**	**Description**
1	0.05 m	Central zone
2	0.08 m	Near the center
3	0.11 m	Midsection
4	0.13 m	Near the tip
5	0.15 m	Full radius

Chord Length for Each Section:

Determining the Chord Length for Each Section:

$$c(r) = \frac{8\pi r}{NC_L}(1 - cos\phi), \text{unde } \phi = \arctan\left(\frac{v}{wr}\right)$$

Table 5. Chord length by section

Section	**ωr (m/s)**	**ϕ (degrees)**	**cos(ϕ)**	**Chord c(r) (mm)**
0.05	40	26.57°	0.894	49 mm
0.08	64	17.35°	0.954	29 mm
0.11	88	12.85°	0.975	19 mm
0.13	104	10.85°	0.983	15 mm
0.15	120	9.46°	0.987	12 mm

Knowing the optimal angle of attack (AOA) for the S1223 air foil profile (6°), the twist angle is calculated using the following formula:

$$\theta(r) = \phi(r) - \text{AOA}$$

Table 6. Angle of Attack by Section

Section	ϕ (degrees)	Twist Angle θ (degrees)
Section	26.57°	20.57°
0.05	17.35°	11.35°
0.08	12.85°	6.85°
0.11	10.85°	4.85°
0.13	9.46°	3.46°

The design of the turbine shown in Figure 8 was carried out based on the previously presented calculations.

In the conceptual stage, the collector turbine will be connected to a direct current (DC) motor, which will convert the mechanical energy produced by the turbine into electrical energy, thereby demonstrating the system's functionality.

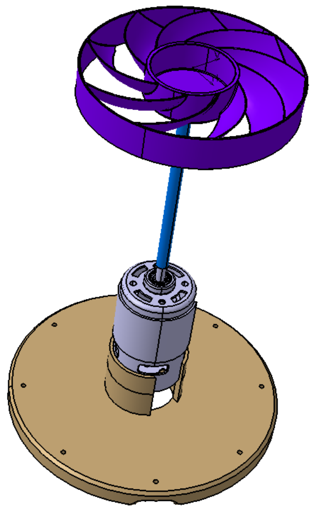

Fig. 8. Design of the Wind Turbine Connected to an RS-775 DC Motor

7. Conclusions

Through the direction of this research, an innovative biomimetic concept was proposed and developed, combining two forms of sustainable energy generation.

The key elements underlying the innovation of this concept are:

1. The adoption of a highly efficient construction technology for electrical power generation;
2. Analysis of the current state of research and competing products to identify key points for product development;
3. Development of a robust structure to withstand strong wind currents;
4. Integration of a solar tracking system to maximize the efficiency of the photovoltaic panels;
5. Execution of a preliminary economic calculation to assess the project’s feasibility;
6. Design and calculation of the conceptual elements and parameters of the wind turbine.

8. Bibliography

[1] G. Resch, L. Liebmann, and R. Hirner, *"Study on the Wind Power Potential in Bulgaria, Hungary, and Romania,"* presented at the International Conference on Renewable Energy Resources, vol. 3, no. 2, pp. 45-56, 2023.

[2] N. M. Ali and H. Ammari, “Design of a hybrid wind-solar street lighting system to power LED lights on highway poles,” AIMS Energy, vol. 10, no. 2, 2022, doi: 10.3934/ENERGY.2022010.

[3] Y. F. Nassar, H. J. El-Khozondar, and M. A. Fakher, *"The Role of Hybrid Renewable Energy Systems in Covering Power Shortages in Public Electricity Grid: An Economic, Environmental and Technical Optimization Analysis," Renewable Energy Journal*, vol. 75, no. 1, pp. 123–135, 2024.

[4] “GES-500 Solar Wind system.” Accessed: Apr. 06, 2025. [Online]. Available: https://www.kandh.com.tw/ges-500-wind-and-solar-hybrid-system-ges-500.html

[5] “Sistem eoliana-fotovoltaic off-grid 5KW.” Accessed: Apr. 06, 2025. [Online]. Available: https://www.voltecon.ro/produs/sistem-eoliana-fotovoltaic-off-grid-5kw/

[6] D. Jesús and Y. Villarreal, "VIV resonant wind generators." [Online]. Available: www.vortexbladeless.com
[7] C. Dumitraș și C. Opran, "*Prelucrarea materialelor compozite, ceramice și minerale*" Bucharest: Publisher Editura Tehnică, 1994. ISBN 973-31-0602-X
[8] C. Opran, N. Vasile, V. Racicovschi, P. Pencioiu, I. Păuna, M. Casariu, G. Mohan și A. Ardelean, "*Biostructuri polimerice degradabile în mediul natural*" Arad: Vasile Goldiș University Press, 2004. ISBN 973-664-041-8.
[9] C. G. Opran, "*Tehnologia produselor din materiale avansate*" București: Publisher Bren, 2017. ISBN 978-606-610-087-8.

DESIGN AND DEVELOPMENT OF AN EXPERIMENTAL MODEL OF A ROBOT FOR HANDLING PLANT POTS IN A WAREHOUSE

COJOCARU Leonard Mihai, OANCEA Maria Emilia, PĂSĂRIN Flavius Mihail, PUIU Elena Bianca, Liviu-Daniel GHICULESCU(Conducător științific)
Faculty: Industrial Engineering and Robotics, Specialization: Economic Engineering and Business Management, Year of study: Master's 2nd year ,
E-mail: maria.emilia.oancea @gmail.com

ABSTRACT: The paper presents the design and development of an autonomous robot for handling plant pots in warehouses, as a solution to the increasing demand in the horticultural sector. Market requirements were analyzed, technical specifications were established, and the most suitable robotic design solutions were selected. The prototype was modeled in 3D, with components produced using 3D printing technology and PLA material. Electronic components (motors, sensors, Arduino) were purchased and tested. After the physical and electronic assembly, code was developed in the Arduino IDE to enable the robot's autonomous operation.

KEYWORDS: robot, plants, handling, design, manufacturing

1. Introduction

The rapid growth of the flower market in Romania and the increasing demand for ornamental plants have emphasized the need to optimize logistical processes in warehouses. In this context, the development of a robot designed for plant handling represents an efficient solution for reducing pot handling time, while also ensuring the protection of both plants and containers [1].

This paper analyzes the conception, design, and implementation of a robot that ensures the safe handling of plant pots by integrating modern technologies such as gripping mechanisms, handling systems, and mobility on a mobile platform. It addresses the stages of CAD design, additive manufacturing of components, mechanical and electrical assembly of the robot, as well as its programming.

2. Current state

Up to the current stage of research, several important steps have been completed in the development of a robot designed for handling plants in storage environments. A strategic marketing analysis was conducted to identify market requirements related to the automation of pot handling processes in the horticultural sector. Based on this data, the functional and technical specifications of the system were established, considering parameters such as maximum supported load and the need for delicate handling suitable for fragile objects.

During the conceptual design phase, multiple robotic architecture variants were developed and compared, and the configuration offering the best balance between efficiency, cost, and operational flexibility was selected. Subsequently, in the detailed design phase, the component elements of the assembly were defined, along with the type of mechanical transmission and the general principles of operation of the robotic system.

The research also included an applied study on grippers, analyzing various existing types (mechanical, pneumatic, flexible), as well as the materials used for the contact surfaces, with the aim of reducing the risk of damaging the plants during handling. In parallel, solutions were identified for sealing and insulating the cables, necessary for protecting the electrical components under conditions of high humidity and temperature variations specific to storage spaces.

3. Design and development of the robot

The prototype of the plant-handling robot was developed using specialized 3D modeling software, based on dimensions extracted from the technical datasheets of the components to be mounted on the chassis [2]. The precise dimensions of the parts were determined to ensure compatibility between components, proper system functionality, and integration within the available warehouse space. The final dimensions of the device, resulting from these constraints, are 265 × 192 × 502 mm (L × W × H), as shown in Fig. 1.

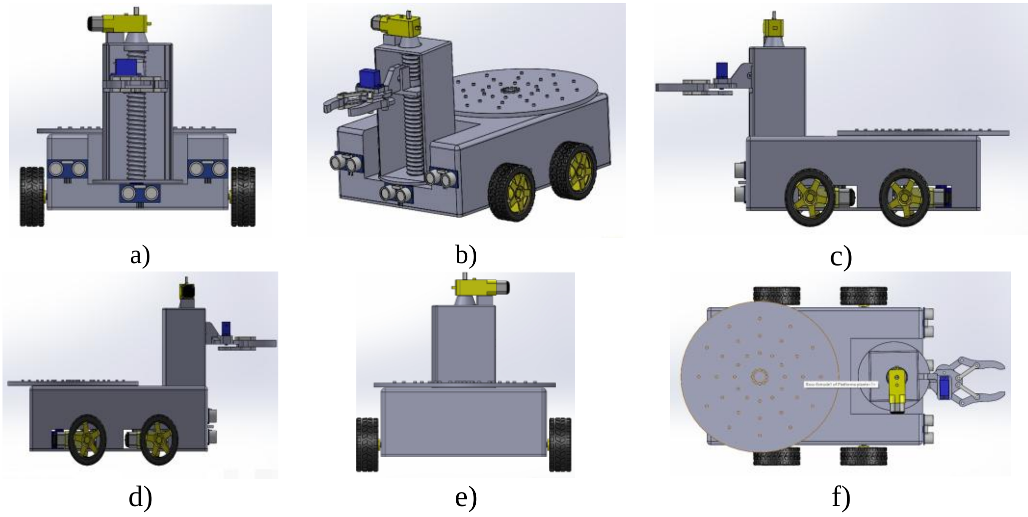

Fig. 1 Handling robot a)Front view, b) Isometric view, c-d)Side view, e) Back view, f) Top view

The assembly drawing of the plant-handling robot can be seen in the figure below:

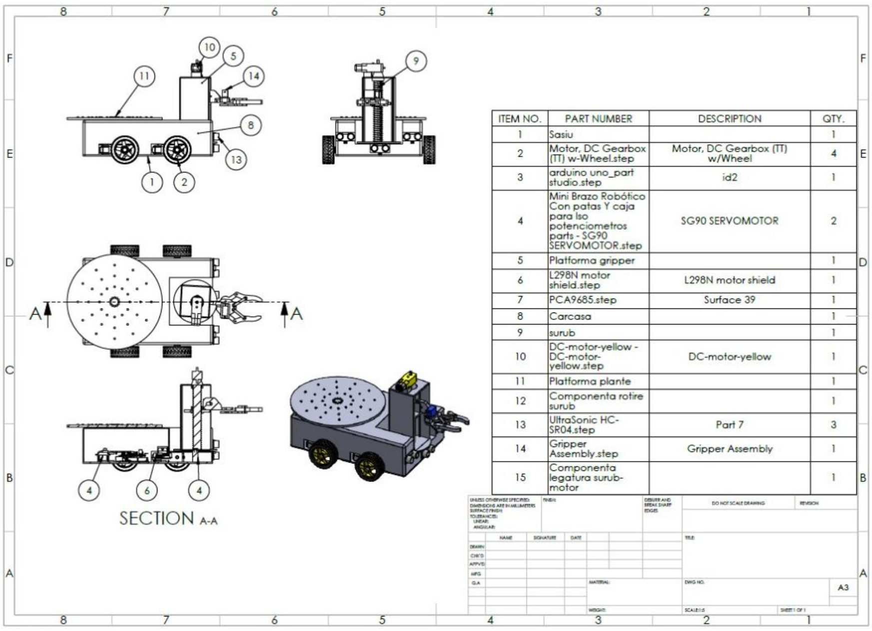

ITEM NO.	PART NUMBER	DESCRIPTION	QTY.
1	Sasiu		1
2	Motor, DC Gearbox (TT) w-Wheel.step	Motor, DC Gearbox (TT) w/Wheel	4
3	arduino uno_part studio.step	id2	1
4	Mini Brazo Robótico Con patas Y caja para lso potenciometros parts - SG90 SERVOMOTOR.step	SG90 SERVOMOTOR	2
5	Platforma gripper		1
6	L298N motor shield.step	L298N motor shield	1
7	PCA9685.step	Surface 39	1
8	Carcasa		1
9	surub		1
10	DC-motor-yellow - DC-motor-yellow.step	DC-motor-yellow	1
11	Platforma plante		1
12	Componenta rotire surub		1
13	UltraSonic HC-SR04.step	Part 7	3
14	Gripper Assembly.step	Gripper Assembly	1
15	Componenta legatura surub-motor		1

Fig. 2 Assembly drawing

3.2 Additive manufacturing

To manufacture the robot components, additive manufacturing through 3D printing was used. The designed models were processed in Ultimaker Cura software, which generated the files necessary for printing. This method allowed for the rapid production of parts with precise geometry, optimized for final assembly and testing (Fig. 3a, 4a). In terms of costs and printing time, the material chosen was PLA (Polylactic Acid) [3] [4] [5].

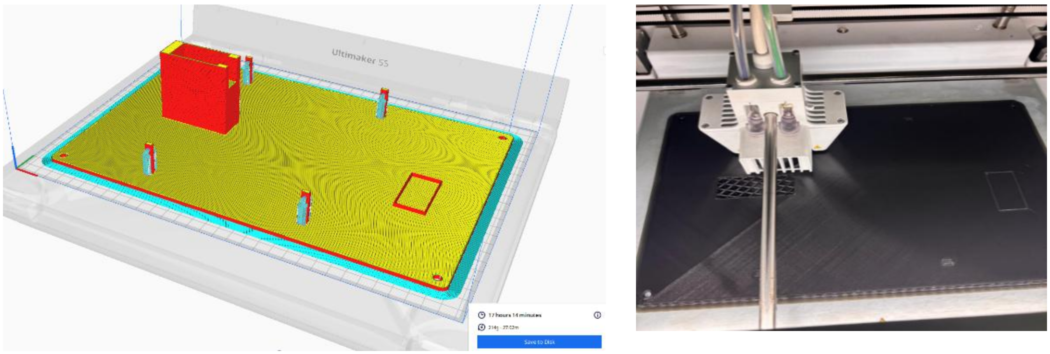

a) b)

Fig. 3. Chassis:: a) Part presentation in Ultimaker Cura, b) Chassis during the printing process

The next step was to make the settings for the upper casing, which were compared to choose the best additive manufacturing technology in terms of cost, printing time, and strength. The printer used for the components was the Ultimaker 5S and Creality CR-20 PRO, and the material chosen after the study was PLA.

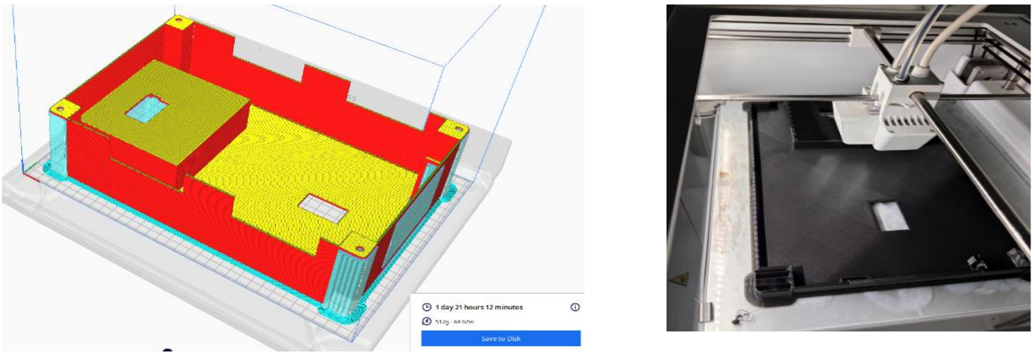

a) b)

Fig. 4 a) Part presentation in Ultimaker Cura, b) Casing during the printing process

Another component made through 3D printing was the gripper, designed for gripping and handling the plant pot. It is shown in Fig. 5.

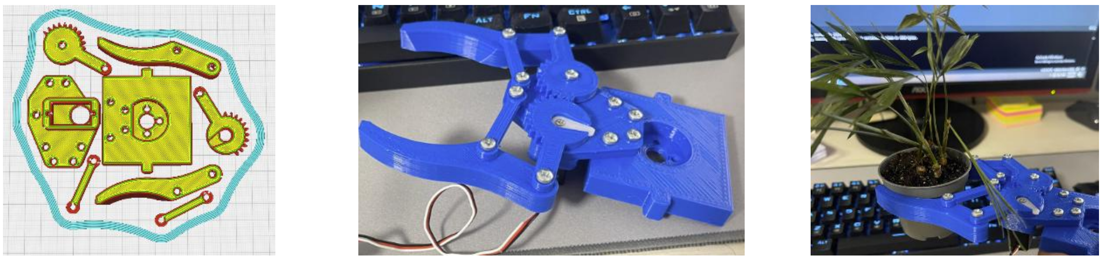

a) b) c)

Fig. 5 a) Gripper presentation in Ultimaker Cura, b) Assembled gripper, c) Gripper with plant pot

The next step in the process of developing the robot prototype was the acquisition of the electronic components necessary to ensure the system's functionality, as presented in Table 1.

Table 1. Electronic components

Nr. crt.	Name	Quantity	Representation	Nr. crt.	Name	Quantity	Representation
1.	Wheel	4		4.	Ultrasonic Sensor hc-sr04	3	
2.	Motor	5		5.	Battery casing	1	
3.	Arduino Board	2		6.	Battery	2	
7.	L298N	1	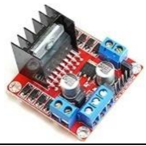	10.	Breadboard	1	
8.	Servomotor SG90	2		11.	Servomotor MG995	1	
9.	Start-Stop Button	1		12.	Motor mounting bracket	4	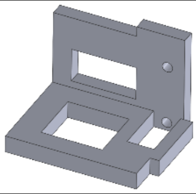

4. Motor and servomotor testing

After the parts were printed and the electronic components were assembled, each part of the system was tested. Testing the motors and servomotors is necessary to verify that they function correctly and meet the performance requirements of the robot. For this stage, a specialized programming language was used, providing tools for signal analysis, data processing, and automatic control, thus enabling efficient and accurate testing [6] [7].

4.1 DC Motor Programming

In the project, an L298N motor driver was used to control the DC (direct current) motors— a module commonly found in automation and robotics applications. This driver allows simultaneous control of two DC motors, providing essential functions such as changing the direction of rotation and adjusting speed through PWM (Pulse Width Modulation) signals. The motors were programmed using an Arduino board, which sends logic signals to the driver to execute the desired commands.

```
Cod_Placa_1.ino
#include <NewPing.h>  // Ultrasonic sensor function library

// Motor control pins
const int LeftMotorForward = 7;
const int LeftMotorBackward = 6;
const int RightMotorForward = 5;
const int RightMotorBackward = 4;

// LED indicators
const int ForwardLED = 8;
const int BackwardLED = 9;
const int LeftLED = 11;
const int RightLED = 12;

// Sensor LEDs (optional for visual feedback)
const int LeftSensorLED = 13;
const int RightSensorLED = 3;

// Ultrasonic sensor pins
#define left_trig A1
#define left_echo A2
#define right_trig A3
#define right_echo A4
#define maximum_distance 200

// Timing variables
unsigned long lastDetectionTime = 0;
const unsigned long detectionTimeout = 1500; // 1.5 seconds

// Create sonar objects for left and right front sensors
NewPing leftSonar(left_trig, left_echo, maximum_distance);
NewPing rightSonar(right_trig, right_echo, maximum_distance);

void setup() {
  // Motor pins
  pinMode(RightMotorForward, OUTPUT);
  pinMode(LeftMotorForward, OUTPUT);
  pinMode(LeftMotorBackward, OUTPUT);
  pinMode(RightMotorBackward, OUTPUT);

  // LEDs
  pinMode(ForwardLED, OUTPUT);
  pinMode(BackwardLED, OUTPUT);
  pinMode(LeftLED, OUTPUT);
  pinMode(RightLED, OUTPUT);
  pinMode(LeftSensorLED, OUTPUT);
  pinMode(RightSensorLED, OUTPUT);

  // Initialize state
  moveStop();
}
```

```
void loop() {
  delay(50);

  int leftDistance = readLeftPing();
  int rightDistance = readRightPing();
  int minDistance = min(leftDistance, rightDistance);

  // Optional: show sensor LED activity
  digitalWrite(LeftSensorLED, leftDistance <= 45 ? HIGH : LOW);
  digitalWrite(RightSensorLED, rightDistance <= 45 ? HIGH : LOW);

  if (minDistance <= 45) {
    // Obstacle detected
    lastDetectionTime = millis();
    moveStop();
    delay(300);
    moveBackward();
    delay(400);
    moveStop();
    delay(300);

    // Decide turn direction
    if (leftDistance > rightDistance) {
      turnLeft();
    } else {
      turnRight();
    }

    moveStop();
  } else {
    // No object detected recently
    if (millis() - lastDetectionTime >= detectionTimeout) {
      moveForward();
    }
  }
}
```

```
int readLeftPing() {
  delay(70);
  int cm = leftSonar.ping_cm();
  return (cm == 0) ? 250 : cm;
}

int readRightPing() {
  delay(70);
  int cm = rightSonar.ping_cm();
  return (cm == 0) ? 250 : cm;
}
```

```
void moveStop() {
  setMotors(LOW, LOW, LOW, LOW);
  digitalWrite(ForwardLED, LOW);
  digitalWrite(BackwardLED, LOW);
  digitalWrite(LeftLED, LOW);
  digitalWrite(RightLED, LOW);
  digitalWrite(LeftSensorLED, LOW);
  digitalWrite(RightSensorLED, LOW);
}

void moveForward() {
  setMotors(HIGH, LOW, HIGH, LOW);
  digitalWrite(ForwardLED, HIGH);
}

void moveBackward() {
  setMotors(LOW, HIGH, LOW, HIGH);
  digitalWrite(BackwardLED, HIGH);
}

void turnRight() {
  digitalWrite(RightLED, HIGH);
  setMotors(HIGH, LOW, LOW, HIGH); // Right turn
  delay(250);
}

void turnLeft() {
  digitalWrite(LeftLED, HIGH);
  setMotors(LOW, HIGH, HIGH, LOW); // Left turn
  delay(250);
}

void setMotors(int leftForward, int leftBackward, int rightForward, int rightBackward) {
  digitalWrite(LeftMotorForward, leftForward);
  digitalWrite(LeftMotorBackward, leftBackward);
  digitalWrite(RightMotorForward, rightForward);
  digitalWrite(RightMotorBackward, rightBackward);
}
```

Fig. 6 DC Motor Program [8]

4.2. Program for SG90/MG995 Servomotor

This subsection presents the use of SG90 and MG995 servomotors within the project, essential components for achieving precise and controlled movements. The servomotors are driven by PWM signals and are used in various parts of the mechanism: for rotating the platform that holds the plant pots, for the rotary platform that releases the pot through a 180° rotation, as well as for the opening and closing of the gripper.

Cod_Placa_2.ino

```
#include <Servo.h>

Servo Servo_1;
Servo Servo_2;

bool servomotor = false;

void setup() {
  Serial.begin(9600);

  Servo_1.attach(9);
  Servo_2.attach(10);

  // Verifica pozitie servomotoare
  Servo_1.write(0);
  Servo_2.write(0);

  delay(3000);
}
```

```
void loop() {
  if (!servomotor) {

   // Step 1: Miscarea Servomotorului 1 la 180 grade
   //Servo_1.write(180);
   //delay(2000);
   moveServo1Slowly(0, 180);
   delay (2000);

    // Step 2: Miscarea Servomotorului 2
    moveAndCount(0, 60);
    moveAndCount(60, 120);
    moveAndCount(120, 180);

    // Step 3: Miscarea Servomotorului 1 la 0 grade
    //Servo_1.write(0);
    //delay(1000);
    moveServo1Slowly(180,0);

    // Se valideaza loop-ul ca fiind complet
    servomotor = true;
  }
}
```

```
void moveAndCount(int start, int end) {
  Serial.print("Moving to: ");
  Serial.print(end);
  Serial.println(" degrees");

  moveSlowly(start, end);
  countTo10();
}

void moveServo1Slowly(int startAngle, int endAngle) {
  int steps = abs(endAngle - startAngle);
  int delayTime = 40;

  if (startAngle < endAngle) {
    for (int pos = startAngle; pos <= endAngle; pos++) {
      Servo_1.write(pos);
      delay(delayTime);
    }
  } else {
    for (int pos = startAngle; pos >= endAngle; pos--) {
      Servo_1.write(pos);
      delay(delayTime);
    }
  }
}

void moveSlowly(int startAngle, int endAngle) {
  int steps = abs(endAngle - startAngle);
  int delayTime = 35;

  if (startAngle < endAngle) {
    for (int pos = startAngle; pos <= endAngle; pos++) {
      Servo_2.write(pos);
      delay(delayTime);
    }
  } else {
    for (int pos = startAngle; pos >= endAngle; pos--) {
      Servo_2.write(pos);
      delay(delayTime);
    }
  }
}
```

```
void countTo10() {
  for (int i = 1; i <= 10; i++) {
    Serial.print("Count: ");
    Serial.println(i);
    delay(500);
  }
}
```

Fig. 7 Servomotor program

5. Robot assembly and final code development

The first step in making the robot operational was establishing the electrical connections between the components, as shown in Fig. 8. This image illustrates how the motors, servomotors, sensors, and Arduino Uno R3 boards were connected using cables.

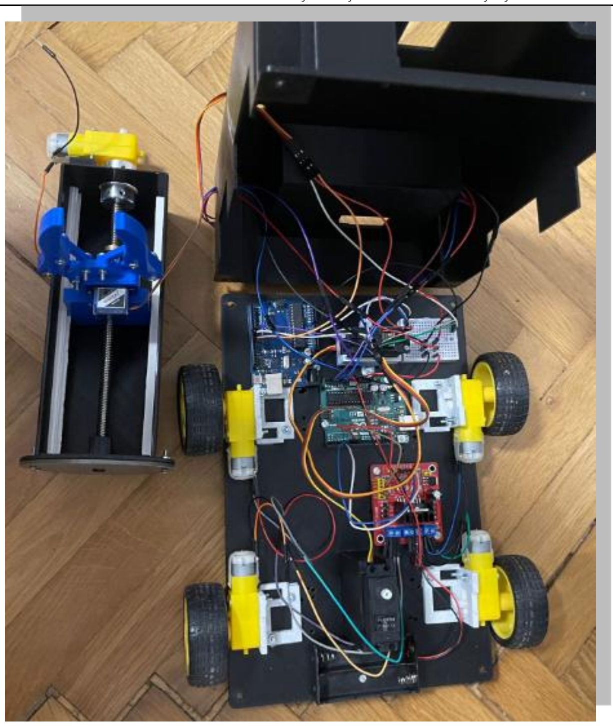

Fig. 8 Interior of the robot

Figure 9 shows the final assembly of the robot. To achieve this, the electronic connections and the component parts presented in Table 1 were taken into consideration.

a) b) c)

Fig. 9 Robot : a) Robot front view, b) Robot front view with plant pot, c) Robot side view

The second step is the integration of the individual codes, ensuring that all electronic components work together as a unified system. After testing, a program was developed in Arduino IDE, configured to run continuously until the user presses the STOP button.

6. Conclusions and future developments

The project "Autonomous Robot for Handling Plants in a Warehouse" investigates a robot that can be used in various types of warehouses or flower markets. Following the development of the chapters, the following conclusions can be listed:

- A market analysis was conducted to identify the needs in the horticultural sector regarding the automation of plant handling;
- Several robotic architecture variants were designed, and the optimal configuration was selected;
- Additive manufacturing technology (3D printing) was used to produce the parts;
- The necessary electronic components for the system's operation were purchased;
- A complete electrical connection diagram was developed between all components;
- Individual tests of the motors and servomotors were conducted to validate their functionality;
- A complete code was written and integrated in Arduino IDE, with continuous operation until the STOP button is pressed;

Future developments:

- Improvement of the precision with which the robot positions and handles the plant pots;
- Optimizing the gripper for a more delicate and secure handling of the plants;
- Reducing energy consumption to operate more efficiently;
- Adapting the design to function in smaller spaces or different types of warehouses;

7. Bibliography

[1]. Savu, C., *România a devenit o piață importantă pentru plante și flori. Nu mai producem industrial, dar afacerile românești prosperă*, available at: https://stirileprotv.ro/romania-te-iubesc/romania-a-devenit-o-piata-importanta-pentru-plante-si-flori-nu-mai-producem-industrial-dar-afacerile-romanesti-prospera.html, accesat la 06.05.2024.

[2]. Filip, V., Marin, C., Grunoiu, L., & Negrea, A. (2008). *Proiectarea, modelarea, simularea sistemelor mecanice utilizând SolidWorks, CosmosMotion și CosmosWorks*. Târgoviște: Valahia University Press.

[3]. Popescu, D., & Cazacu, A. (2017). *ECDL 3D Printing*. București: Editura ECDL România.

[4]. Doicin, C. (2023). *Curs: Tehnologii de Fabricare Aditivă*, Universitatea Politehnica din București, available at https://archive.curs.upb.ro/2023/login/index.php.

. [5]. Ulmeanu, M., & Doicin, C. (2018). *Dezvoltarea produselor fabricate aditiv*. București: Editura BREN.

[6]. Anghel, T. (2020). *Programarea plăcii Arduino*. Pitești: Editura Paralela 45.

[7]. Duguleană, M. (2011). *Învățarea roboților mobili pentru deplasare și manipulare în medii industriale*. Brașov.

[8]. ***. How *to Make Arduino Obstacle Avoiding Robot*, disponibil la: https://robotlk.com/how-to-make-arduino-obstacle-avoiding-robot/, accessed at 15.03.2025.

EVALUATION OF INERTIAL EFFECTS ON THE STRUCTURAL BEHAVIOR AND PRECISION OF A DELTAPOD ROBOT

COSTEA Mihai, STOIAN Bogdan-Nicolae, NĂSTASE Marian-Sebastian, JIGA Gheorghe-Gabriel(Conducător științific)

Faculty of Industrial Engineering and Robotics, Domain: Safety and Structural Integrity of Structures, Ist year master's student, e-mail: mihai.costea2210@upb.ro

Parallel-actuated robots are increasingly used in automated manufacturing cells due to their superior precision and speed. These robots are essential in modern production processes, which often include such robotic systems. In recent decades, technological advancements have led to a deeper integration of parallel-actuated robots in automated factories, significantly contributing to increased efficiency and production quality.
The fabrication of solutions dedicated to the placement and support of parallel-actuated robots, such as DELTAPOD, presents significant challenges concerning the maintenance of structural integrity and positioning accuracy. These modular structures must withstand both internal and external forces without compromising the robot's performance. Studying the behavior of these structures during manufacturing processes is essential, as any deformation or fabrication error can directly affect the robot's positioning precision. In this context, the analysis of structural integrity becomes a crucial domain within mechanical engineering, given its impact on the performance and reliability of robotic systems.

CUVINTE CHEIE: DELTAPOD Robots, Structural analysis, Modular Structures, Positioning accuracy, Finite Elements Method.

1. Introduction

This article outlines a comprehensive methodology employed in the design and validation of the DELTAPOD robot's mounting structure, specifically the ABB IRB 390. By integrating both dynamic and static analyses, the study effectively guarantees the structural robustness and operational accuracy of the robot. The design process encompasses multiple key phases, including CAD modeling, kinematic and static evaluations, and real-world application, all aimed at achieving the most efficient design. The novel combination of rigid body dynamics with finite element modeling (FEM) allows for a thorough and precise optimization of structure design, making it highly suited for industrial applications [1].

2. State of the art

The current stage focuses on the production of such structures used in industrial environments, highlighting the practical applicability of the proposed solutions. The analysis performed using the finite element method plays a crucial role in evaluating nodal displacements, while also providing valuable insights into identifying areas susceptible to deformation. This information enables the proposal of localized stiffening measures aimed at ensuring that the robot's positioning accuracy remains unaffected by the elastic behavior of the load-bearing structure [2].

The ABB IRB 390 represents a high-performance industrial robot characterized by parallel kinematic architecture, specifically developed to meet the demands of high-speed, high-precision applications. As depicted in Figure 1, its advanced structural configuration and modular design contribute to its adaptability across a wide range of industrial settings.

The robot's reduced mass facilitates efficient execution of pick-and-place operations, which are integral to fields such as packaging, logistics, and electronics manufacturing. Moreover, the parallel kinematic arrangement promotes uniform load distribution, thereby mitigating mechanical stress on individual joints and enabling rapid, accurate positioning.

Fig. 1. ABB IRB 390 – Parallel acting Industrial Robot

3. Statement of Contribution

This study contributes to the field of industrial robotics by presenting a comprehensive methodology for the design and verification of the mounting structure of a high-speed parallel robot, specifically the ABB IRB 390. The primary contributions include the development of a CAD-based structural model, the integration of kinematic and static analyses to evaluate mechanical performance, and the application of finite element methods to identify critical deformation zones. Additionally, the research proposes targeted stiffening strategies to enhance positioning accuracy, ensuring structural integrity under dynamic loading conditions.

By bridging theoretical modeling with practical implementation, the work demonstrates the feasibility and effectiveness of simulation-guided design in optimizing robotic structures for industrial applications.

The mounting structure of the ABB IRB 390 parallel acting robot was designed with a modular architecture aimed at optimizing spatial efficiency for seamless integration within industrial work cells. The design prioritizes structural rigidity to preserve high-precision positioning, while also mitigating the risk of vibrations or resonant phenomenon that could compromise operational safety. Moreover, it is tailored to withstand dynamic loading conditions without sacrificing structural stability [3], [4].

Figure 2 illustrates the key reinforcement components that contribute to the system's mechanical rigidity. Material selection was carefully calibrated to achieve an optimal balance between strength and weight, employing high-performance aluminum alloys for the main frame and structural steel in zones subjected to significant mechanical stresses.

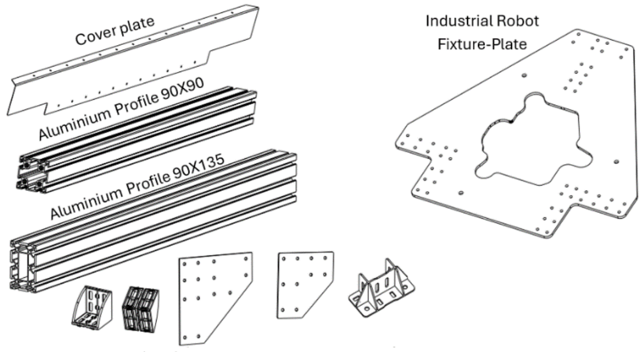

Fig. 2. Constitutive elements for the modular structure

The use of CAD modeling played a crucial role in defining both the structural configuration and spatial parameters of the mounting system. As illustrated in Figure 3, the modular design and its final dimensions were tailored to align precisely with the robot's operational envelope and the required range of motion for its components. Through a parametric, iteration-based approach, the model was progressively refined to ensure full compatibility with the robot's kinematic behavior, all while meeting the spatial limitations typical of industrial environments.

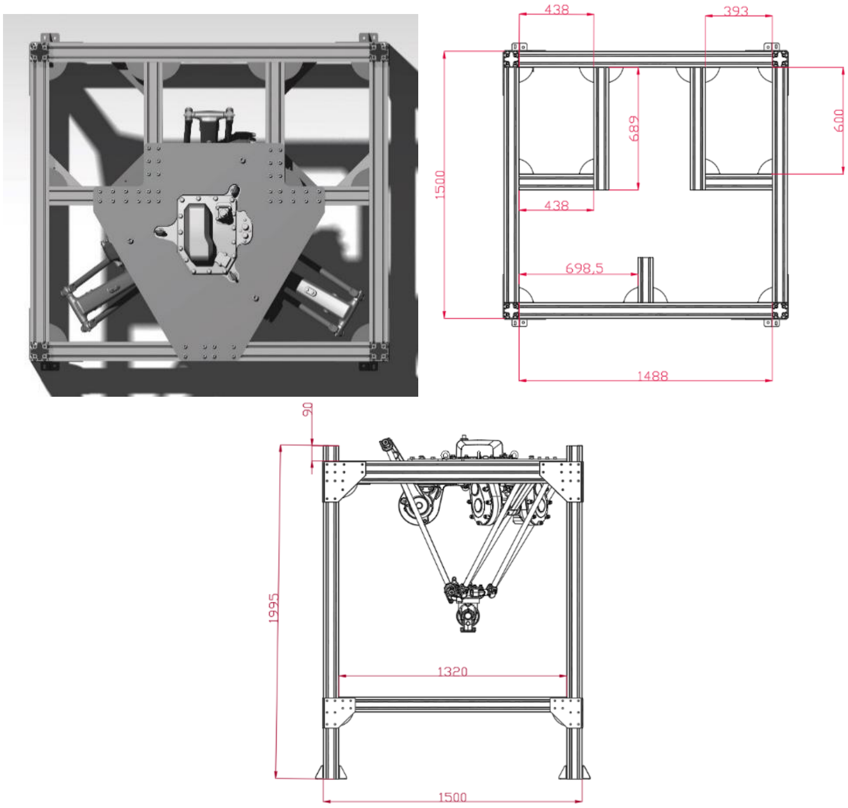

Fig. 3. General dimensions for modular designed structure

One of the main advantages of the developed structure lies in its modularity. In industrial settings, the position and orientation of components are frequently adjusted to accommodate ongoing modifications within flexible manufacturing cells. To meet these requirements, the structure was designed using standardized extruded aluminum profiles, selected for their enhanced bending stiffness, which makes them highly suitable for such applications. Additionally, to further increase the rigidity of the assembly, aluminum brackets were incorporated, while fastening is ensured through components made of heat-treated steel, thereby enhancing the overall stability and durability of the structure [5].

Table 1 presents all the components used in the manufacturing of the load-bearing structure of the DELTAPOD robot.

Table 1. Constitutive elements for robot mounting structure

ID	Functional Role	Material	Dimensions (L x l x h) [mm]	Quantity
1	Support columns	Alluminium Alloy extruded profile	90 x 90 x 2000	4
2	Upper crossbeam	Alluminium Alloy extruded profile	135 x 90 x 1320	2
3	Upper crossbeam	Alluminium Alloy extruded profile	135 x 90 x 1488	2

4	Cantilever beam	Alluminium Alloy extruded profile	135 x 90 x 689	2
5	Cantilever beam	Alluminium Alloy extruded profile	135 x 90 x 438	1
6	Cantilever beam	Alluminium Alloy extruded profile	135 x 90 x 392	1
7	Cantilever beam	Alluminium Alloy extruded profile	135 x 90 x 252	1
8	Bottom crossbeam	Alluminium Alloy extruded profile	135 x 90 x 1488	2
9	Bottom crossbeam	Alluminium Alloy extruded profile	90 x 90 x 1320	2

This configuration ensures structural stability and strength, tailored to support high-precision performance and adaptability within industrial environments.

Since the components of the industrial robot cannot be modified or adapted through machining, it is necessary to develop a 3D model and manufacture a dedicated element capable of supporting the robot's weight (140 kg). This structural component, responsible for the positioning of the robot, must maintain high rigidity to prevent excessive deformation that could negatively impact the robot's positioning accuracy, an essential parameter in the applications for which the system was designed. Therefore, steel was selected as the material for the primary support, mounting, and orientation element, due to its favorable mechanical properties and cost-effectiveness.

In figure 4 the structure used as a mounting structure for ABB IRB 390 - parallel acting robot is presented.

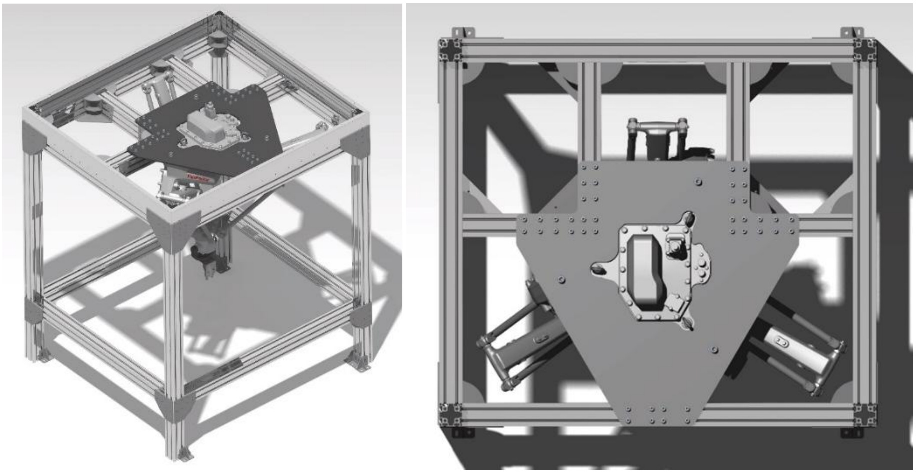

Fig. 4. Virtual prototype of designed structure

3. Study of Inertial influences on structural behavior

To assess the structural behavior under inertial loads generated during the operation of the industrial robot, the finite element method (FEM) is employed. This numerical technique is widely used for evaluating the mechanical response of structures, optimizing their geometry, and validating their performance under real operating conditions.

The rigid body dynamics analysis is performed to obtain numerical values as well as to determine the loading conditions imposed on the structure during operation. In every industrial application involving a robot, a motion cycle referred to as a cyclogram defines the robot's movements in real use. To accurately simulate real working conditions, a representative motion cyclogram is defined and implemented within the numerical analysis in ANSYS module [6].

In figure 5 the simulated working cycle for industrial robots is presented.

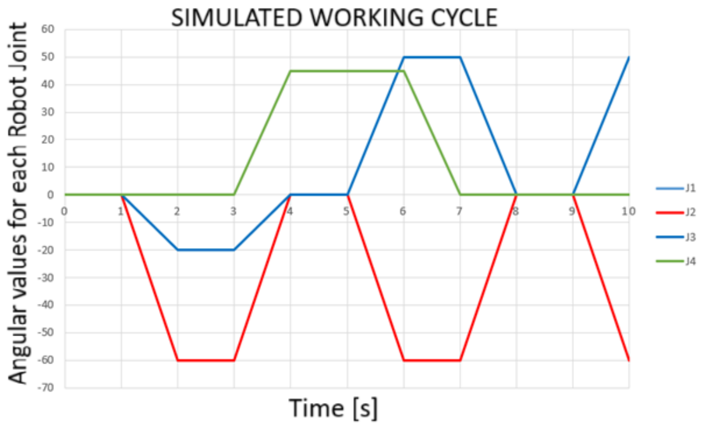

Fig. 5. Simulated working cycle for a real application

Through kinematic analysis, the inertial forces influencing the structural response during dynamic operation were quantified. A hybrid modeling approach was employed, combining three-dimensional solid elements for complex regions with one-dimensional bar elements to optimize the computational load. Figure 6 presents the recreated structural geometry, cross-sectional characteristics, and the applied meshing technique. The simulation not only enabled an efficient representation of the physical system but also highlighted the mechanical interplay between the robot and its support, identifying critical areas prone to elevated stress under dynamic conditions.

Maximum inertial loads are observed in the robot's most critical or disadvantageous operating configuration. This critical configuration corresponds to the position in the work cycle where the robot's segments are most extended. Figure 6 illustrates the posture associated with the highest inertial forces recorded in the simulated application.

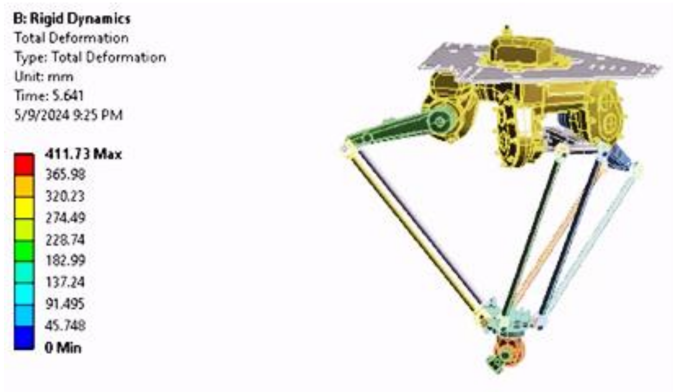

Fig. 6. Critical robot configuration

The structural model is developed using a combination of 3D solid elements and 1D beam elements, as a full discretization with solid elements may lead to the generation of large stiffness matrices. This increases computational demand, since the solver must process a significantly higher number of equations, which can reduce simulation efficiency.

In figure 7 is presented the geometry designed/simplified in ANSYS Workbench.

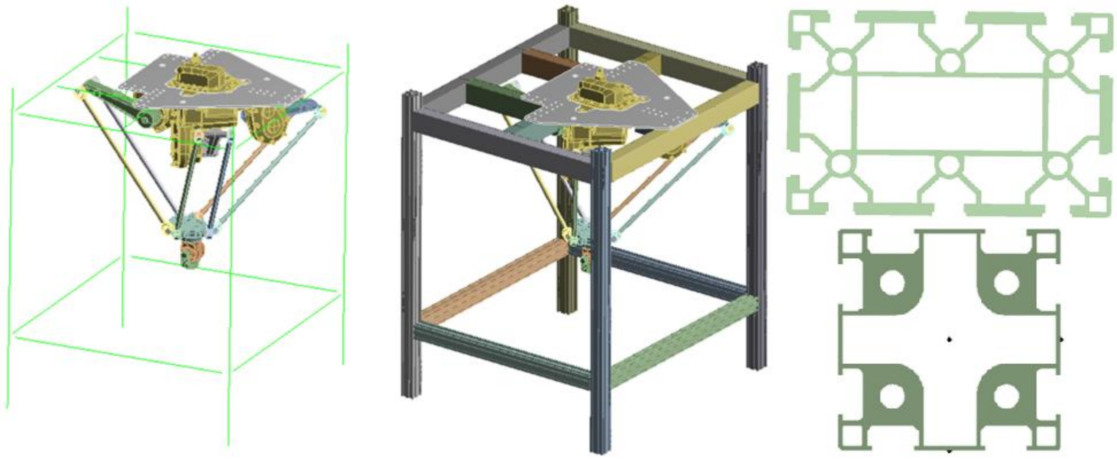

Fig. 7. ANSYS modeling using BEAM (1D) elements

The use of 1D beam elements in structural modeling provides a highly efficient and accurate method for analyzing frameworks composed of elongated components such as columns, beams, and support frames. This approach simplifies geometry by representing each structural member as a line element with defined cross-sectional properties, enabling a significant reduction in computational cost compared to full 3D solid mesh.

Beam elements capture both axial and bending behavior and allow the extraction of internal forces and moments directly, offering clear insight into load paths and structural performance. As such, this method is particularly suitable for modular assemblies, load-bearing frames, and other applications where high computational efficiency and reliable mechanical evaluation are essential.

In the present study, data obtained from the rigid body dynamic analysis (specifically the inertial forces generated by the movement of the robot segments during a working cycle) will be used as input for the static structural analysis. The purpose of the static analysis is to determine the stress distribution within the robot base mounting component, as well as to evaluate the nodal displacements under operating conditions.

Considering all inertial forces obtained from the dynamic analysis, Figure 8 illustrates the boundary conditions and loading scenarios applied in the static analysis.

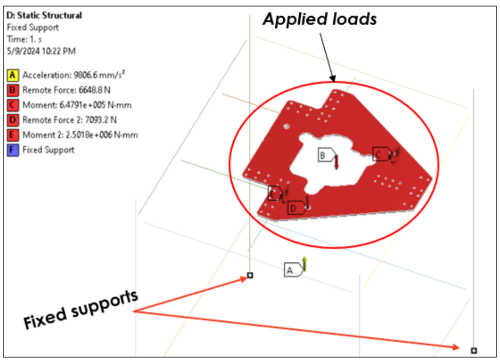

Fig. 8. Boundary conditions and applied loads on the model

One of the original aspects of the present approach lies in the hybrid discretization strategy, which combines one-dimensional and three-dimensional elements. Structural members such as beams and crossbars are modeled using 1D BEAM elements, while the robot's mounting plate is discretized using tetrahedral 3D elements.

In finite-element analysis, Element Quality encompasses a series of geometric and numerical metrics that gauge the fidelity of a mesh relative to ideal element shapes, with direct consequences for solution accuracy and convergence behavior.

Elements exhibiting near-unity aspect ratios, minimal skew and warping, and uniformly positive Jacobians produce well-conditioned stiffness matrices, thereby improving solver stability and reducing numerical error. In contrast, poorly shaped elements can introduce stress singularities, impede convergence, or even cause solver divergence.

Modern mesh-generation software reports Element Quality on a standardized scale (0-1 or 0-100 %), allowing engineers to detect substandard regions and apply corrective measures, such as local mesh refinement, node smoothing, or element-type substitution, prior to executing the final analysis. Figure 9 illustrates the finite-element mesh of the top fixture plate.

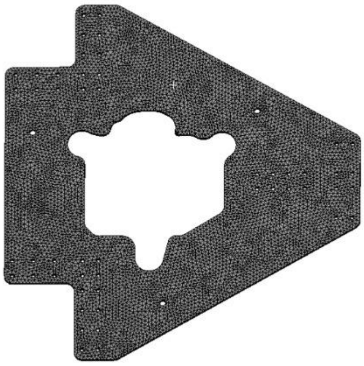

Fig. 9. Global tetrahedral mesh

The model has been meshed using tetrahedral elements with a uniform global mesh size of 10 mm. This meshing strategy was selected for its ability to furnish insightful results expeditiously, striking an optimal balance between solution fidelity and computational efficiency.

Depending on the specific application of the structural analysis, there exist benchmark values for assessing mesh quality. A suitably refined mesh is essential to obtain realistic results. In finite-element theory, load transfer occurs through nodes and thus through the associated elements. Excessively distorted elements can compromise accurate force transmission. Therefore, established meshing criterion is critical to ensure that the computed stress and deformation fields faithfully represent the true structural behavior.

In the present study, mesh elements are required to exhibit no more than 20% geometric distortion from their ideal shape. Accordingly, the average quality score for elements meeting this criterion is 80%. Figure 10 presents the global mesh evaluation criterion [7].

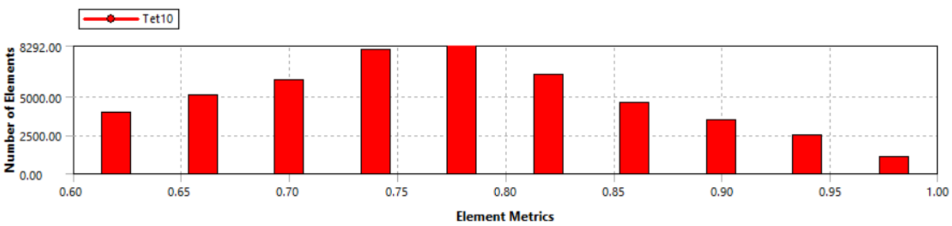

Fig. 10. Global meshing criterion

3. Static analysis results

Considering the loading conditions derived from the rigid-body dynamic analysis (Figure 8), the maximum nodal displacements of the entire support structure are evaluated, alongside the von Mises equivalent stresses. By examining the displacements, one can estimate the actual positioning error introduced over a robotic work cycle. In industrial practice, motion data are acquired using the robot controller, which records the sequence of movements (the motion cyclogram) for subsequent analysis.

Figure 11.a. highlights the region of the structure experiencing the greatest deformations. The highest total displacement measured at the cantilevered beams (fixed at one end and free at the other) is 6 [µm]. Given the robot's nominal positioning precision of 70 [µm], this deformation incurs an approximate 8.57 % reduction in accuracy.

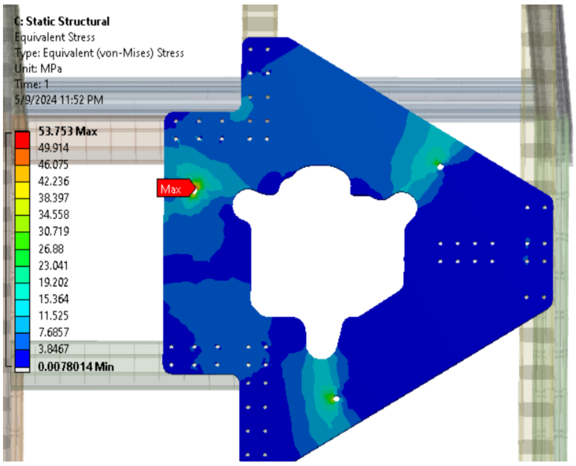

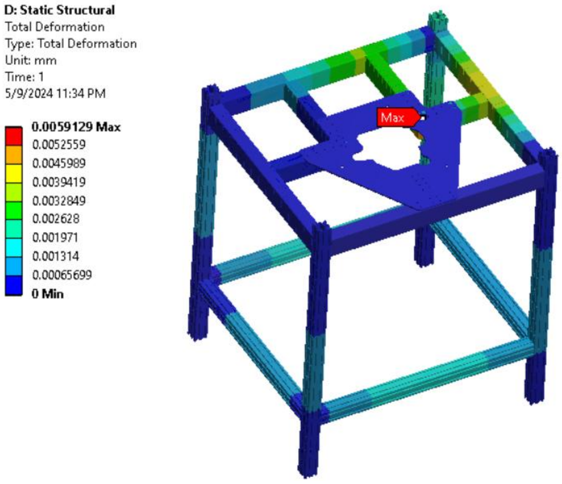

a. b.

Fig. 11. a. b. Distribution of total displacements and von Mises equivalent stresses

The von Mises stress is a scalar value derived from the combination of the three principal stresses acting on a material. This equivalent stress allows for the comparison of complex stress states with the material's yield strength, facilitating the assessment of structural safety. If the von Mises stress exceeds the material's yield limit, it is considered that the material will undergo plastic deformation, which may lead to structural failure.

In the context of analyzing the support structure of an industrial robot, the application of the von Mises criterion is essential for identifying critical areas where stress concentrations may occur. This evaluation allows engineers to determine whether the structure can withstand the dynamic loads imposed by the robot's movements without compromising structural integrity or operational precision.

Therefore, applying the von Mises criterion in structural analysis provides a clear perspective on material behavior under complex loading conditions and serves as an indispensable tool in the design and evaluation of modern mechanical structures.

3. Conclusions

The analysis indicates that the maximum total displacement of 6 [μm] represents approximately 8.45% of the robot's positioning accuracy, suggesting a minimal impact on operational precision. Stress concentrations identified at cantilever joints are effectively mitigated through reinforced closed-frame designs, enhancing structural durability. The modular structure's compactness and ease of integration make it adaptable for various industrial applications. Using an integrated approach that combines kinematic and static analyses offers a robust framework for thoroughly assessing and enhancing both the dynamic and static performance characteristics of mechanical systems. This methodology enables engineers to evaluate motion-related behaviors alongside structural responses, facilitating informed design decisions that optimize overall system performance.

8. Bibliography

[1]. Grabiec, J., Pajor, M., Dunaj, P., "Finite Element Modeling of Dynamic Properties of the Delta Robot with Base Frame" in Materials 2022, 15, 6797, https://doi.org/10.3390/ma15196797;

[2]. Shehata, M., Elshami, M., Bai, Q., Zhao, X., "Parameter Estimation for Multibody System Dynamic Model of Delta Robot from Experimental Data" in IFAC Proceedings, Volume 54, Issue 14, 2021, Pages 72-77, ISSN 2405-8963, https://doi.org/10.1016/j.ifacol.2021.10.331;

[3]. Mirz, C., Hüsing, M., Takeda, Y., Corves, B. "Low-cost delta robot for the experimental validation of frame vibration reduction methods" in Symposium on Robot Design, Dynamics and Control (pp. 332-339), Springer International Publishing, 2022;

[4]. Costea, M., Năstase, M. S., Ancuța, A. A., "Determination of the Stress and Strain state in the mounting solution of parallel acting Industrial Robot", Scientific communication session, National University of Science and Technology POLITEHNICA Bucharest, 2023, industrialengineeringjournal.eu;

[5]. Guler, S., Karagülle, H., "Finite Element Analysis of Structures with Extruded Aluminum Profiles Having Complex Cross Sections" in Latin American Journal of Solids and Structures. 13. 1499-1514. 10.1590/1679-78252755;

[6] Pilz, S., "Multibody Dynamics: Rigid and Flexible Methods", ANSYS Advantage Volume II, Issue 4, 2008, pag. 40-42;

[7]. Chen, X., Liu, Y., (2018), "Finite Element Modeling and Simulation with ANSYS Workbench", Second Edition, CRC Press, https://doi.org/10.1201/9781351045872;

PNEUMATIC EQUIPMENT DESIGNED FOR BENDING METAL SHEETS USED IN THE COVERING OF MODULAR CONTAINERS

CUCU Andrei, MAN Giulia-Maria, COSTEA Mihai, JIGA Gheorghe-Gabriel(Conducător științific)

Faculty of Industrial Engineering and Robotics, Specialization: Robotics, Year of Study: II, e-mail: andrei.cucu44@yahoo.com

The paper presents the development of an innovative pneumatic device for bending metal sheets used in the covering of modular containers, aiming to improve production efficiency. The solution involves the use of a pneumatic piston that transforms translational motion into rotational motion, enabling the precise bending of metal sheets in 500 mm segments. The prototype, initially 3D printed, was tested and later manufactured in metal, demonstrating high reliability and efficiency. Finite element analysis enabled the correct sizing of components, while integration into the factory's pneumatic system was optimized for safety and ergonomics. The results showed a significant increase in productivity, cost reduction, and improved quality of the final product.

KEYWORDS: Pneumatic device, Modular container, Process mechanization, Industrial prototype, Productivity optimization

1. Introduction

This paper focuses on optimizing a critical process in the manufacturing of modular containers—bending the metal sheets used for roofing—a stage which, until recently, was performed manually (see Fig. 1), with high consumption of time and resources. The main objective was the development of a pneumatic device capable of automating this operation, replacing inefficient traditional methods and ensuring fast, precise, and repeatable processing.

The proposed solution consists of a system that uses a pneumatic piston to convert translational motion into rotational motion, enabling controlled bending of the sheet along the container's profile. The development process included 3D modeling, rapid prototyping, functional testing, and finite element analysis for structural validation.

Through the implementation of this device, the project achieved its goals: increased productivity, reduced physical effort for operators, and improved quality of the final product.

Fig. 1. Initial Bending Process

2. Current state of the art

The bending of sheet metal for modular container roofing currently represents one of the most inefficient stages in the production process. At CERES CONTAINER, this operation was carried out manually, through repeated hammer blows and clamping with pliers, requiring a large number of workers and significant execution time. The traditional method is slow, imprecise, and physically demanding, leading to variations in product quality and negatively impacting productivity.

Research has shown that none of the factories in Romania or elsewhere in Europe employ an automated process for this operation, due to the challenges posed by the narrow profile of the containers and the variable dimensions of the sheet metal. The sheets used range in surface area from 1×2 m² to 4×12 m², and the container profile is very narrow (see Fig. 2), which precludes the use of bulky equipment. These technological limitations highlight the need for a compact and efficient pneumatic solution capable of automating this essential process.

Fig. 2. The Profile on Which the Sheet Metal Is Bent

3. Design, 3D printing, FEM analysis, and pneumatic structure

The bending device was entirely modeled in SolidWorks (see Fig. 3), using advanced parametric design tools to adapt each component to the constraints imposed by the geometry of the container profile. The design included a fixed “T”-shaped part welded to the container roof frame and a movable part articulated through six welded hinges, allowing controlled rotation around a single axis. Special attention was given to the positioning of the piston rod, which is connected to a ring-section bar positioned eccentrically relative to the hinge axis, enabling the efficient transformation of translational motion into rotational movement of the mobile part. Precise dimensions, such as the 70 mm distance between the hinges and the force application point, were established to obtain an optimal bending torque. Additionally, an active working area of 500 mm in length was modeled, corresponding to the device’s useful span, allowing for segmented coverage around the full perimeter of the container.

To verify the form, functionality, and ergonomics of the system, a physical prototype was created using FDM 3D printing technology, with PLA filament on a Bambu Lab P1S printer (see Fig. 4). The printed model enabled testing of hinge positioning, functional clearances, and overall geometry before proceeding with steel fabrication.

Several versions were printed in different colors to distinguish components during the validation process. Based on observations during prototype handling, minor design adjustments were made—such as modifying the thickness of the movable part and integrating mounting points for an interchangeable handle, adaptable for both left- and right-handed users.

Finite Element Method (FEM) analysis was carried out to determine the force required by the pneumatic piston to bend the galvanized sheet with a thickness of 0.6 mm (see Fig. 5). The sheet material was modeled with bilinear behavior, including an elastic region according to Hooke's Law and a plastic region with a reduced hardening modulus. The stress–strain curve was generated based on the properties of galvanized S235 steel, and the geometry of the device was discretized into solid elements for high accuracy. Forces were applied iteratively (see Fig. 6), and the analysis revealed the distribution of equivalent von Mises stresses and the maximum deformations occurring in the hinge area and the movable part. Results led to the selection of a piston with a force of 1800 N to ensure proper bending without residual deformation of the sheet or structural failure [3], [4].

The pneumatic structure (see Fig. 7) was dimensioned to integrate effectively into the factory's compressed air system, which operates at a pressure of 8 bar. The selected pneumatic cylinder has a 100 mm stroke, an M16 threaded rod, and is mounted using two types of supports: PHSA M16 rod ends at the front and CB and YB mounts at the rear. The pneumatic valve used is a 5/3 G1/4 model, manually actuated with automatic spring return, ensuring safe operation and the ability to stop the piston at any point. The entire system is supplied via an XOU G1/4 air preparation unit, which includes a filter, lubricator, pressure regulator, and moisture separator to ensure a clean and steady air flow. Pneumatic connections are made using PTFE hoses with Ø10 mm diameter, connected via G1/4 quick couplings, and equipped with throttles for regulating the piston's advance and return speed. For operator comfort, a noise muffler was added to reduce acoustic impact during repeated use. This configuration ensures reliability, minimal maintenance, and easy integration into the factory's production flow [1], [2], [5].

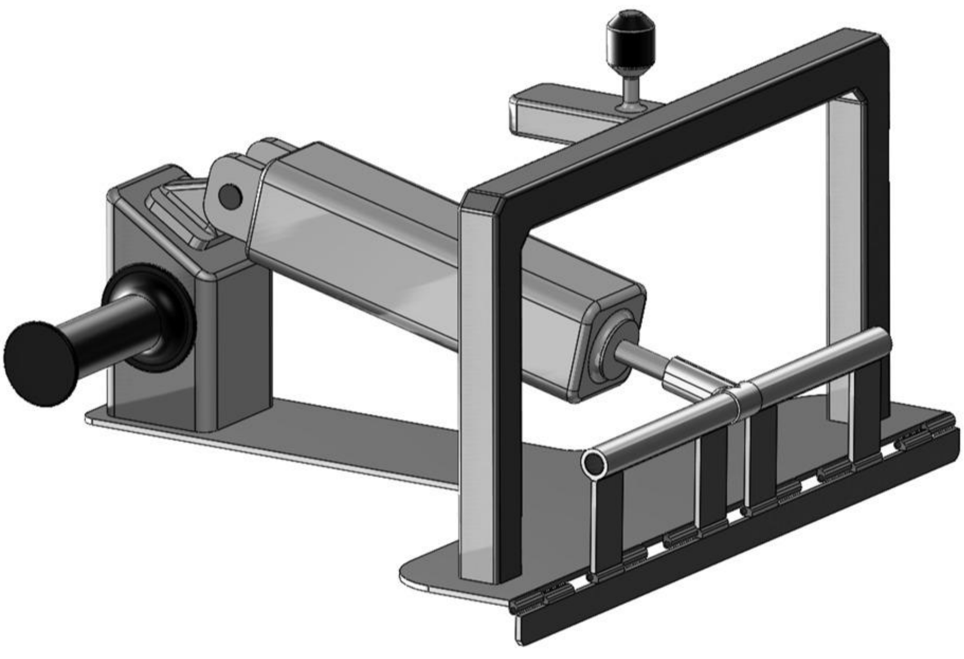

Fig. 3. 3D Model of the Device Designed in SolidWorks

Fig. 4. 3D Printed Model

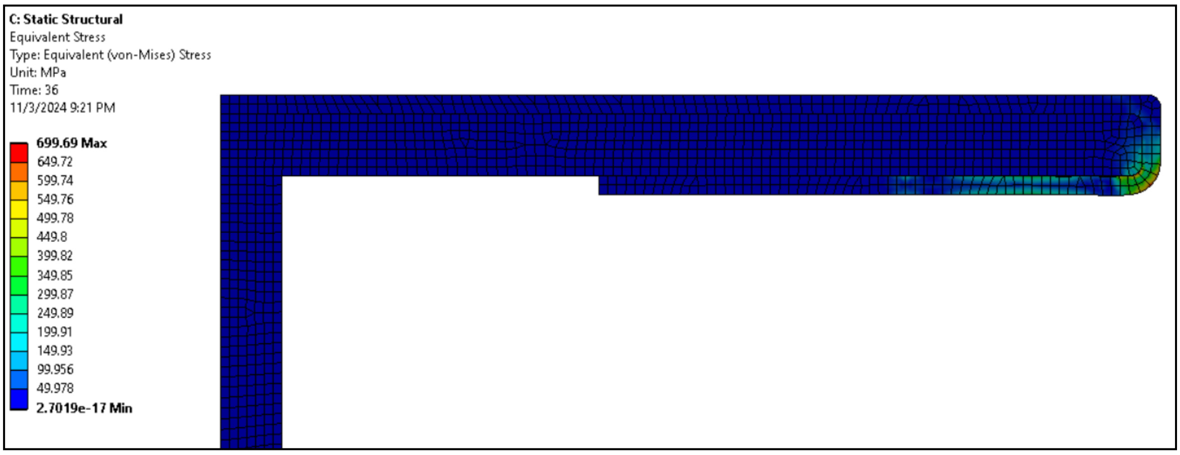

Fig. 5. Distribution of von Mises Equivalent Stresses

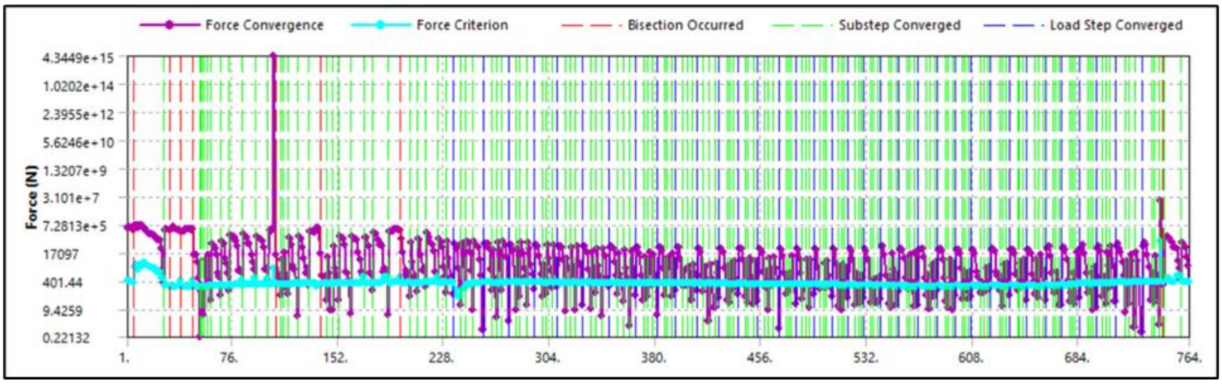

Fig. 6. Convergence of Iteratively Applied Forces

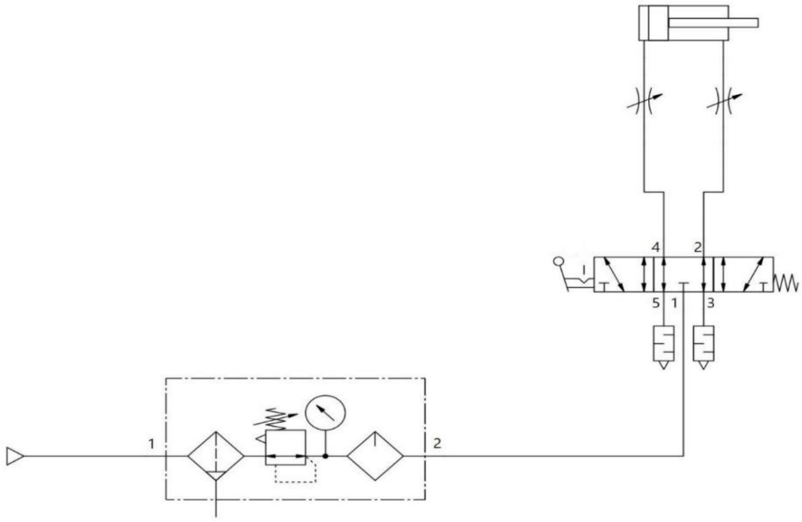

Fig. 7. Pneumatic Schematic

4. Selection of components, materials and fabrication

For the development of the pneumatic sheet metal bending device, the selection of components and materials was based on requirements such as mechanical strength, compatibility with the existing compressed air system, reduced weight, and the ability to be integrated into the limited space imposed by the container profile. The metal structure of the device was constructed from S235JO structural steel, chosen for its good mechanical properties, ease of machining and welding, and cost-effectiveness. The thicknesses used were 4 mm for the movable part and 6 mm for the fixed base, values determined through FEM simulations and practical testing. For the bending area, a circular-section bar was selected to ensure uniform transmission of force from the piston rod to the metal sheet.

The pneumatic cylinder selected provides a force of 1800 N, with a stroke of 100 mm, and operates at a working pressure of 8 bar, fully compatible with the factory’s compressed air network. Mounting was achieved using standardized accessories: PHSA M16 rod ends for the front connection and CB and YB supports for the rear fixation. The valve used is a 5/3 G1/4 type, manually actuated with automatic spring return, ensuring safe and precise control over piston movement. Additional components include: PTFE hoses Ø10 mm, G1/4 connectors, flow control valves (drosels) for speed adjustment, a BSL G1/4 noise muffler, and the XOU G1/4 air preparation unit, which incorporates a filter, lubricator, and pressure regulator.

The physical fabrication of the device (see Fig. 8) began with plasma cutting of the metal parts, followed by finishing using an angle grinder. Welding was performed using the MIG process, with CORGON shielding gas (a mix with 18% Argon), to obtain clean and strong joints. The hinges, elevation components, and actuation bar were welded with high precision. Afterward, the entire assembly was sandblasted and painted to provide corrosion protection and a uniform appearance.

For improved ergonomics, a threaded rear handle was added, which can be positioned on either the left or right side of the device depending on the operator's preference. Upon completion of the assembly, functional tests were conducted to verify the full piston stroke, the sealing of the pneumatic circuit, and the effectiveness of the bending process.

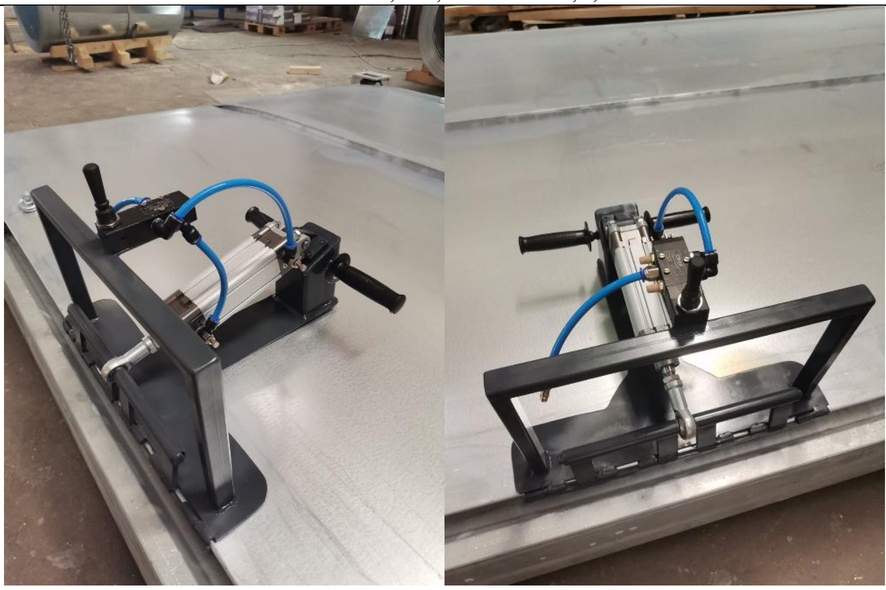

Fig. 8. Final Device

5. Conclusions

The development and implementation of the pneumatic sheet metal bending device have led to a major improvement in the modular container production process. By eliminating the manual method—which was slow and physically demanding—a semi-automated, efficient, and precise workflow was achieved.

Productivity increased by over 350% per worker, as the number of operators was reduced from six to two, while maintaining a steady output of six containers per day. Furthermore, the bending process became uniform and repeatable, improving the quality and consistency of the final product.

The device also brought significant ergonomic benefits, reducing physical effort and minimizing the risks associated with manual labor. The pneumatic system is reliable, easy to maintain, and adaptable to various profile dimensions, allowing seamless integration into the existing production line.

This technical solution has proven to be practical, cost-effective, and scalable, with strong potential for wider application in the container industry and beyond.

6. References

[1]. Prodan, D., Dușan, C., & Bucureșteanu, A. (2004). *Acționări pneumatice. Elemente și sisteme*. Editura Printech. ISBN: 973-718-020-8;

[2]. Taca, C., & Păunescu, M. (2007). *Acționări hidraulice și pneumatice*. Editura Universității Politehnica din București. ISBN: 978-973-755-388-1;

[3]. Dumitras, C. (2011). *Aplicații ale metodei elementelor finite în inginerie*. Editura Performantica. ISBN: 978-973-730-895-5;

[4]. Reddy, J. N. (2005). *An Introduction to the Finite Element Method* (3rd ed.). McGraw-Hill Education. ISBN: 978-0-07-246685-0;

[5]. Liu, Y., & Zhang, Z. (2019). *Methods to Evaluate and Measure Power of Pneumatic System and Components*. Chinese Journal of Mechanical Engineering, 32(1), 1–12. https://doi.org/10.1186/s10033-019-0354-6

THERMAL EFFECTS ON MIRROR COATING INTEGRITY IN HIGH-POWER LASER SYSTEMS AND NUCLEAR APPLICATION

1. **ENE Cosmina-Cristiana, and Prof. Dr. Ing. JIGA Gabriel(Conducător științific)**

Faculty: Industrial Engineering and Robotics, Specialization: Mechatronics and Robotics,Year of Study: I, e-mail: cosmina.36.ene.9@gmail.com

SUMMARY: This study investigates how dielectric, silver, and gold mirror coatings respond to thermal stress from high-energy laser pulses, as observed through experimental interferometry and spectral analysis. Conducted at the Extreme Light Infrastructure - Nuclear Physics facility in Magurele, Romania, this research explored deformation, stress behavior, and optical resilience in real-world laser interactions. Dielectric coatings showed minimal expansion and deformation, maintaining optical integrity, while silver and gold absorbed more energy and experienced notable thermal distortion. These findings support the use of dielectric mirrors in extreme photonic environments such as industrial laser processing and nuclear research.

KEYWORDS: mirrors, lasers. thermal stress, dielectric materials, strength

2. Introduction

In the world of high-power photonics, mirrors are no longer passive components. They are precision-engineered, multilayered interfaces responsible for controlling and guiding some of the most intense energy fluxes produced by humanity. From ultrafast laser systems to advanced industrial applications, mirrors are tasked with reflecting beams that can burn through steel, initiate nuclear reactions, or trigger femtosecond-scale diagnostics. Yet these mirrors remain vulnerable to their own function. When faced with high fluence and rapid thermal cycling, even a nanometer defect or distortion can spiral into catastrophic failure. As laser powers increase into the petawatt range, understanding how different mirror coatings behave under thermal stress becomes essential not just for system performance, but for the survival of the optical elements themselves. This research investigates three widely used coating materials (dielectric stacks [1], silver, and gold) under thermal stress generated by high-energy laser pulses. By coupling experimental fringe analysis with thermal modeling and spectral diagnostics, we quantify how each coating type reacts, deforms, and potentially fails. Our goal is to identify which materials are most thermally robust, and what trade-offs exist in choosing coatings.

3. Scientific background

Mirror coatings represent the interface between optical precision and material science. When subjected to high-power laser beams, they undergo thermal phenomena governed by physical parameters such as: absorption of energy, leading to localized heating; thermal expansion, disorting surface geometry; stress gradients from uneven heating, risking deformation or delamination.

Dielectric coatings (typically multilayer stacks of SiO_2 and TiO_2 or Ta_2O_5) are engineered for minimal absorption and precise spectral control but require complex thermal management. Silver offers superior reflectivity in the visible range but tends to overheat due to absorption in the near-infrared. Gold performs better thermally than silver in the infrared spectrum, though its density and moderate absorption limit its use under extreme laser fluences.

4. Experimental setup – Mach-Zehnder interferometer

The investigation combined optical interferometry to assess deformation and energy absorption.
The Mach-Zehnder interferometer splits a coherent laser beam into two optical paths: one serving as reference, and the other directed onto the test mirror [2]. Upon recombination, any phase distortion caused by surface deformation leads to fringe pattern shifts. These fringe distortions serve as direct indicators of thermally induced stress and optical surface expansion.

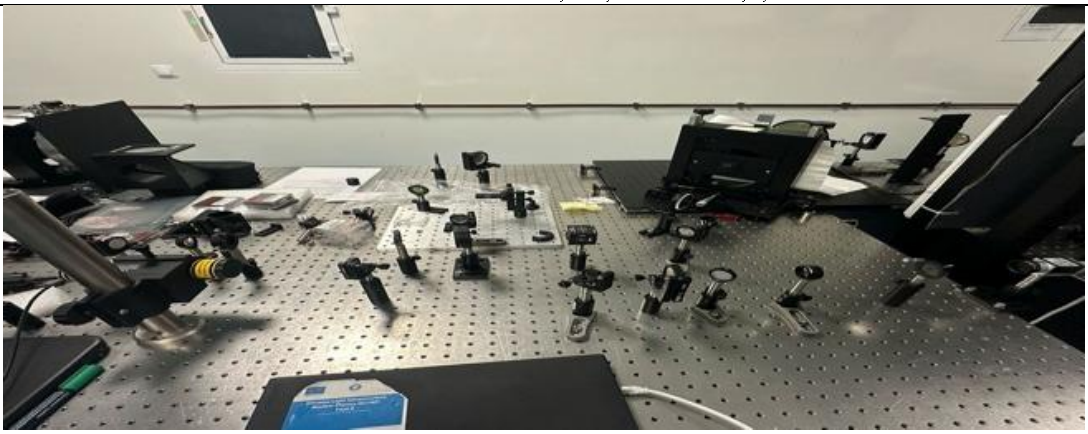

Fig. 1. Interferometer setup in the Optics Laboratory, Magurele

The interferometric system was built using four high-reflectivity planar mirrors, two precision beam splitters (BS1 and BS2), a set of collimating lenses for spatial coherence, a high- resolution Basler camera paired with Pylon software [3], the laser source and the analysed mirror with the specific coating.

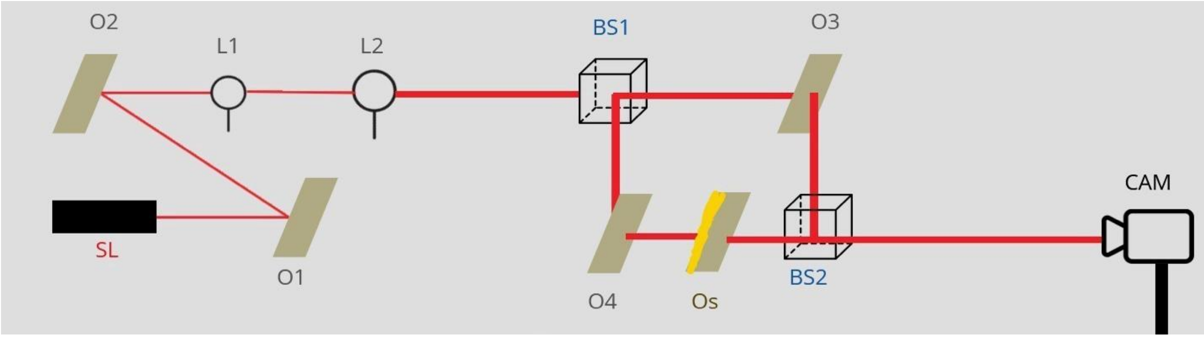

Fig. 2. Schematic of the interferometer

Fig. 3. Fringes seen with the naked eye

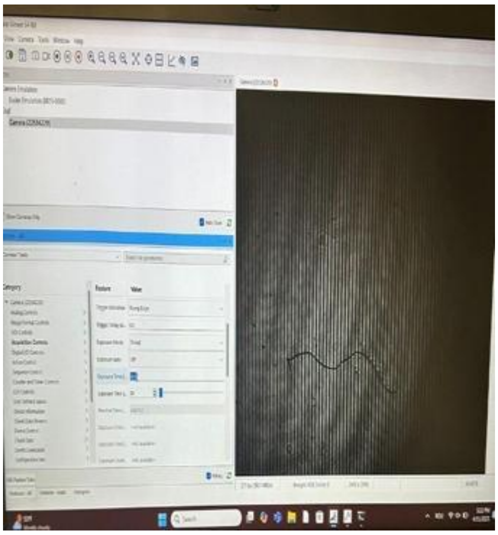

Fig. 4. Pylon software

4. **Group delay dispersion evaluation**

To better understand the phase integrity and temporal behavior of laser pulses interacting with optical coatings, a detailed analysis of **Group Delay Dispersion (GDD)** was conducted for each mirror type. GDD is a second-order dispersion parameter defined as the derivative of the group delay with respect to angular frequency or wavelength [4]. In essence, it quantifies how much different spectral components of a pulse travel at different speeds through a material or are reflected with different phase delays. This becomes especially critical in femtosecond laser systems, where even slight phase mismatches across the spectrum can stretch a pulse temporally, introduce chirping, or reduce the peak intensity upon focusing.

The dielectric mirror exhibited a controlled GDD curve, indicating minimal distortion introduced during broadband reflection. This performance is a result of the mirror's carefully engineered multilayer stack, typically alternating layers of high- and low-index materials (e.g., Ta_2O_5 and SiO_2) designed to achieve both high reflectance and controlled phase response. In practice, the measured GDD for this mirror stayed well below ± 100 fs² across the 700–900 nm interval, which is within acceptable limits for pulse durations below 30 fs. This makes the dielectric coating the most suitable candidate for chirp-free propagation in ultrafast beamlines, particularly when maintaining Fourier-limited pulse duration is necessary for precision interactions with matter.

In contrast, the silver-coated mirror displayed erratic GDD behavior, with measured values fluctuating rapidly and exceeding ± 400 fs² at multiple wavelengths. These oscillations are caused by the intrinsic material properties of silver, which lacks the dispersion-engineered structure of dielectric stacks. The result is a spectral phase profile that severely alters the time structure of any femtosecond pulse, potentially increasing the duration by an order of magnitude and weakening the fluence at the focus. For this reason, despite its excellent reflectance in the visible range, silver coatings are generally unsuitable for use in front-end compressors or ultrafast diagnostics where phase linearity is critical.

The gold-coated mirror offered a more stable, though still moderate GDD performance. Its GDD curve featured a smoother profile than silver's, with a broad peak near 720–740 nm followed by a gradual descent toward the infrared. While values were not as low or flat as those observed in the dielectric case, they remained within ± 200 fs² over most of the spectrum. This makes gold a viable option for applications involving longer pulses (e.g., >100 fs), mid-IR wavelengths, or situations where thermal durability outweighs the need for strict dispersion control.

Quantifying GDD is vital not only for characterizing temporal fidelity, but also for predicting cumulative effects when multiple optical elements are involved. In high-power laser systems like those operated at ELI-NP, even a small phase error introduced at each bounce can accumulate over beam paths of tens of meters, distorting temporal pulse structure and reducing system efficiency.

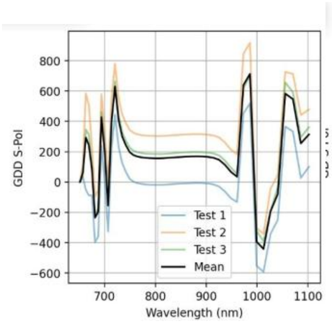

Fig. 5. GDD Dielectric mirror

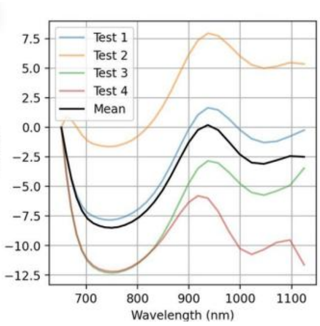

Fig. 6. GDD Silver Mirror

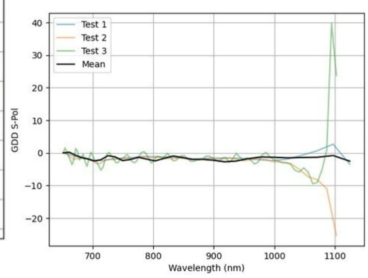

Fig. 7. GDD Gold mirror

5. Finite element analysis

To complement the interferometric and GDD evaluations, finite element analysis (FEA) and heatmap visualization in MATLAB were performed on all three mirror types to estimate thermal stress, energy absorption, and surface deformation under simulated laser exposure. The dielectric-coated mirror showed a uniform, low-intensity absorption profile. Despite the appearance of red regions in the heatmap, the absorbed energy never exceeded ~0.0027 J/cm², well below its damage threshold. The mirror maintained energy stability across the surface, highlighting its suitability for ultrafast optics.

The gold-coated mirror revealed central energy concentration between 0.15–0.5 J/cm², forming concentric rings likely caused by local roughness or interference. Absorption exceeded the damage threshold (~0.1 J/cm²), indicating higher risk of localized thermal failure. Despite excellent IR reflectance, gold's density and absorption require strict thermal management. Silver-coated mirrors exhibited the highest and most uneven absorption— ranging from 0.3 to 0.8 J/cm², significantly surpassing their known damage threshold (~0.225 J/cm²). The presence of concentric high-intensity zones aligned with micro-defect interference suggests a combination of poor phase stability and local absorption spikes. These behaviors reinforce previous observations from GDD and fringe deformation.

To explain these results at the atomic level, we must consider the microstructure and crystal arrangement of each coating material. Dielectric coatings are typically composed of alternating layers of non-metallic oxides, such as SiO_2 and Ta_2O_5. These materials are amorphous or polycrystalline and do not contain free electrons,

which minimizes both absorption and conduction of heat. Their structure is tightly bonded, with wide band gaps that prevent significant energy uptake from incident photons, contributing to the uniform heatmap observed.
In contrast, both silver and gold are metals with a face-centered cubic (FCC) lattice structure. This crystal arrangement allows for high packing density and malleability but also results in a high density of free electrons in the conduction band. When exposed to intense laser light, these free electrons absorb and re-emit energy, causing localized heating. The increased electron mobility facilitates non-radiative energy transfer, which elevates temperature gradients in small regions.
Silver, in particular, has a relatively low melting point and surface hardness, making it more susceptible to deformation and damage when microstructural imperfections—such as dislocations or surface roughness—enhance localized absorption. Gold is slightly more thermally stable but still shares the same FCC structure and free-electron behavior [5], which explains the concentric thermal absorption rings and higher central intensities.

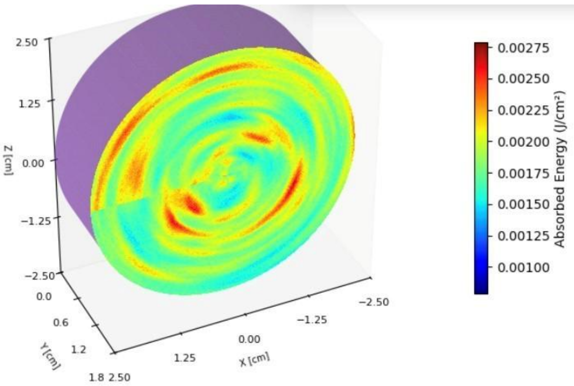

Fig. 8. Dielectric mirror heatmap

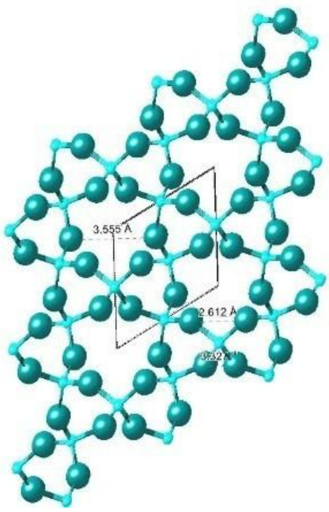

Fig. 9. SiO2 base structure

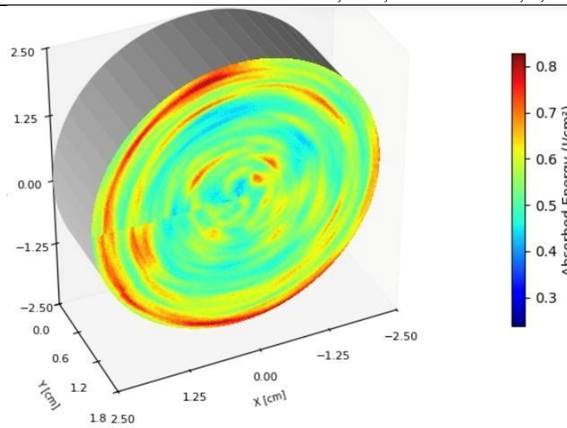

Fig. 10. Silver mirror heatmap

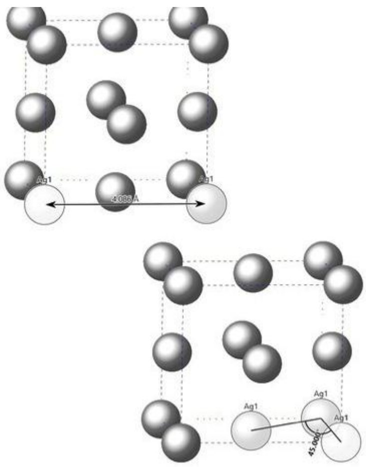

Fig. 11. Ag atomic structure

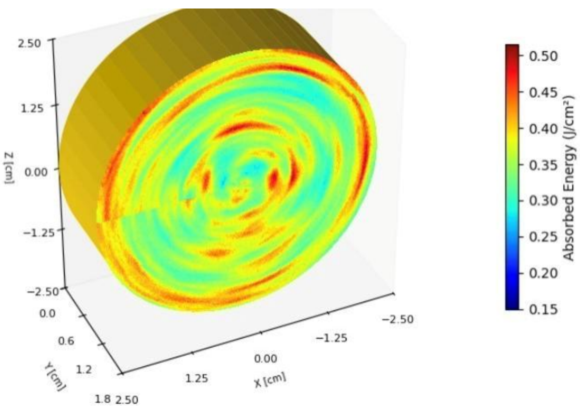

Fig. 12. Gold mirror heatmap

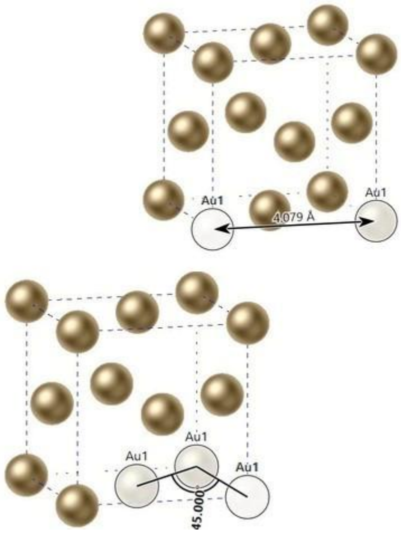

Fig. 13. Au atomic structure

6. **Conclusions**

Dielectric-coated mirrors show the highest thermal and optical stability under high-power laser exposure, with minimal deformation and low absorption.
Although the manufacturing of dielectric stacks can be more demanding due to layer precision and angular sensitivity, their benefits in long-term stability, damage threshold, and spectral control far outweigh these challenges. Their performance under femtosecond-scale fluences confirms their superiority in environments where thermal resilience and optical coherence are critical.
The increasing complexity of high-power laser systems demands optical components that can withstand extreme thermal and mechanical stress while maintaining phase stability. This study highlights how material structure, electronic properties, and coating design influence mirror performance under such conditions. By combining experimental data with simulation and atomic- scale analysis, we gain insight into the mechanisms behind deformation and energy absorption, paving the way for future innovations in photonic materials and thermal-resistant coatings.

Bibliography

[1] Joannopoulos, J. D., Meade, R. D., & Winn, J. N. (1995), Photonic Crystals: Molding the Flow of Light, Princeton University Press, Princeton, ISBN 978-0-691-04317-4.

[2] Leuthold, J. (1999), Advanced Indium-Phosphide Waveguide Mach-Zehnder Interferometer All-Optical Switches and Wavelength Converters: Theory, Design Guidelines & Experimental Results, Hartung-Gorre Verlag, Konstanz, ISBN 978-3- 89649-410-9.

[3] Basler AG (2022), pylon Software Suite Documentation, Basler AG, Ahrensburg: https://docs.baslerweb.com/pylon-software-suite.

[4] Chen, X., Hurley, J. E., Nord, J. L., Nikulin, I., Dainese, P., Sauer, M., & Li, M.-J. (2025), Measurements of Group Delay and Chromatic Dispersion of Hollow-Core Fiber Using a Frequency Domain Method, Photonics, 12(1), 47: https://doi.org/10.3390/photonics12010047.

[5] Tilley, R. J. D. (2006), Crystals and Crystal Structures, John Wiley & Sons, Chichester, ISBN 978-0-470-01820-0.

VERIFICATION OF THE STRUCTURAL INTEGRITY OF A ROBOTIC ARM WITH 6 NCA USING THE FINITE ELEMENTS METHOD

ȚENESCU Matei-Mihai1, MANOLE Robert Vasile, CÎRJA Rareș, DINICĂ Bogdan-Andrei, BLEAH Dionisie Cristian, ZAMFIROIU Mihai Alexandru, JIGA Gheorghe-Gabriel (Conducător științific)
[1]Faculty of Industial Engineering and Robotics, Specialization: Robotics, Year of study: II,
e-mail:tenmatei760@gmail.com

ABSTRACT: This report starts with determining the motion loads developed in predetermined points of interest in the structure of a 3D printed robot, by analyzing a motion cyclogram in Ansys Rigid Dynamics Module. As an added benefit the required torque of used DC motors can also be determined with the same analysis. After determining the motion loads, they were imported into Ansys Static Structural to evaluate stress and deformation that appears in the structure. As of the publishing date, topological optimization of the 3D printed components is in progress to achieve a lighter structure, reduce strain on the motors, and ensure smoother operation.

KEY WORDS: articulated arm robot, finite element modelling, topology optimization, structural integrity

1. Introduction

This paper presents a verification of the structural integrity of a six-axis robotic arm designed as a simple-to-manufacture and easily configurable alternative to conventional industrial robots [1]. The proposed approach focuses on cost optimization by utilizing FDM 3D printing for the fabrication of joining components, which are combined with off-the-shelf standardized metallic parts [2].

This strategy ensures a reliable supply chain for replacement parts and enables modifications at a significantly reduced cost. The structural analysis aims to confirm the conformity of the stresses developed within the mixed-material structure.

2. Dynamic analysis

The analysis begins in Ansys Rigid Dynamics Module, using a predetermined cyclogram (Fig. 1) applied to a slightly simplified model of the robotic arm (Fig. 2) manipulating a point mass of 2 [kg]. All connections between components are modeled using joints, specifically fixed and revolute types [3].

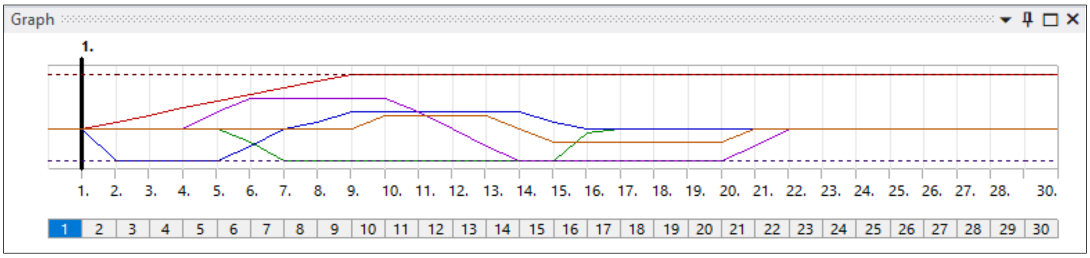

Fig. 1. Movement cyclogram for all kinematic joints

Following the completion of the dynamic analysis, the required motor torque was identified as 9.84 [Nm]. The motion loads export function was then used to transfer the results from the dynamic analysis into the static analysis.

3. Static analysis

The structural analysis continues in Ansys Static Structural, where motion loads (Fig. 3) are applied to the components of interest and each component is analyzed individually.
Components are meshed using the tetrahedron method with a mesh size of 2 [mm], selected for its superior accuracy compared to cartesian or multizone approaches in this context. This meshing strategy resulted in 114,389 nodes and 65,959 elements, with most elements exhibiting quality values in the 0.63–0.88 range, indicating overwhelmingly positive results (Fig. 4).

Although the same meshing method was applied to all components, certain complex geometries required additional refinement in specific regions with a smaller mesh size to maintain element quality.

Fig. 2. Simplified structure

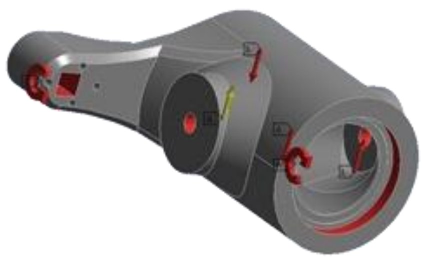

Fig. 3. Motion's loads effects

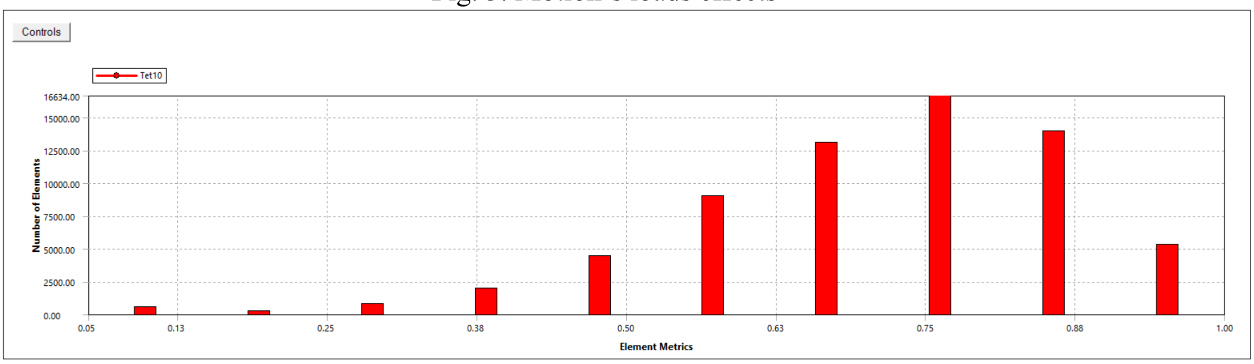

Fig. 4. Element quality criterion

The results obtained from the static structural simulation indicate that all components remain within the maximum allowable stress and deformation limits for the intended application. However, a few locations exhibit elevated stress concentrations that, while not exceeding the permissible values, will require further optimization [4]. All eight 3D-printed components were analyzed to ensure rigidity and compatibility with the standardized metallic parts. Of these, three components display areas that will require additional reinforcement (Fig. 5, Fig. 6, Fig. 7).

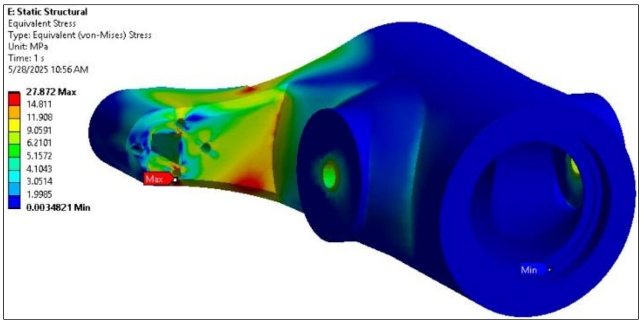

Fig. 5. Equivalent stress using von Mises principle in outer “roll” segment

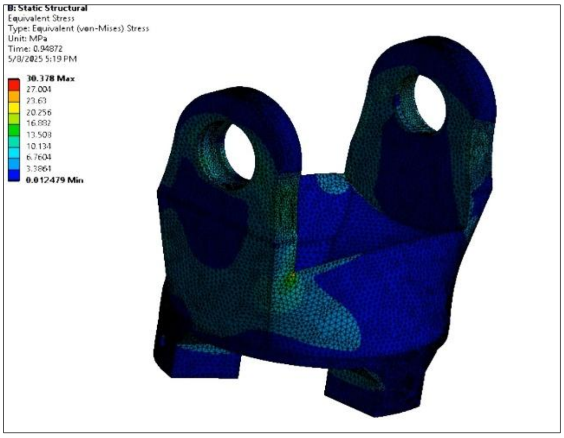

Fig. 6. Equivalent stress using von Mises principle in “pitch” segment

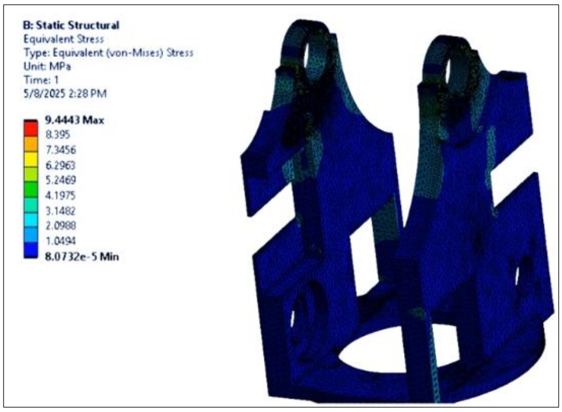

Fig. 7. Equivalent stress using von Mises principle in base segment

4. Topological analysis

Based on the results of the static structural analysis, a topological optimization of the components was initiated. The Ansys Static Structural results were imported into Ansys Topology Optimization, yielding several preliminary outcomes (Fig. 8) after 10 to 13 iterations.

While these initial results appear acceptable, further refinement will be necessary to produce manufacturable components.

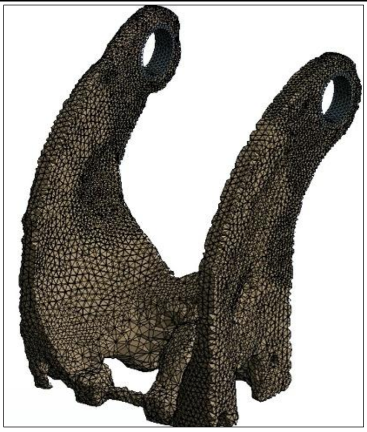

Fig. 8. Preliminary results

5. Conclusions

The analysis confirms that the initial design is fully capable of performing the required workload under standard conditions and is suitable for production after addressing the identified weak points. Ongoing research will focus on optimizing the geometry of the verified components by refining mesh quality and increasing the number of iterations in the topological analysis, with the aim of developing structurally optimized components for future versions of the robotic arm.

The use of the Finite Element Method has been essential for evaluating the structural behavior of the robotic arm, enabling informed design decisions. By combining structural verification with topological optimization, the goal is to create a more lightweight and reliable robot, prepared to meet both current and future performance requirements. Future efforts will concentrate on achieving better mass distribution and integrating more powerful motors, allowing the robot to manipulate heavier loads more efficiently.

The observed maximum deformation of 1.31 [mm] at the connection between the closed kinematic chain and the second link significantly impacts the robotic arm's precision and accuracy. Structural deformation at this critical joint directly translates into positional errors at the robot's end-effector, as even minor deflections can amplify considerably through subsequent links.

6. Bibliography

[1]. Adrian T. (2019), Title: *Precizia robotilor industriali. Studiul monografic*, Tehnica-Info Chișinău, Chișinău, ISBN 978-9975-63-449-6.

[2]. Niku SB., (2020), Title: *Introduction to Robotics – Analysis, Control, Applications 3rd Edition*, Wiley, Chichester, United Kingdom, ISBN: 978-1119-52-762-6.

[3]. Huei-Huang L., (2023), Title: *Finite Element Simulations with ANSYS Workbench 2023*, SDCpublication, ISBN 978-1-63057-615-8.

[4]. Ion S., Ion I., Liviu C., (2008), Title: *Mecanismele robotilor industiali vol. I*, A.G.I.R, ISBN: 978-973-720-206-2.

[5]. Theodor B., Alexandru D., Florin D.A., (2010), Title: *Programarea robotilor*, A.G.I.R, ISBN 978-973-720-337-3.

PRINCE RUPERT'S DROPS – THE INFLUENCE OF GLASS TYPE ON THE MECHANICAL PROPERTIES

ZGREABĂN Francesca-Rosemarie, BUJOREANU Ioan-Matei,JIGA Gabriel (Conducător științific)

Faculty: Industrial Engineering and Robotics, Specialization: Mechatronics and Robotics,Year of Study: I, e-mail: francescazgreaban@gmail.com

SUMMARY: The study investigates the mechanical properties of Prince Rupert's Drops (also known as Batavia's Tears), with a focus on how the glass used influences their strength and fracture behaviour. We produced drops from two different glass compositions: soda-lime and borosilicate. Through compression and impact testing , we managed to highlight the role of thermal stress distribution and material properties. The results reveal significant differences in the mechanical performance of the drops depending on the glass type, offering insights into the connection between rapid cooling, internal stresses, and fracture mechanics in brittle materials.

KEYWORDS: fracture, stress, impact, glass, strength

1. Introduction

Prince Rupert's Drops were discovered as a scientific marvel in the 17th century, in the Netherlands, hence their name [1]. At that time, Prince Rupert brought several drops to England and presented them to King Charles II, who offered them for study to the Royal Society of London [1]. For nearly 400 years, Batavia's Tears have been studied in an attempt to explain their counterintuitive behavior: the bulbous head does not break even under strong impact, while a light touch to the tail causes the entire drop to shatter. These remarkable glass structures are formed by dropping molten glass into cold water, resulting in a teardrop shape characterized by a bulbous head and a thin, curved tail. The extreme cooling process introduces compressive stresses in the outer layer and tensile stresses in the core. This internal stress profile is responsible for the high strength of the head and the catastrophic failure initiated by the tail. The principle behind these properties paved the way for the development of modern tempered glass (patented in 1874), which is now used in windshields, safety windows and smartphone cases [2].

Our study aims to further investigate the influence of glass composition on the mechanical properties of Prince Rupert's Drops. The main objective of this work is to produce Batavia's Tears using both soda-lime and borosilicate glass under similar conditions, and to compare their behavior through practical impact, fracture and compression tests. By examining their structural response, this research contributes to a better understanding of how material selection affects the performance of glass structures subjected to rapid cooling and internal stress development.

Thus, Batavia's Tears are not only a historical curiosity, but also a key milestone in the evolution of Strength of Materials, illustrating the concept of internal pre-compression to increase the resistance of a brittle material.

2. State of the art

Modern scientific explanations became possible with advancements in technology, particularly through the use of high-speed cameras and numerical simulations [1]. It has been demonstrated that the rapid cooling of molten glass in water creates an outer layer under compressive stress, while the interior remains under tensile stress. This internal stress distribution is responsible for the drops' unique strength and fracture behavior.

Despite the multitude of research describing the general behavior and physical principles underlying Prince Rupert's Drops, comparative studies that investigate the specific influence of glass composition remain relatively scarce. Most existing literature tends to focus on the internal stress distributions and the dramatic fracture patterns, often using theoretical models or high-speed imaging to illustrate the failure mechanisms. However, fewer studies explore how different types of glass - such as soda-lime and borosilicate - impact the mechanical behaviour, resistance to shock, or the threshold at which catastrophic failure occurs.

This gap is particularly noticeable in the context of hands-on, reproducible experimental procedures that can be replicated in academic or educational environments. While the general phenomenon is well known, the lack of accessible, comparative testing leaves important questions unanswered, such as: "How do different glass compositions influence the magnitude and distribution of internal stresses?", "Does borosilicate glass, known for its thermal stability, produce tears with different fracture patterns or strengths compared to soda-lime glass?".

Addressing these questions is crucial not only for understanding the fundamental physics of brittle materials but also for enhancing the educational value of Prince Rupert's Drops as teaching tools in Strength of Materials. Therefore, this project aims to fill that gap by designing and conducting a series of controlled experiments that produce Batavia's Tears from different glass types under similar thermal conditions. The mechanical responses—such as resistance to compression, impact, and tail-induced fracture—are then analyzed and compared.

3. Properties and structure

Soda-lime glass is mainly composed of silicon dioxide (SiO_2 ~70–73%), with sodium (Na_2O) and calcium oxides (CaO), plus small amounts of other oxides. These modifiers lower the melting point but introduce non-bridging oxygens that weaken the structure. As a result, soda-lime glass is inexpensive and easy to process but has low thermal shock resistance and moderate hardness (~6 Mohs) due to its higher thermal expansion and disordered network [3].

Borosilicate glass contains more SiO_2 (~80%) and boron trioxide (B_2O_3 ~12–13%), which acts as a network former. This results in a more uniform structure with fewer defects, leading to greater chemical and thermal resistance, lower thermal expansion, and higher hardness (~7.5 Mohs). However, it requires higher processing temperatures and is more costly.

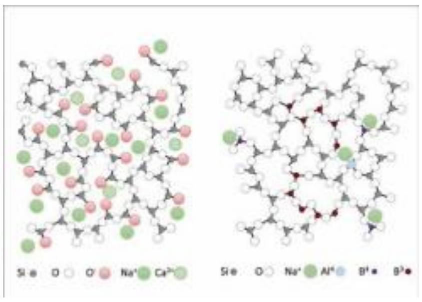

Fig. 1. Structure of soda-lime and borosilicate glass

Both are amorphous materials with SiO_4 tetrahedra [4]. The key difference lies in their internal structure: soda-lime glass has more disrupted bonds due to network modifiers (Na^+, Ca^{2+}), while borosilicate glass has stronger B–O bonding and fewer discontinuities. These differences directly influence the mechanical behaviour of Batavia's Tears made from each type.

Prince Rupert's Drops are created by dripping molten glass into cold water, which causes the surface to solidify extremely rapidly. The outer layer cools and hardens first, while the inner core remains hot and cools more slowly. As the interior contracts during cooling, it is constrained by the already solidified shell, resulting in a complex system of residual thermal stresses: compressive stress in the outer layer and tensile stress in the core.

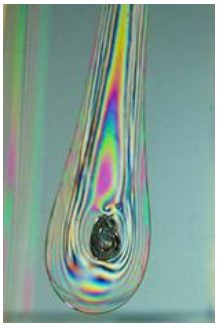

Fig. 2. Photoelastic analysis of a Batavia Tear

The compressed outer shell acts as a "pre-stressed skin" (similar to tempered glass), capable of withstanding extremely high forces without failure. Any surface crack must first overcome the strong compressive field, making it difficult for the head to fracture. As a result, the bulbous head can resist hammer blows, hydraulic pressure, and even bullets. Experiments have recorded forces in the range of ~664 kN before failure, with surface compression stresses reaching up to 700 MPa, values comparable to high-strength steels.

In contrast, the narrow tail contains material under internal tensile stress. As glass is inherently brittle, even a slight crack or fracture at the tail tip releases the built-up stress, triggering a rapid crack propagation towards the head. High-speed camera studies have observed crack velocities of 1,500–1,900 m/s, with repeated bifurcations. Within microseconds, the entire drop disintegrates explosively into fine glass powder, releasing the stored energy.

4. Process of obtaining the drops

In this study, two types of Prince Rupert's Drops (Batavia's Tears) were produced using different glass compositions and diameters: small-diameter drops made from soda-lime glass, large-diameter drops made from borosilicate glass.

The first series of drops was created using 5 mm diameter soda-lime glass rods heated with an oxyacetylene torch adjusted to a minimal flame. These initial attempts frequently resulted in the drops breaking. Consequently, experimental parameters were progressively adjusted, such as the angle of the rod and the heating duration.

A significant issue observed was the formation of air bubbles inside the drops. These bubbles disrupted the continuity of the vitreous network during cooling and became stress concentration points, often initiating spontaneous internal cracking as the glass contracted. To improve the outcome, a second series was performed using thicker soda-lime glass, sourced from the fragments of a bottle. The same oxyacetylene torch was used for heating. The resulting drops had a visibly larger volume and were more stable, showing fewer signs of spontaneous failure. It was noted that thicker glass retains heat longer, allowing the thermal gradient necessary for internal stress development to form properly. As a result, larger diameters correlated with higher success rates, due to more favorable cooling dynamics and better structural stability.

The third series also used 5 mm soda-lime glass rods but replaced the oxyacetylene torch with a Flamex butane microtorch. This offered greater control over the heating process, albeit with a lower flame intensity. Drops formed more slowly, giving better control over their shaping and cooling.

Initially, some drops exhibited minor internal fractures due to insufficient temperature gradients. To prevent this, the glass was no longer heated until dripping, but rather gently immersed into water while still attached to the rod, allowing gradual separation and more uniform cooling. This method produced intact, flawless drops, indicating an optimal balance between temperature, viscosity, and immersion timing.

For borosilicate glass drops, collaboration with a specialized glass working facility was necessary, as borosilicate requires higher working temperatures. A concentrated oxigas torch was used, specific for processing borosilicate, and the rod diameter was increased to 15 mm. The resulting drops were larger and uniformly successful, achieving a 100% success rate. This indicates that borosilicate's slower thermal expansion and higher viscosity at working temperature can provide better control over the solidification process, provided that the thermal gradient is carefully managed.

Thermal behavior was visually tracked during immersion into water. The drops exhibited bright exterior solidification within moments of contact with water, confirming the extremely fast surface cooling that generates internal residual stresses.

5. Experimental data and analysis

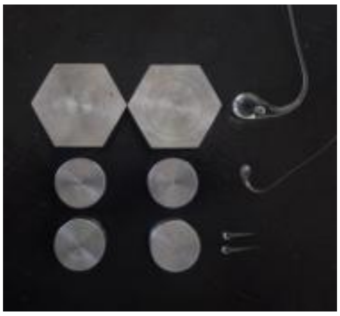

Fig. 3. Materials used

Fig. 4. Used hydraulic press

To evaluate the mechanical resistance of the two types of Prince Rupert's Drops, we applied two experimental testing methods: compression testing using a hydraulic press, impact testing using a hammer.

The tests were conducted using a W+R hydraulic press equipped with digital force measurement. Each drop was positioned vertically between two solid steel compression plates, and force was gradually applied until structural failure occurred. The force required to fracture the drop was so high that visible indentations were left on the steel plates.

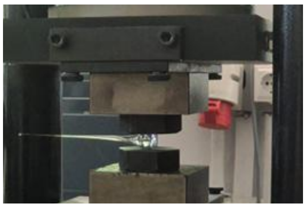

Fig. 5. Borosilicate drop during testing

Fig. 6. Indentations in steel plates

The borosilicate glass drop, produced from a 15 mm rod, exhibited exceptional compressive resistance, with failure occurring at 80 kN. This indicates a high degree of internal pre-compression and a well-structured internal network. The force applied was sufficient to leave marks on the steel plates, highlighting the drop's incredible strength.

Three soda-lime drops with a 5 mm diameter were tested: drop 1 failed at 23 kN, drop 2 failed at 16.5 kN, drop 3 failed at 7.3 kN.

Although the borosilicate drop with larger diameter demonstrated the highest absolute resistance, it is important to note that soda-lime glass drops performed better relative to their size. When normalized by diameter, soda-lime drops exhibited greater strength per unit cross-sectional area, suggesting that smaller drops may accumulate more favorable internal stress distributions under rapid cooling. This suggests that it is not size alone, but the intrinsic characteristics of the glass that govern the mechanical performance of Batavia's Tears under thermal shock.

6. Conclusions

Due to fabrication constraints, we were only able to test specific combinations of diameter and material: 5 mm soda-lime drops and 15 mm borosilicate drops. To allow a comprehensive comparison, we applied a normalization method based on compressive strength values reported in the scientific literature. According to known mechanical data: soda-lime glass has a compressive strength of approximately 700 MPa and borosilicate glass has a compressive strength of approximately 580–600 MPa [4]. This results in a performance ratio of roughly 0.83, which we used as a correction factor to estimate what a borosilicate drop would resist under the same geometry as soda-lime:

$$F_{echiv,borosilicate} = 24 \times 0.83 = 20kN \tag{1}$$

Conversely, the inverse factor (1.2) was used to estimate the resistance of a soda-lime drop of 15 mm diameter, using the actual borosilicate result as a reference:

$$F_{echiv,sodalime} = 80 \times 1.2 = 96kN \tag{2}$$

Using this approach, we extended our analysis to multiple diameters (5 mm, 15 mm, and 30 mm) for both materials. While direct testing was only performed on select samples, this method allowed us to interpolate and extrapolate realistic estimates for the missing combinations.Thus, our conclusions are based on both experimental measurements and material-

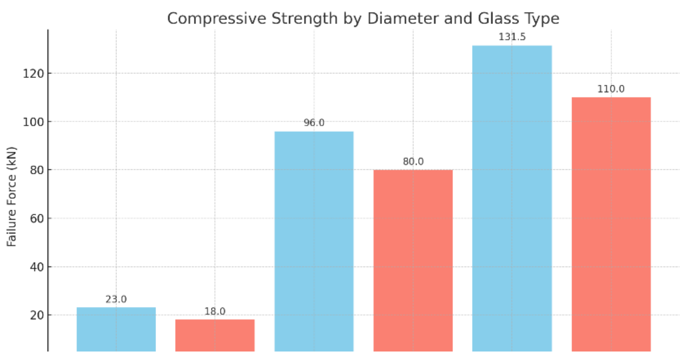

Fig. 7. Bar chart of Batavia's Tears

specific scaling, enabling a robust comparison of the compressive strength of Batavia's Tears as a function of both material type and geometry.

The bar chart shows the compressive resistance of Batavia's Tears as a function of both glass type and drop diameter. Consequently, there resulted some observations.

Soda-lime glass outperforms borosilicate glass at all tested diameters. This aligns with the higher compressive strength of soda-lime (approx. 700 MPa) compared to borosilicate (approx. 580–600 MPa). The performance gap between the two materials increases almost linearly with diameter: At 5 mm the difference is 5 kN, at 15 mm the difference is 16 kN and at 30 mm the difference is 21.5 kN.

Soda-lime glass, being mechanically stronger than borosilicate glass, allows the drops to withstand significantly higher forces before failure—estimated to be approximately 20% more under similar conditions. This difference arises from the higher compressive strength and thermal expansion of soda-lime glass, which enable the generation of stronger residual stresses during quenching. Additionally, when analyzing drops made from the same material, we observed that compressive resistance increases as the diameter increases, but the trend is sublinear. In other words, although larger drops are stronger in absolute terms, the rate of increase in strength slows down at higher sizes.

These results highlight two key principles:

1. Material properties dominate the mechanical performance, even more than size alone.
2. Optimizing drop geometry and thermal gradients is crucial for achieving maximum strength.

Future research on Prince Rupert's Drops could benefit from finite element simulations to model internal stress distributions as a function of material, geometry, and cooling rate [5]. High-speed imaging would also allow deeper investigation into the fracture dynamics and energy release during failure.

Further studies using SEM and XRD could clarify how microstructural features influence drop performance, while expanding to alternative glass types such as fused silica or transparent ceramics may uncover new behaviors under thermal shock.

Improving thermal control during quenching through programmable setups could enhance reproducibility and allow systematic studies of stress formation. Moreover, the principles behind these drops could inspire impact-resistant material designs and biomimetic structures. Due to their visually striking behavior, they also hold strong potential as educational tools in strength of materials and physics [6].

7. Bibliography

[1]. Bradt, R. C. and Bradt, N. R. E. (2012), „The Prince Rupert's drop: Glass, strength, and science history”, Journal of the American Ceramic Society, vol. 95, no. 11, pp. 3600–3606, ISSN 0002-7820 (print), 1551-2916 (online).
[2]. Varshneya, A. K. (1993), *Fundamentals of Inorganic Glasses,* Academic Press, New York, ISBN 0-12-714970-8.
[3]. Westlab (2017), "What is the Difference Between Soda-lime Glass & Borosilicate Glass?", Available: https://www.westlab.com/blog/what-is-the-difference-between-soda-lime-glass-and-borosilicate-glass

[4]. Möncke, D. and Smedskjaer, M. M. (2019), „Structure and properties of soda-lime silicate and borosilicate glasses: A short review”, Journal of Non-Crystalline Solids, vol. 521, pp. 1–17, ISSN 0022-3093.
[5]. Bradt, R. C. and Bradt, V. H. (2006), „Residual stresses in Prince Rupert’s drops”, in: Varner, J. R., Quinn, G. D. and Wightman, M., “Fractography of Glasses and Ceramics” V, Wiley-American Ceramic Society, Hoboken, pp. 181–188, ISBN 978-0-470-09737-3
[6]. S. Arbesman (2014), “Prince Rupert: Philosophic Warrior”, Wired Magazine, Available: https://www.wired.com/2014/06/prince-rupert-philosophic-warrior/.

PROGRAMMING AND OFFLINE SIMULATION OF A ROBOTIC CELL FOR PALLETIZING USING PROCESS SIMULATE ENVIRONMENT

CICÎRÎC Diana-Maria, Cristina PUPĂZĂ

Faculty: Industrial Engineering and Robotics, Specialization: Robotics, Master student, Year of study: 2
E-mail: diana_maria.ciciric@stud.fiir.upb.ro

This research encompasses the virtual prototype of a robotic cell designed for palletizing parallelepiped boxes containing milk cardboard containers. The cell integrates two articulated arm industrial robots with six numerically controlled axes and equipped with two poly-functional effectors. This study is a continuation of the Bachelor Thesis and it is focused on the signal-based simulation of the cell employing Siemens Process Simulate environment.

KEY WORDS: palletizing, sensors, signals, Process Simulate.

1. Introduction

This research is focused on a signal-based simulation of a robotic cell's functioning in Siemens Process Simulate environment - a Digital Twin employed to verify the manufacturing processes in a three-dimensional environment and to virtually check the designed workflows throughout their entire lifecycle.

The main goals of a signal-based simulation are the reduction of the development time and the increase of the precision and reliability. The working cycles of the robots are tested, the operating parameters can be changed without needing to turn off the production in real time and possible collisions between equipments are visualized and eliminated. It is a fundamental step towards Virtual Commissioning.

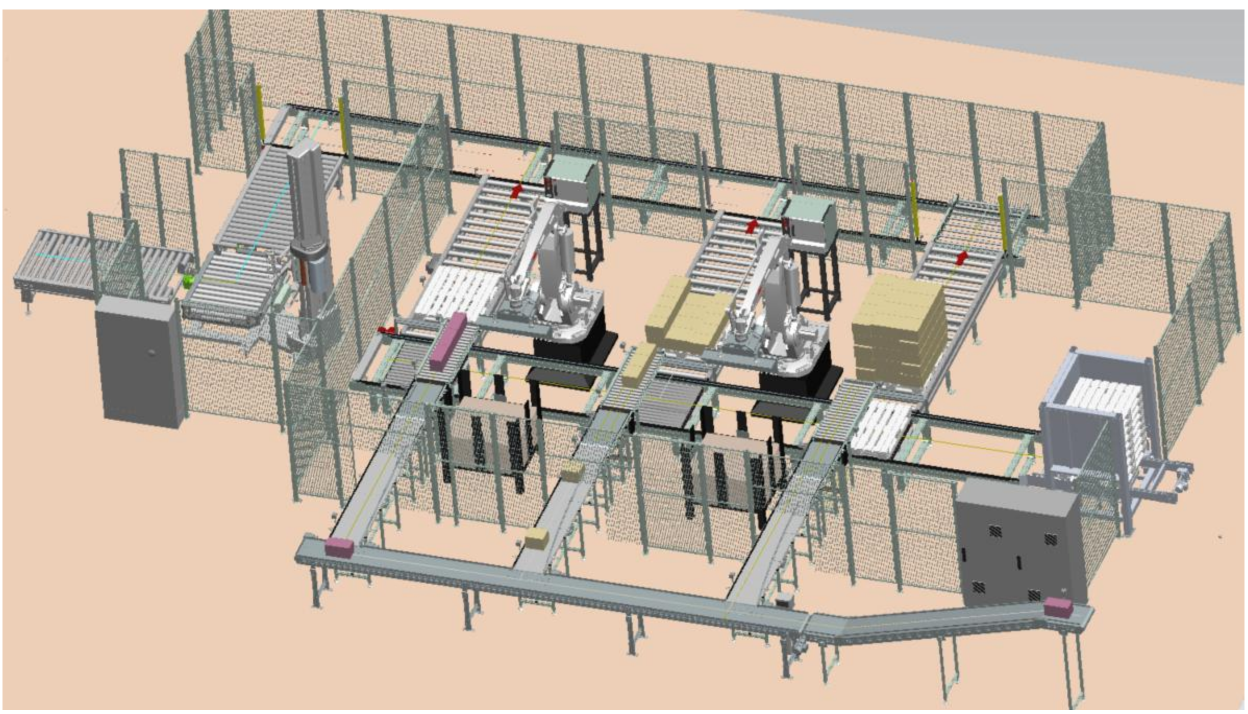

Fig. 1 Overview of the robotic cell developed in Process Simulate environment

The logical operation process of the studied palletizing cell is presented in Fig.2, in the application's functional organization chart (flowchart).

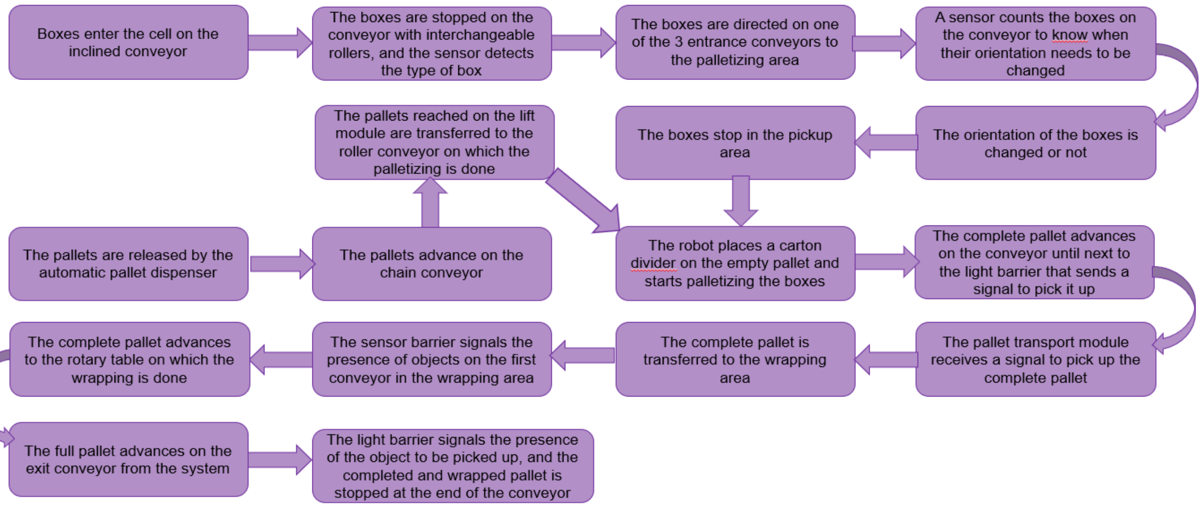

Fig. 2 Functional flowchart of the robotic cell

2. The event and signal-based programming of the entire application

The first step in conducting the simulation in Process Simulate involves the definition and positioning of the photoelectric sensors within the robotic cell. The sensor's location is illustrated in Fig. 3 - the presence of the safety barriers is marked with the red color, the photoelectric sensors with diffusion are yellow, and the photoelectric sensors with reflection with the green color.

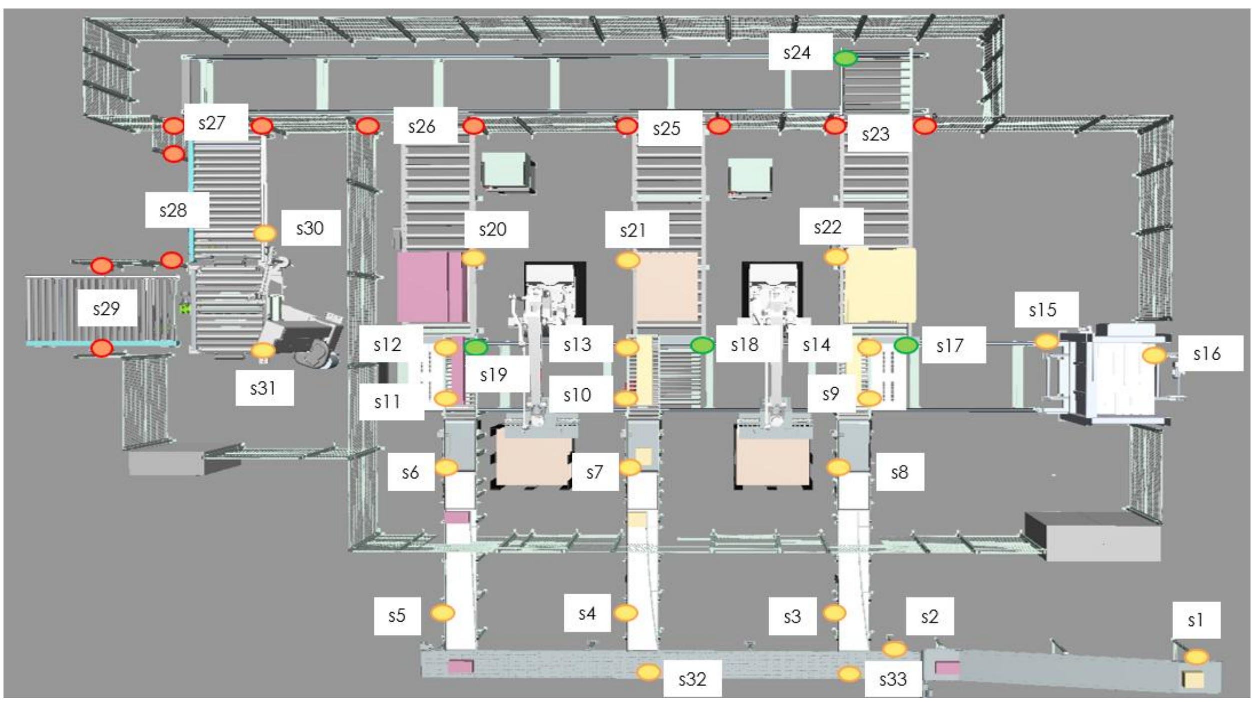

Fig. 3 Location of the sensors in the robotic cell

Fig. 4 illustrates both the "Object Tree" window, displaying the sensors defined within the robotic cell, and the "Simulation Panel" window, showing the defined signals and their corresponding values.

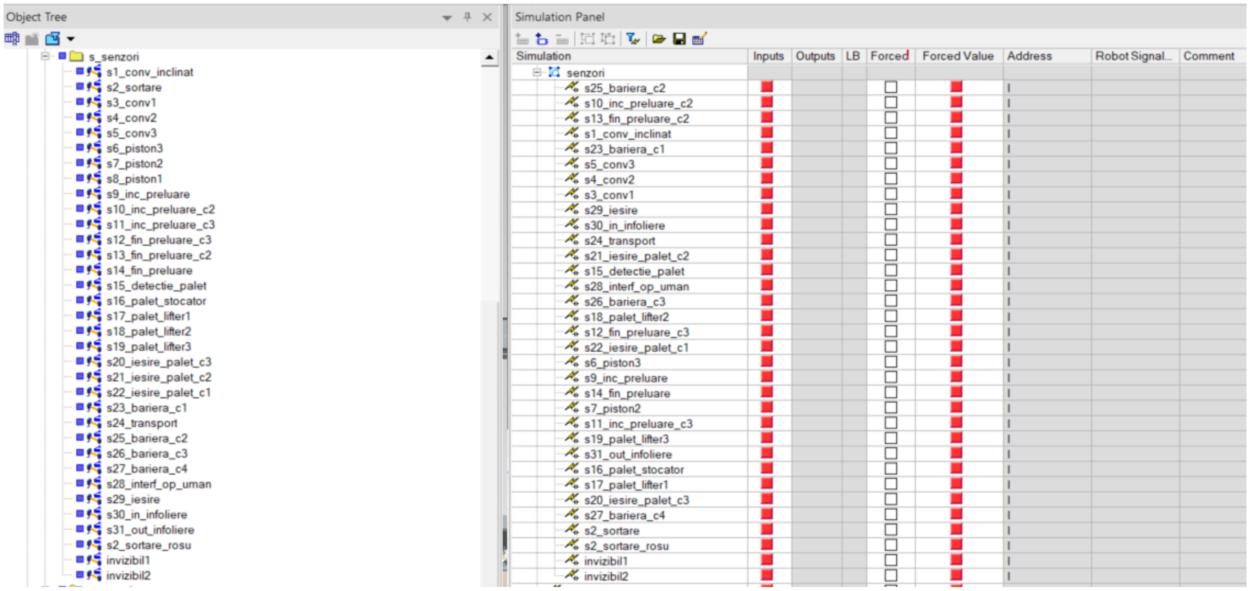

Fig. 4 Photoelectric sensors defined within the robotic cell and their signals

The next research steps in carrying out the simulation were:

- definition of the main compound operation called „LineOperation” (Fig.5, represents a collection of all operations);
- definition of the CEE operation (the “Cyclic Event Evaluator” tool is used to control the logical progression of the mechanical system simulations, based on events, and allows the simulation to be reset to the initial position after the completion of all operations);
- generation of the appearances of the manipulated objects - boxes, pallets, paper separators, within the simulation. An appearance acts as a duplicate of the original objects; three independent operations were defined: generation, maintenance and deletion, based on the object type;

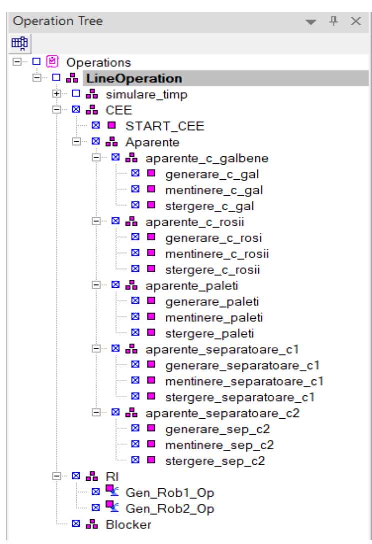

Fig. 5 The compound or simple operations defined in the Operation Tree window

- insertion of the operations in the „Sequence Editor” window to run the simulation and add events;
- addition of the device signals according to the positions of mechanisms in the „Simulation Panel” window, an essential tool for debugging of the signal-based simulations, which allows viewing and modifying signal values;

- definition of the logic blocks for each intelligent object in the application (connecting internal input/ output signals to module-specific signals);
- specifying the type of the object detected for each photoelectric sensor in the robotic cell;
- generating trajectories, definition of the stopper points, tolerances and speed for each conveyor in the cell.

3. Offline simulation of the entire application's functionality

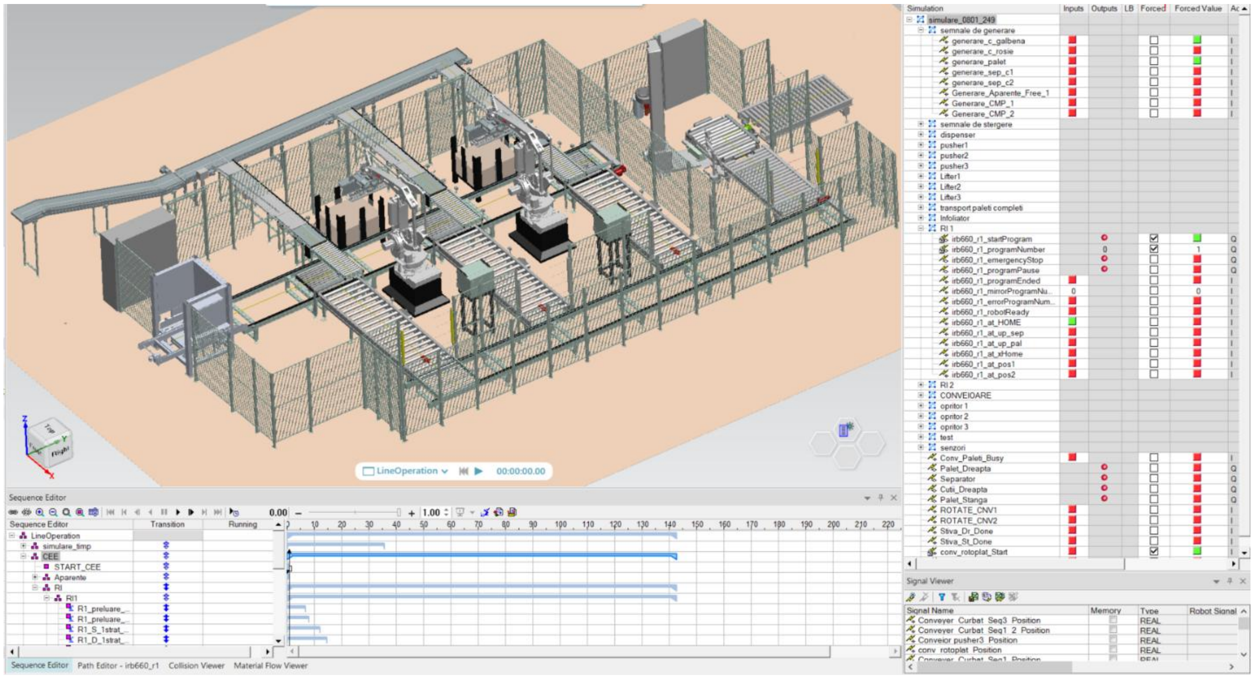

Fig. 6 Cell overview prior to the start of the simulation

In the analyzed robotic cell the boxes are introduced into the system by a slanting entrance conveyor, followed by a roller conveyor with interchangeable orientation. Their presence is sensed by a photoelectric sensor. The boxes are analyzed by a barcode scanner, after which the first yellow box is redirected to the first conveyor, the second to the middle conveyor, and the red box to the last conveyor.

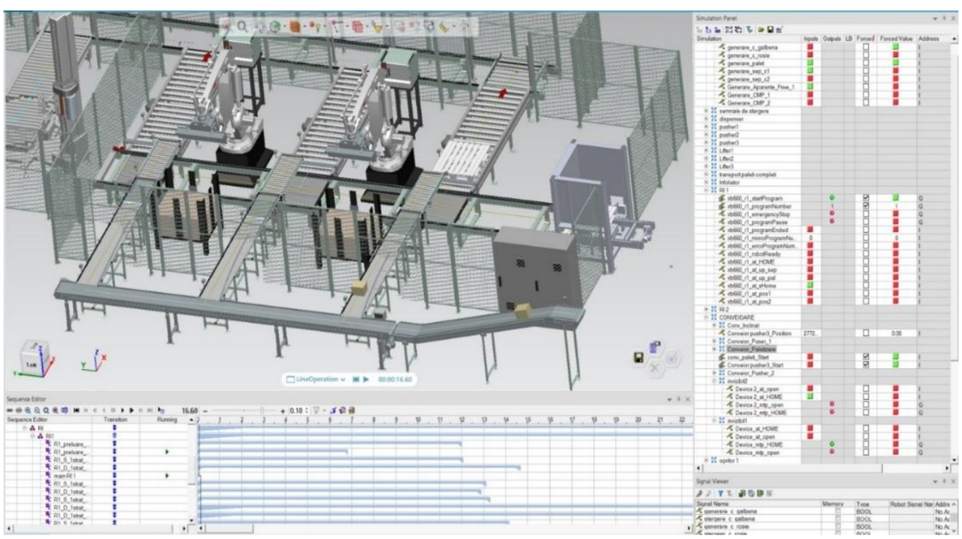

Fig. 7 Entrance of the yellow box on the first belt conveyor. Entrance of the pallet on the first roller conveyor

The pallets are generated by the automatic feeding system. A photoelectric actuator senses the presence of the pallets and they are transported on a chain conveyor to the lift module, within the range of the reflective photoelectric sensors. The lifting module transfers the pallets to the roller conveyor on which they are filled (Fig.9). The pallets stop in the palletizing area, the position being indicated by the diffusion photoelectric sensors placed at the end. The robot places a cardboard divider from the designated storage on the surface of the pallet (Fig.8).

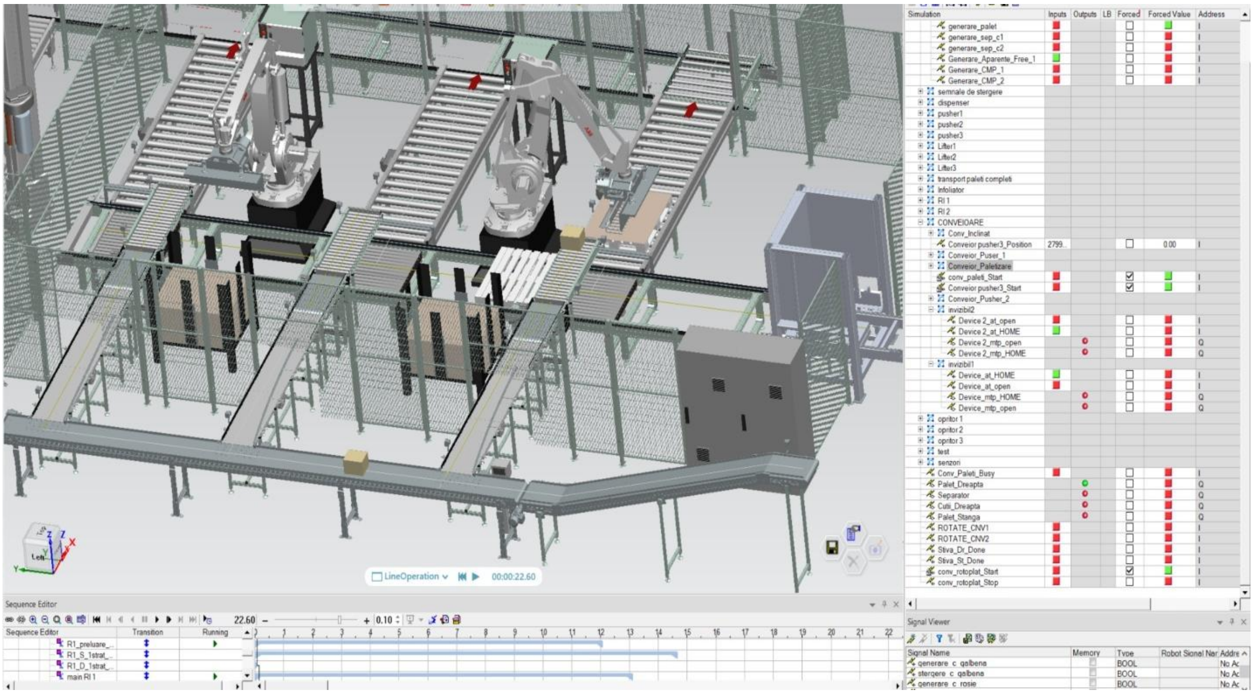

Fig.8 Placement of a separator on the pallet by the first industrial robot. Movement of the pallet to the second lifting module. Movement of the box to the second belt conveyor

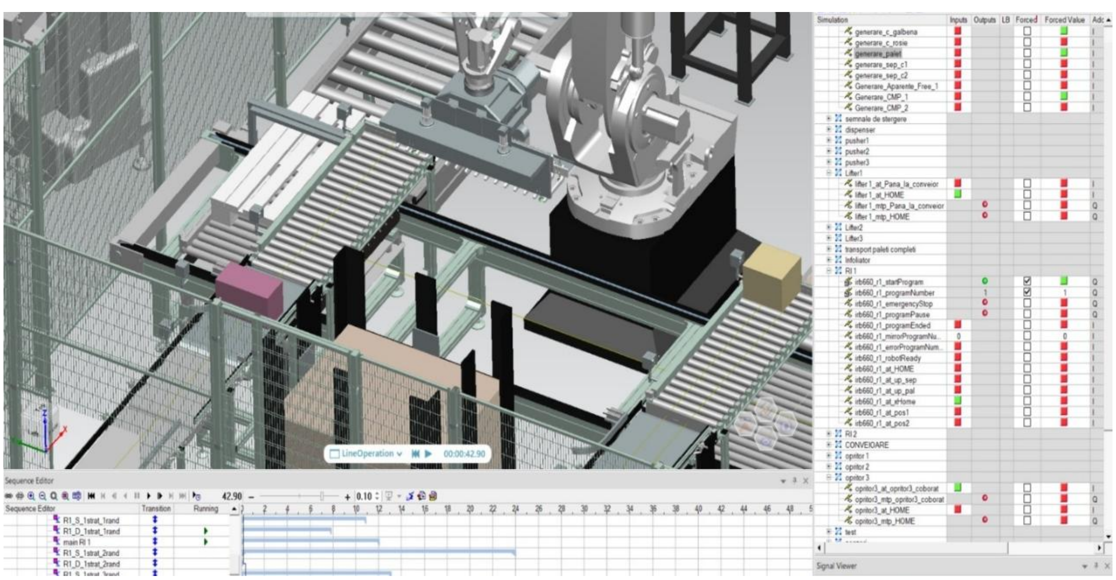

Fig.9 Lifting of the pallet from the lifting module to the third roller conveyor. The box stopper is lowered

Boxes are selected and redistributed to the designated industrial robot, through a sequence of belt conveyors accumulating, accelerating and changing the orientation of the boxes. The boxes are counted by the signals transmitted by the photoelectric sensors - positioned at the entrance on the three conveyors, to the information unit. Once the desired number is reached, a change in orientation of the boxes is performed with the help of a pneumatic piston with an adjustable curved rod (Fig.11).

The boxes advance on a roller conveyor, equipped with two photoelectric sensors (at the position of the first and last box to be picked up respectively, in order to comply with the imposed palletizing scheme). When both sensors detect objects, the stopper is raised and the boxes are picked up by the industrial robot equipped with a bifunctional effector, compatible with the spaces between the rolls (Fig.10). Boxes are then placed on a pallet.

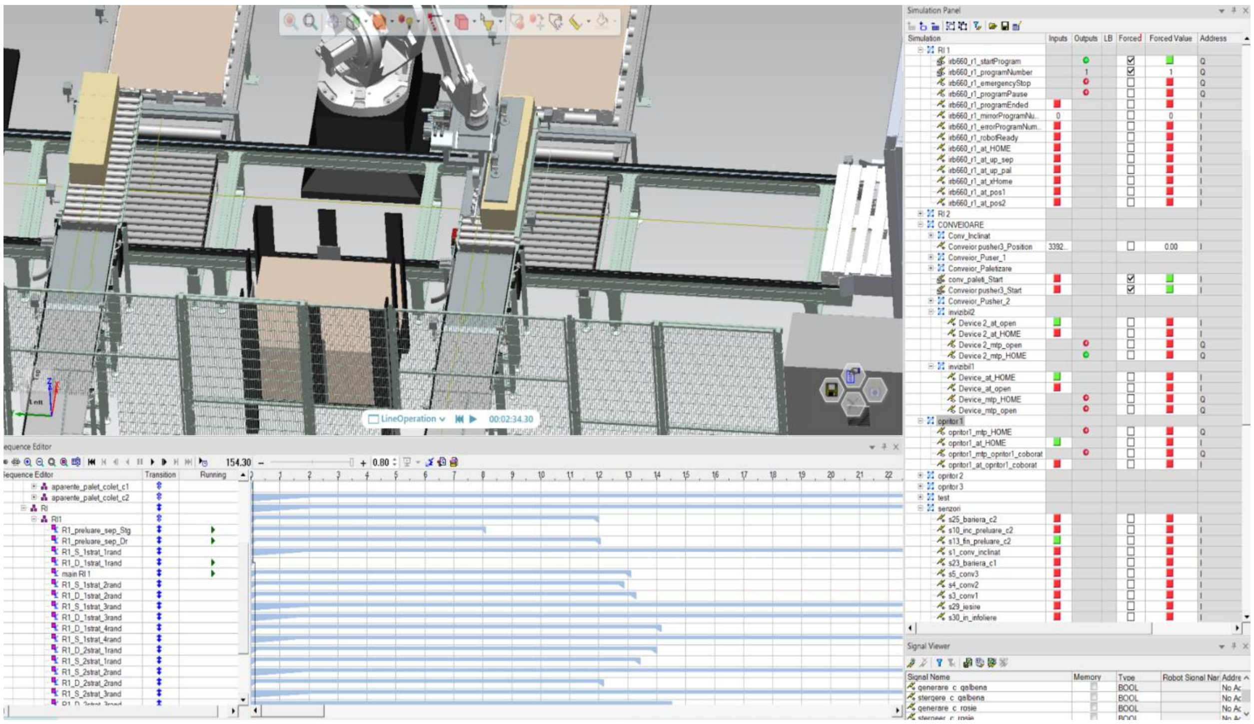

Fig.10 Start of the palletizing process for the first set of 5 boxes

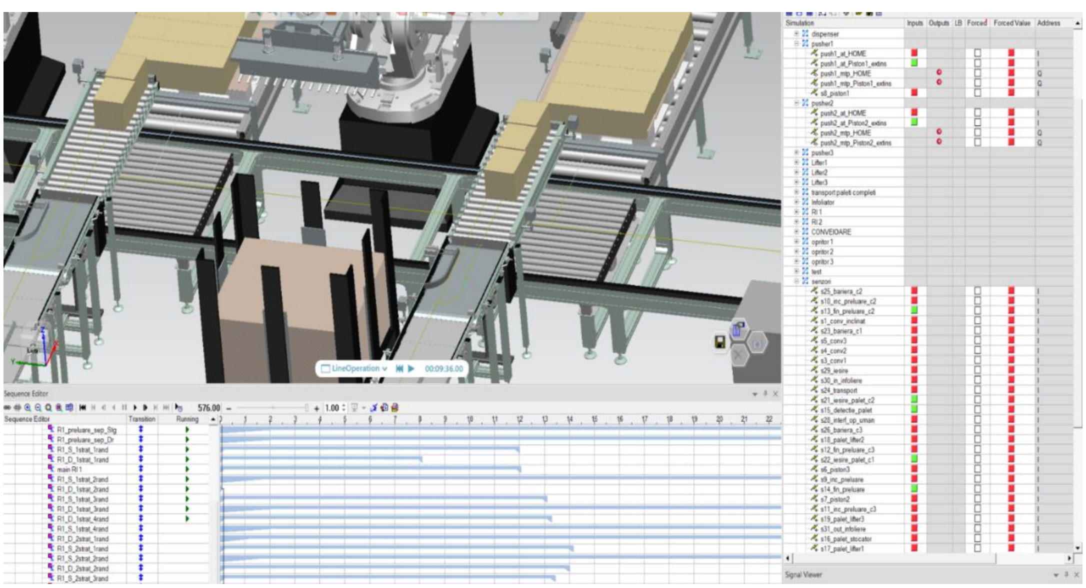

Fig.11 Rod extension for changing the orientation of the boxes

The complete pallet advances on the roller conveyor on which the palletization was done, up to the light barrier (Fig.12), and it is picked up by a transport module (Fig.13), consisting of a chain conveyor and a roller conveyor, equipped with photoelectric sensors with reflection that transmit information about the picking and positioning points of the pallet on the roller conveyor.

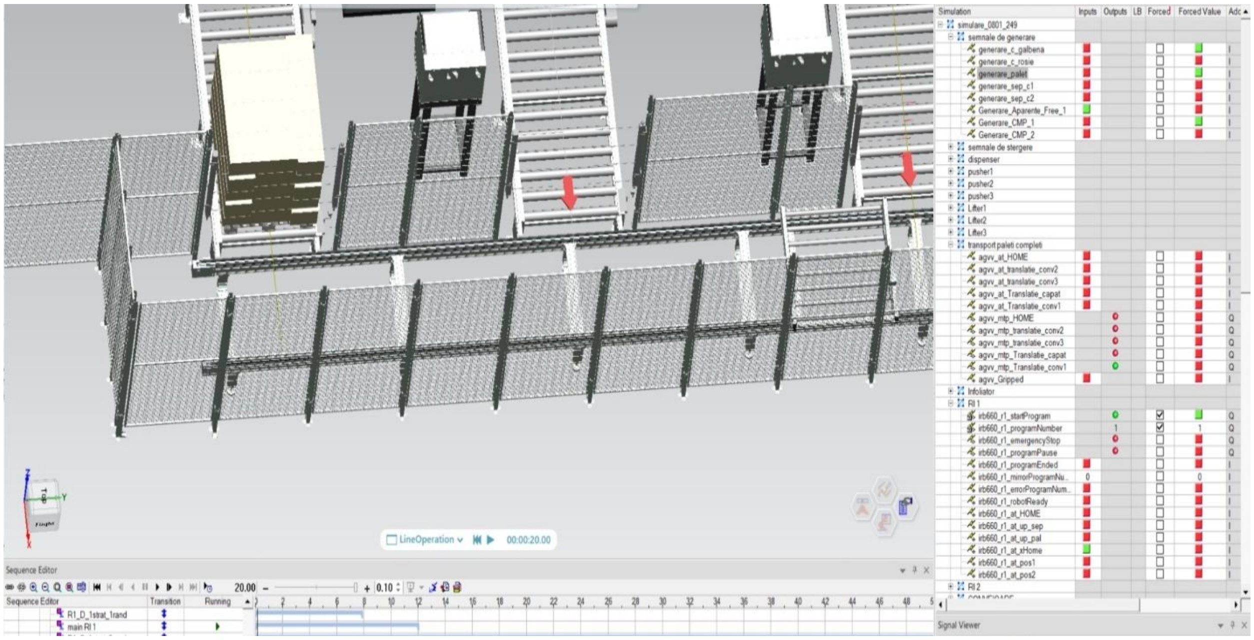

Fig.12 Generation of a complete pallet pickup command from the first conveyer to the transport module

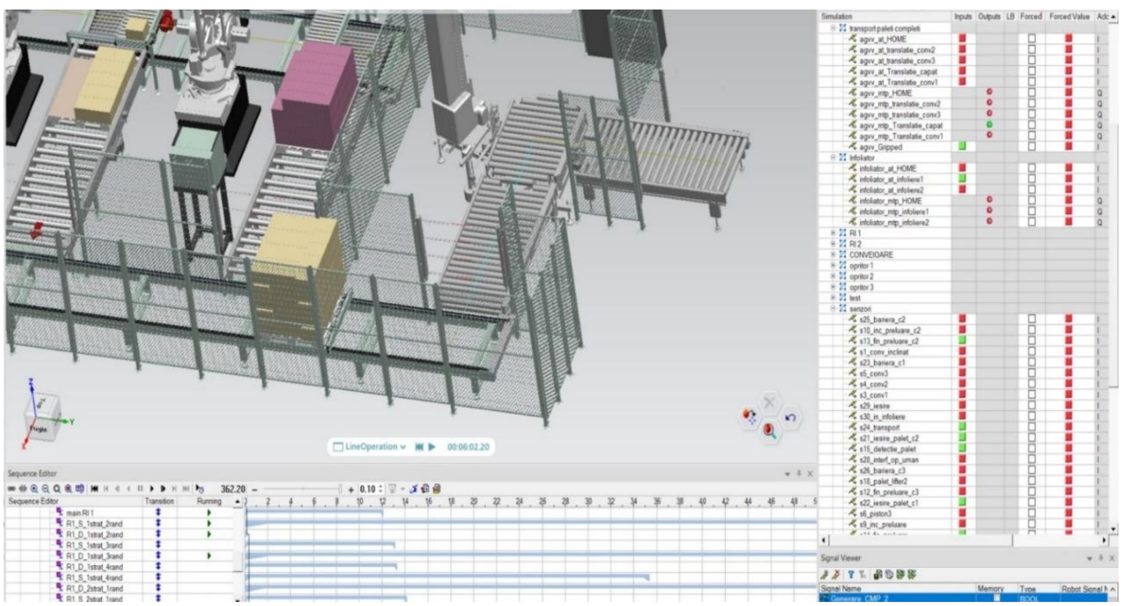

Fig.13 Transfer of the complete pallet to the wrapping area

The complete pallet passes through the light barrier on the exit roller conveyor. The role of the safety light barrier is to identify the presence of the human operator in the transfer space to the wrapper and to stop the process during the reception of signals for operator presence. The full pallet is transported to the rotary table enwrapper (Fig.14), equipped with photoelectric sensors, and then leaves the cell via another roller conveyor to the last light barrier which signals that the pallet is ready to be picked up by the human operator (Fig.15).

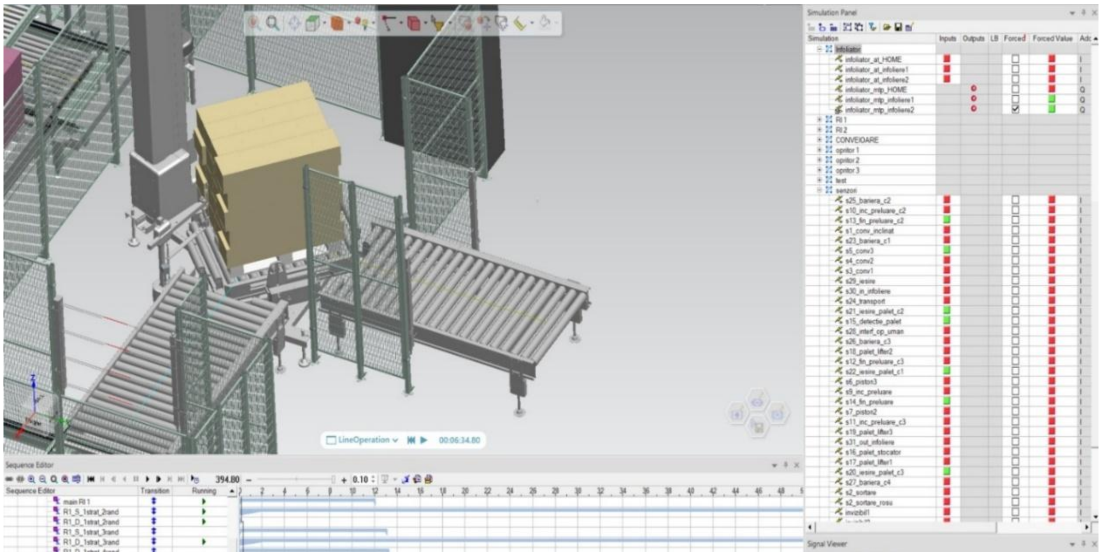

Fig. 14 Pallet wrapping process

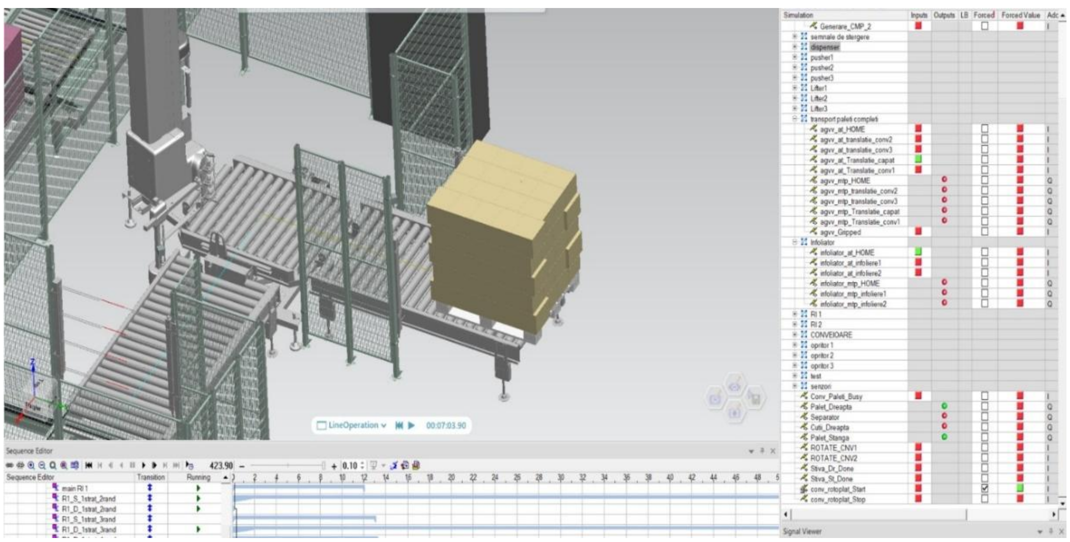

Fig. 15 The wrapped pallet awaits pickup by a human operator for system exit

4. Conclusion

The original contributions of this research are: a 3D CAD synthesis of the robotic cell using NX, the development of the subsystem mechanisms in Process Simulate in order to enable simulation of the component movements from the palletizing cell, the elaboration of the flowchart with all the details of the specific processes, events and signals. Additionally, the sensor-based mapping of the entire application was completed. The logical blocks and the signals corresponding to the sensors, robots, and smart objects were defined. Conveyor trajectories and stopper control points were described, along with their associated logical conditions.

5. References

[1]. Process Simulate - Siemens Digital Industries Software. Tecnomatix Process Simulate Version 16.1 (2024) https://docs.sw.siemens.com/en-US/doc/288782031/PL20231017544579710.tecnomatix_eMS.xid1015765/xid1657141.

OFFLINE PROGRAMMING AND SIMULATION OF A ROBOTIC CELL FOR PAPER ROLL PALLETIZING INTEGRATING TWO INDUSTRIAL ROBOTS USING THE PROCESS SIMULATE ENVIRONMENT

BADEA Marian-Cristian,PUPĂZĂ Cristina(Conducător științific)
Faculty of Industrial Engineering and Robotics, 2nd Year, Robotics Master's Program

This thesis presents the development and simulation of an industrial palletizing application for stacks of paper towel packages using two industrial robots. The system integrates real-time signal-based and event-based programming in Tecnomatix Process Simulate to manage object flow, orientation, and automation of tasks such as palletizing and wrapping. The project emphasizes the digital design, configuration, and synchronization of all functional units within the robotic cell to create a fully automated and realistic workflow.

Keywords: Robotic palletizing, event-based programming, digital twin simulation.

1. Introduction

The goal of this thesis is to simulate a fully automated robotic palletizing cell designed to handle paper towel packages. The process includes generating packages and pallets, transporting them through conveyors, centering and orienting them, stacking the items using robots, and finally wrapping the completed stacks.

The project began with the 3D design of the cell in Siemens NX, incorporating two industrial robots, a conveyor system, a wrapping station, and supporting hardware. This digital model was then transferred to Process Simulate, where offline programming and signal-based logic were used to model real-time behavior and interactions.

By using Tecnomatix Process Simulate, the system achieves realistic control over the workflow using a signal-event framework, allowing for coordination without direct communication between the two robots. A complete map of sensor inputs and equipment responses is included, highlighting industrial feasibility.

2. Current Stage

2.1 Signal-Based Programming in Process Simulate

The simulation environment was configured for "Line Simulation" mode, allowing signal-based and event-based interactions. Intelligent components and sensors were defined to trigger object appearances and coordinate actions across the system.

Signals were created to manage the appearance and removal of packages and pallets. Conveyors were modeled with associated conveying frames and control points, ensuring accurate movement along predefined paths. Logic was developed for centering systems, pallet dispensers, and lift-mode conveyors.

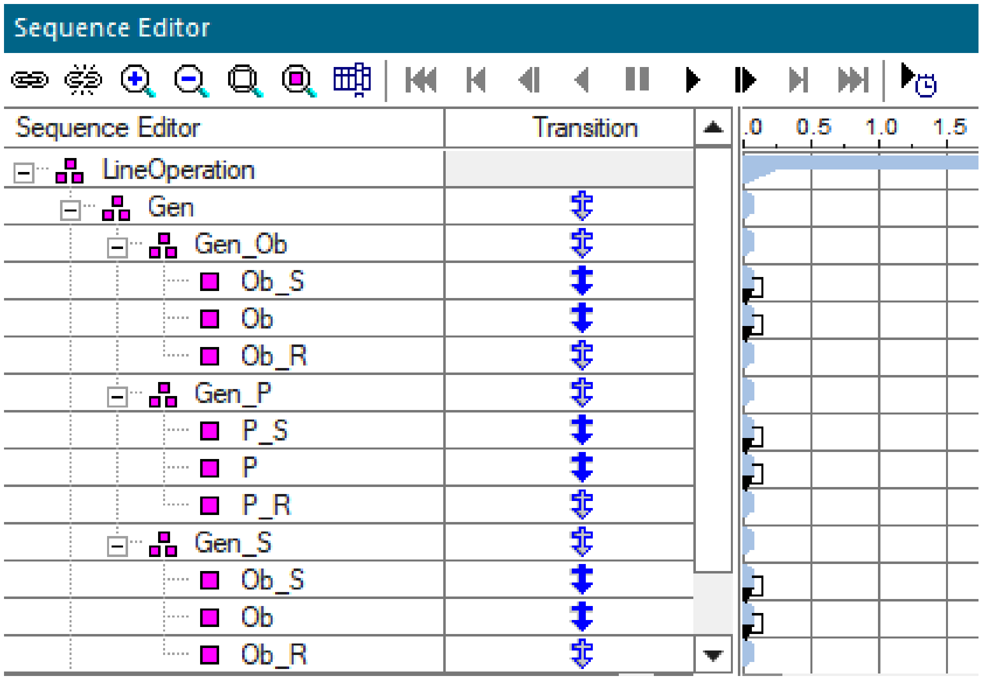

Fig.1 Operations required for generation

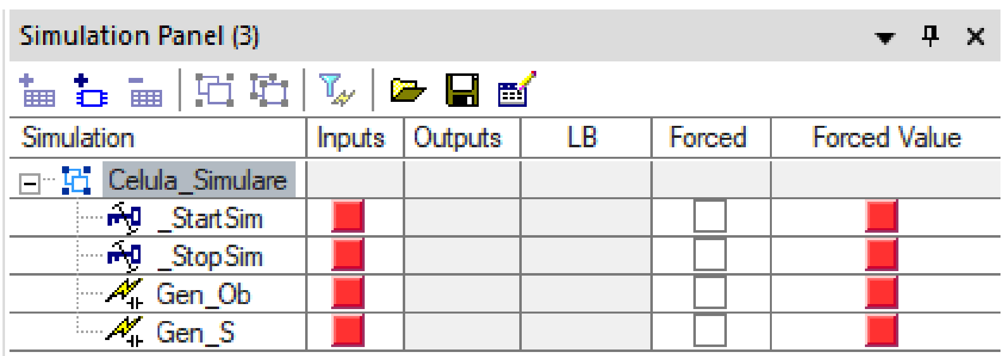

Fig.2 Signals for creation and deletion of appearances

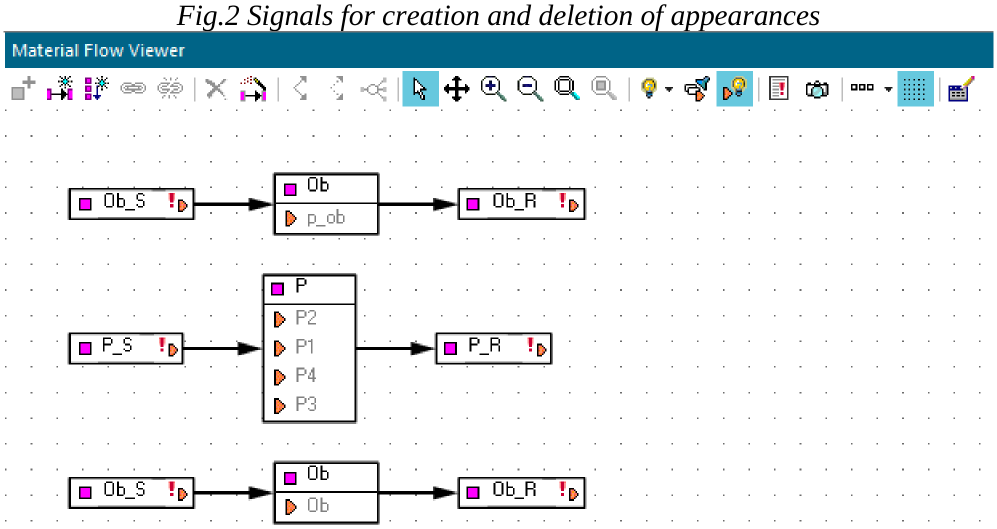

Fig.3 Signals for creating and deleting appearances

Robot signals and programs were defined separately for a 6-axis manipulator and a MOTOMAN PL190, handling the package rotation and palletizing operations respectively. The logic included:

- Initial package generation
- Conveyor-based transport and orientation
- Pallet feeding and alignment
- Object stacking by robots
- Wrapping using a rotary table equipped with a film cutter and holder

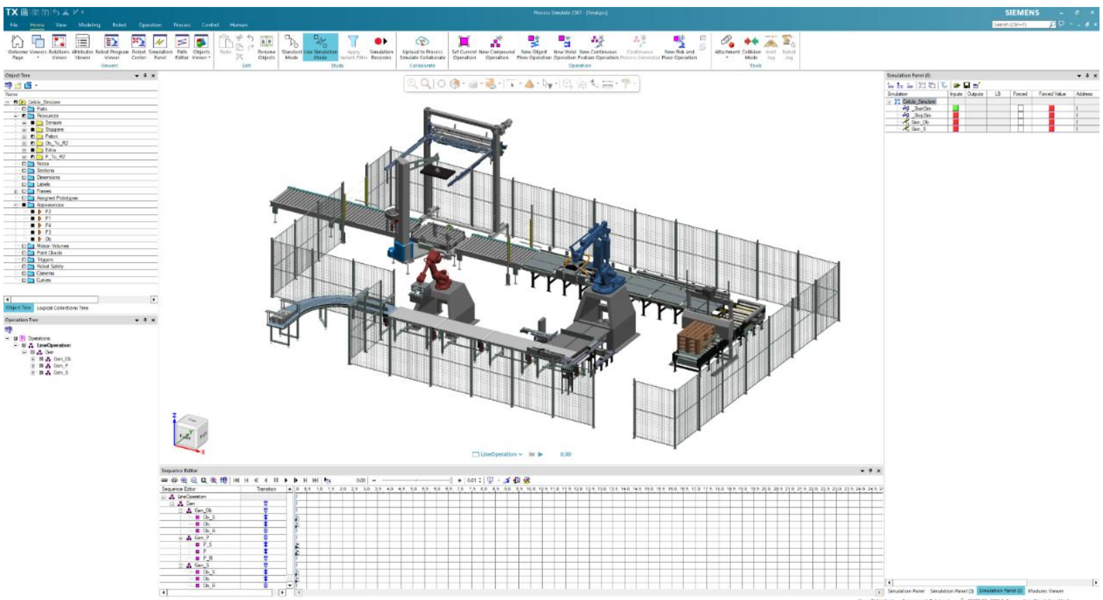

Fig.4 Initial appearance generation

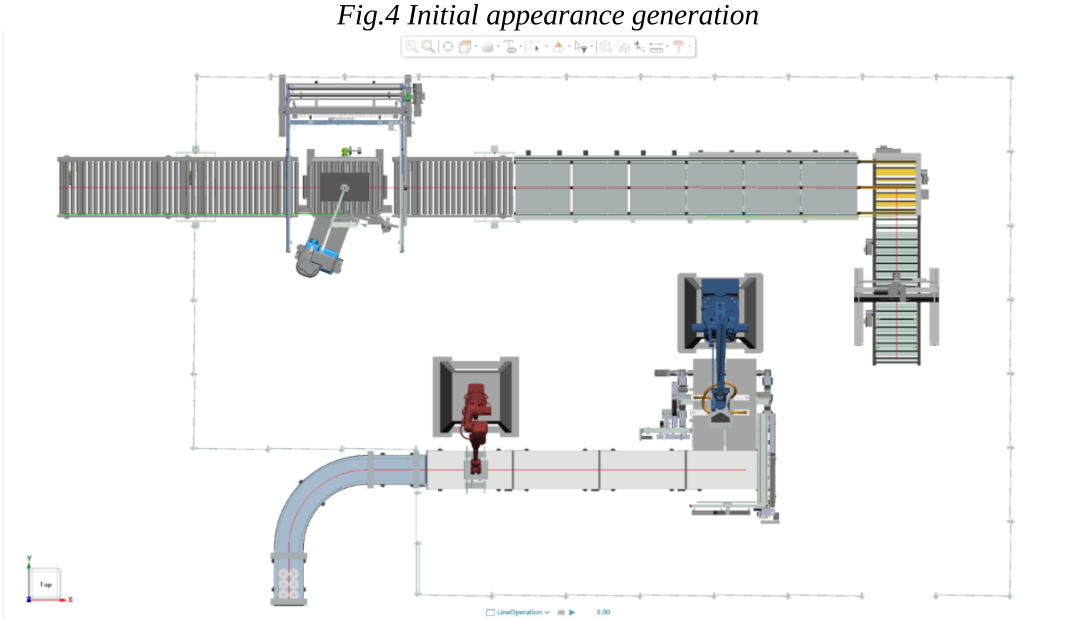

Fig.5 Highlighting the straight lines and the curve

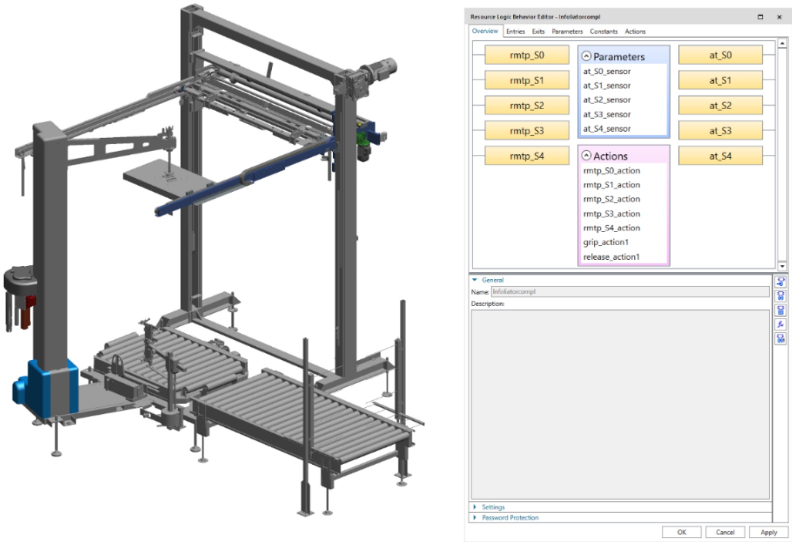

Fig.6 The logic of the rotary table wrapper equipped with scissors and a system for holding and cutting the film at a fixed height

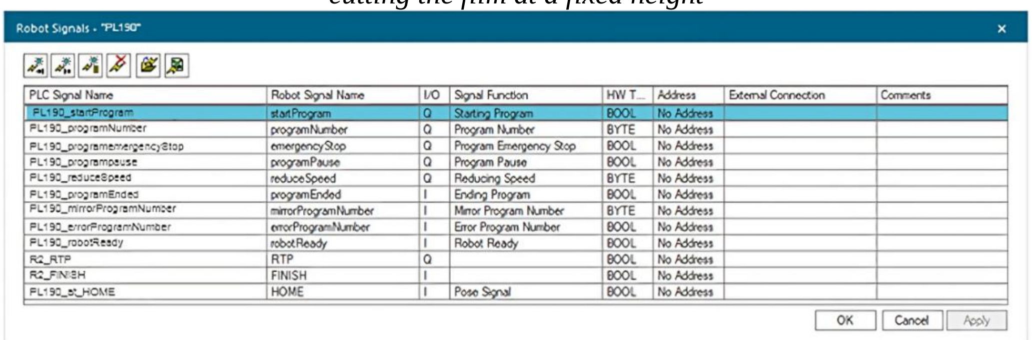

Robot Signals - "PL190"

PLC Signal Name	Robot Signal Name	I/O	Signal Function	HW T...	Address	External Connection	Comments
PL190_startProgram	startProgram	Q	Starting Program	BOOL	No Address		
PL190_programNumber	programNumber	Q	Program Number	BYTE	No Address		
PL190_programemergencyStop	emergencyStop	Q	Program Emergency Stop	BOOL	No Address		
PL190_programpause	programPause	Q	Program Pause	BOOL	No Address		
PL190_reduceSpeed	reduceSpeed	Q	Reducing Speed	BYTE	No Address		
PL190_programEnded	programEnded	I	Ending Program	BOOL	No Address		
PL190_mirrorProgramNumber	mirrorProgramNumber	I	Mirror Program Number	BYTE	No Address		
PL190_errorProgramNumber	errorProgramNumber	I	Error Program Number	BOOL	No Address		
PL190_robotReady	robotReady	I	Robot Ready	BOOL	No Address		
R2_RTP	RTP	Q		BOOL	No Address		
R2_FINISH	FINISH	I		BOOL	No Address		
PL190_at_HOME	HOME	I	Pose Signal	BOOL	No Address		

OK Cancel Apply

Fig.7 The signals of the PL190 robot

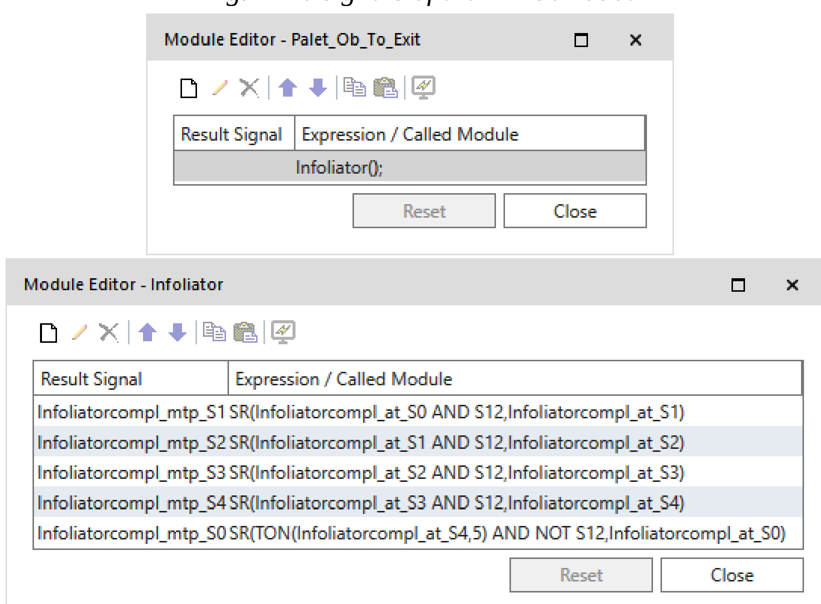

Fig.8 The modules used for the rotary table wrapper equipped with scissors and a system for holding and cutting the film at a fixed height

2.2 Offline Simulation Workflow

The process starts with generating packages and placing them on conveyors. The 6-axis robot aligns and orients packages, while pallets are prepared and aligned using piston-controlled guides. Once a complete layer is ready, it is transferred to the working area of the palletizing robot.

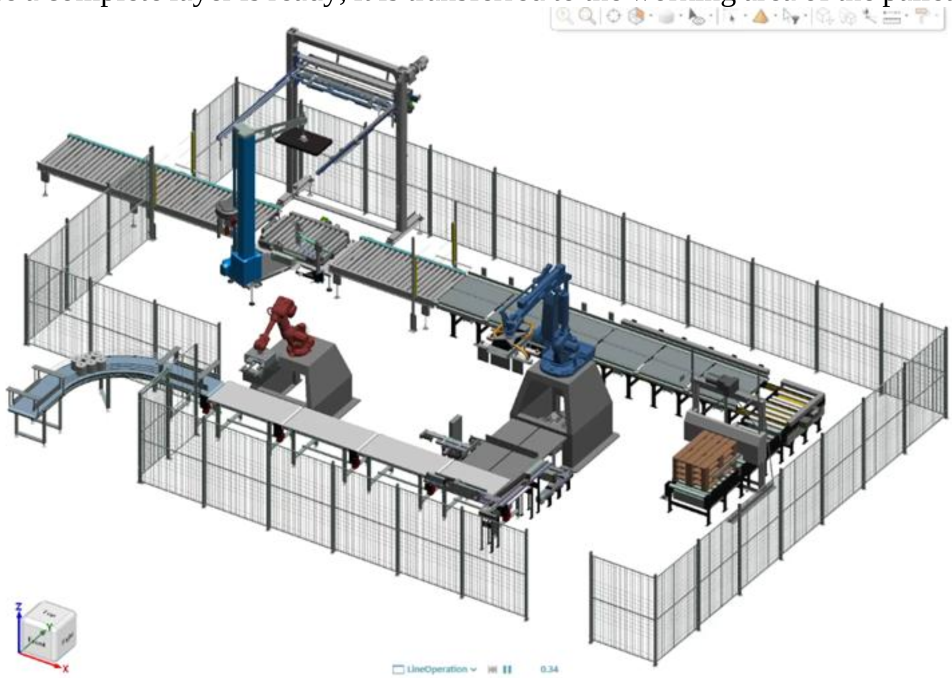

Fig.9 Generation and insertion of parts

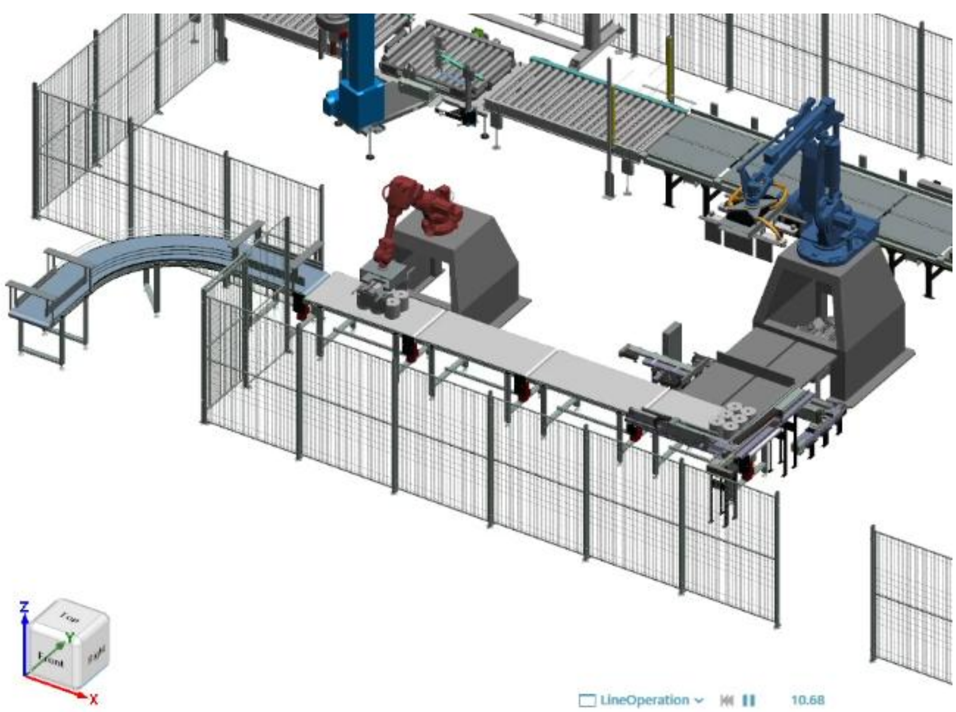

Fig.10 Modification of object positions by the 6-axis

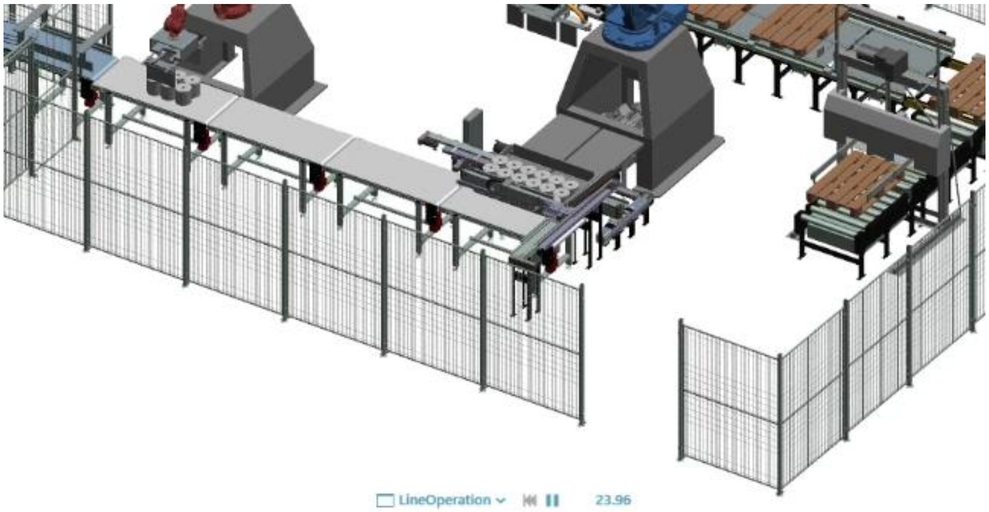

Fig.11 Transfer of object layers

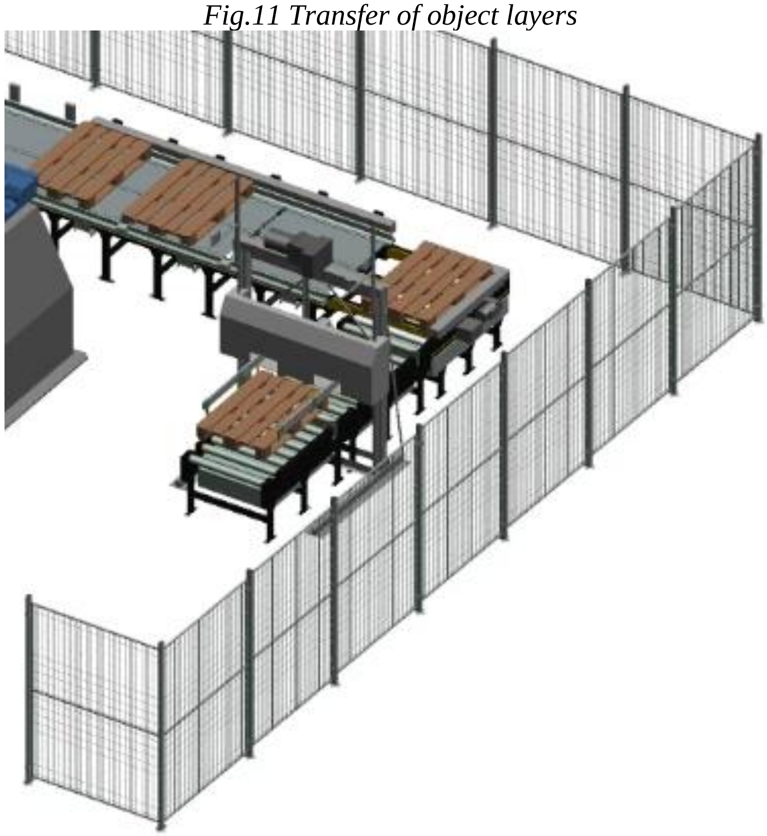

Fig.12 Feeding the system with pallets, changing their orientation by 90 degrees, and aligning them by activating the pistons.

The MOTOMAN PL190 robot then stacks the packages layer by layer. When the stack is complete, it is transferred to a rotary wrapping station, where wrapping is initiated and completed based on sensor signals. Finally, the stack exits the cell, completing one full cycle of the automated system.

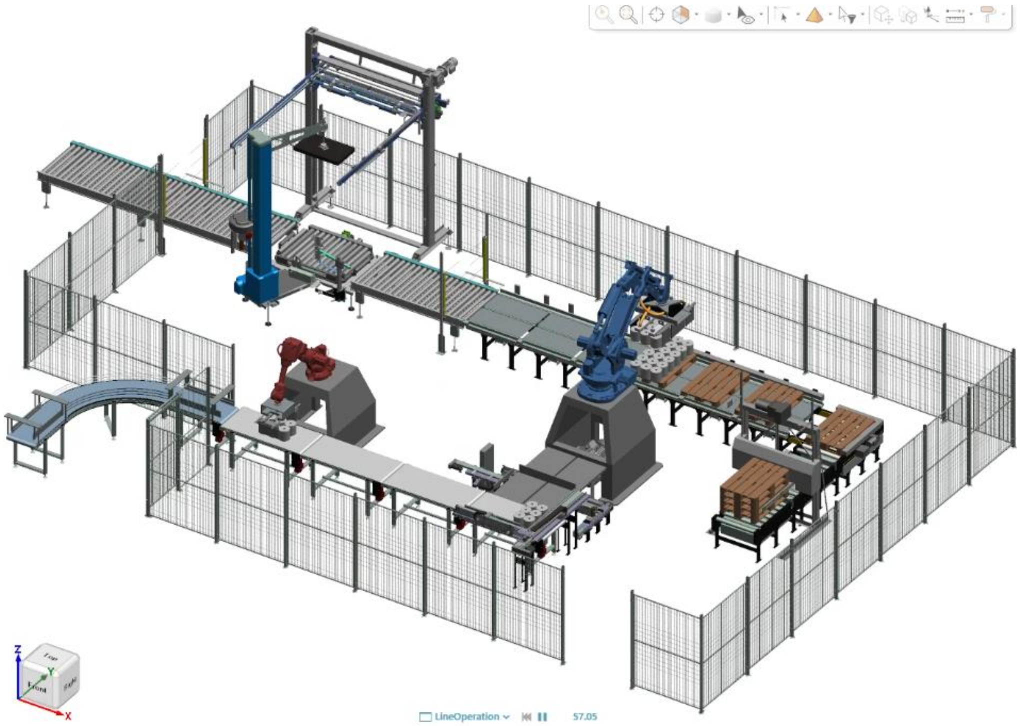

Fig.13 Palletizing object layers by the 4-axis robot

Fig.14 Wrapping the complete stack of objects

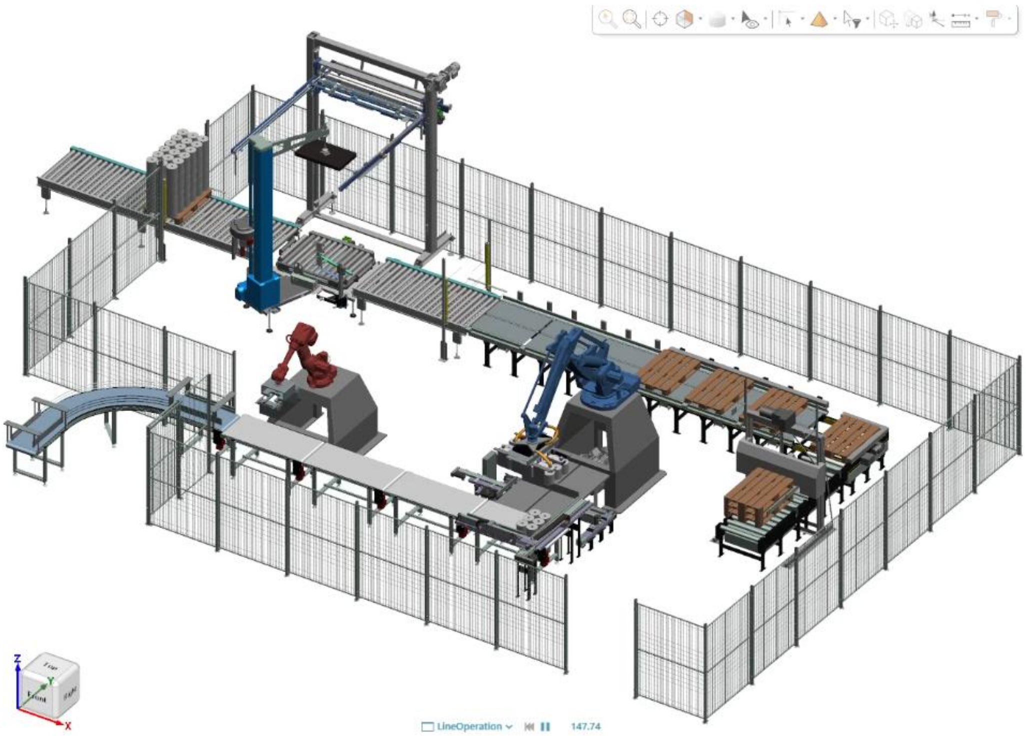

Fig.15 The exit of the complete and wrapped object stack from the cell

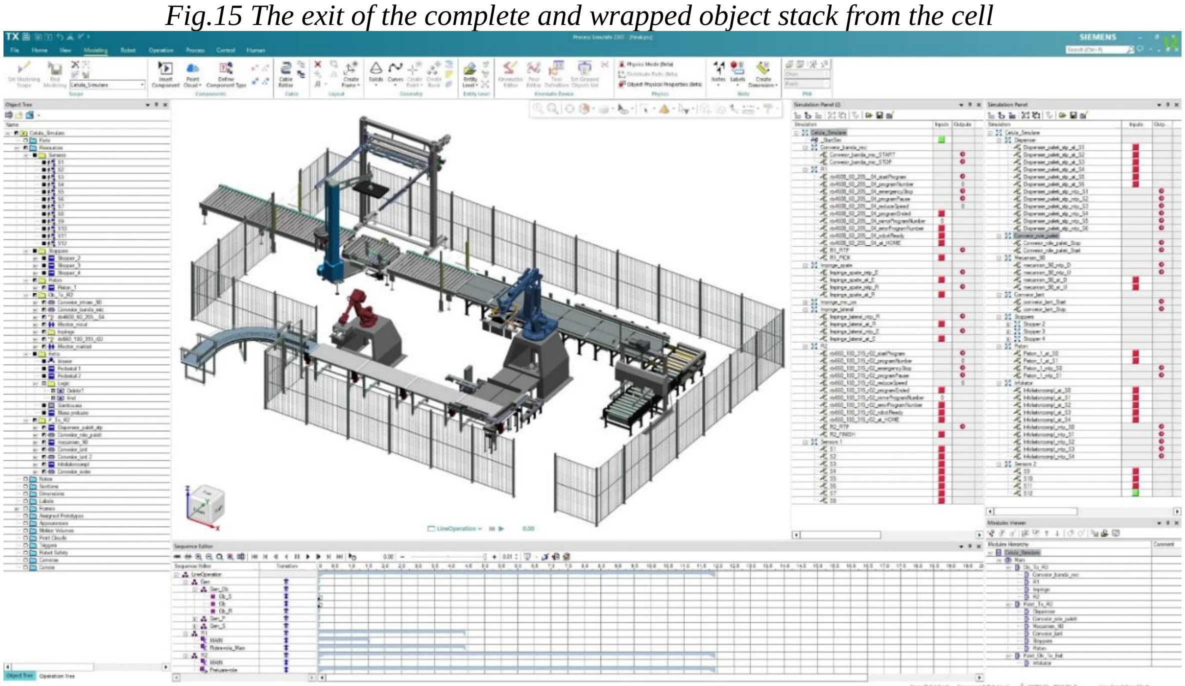

Fig.16 The overall view with the simulation at the moment the application starts

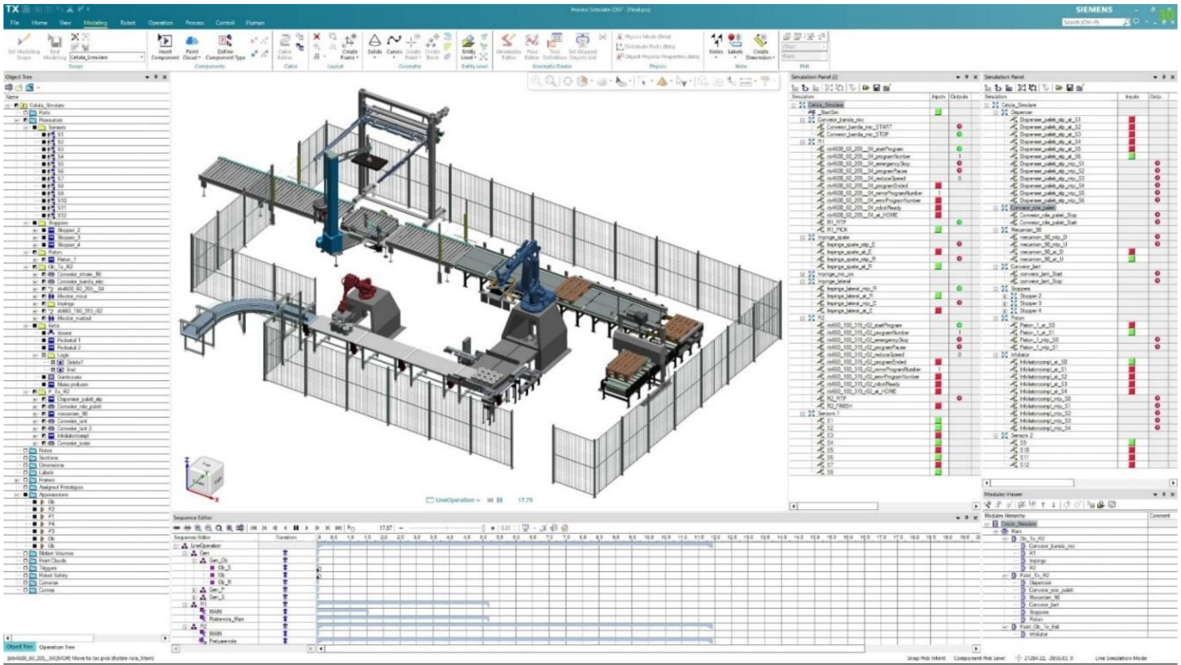

Fig.17 The overall view with the simulation during the application's execution

3. Conclusions

Contributions to Modeling:

- Full 3D design of the robotic cell in NX, including integration of sensors and mechanical systems.
- Detailed event-based logic created in Process Simulate, enabling stepwise control over object flow.
- Simulation of realistic conveyor behavior using control points and signaling systems.
- Logic development for major equipment: dual robots, pallet dispenser, and wrapping station.
- Use of "Key" and "Input" signals for precise control of the sequence and material flow.

Additional Contributions:

- Creation of a comprehensive flowchart mapping all system processes.
- Categorization and mapping of all sensor signals and I/O logic.
- Integration of transport modules for both paper packages and pallets, ensuring a continuous and autonomous workflow.

This project demonstrates the feasibility of modeling a real industrial palletizing system using Tecnomatix Process Simulate. By employing a modular, signal-driven approach, the system ensures efficient operation with minimal direct robot interaction, simulating a realistic production environment with high fidelity.

4. Bibliography

- Bucureșteanu A. – Pneumatic Actuation of Industrial Robots, UPB course notes, 2021
- Bucureșteanu A. – Pneumatic Elements and Systems for Industrial Robot Actuation, Printech Publishing, ISBN 978-606-23-0081-4, Bucharest 2013.
- Cristoiu C. – Computer-Aided Design 3 - NX CAD, course notes and application support, UPB, 2021
- Cristoiu C. A., Nicolescu A. F. – NX CAD-Basic - Computer-Aided Design
- Cristoiu C. – Programmable Logic Controllers, course notes and application support, UPB, 2020
- Dobrescu T. – Basics of Kinematics of Industrial Robots, Bren Publishing, ISBN-973-9427-02-2, Bucharest, 1998
- Dorin A., Dobrescu T., Pascu N., Ivan I., – Kinematics of Industrial Robots, Bren Publishing, ISBN-978-973-648-970-9, Bucharest, 2011
- Dorin Al., Dobrescu T. – Pneumatic Actuation of Robots, Bren Publishing, ISBN-973-648-060-7, 2002
- Dorin Al., Dobrescu T., Bucureșteanu A. – Hydraulic Actuation of Industrial Robots, Bren Publishing, 2007
- Enciu G., Popescu A. – Industrial Sensors, course notes, UPB, 2021
- Nicolescu A., Coman C. – Robotics 2, course notes and applications, UPB, 2019
- Nicolescu A., Coman C. – Robotics 3, course notes and applications, UPB, 2020
- Nicolescu A., Coman C. – Electric Drives for Mechatronics and Robotics, course notes and design methodologies, UPB, 2020
- Nicolescu, A. – Concept and Exploitation of Industrial Robots 1, course notes and applications, UPB, 2021
- Nicolescu, A. – Concept and Exploitation of Industrial Robots 2, course notes and design methodologies, UPB, 2021
- Nicolescu, A., Industrial Robots, ISBN 973 – 30 – 1244 – 0, Didactic and Pedagogical Publishing House, CNCSIS code 165, 2005, Bucharest
- Nicolescu A. F., – Concept and Exploitation of Industrial Robots - Calculation Methodologies for Design and Verification of Industrial Robots' Exploitation Conditions, 473 pages, Politehnica Press, 2021, CNCSIS Code 19, ISBN 978-606-515-916-7, CIP BNR 2020-14500
- Nicolescu A., Dobrescu T., Ivan M., Avram C., Brad S., Doroftei I., Grigorescu S. – Industrial Robots, Robotic Production Technologies and Systems, 190 pages, Academy of Scientists Publishing House, Romania, 2011, ISBN 978 – 606 – 8371 – 48 – 1, CIP BNR 2011-21962, BNR Code III 307660
- Nicolescu, A. – Implementation of Industrial Robots in Production Systems, course notes and design methodologies, UPB, 2022
- Nicolescu, A. – Concept and Exploitation of Robotic Production Systems, course notes and design methodologies, UPB, 2022
- Silvestru C. – Basics of Offline Programming of Industrial Robots, course notes and application support, UPB 2022
- Badea Marian-Cristian. – Diploma project "Robotic Cell for Palletizing Paper Rolls Integrating Two Articulated Arm Industrial Robots"

TRANSIENT ANALYSIS (FEM) OF THE CONVEYOR LOAD-BEARING STRUCTURE WHEN DISCHARGING NON-COMPLIANT BAGS

NICOLESCU Răzvan Florin, Tiberiu Dobrescu(Conducător științific)
Faculty of Industrial Engineering and Robotics, Robotics specialisation, 4th year
nicolescu.razvan@yahoo.com

I Introduction

During the application, the robot freely drops a bag from a height of 150mm. It drops onto a 2m long roller conveyor with a 30º incline and moves freely.

Fig. 1 Conveyor removing non-compliant bags

The objectives of the research are to verify the operational safety of the conveyor belt bars, and to verify the fall of the bags on the conveyor when tilting at the required incline.The working stages were:

- Bibliographic research
- Simplification of the model
- Reducing the computing model from 3D to 1D
- Meshing was done with Courant number calculation - taking the shock wave into account
- The solution parameters were set in the explicit dynamic analysis according to the normal ...
- Energies affecting the system were monitored in real time
- The results were processed in order to check the structural elements of the conveyor.

II Analysis

The analysis was performed in the Ansys Explicit Dynamics module, due to the time efficiency compared to Transient Structural.

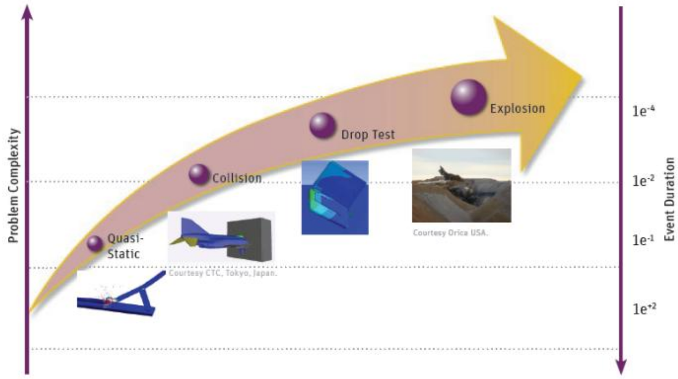

Fig. 2 Complexity - duration graph regarding Explicit Dynamics

The selection criteria for the type of analysis are:

- The application is short in length
- The application contains extreme non-linearities (granular material inside the bag)

- The time step is calculated according to the discretization in order to visualize the dispersion of shock waves

The explicit analysis does not calculate the stiffness matrix. In the current case, consider the mass and inertia forces, using a method containing the CFL (Courant-Friedrichs-Levi) time step. Thanks to this method, it is possible to observe the formation of shock waves in the form of waves along the bag.

Fig.3 Courant time step

Explicit analysis works relatively easily with contact elements and nonlinear materials. The equations of

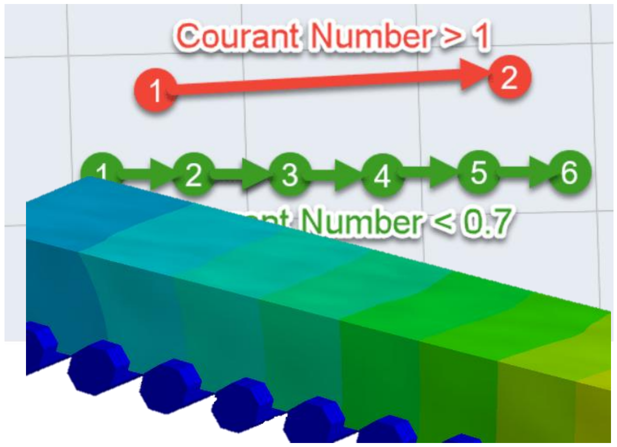

motion express (respect) the conservation of mass, momentum and energy in Lagrangian coordinates. They, together with a given material model and a set of initial data (e.g. initial velocities, etc.) and boundary conditions (constraints imposed on the model), completely define the dynamic phenomenon to be solved.

Fig.4 Total displacement and shock propagation

Calculation algorithm: calculate the accelerations {ü} at time n, the velocities {u̇} at time n + ½ and the displacements {u} at time n+1. With the displacements {u} the specific deformations {ε} are determined. With the specific deformations {ε} the stress {σ} are calculated. And the cycle is repeated for the next time step.

For Lagrange formulations, the discretization lattice shifts and distorts with the material it models, so that mass conservation is automatically satisfied.

Conservation of mass. The density can be determined at any time from the current volume (V), the initial mass (m_0) and the initial density:

$$\frac{\rho_0 V_0}{V} = \frac{m}{V} \qquad (1)$$

The partial differential equations expressing the conservation of momentum include the acceleration of the stress tensor σ_{ij}:

$$\rho\ddot{x}=b_x+\frac{\partial\sigma_{xx}}{\partial x}+\frac{\partial\sigma_{xy}}{\partial y}+\frac{\partial\sigma_{xz}}{\partial z}$$
$$\rho\ddot{y}=b_y+\frac{\partial\sigma_{yx}}{\partial x}+\frac{\partial\sigma_{yy}}{\partial y}+\frac{\partial\sigma_{yz}}{\partial z} \qquad (2)$$
$$\rho\ddot{z}=b_z+\frac{\partial\sigma_{zx}}{\partial x}+\frac{\partial\sigma_{zy}}{\partial y}+\frac{\partial\sigma_{zz}}{\partial z}$$

Energy conservation is expressed by the relation:

$$\dot{e}=\frac{1}{\rho}\left(\sigma_{xx}\dot{\varepsilon_{xx}}+\sigma_{yy}\dot{\varepsilon_{yy}}+\sigma_{zz}\dot{\varepsilon_{zz}}+2\sigma_{xy}\dot{\varepsilon_{xy}}+2\sigma_{yz}\dot{\varepsilon_{yz}}+2\right)\sigma_{zx}\dot{\varepsilon_{zx}} \qquad (3)$$

For each time step these equations are solved explicitly for each element in the model, based on the input values at the end of the previous step. At the first time step they are solved based on the initial conditions.

Only conservation of mass and momentum apply in the solution. However, in explicit simulations, mass, momentum and energy should be conserved. Therefore, the conservation of energy is constantly monitored on the graph that also expresses the quality of the results (as opposed to the convergence tolerances in the implicit transient dynamics).

The Explicit solver uses a differential time integration scheme called the Leapfrog method. After calculating the forces in the nodes (resulting from internal stress, contact or boundary conditions), the nodal accelerations are obtained by dividing the force by the mass:

$$\ddot{x_i}=b_i+\frac{F_i}{m} \qquad (4)$$

where $\ddot{x_i}$ are the components of nodal acceleration (i = 1,2,3), Fi are the nodal forces, bi are the components of body acceleration (x,y,z) and m is the mass.

With the accelerations at time n - ½ determined, the velocities at time n + ½ are calculated:

$$\dot{x}_i^{n+1/2} = \dot{x}_i^{n-1/2} + \ddot{x}_i^{n} \Delta t^{n} \quad (5)$$

Finally, the node positions are updated at time n + 1 by integrating the velocities:

$$x_i^{n+1} = x_i^{n} + \dot{x}_i^{n+1/2} \Delta t^{n+1/2} \quad (6)$$

III Geometry + Discretization

To decrease processing time, was opted to use 1D bars for the conveyor, and of 3D bodies for bag and contents. The computational model focused only on the area of on the conveyor where the bag drop occurs.

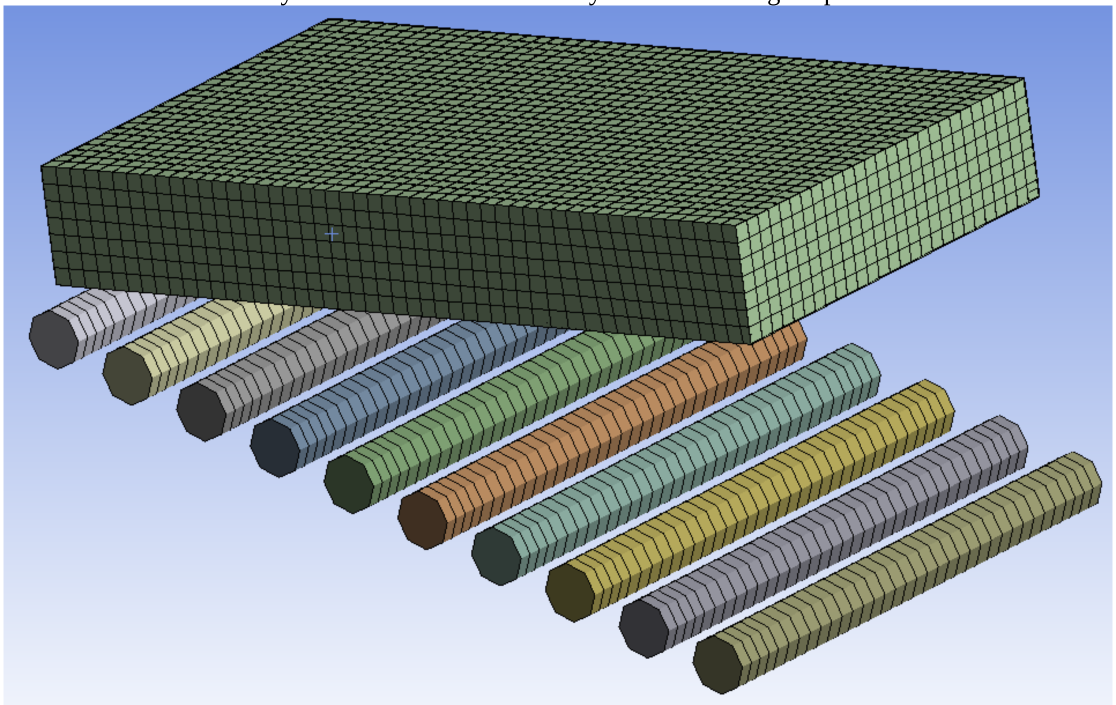

Fig. 5 Discretization

The object was positioned at a distance of 0.1 mm from the first roll in order to shorten the computation time while respecting the impact velocity.

The bag discretization was controlled using the size of the elements to ensure the square shape of the finite elements.

The sizes of the objects are as follows:

- Bag: Prism 700x400x100 mm
- The 10 conveyor rollers: 150 mm x 50 mm Ø

IV Materials

Three types of materials were used in the analysis:

- For conveyor: Aluminum (Aluminum Alloy) with linear behavior
- For the bag: custom cardboard material
- For bag contents: granular material from the Ansys explicit library

Table nr.1 Materials

	Density [kg/m^3]	Young's Modulus[Mpa]	Poisson's Ratio
Alluminium Alloy	2770	7110	0.33
Carton	892.86	4020	0.34

Bag content material:

25 kg mass – According to density

Composed of a granular material

Details of "Analysis Settings"

Analysis Settings Preference	
Type	Efficiency
Step Controls	
Number Of Steps	1
Current Step Number	1
End Time	0.75
Resume From Cycle	1.3567e+06
Maximum Number of Cycles	1e+07
Maximum Energy Error	0.1
Reference Energy Cycle	1e+07
Initial Time Step	Program Controlled
Minimum Time Step	Program Controlled
Maximum Time Step	Program Controlled
Time Step Safety Factor	1.
Characteristic Dimension	Opposing Faces
Automatic Mass Scaling	Yes
Minimum CFL Time Step	1.e-007 s
Maximum Element Scaling	1000.
Maximum Part Scaling	1000.
Update Frequency	0

Details of "Velocity"

Scope	
Scoping Method	Geometry Selection
Geometry	2 Bodies
Definition	
Input Type	Velocity
Pre-Stress Environment	None Available
Define By	Components
Coordinate System	Global Coordinate System
X Component	0. mm/s
Y Component	0. mm/s
Z Component	-1741. mm/s
Suppressed	No

Properties of Outline Row 6: SAND

	A	B	C
1	Property	Value	Unit
2	Material Field Variables	Table	
3	Density	892.86	kg m^-3
4	MO Granular		
5	MO Granular Pressure Hardening	Tabular	
6	Scale	1	
7	Offset	0	Pa
8	MO Granular Density Hardening	Tabular	
9	Scale	1	
10	Offset	0	Pa
11	MO Granular Variable Shear Modulus	Tabular	
12	Scale	1	
13	Offset	0	Pa
14	Shear Modulus	7.69E+07	Pa
15	Tensile Pressure Failure		
16	Maximum Tensile Pressure	-1000	Pa
17	Compaction EOS Linear		
18	Solid Density	2641	kg m^-3
19	Compaction Path	Tabular	
20	Scale	1	
21	Offset	0	Pa
22	Linear Unloading	Tabular	
23	Scale	1	
24	Offset	0	m s^-1

Fig.6 Granular material properties

V Initial conditions

The whole system was subjected to gravity.
An initial velocity of 1.741 m/s was added to the body using the formula $v = \sqrt{2gh}$, it is fixed using *fixed support* by selecting points at the end of the bars.

Results processed:

- moving
- total tension
- shear strength

Measurements were also added for:

- internal energies
- pressure
- axial forces in bars

Fig. 7 Analysis settings

Fig. 8 Velocity added to object

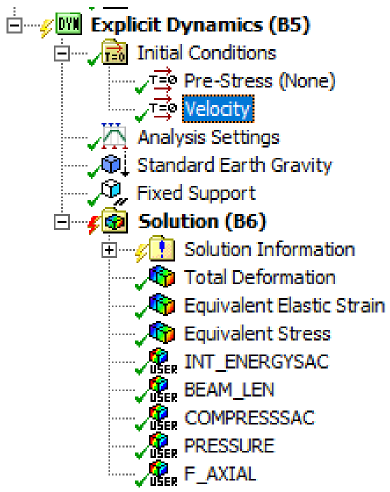

Fig. 9 Actions and results

VI Present Energies

Kinetic energy, potential energy, contact energy and hourglass effect were monitored during the calculations. It is observed that the energy of the system is conserved throughout the analysis. It can also be easily seen from the graph that the distortion of the finite elements during impact is negligible.

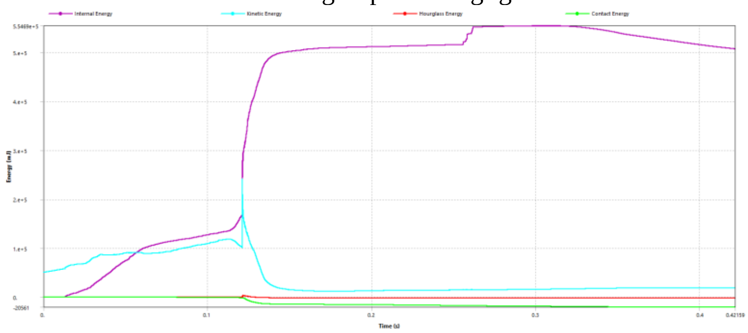

Fig. 10 Present energies

VII Total displacement

On impact with the full length of the bag, the granules begin to change the structure of the bag, forming waves as in the adjacent figure.

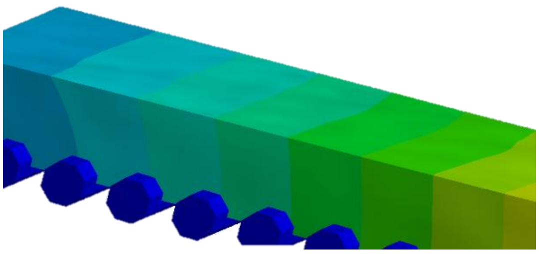

Fig. 11 Total displacement and shock propagation

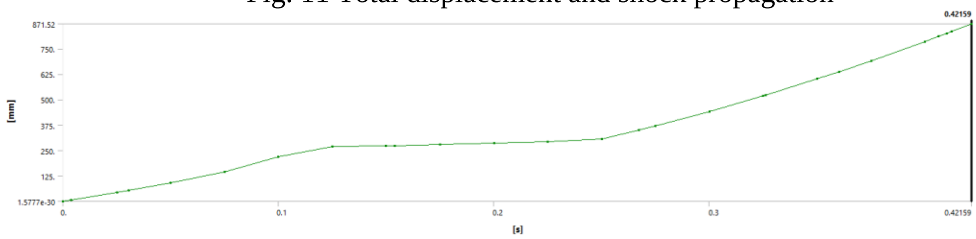

Fig. 12 Results graph Total displacement

VII Tension (Von-Mises)

Fig. 13 and 14 Color coding of tension and stress at t = 0.125s

The stress in the granular material are low due to grain dissipations with maxima in the areas where the particles concentrate, and towards the end of the analysis a stress concentrator is observed in the center of gravity.

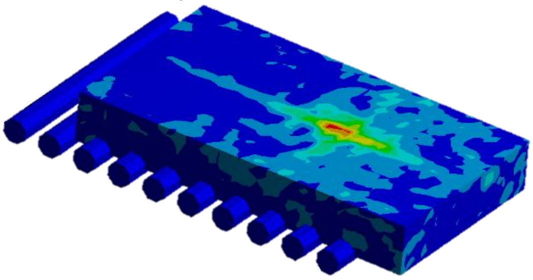

Fig. 14 Tension at t = 0.375s

VII Internal energy in the object

Throughout the simulation, it is observed that the internal energy is increased in the center of gravity of the bag, but also increases behind it.

Towards the end it is observed how, as the object slides off the conveyor, the energy is transferred to the front of the bag.

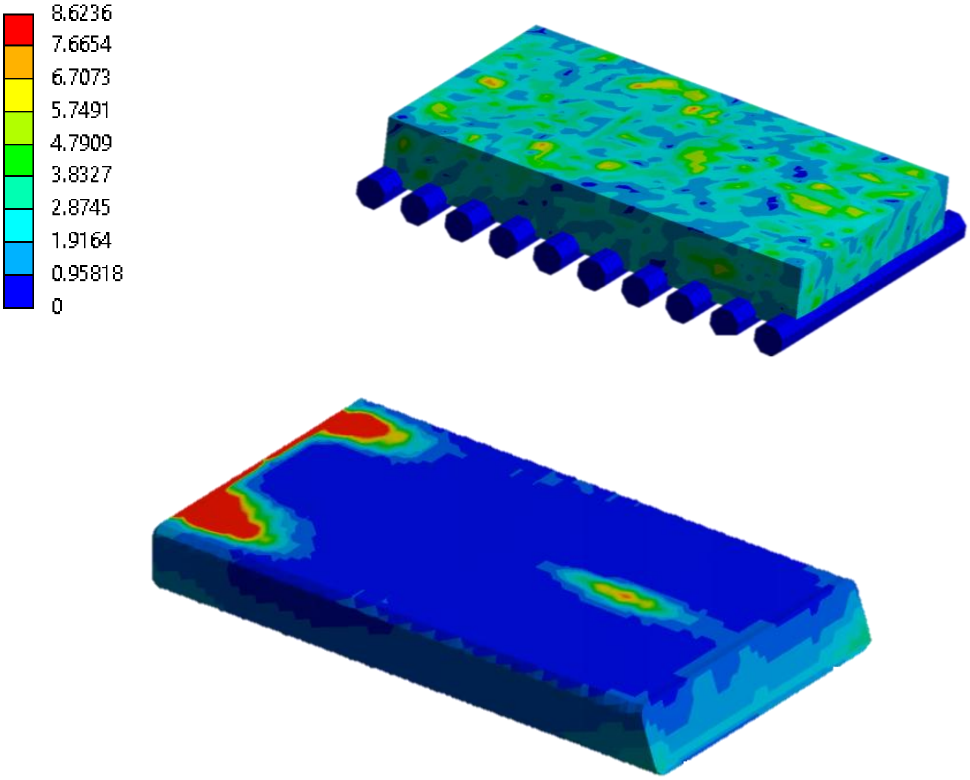

Fig. 16 Internal energy in the object at the end of the analysis

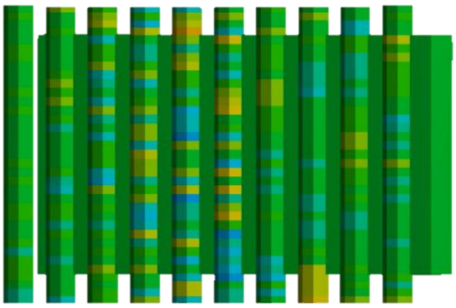

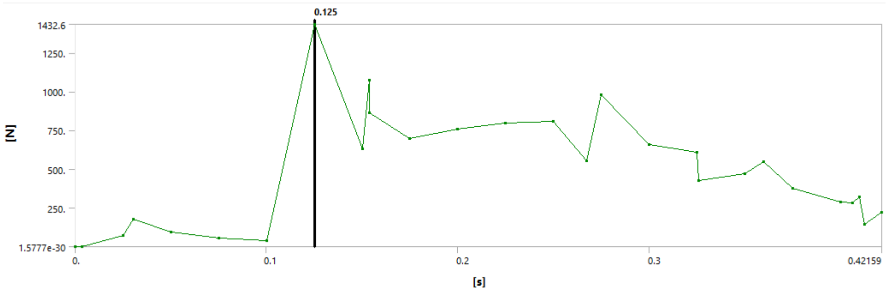

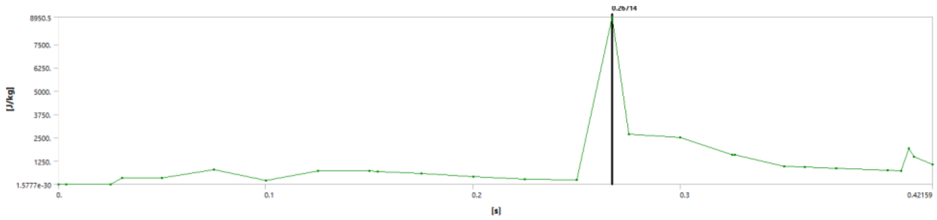

Fig. 17 Internal energy graph

VII Pressure

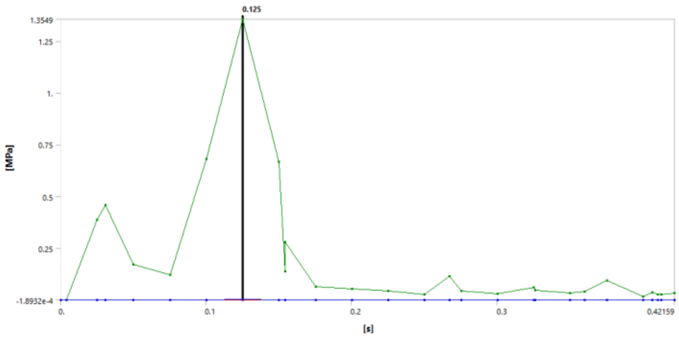

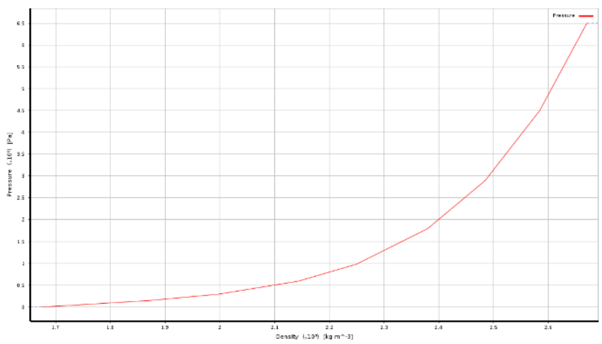

Fig. 18 and 19 Pressure and Material compaction graph

According to the compaction graph, the pressure created on impact has no effect on the density of the material.

The pressure of 1.35 MPa is far too low to have a measurable effect (the graph uses 100 MPa increments).

VII Axial forces in bars

In the adjacent picture can be seen the dispersion of axial forces applied on the bars. They follow the waves formed by the granules inside the bag.

Fig.20 Shock wave propagation at the bars Fig.21 Axial force graph

VIII Conclusions and points of originality

Taking into account the results of the explicit analysis and the comparison with similar current research the following can be stated:

- The research presented is original
- The material models used in the simulation were validated
- Impact between bag and conveyor does not damage the conveyor

Using *ScienceDirect*, we found research on the impact of heavy objects on conveyors dating back as far as 2014.

[1] Feodorko, from the Univ. of Košice did in 2014 experimental impact research for belts when sharp objects fall

[2] In 2020 Andrejiova, at the same university, continued experimental impact tests and created models with mathematical regression for these situations.
[3] Also in 2020, Grincova makes it clear that tests on belts should focus on finding new materials with higher strength.
However, I did not find any FEM simulations on the current research topic.

IX Bibliography

[1] Fedorko, Gabriel, et al. "Failure analysis of belt conveyor damage caused by the falling material. Part I: Experimental measurements and regression models." *Engineering Failure Analysis* 36 (2014): 30-38.
[2] Andrejiova, M., A. Grincova, and D. Marasova. "Monitoring dynamic loading of conveyer belts by measuring local peak peak impact forces." *Measurement* 158 (2020): 107690.
[3] Grincova, Anna, et al. "Measurement and determination of the absorbed impact energy for conveyor belts of various structures under impact loading." *Measurement* 131 (2019): 362-371.
[4] Pupăză, C., Parpală, R.C. - *Structural modeling and analysis with ANSYS Workbench*, Editura Politehnica Press, 2011
[5] Pupăză, C. - *CAD-FEM modeling*. Editura Politehnica Press, 2013
[6] CAE program manuals: Ansys Workbench, Nastran, SIMULIA - ABAQUS, LS-DYNA, etc.
[7] Written and electronic support on Moodle platform 2024-2025

RESEARCH AND DEVELOPMENT OF A FLEXIBLE THERMOS INTEGRATING MATERIAL LIBRARIES USING PYTHON SCRIPTS

CIOCONEA Adina[1], Pupăză Cristina(Conducător științific)

[1]Facultatea: Inginerie Industrială și Robotică, Specializarea: Integrated Engineering, Anul de studii: 4, e-mail:cioconea.adina@gmail.com

SUMMARY: The study follows the idea of developing an innovative thermos with minimal size when empty and yet keeping a good thermal insulation. The research is focused on material selection and material model validation and encompasses scripting to automate, extract and organize material properties as inputs in CAE simulation, as well as result post-processing. A physical flexible bottle from the market was employed to prove the material model and properties. The simulation software was appropriate for simulating the thermos behavior in a prescribed, easy-to-reproduce procedure. Original Python scripts were developed to run multiple simulation scenarios without involving manual inputs for parameters change and extraction and categorizing the simulation results. The approach proved how combining material knowledge, FEM solvers and automation procedures can help the researcher to validate and collect data for realistic simulation results.

Keywords: innovative thermos, material, Python scripting, simulation, automation.

1. Introduction

In today's world, innovative materials are employed for various products - from food containers to new consumer goods. The basic concept for an innovative thermos is to minimize the size of the product, to offer excellent flexible properties, keeping heat transfer caused by conduction, convection, or radiation at minimum. Regarding food and beverage transport capabilities, the new structure is mostly conservative - a double wall concept, an insulation layer in between, a tight lid or cap, and maybe even a shiny reflective surface on the inner wall.

Current design solutions for food and drinks take up space. They're not always portable, customizable, or even size convenient. The goal of this research is to develop a new concept of a thermos that is portable, flexible, has good thermal isolation capabilities, and is robust, easy to clean and food safe.

The article is structured as follows: the first section describes the new concepts that lead to a new design, then a material validation study is performed employing material libraries and automatic inputs in the simulation model using Python scripting. The simulation results and thus the new material model are verified by experiments. Finally the simulation outputs are also processed by original automated procedures that pave the way for the use of AI in CAE scenarios.

2. Problem statement

The present research is focused on verifying the structural response of a new flexible container intended for thermal use. A commercially produced collapsible bottle made of food-grade silicone served as both inspiration for a new design, but also as a reference model for material validation. The object was also experimentally tested under controlled displacements to observe how it deforms and how it recovers then the initial shape, to tune the material model with the real behavior of the collapsible bottle.

Following this, a 3D model of the bottle was created for the Computer Aided Engineering (CAE) study. The applied displacements mirrored those in the experiment, allowing a meaningful comparison between virtual and real-world behavior. The material was treated as a hyper elastic solid, suitable for high-strain scenarios, and the deformation patterns between the two environments turned out to be closely aligned.

To reduce a repetitive work and to speed up the numerical simulation, a Python-based workflow was written. The script processes input data, adjusts material settings, launches analyses, and collects output figures and numbers. This structure supports recurrent testing with minimal manual involvement, while keeping result interpretation consistent.

The numerical simulation, as well as the experiments confirmed that the new flexible design can hold up under pressure. While thermal insulation tests in progress, the groundwork has been laid. The approach can now be extended to test more complex physical conditions, and the digital process is modular and adaptable and can also be employed for general testing purposes, such as different geometries and material models for various applications.

3. Design and development

After conducting several rounds of analysis and exploration as needs analysis and systemic literature review [1][2][3] the innovative idea was defined. TRIZ and QFD helped solve design challenges and match user needs with functions. Morphological analysis and Su-Field methods guided concept generation, while AHP was employed to pick the best solution, and an initial design direction began to be shaped. The first objective was to develop a thermos that balances portability, flexibility, and thermal performance - all while remaining compatible with food safety standards.

This initial prototype concept is shown in Figure 1 and Table 1, which outlines the modular construction, insulation chamber, and flexible outer wall.

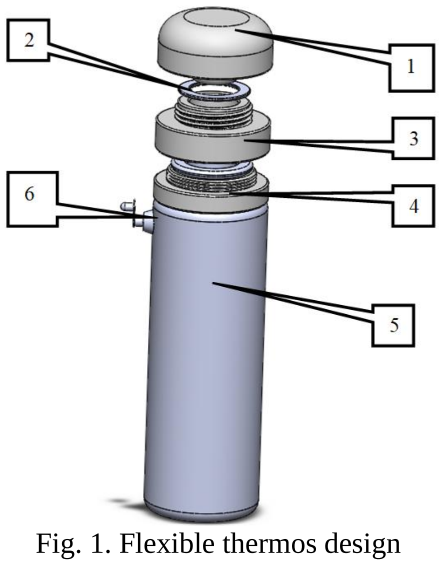

Fig. 1. Flexible thermos design

Table 1. Flexible thermos components

No.	Part name	Quantity	Dimensions [mm]
1	Cup	1	R35 x h40
2	Seal	1	R22 x r15 x h2
3	Top lid	1	R35 x r15 x h 20.5

4	Bottom lid	1	R35 x r20 x h 19
5	Bottle	1	R35 x r30 x h 217
6	Air valve	1	R24 x r5 x h18.7

The resulting concept is a modular thermos with interchangeable components. Its dimensions were carefully selected to fit into common use contexts, like car cup holders, side pockets of backpacks, and standard bottle compartments. In terms of functionality, the bottle is designed to resist deformation under pressure, while still allowing it to collapse when empty. It blocks two of the main thermal transfer mechanisms conduction and convection, with targeted solutions applied to both geometry and materials.

The inspiration for the bottle's soft, flexible body came from the baby bottle nipples, which share similar requirements: food-safe materials, flexibility, ease of cleaning, and durability. For the insulation component, the idea was drawn from inflatable systems - like the ones used in sports balls. The air layer created between two flexible walls forms a barrier against the thermal exchange, mimicking vacuum-insulated behavior in a much simpler structure. Also, the model is thought to permit additional features as adding a custom bottle sleeve, thermometer integration into the cup or a straw.

4. Static structural hyperelastic simulation

For the CAE simulations, the materials were selected based on a real-life collapsible silicone bottle used as a reference. According to the product label, the body is made from silicone rubber, while the cap is made from HDPE high-density polyethylene - a common choice for lids due to its durability and rigidity. These same materials were assigned in the simulation to mirror the actual behavior of the components.

The Finite Element Method (FEM) material models in this study were conceived on the Neo-Hookean hyperelastic model, which is commonly employed for materials that undergo large, recoverable deformations like silicone rubber. This model assumes isotropic and nearly incompressible behavior. In this case the stress-strain relationship can be defined as [4]:

$$\sigma \cong 4C_1 \cdot Term_1(\varepsilon) + 2D_1 \cdot Term_2(\varepsilon) \tag{1}$$

where:

- C_1 is related to the initial shear modulus ($\mu = 2C_1$)
- D_1 is the incompressibility parameter
- $Term_1(\varepsilon)$ and $Term_2(\varepsilon)$ are functions of the strain

This model is valid for strains up to ~30-40% in biaxial and 80% in shear strain. This material model was chosen due to its simplicity and suitability for silicone behavior [5].

The purpose of the FEM analysis was to evaluate whether the selected materials are suitable for a flexible thermos, particularly in terms of their performance under deformation. By imposing displacements rather than applying loads. The simulation aimed to replicate the real-life experiment, where the collapsible bottle was manually compressed. This approach aimed to validate the silicone's flexibility and to confirm whether it can maintain its structural integrity during the use in a new innovative product design.

The material properties needed in the FEM analysis were mainly the initial shear modulus μ and the incompressibility parameter. The lid was assumed to be rigid in comparison with the bottle, although the lid capabilities are not important for this analysis. Fig. 2 illustrated a flexible bottle and the 3D replica.

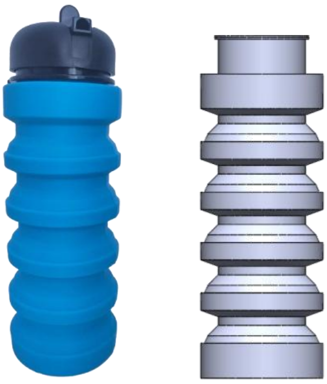

Fig. 2. The physical flexible bottle and the 3D model

The flexible bottle was analyzed on half of the model, due to its symmetry. The mesh has to reach multiple quality criteria. The finite element order has been set to two, the size function of the elements was set to curvature, while for the mesh generation a Hex dominant algorithm was chosen, with edge control sizing on 21 segments per semicercle. Also a face meshing strategy was applied resulting a computational model with 108447 nodes and 22829 elements.

In order to tune the simulation with the experiments on a real flexible multiple boundary conditions ere included. The base of the thermos was fixed on the Y direction and similar on the X direction for the bottom face and the lower face. The flexibility of the bottle was simulated by following the displacements on a remote point, with a -10 mm translation on the vertical direction and a rotation of 30 degrees around its axis.

After the definition of solving parameters, the static hyperelastic analysis was completed. The main processed results were the total deformation of the model, as well as the equivalent von Mises stress and the Equivalent elastic strain. The total deformation, captured on Fig. 3 on each load step proved a maximum value of 57.848 mm and a curved deformed shape.

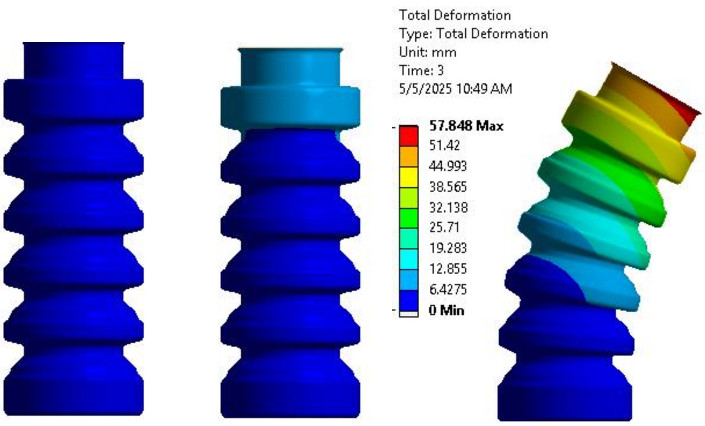

Fig. 3. Total Deformation on steps 1,2 and 3

Regarding the material model applied in this analysis, the obtained results provide solid confirmation of its suitability. The simulated equivalent stress reached a maximum value of 0.226 MPa, while the corresponding strain remained around 3.6% - both well within the elastic range typically tolerated by silicone rubber, which can often endure strains exceeding 100% without permanent deformation. These findings indicate that the Neo-Hookean material model was appropriate for capturing the nonlinear elastic behavior of the material under moderate deformations.

5. Experimental validation of the simulation results

The experiments were conducted employing a silicone bottle bought from the market, and the displacements were set in accordance with the FEM analysis, followed by measurements and assessments. The bottle was set on a flat surface next to a millimetric paper set to match the start with the flat surface on a vertical wall and the margins were noted dimensions for easier readability. Also to imply similar boundary conditions the bottle was held on the bottom surface to prevent the displacement.

The 3 steps displacement was recreated as can be observed on Fig. 4, checking the displacement next to the millimetric paper.

Fig. 4 Normal state and deformation on displacement -10mm and 30 degrees.

At each step, the initial potential maximum displacement was noted on the millimetric paper and as a result, there was a value of about 50-60 mm (on multiple tries), the value that validates the simulation on the real-life flexible bottle.

6. FEM simulation and Python automation

To compare how different flexible materials would perform inside the thermos structure, as well as the material law confirmation, an automated script was built using Python. The script's main task was to avoid repeating manual inputs when testing the material behavior using virtual models.

Material properties (especially initial shear modulus and incompressibility parameter) were taken from an Excel sheet. These were inserted into a standard text-based input file and used to run simulations. The script was designed to work with the mm-N-second (mm-N-s) unit system to match the simulation environment.

Software Requirements:

- Python 3.x (tested with version 3.10)
- ANSYS (version 19.0 or compatible), installed and accessible by command line (e.g., ansys190) [6]
- ANSYS MAPDL solver license available and working in batch mode

The following Python packages must be installed via pip:

- pandas for Excel data handling
- re for string cleaning and parsing
- subprocess for ANSYS execution
- pyvista for 3D result visualization
- numpy and matplotlib for numerical operations and plotting
- ansys.mapdl.reader (PyAnsys) for extracting simulation results

The flowchart of the script is presented on Fig. 5:

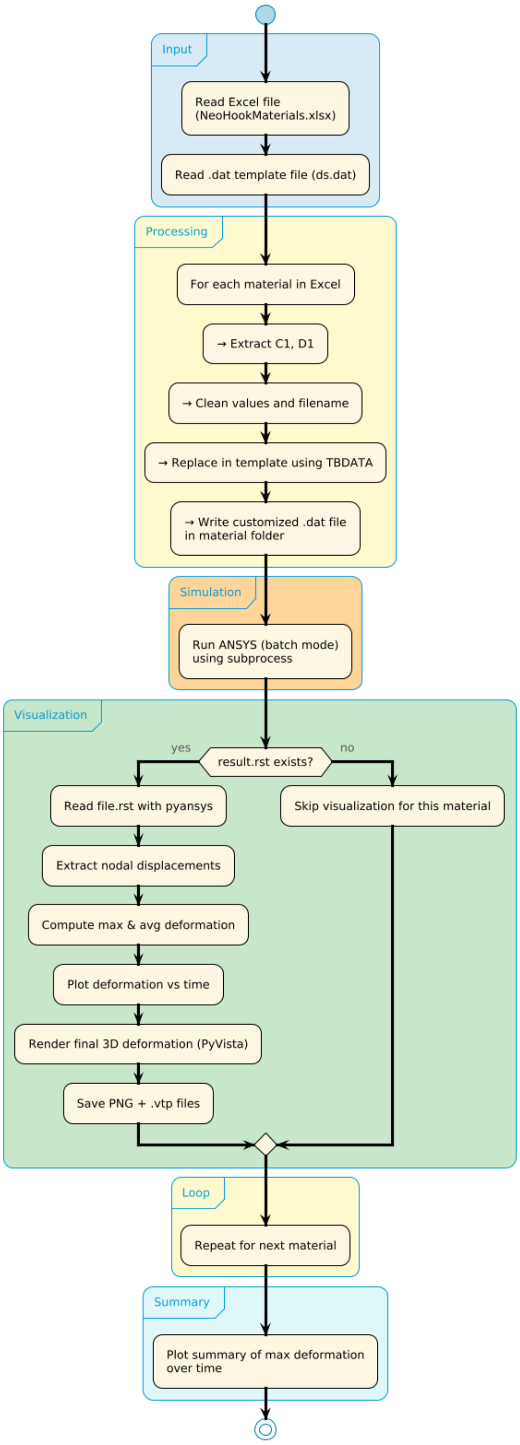

Fig. 5 Script flowchart

Input Files:

- Material Excel File: NeoHookMaterials.xlsx
- Template File: ds.dat
- ANSYS Executable path (e.g., ansy190) or executable Ansys path set into environment variables

The script reads the Excel file, adjusts the material template, starts the simulation, waits for results, and saves both numbers and graphs. Each material gets its own folder with all related files, so it's easy to track and compare results.

The following command was executed in batch mode for each case:

"ansys190 -b -i material_name.dat -o result.rpt"[6]

This ensured results were saved cleanly and each case ran independently.

Outputs:

- Modified input .dat file with updated material parameters
- Report and result files from the simulation
- Plot images showing how much each material bends or stretches
- 3D model views of the final deformation in a VTK file for further inspection

The results can be collected and displayed in many forms automatically using specific functions from data analysis libraries as pandas and matplot, see example in Fig. 6.

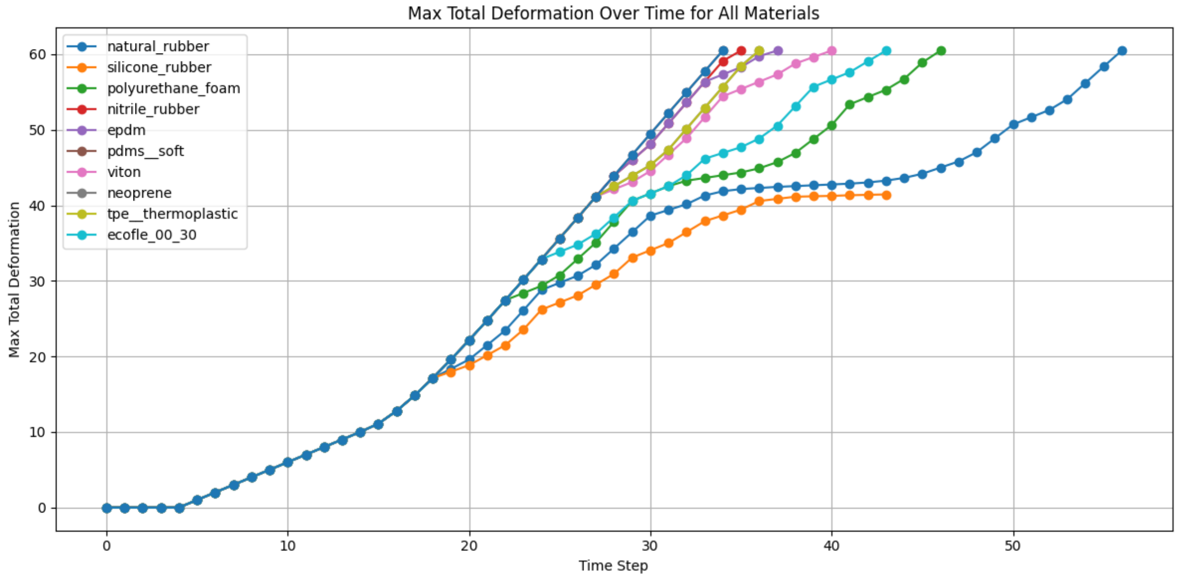

Fig. 6 Cumulate result chart of the total deformation

The script greatly improved testing efficiency by running ANSYS in batch mode, cutting down the time spent on manual setups. By pulling material data from Excel and handling simulations automatically, it removed the risk of input errors and kept the results consistent. Each material's outputs-plots, files, and 3D views-were saved in separate folders, making comparisons straightforward. This structure not only sped up the process but also made decision-making easier through clear, organized data presentation. It also paves the way to introducing AI in CAE procedures.

7. Conclusions

To sum up, this research proved that:

- The flexible thermos can be modeled using Neo-Hookean material law
- Real deformation matches the simulation
- Integrating Python scripts makes the whole process faster, avoids human error and enhances the readability of the results
- Silicone rubber is a good pick for this kind of design

As future work, one of the next steps is to perform both static structural and transient thermal simulations directly on the full thermos design, to prove the thermal retention, flexibility and stiffness of the structure, cycling between CAD and CAE until a satisfactory result.

The Python script turned out to be more than just a time-saver. Running batch simulations became easier and quicker, and extracting the results like deformation, stress and strain values formatting in the preferred way makes the result visualization easier, helping the decision-making between materials. Plus, since its modular, it could easily be adapted for other simulations types, too, such as transient thermal, with just a few parameter changes.

In the long run, this script might even be employed for data collection - feeding information into AI models that predict material behavior, but in also many other CAE scenarios.

8. Bibliography

[1] Alexis, J., Metoda Taguchi în practica industrială-Planuri de experienţe, Bucureşti, Editura Tehnică, 1999

[2] Doicin C., Product development, course notes, academic year 2018-2019, POLITEHNICA University of Bucharest

[3] Ionescu N., Vişan A., Stoicescu D., Creativity and intellectual Property, Editura BREN (Cod CNCSIS 96), București, 2016, ISBN 978-606-610-188-2.

[4]. Kossa, A., Valentine, M.T. & McMeeking, R.M. Analysis of the compressible, isotropic, neo-Hookean hyperelastic model. *Meccanica* **58**, 217–232 (2023). https://doi.org/10.1007/s11012-022-01633-2

[5]. Pupăză C. Modelare CAD-FEM. Editura Politehnica Press, București, 2013

[6]. Pupăză, C., Petrescu, I. - ANSA şi META-Post. Preprocesare şi postprocesare pentru analiza structurală. Editura POLITEHNICA PRESS, București, 2013;

SIMULATION OF THE TRANSIENT STRUCTURAL BEHAVIOR (FEM) OF THE FORK ASSEMBLY WITHIN THE END-EFFECTOR OF THE ROBOT INTEGRATED INTO A FLEXIBLE PALLETIZING LINE

ȘTEFU Mădălina-Georgiana, NICOLESCU Adrian Florin(Conducător științific)

Faculty: Industrial Engineering and Robotics, Specialization: Robotics, Year of Study: IV, e-mail: madalina.stefu@stud.fiir.upb.ro

ABSTRACT:
The work focuses on the transient structural analysis of the fork assembly within the End-effector, using the implicit Finite Element Method. The objective of the study is to simulate the response of the assembly under the action of time-varying forces. In this context, the input data, besides material properties, discretization, initial and boundary conditions, includes time-dependent forces, moments, and displacements, applied in successive time steps, in order to accurately reflect the kinematic behavior of the assembly under real operating conditions. The study also addresses the reduction of the computational model from a full 3D structure to a combination of shell and beam elements, this approach offering the main advantage of significantly reducing computation time and resource requirements, without compromising result accuracy.

KEYWORDS: transient structural analysis, fork assembly, end-effector, model reduction, time-varying forces

1. Introduction

The Finite Element Method (FEM) is one of the most widely used numerical techniques in computer-aided engineering (CAE), applied in the analysis of complex structures with a high level of detail. Initially developed for studying the linear-elastic mechanical behavior of materials, FEM has rapidly expanded to address more complex fields such as nonlinear analysis, computational fluid dynamics (CFD), explicit dynamic analysis, and others [1, 4].

For this study, transient structural analysis was performed using the implicit Finite Element Method (FEM), which employs the Newmark integration scheme. This method uses a Taylor series expansion to approximate displacements, velocities, and accelerations. Within this approach, equilibrium conditions are satisfied at discrete time steps. The smaller the sampling interval, the better the continuity and convergence conditions are met; however, the required computational time increases accordingly. Although many methods adopt equal time steps, in highly nonlinear problems a variable time step can be used, as implemented in the implicit solver in ANSYS [1, 4].

Another method is the direct one, in which the equations are solved in their original form and equilibrium is satisfied only at discrete time steps. A specific variation of displacements and velocities is assumed over each time interval [4].

Within each interval, displacements and velocities are estimated based on the information available at the beginning of the time step. The numerical stability of the direct method is dependent on the size of the time step: to ensure stability, the discrete time steps must be sufficiently small in relation to the system's natural frequencies. This characteristic makes the explicit method efficient for analyzing short-duration, high-intensity phenomena such as impacts or explosions, where extremely small time steps are acceptable [4].

The paper addresses the reduction of the computational model from a 3D structure to a combination of plate and beam elements, as the components were modeled using 1D and 2D approaches. This modeling strategy offers the main advantage of significantly reducing computation time and the computational resources required, without compromising the accuracy of the results in critical areas. By abstracting certain parts of the structure into elements with idealized behavior, more efficient modeling can be achieved, especially in cases where a full 3D analysis would involve an unjustifiably long processing time. At the same time, a significant simplification of the discretization mesh is achieved, leading to a reduced number of finite elements and, consequently, a lower total number of equations to solve.

The fork-style end-effector analyzed in this study was developed as part of the Bachelor's Thesis Project and is used for handling bulk material sacks (rice) weighing 25 and 40 kg. The prototype incorporates four pneumatic cylinders, which simultaneously actuate the gripper assemblies, as well as two linear pneumatic pistons that apply pressure to the sacks.

2. Current state

Up to this point, I have conducted research on the application of the Finite Element Method (FEM) in the analysis of the end-effector, with a focus on transient behavior. This phase also included the study of differences between implicit and explicit methods.

Based on the theoretical knowledge acquired, I modeled the end-effector using a simplification approach, replacing 3D components with equivalent 1D beam and 2D shell structures.

Using this model, a transient simulation was configured in ANSYS software, employing its implicit solver. Material properties, initial and boundary conditions, as well as time-dependent forces and displacements were defined and applied in successive time steps to accurately reproduce the real behavior of the assembly.

At present, preliminary simulations have been completed, and the model is capable of reflecting the kinematic behavior and the stresses developed within the analyzed structure. The next steps involve optimizing the discretization mesh and performing a more detailed analysis of structurally critical areas.

3. Materials

In modeling the fork-style end-effector analyzed in this project, the following materials were used:

- Aluminum Alloy 7068-T6

Tabel 1. Material properties

Property	Value	Unit
Density	2.85	g/cm^3
Young’s Modulus	71100	MPa
Poisson’s Ratio	0.33	-
Yield Strenght	683	MPa

Tabel 2. Material composition

Al	Cr	Cu	Fe	Mg	Mn	Si	Ti	Zn	Zr	Others
88.48 - 88.85%	0.05%	1.6 – 2.4%	0.15%	2.2 – 3.0%	0.10%	0.12%	0.10%	7.3 – 8.3%	0.05 – 0.15%	0.15%

Figure 1 shows the material properties of aluminum alloy 7068-T6 as defined in ANSYS Workbench.

	A	B	C	D	E
1	Property	Value	Unit		
2	Material Field Variables	Table			
3	Density	2.85	g cm^-3		
4	Isotropic Elasticity				
5	Derive from	Young's Mod...			
6	Young's Modulus	71100	MPa		
7	Poisson's Ratio	0.33			
8	Bulk Modulus	6.9706E+10	Pa		
9	Shear Modulus	2.6729E+10	Pa		
10	Tensile Yield Strength	683	MPa		

Fig. 1. Material properties of aluminum alloy 7068-T6

Based on the information in Tables 1 and 2 [5], we can conclude that:

- This is one of the strongest commercially available aluminum alloys, commonly used in critical applications requiring an excellent balance between high mechanical strength, low weight, and fatigue resistance.
- Due to these properties, this material is well-suited for high-performance components such as the gripper fingers in the prehension system, which must handle heavy and deformable sacks in industrial palletizing applications.

- Aluminum Alloy (Al 6061-T6)

Tabel 3. Material properties

Property	Value	Unit
Density	2.77	g/cm^3
Young's Modulus	71000	MPa
Poisson's Ratio	0.33	-
Yield Strenght	280	MPa

Tabel 4. Material composition

Al	Cr	Cu	Fe	Mg	Mn	Si	Ti	Zn	Others
95.8 – 98.6%	0.04 – 0.35%	0.15 – 0.4%	0.7%	0.8 – 1.2%	0.15%	0.4 – 0.8%	0.15%	0.25 %	0.15%

Figure 2 shows the material properties of aluminum alloy 6061-T6 as defined in ANSYS Workbench.

	A	B	C
1	Property	Value	Unit
2	Material Field Variables	Table	
3	Density	2.77	g cm^-3
4	Isotropic Secant Coefficient of Thermal Expansion		
6	Isotropic Elasticity		
7	Derive from	Young's Mod...	
8	Young's Modulus	71000	MPa
9	Poisson's Ratio	0.33	
10	Bulk Modulus	6.9608E+10	Pa
11	Shear Modulus	2.6692E+10	Pa
12	Alternating Stress R-Ratio	Tabular	
16	Tensile Yield Strength	280	MPa
17	Compressive Yield Strength	2.8E+08	Pa
18	Tensile Ultimate Strength	3.1E+08	Pa
19	Compressive Ultimate Strength	0	Pa

Fig. 2. Material properties of aluminum alloy 6061-T6

Therefore, we can state the following about this default aluminum alloy from ANSYS Workbench [5]:

- It is intended for initial or comparative analyses where exact chemical composition or extreme stress behavior is not critical.
- It is suitable for components with moderate requirements, such as frames, plates, housings, or structural parts that are not heavily loaded.

4. Computational Model

Various topology operations were performed on the 3D model in order to simplify it by creating a 1D and 2D representation of the gripper assembly. The claws fall into the category of bar-type structures and were modeled using BEAM elements with a 1D approach, while the plates were built using a 2D SHELL approach. The remaining components of the end-effector were merged, excluding the six pneumatic cylinders, in order to simplify the geometry as much as possible.

Beam elements are used to model elongated components with a small cross-sectional area relative to their length. A beam element transfers axial forces, shear forces, and bending moments, all at a very low computational cost. It is particularly suitable for strength, buckling, or vibration analyses of slender structures [2, 4].

Shell elements are used for modeling components with a small thickness compared to their other dimensions. These elements can capture both bending and stretching effects, making them useful for simulating the mechanical behavior of surfaces without requiring detailed volumetric meshing. They provide a very good balance between accuracy and computational efficiency, especially in dynamic regimes or under distributed loads [2, 4].

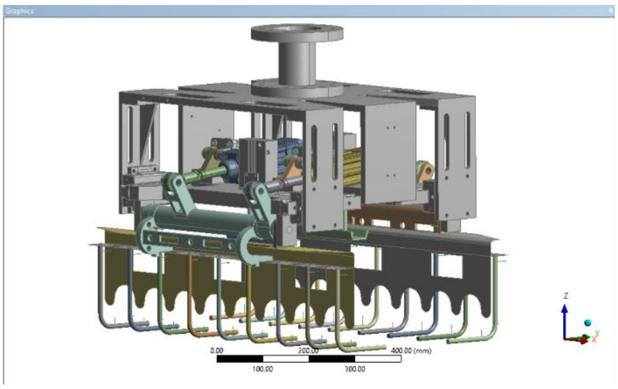

Fig. 3. 3D Model of the end-effector

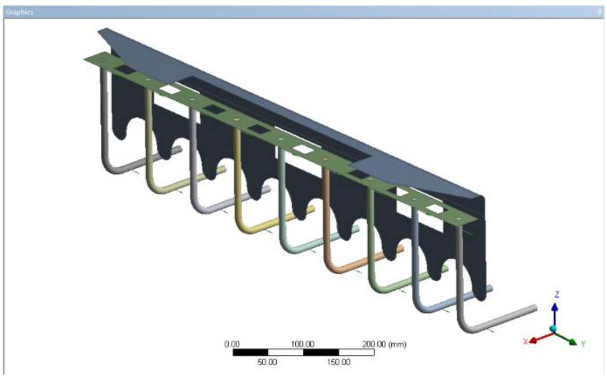

Fig. 4. 1D BEAM and 2D SHELL Approaches

To simplify the simulation, predefined selections were created to facilitate efficient work with complex geometries, allowing for quick identification and grouping of relevant geometric entities - faces, edges, bodies, or vertices - directly in the model tree and for use in defining kinematic joints [3].

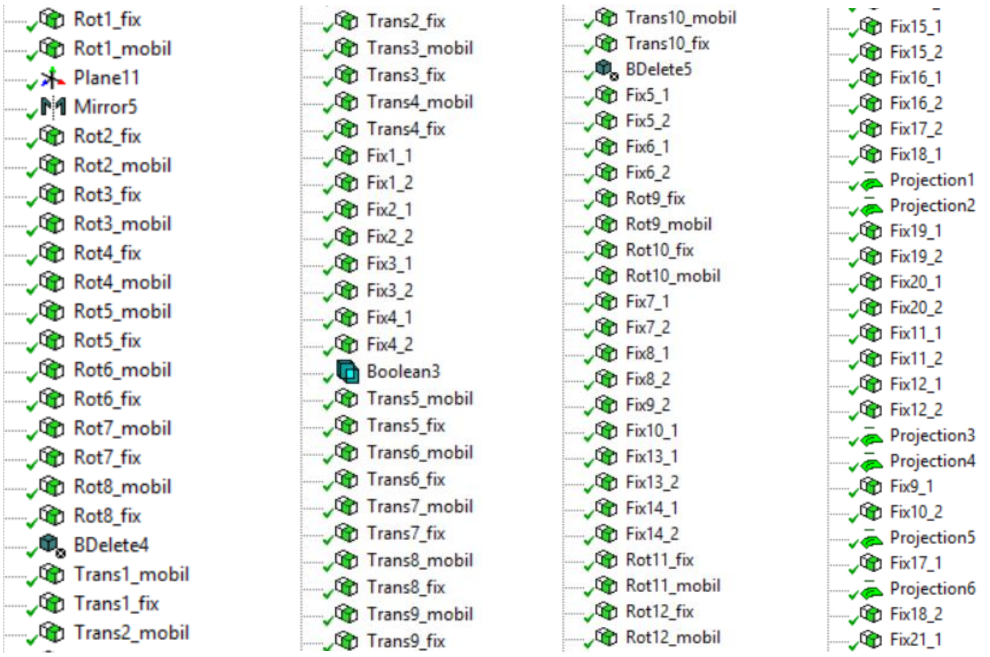

Fig. 5. Named selections

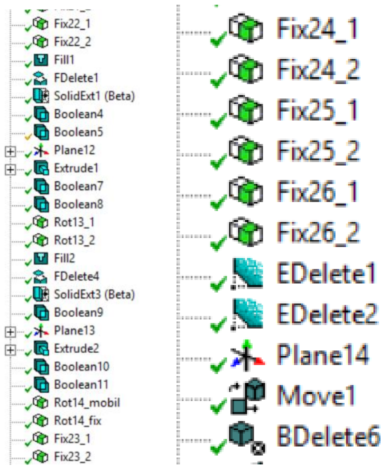

Fig. 6. Named selections

Moreover, in order to accurately represent the kinematic behavior of the assembly under real operating conditions, it was necessary to model in detail the interaction between the mobile components of the system. In this regard, a functional gripping element was created, ensuring guidance and support for the claw assembly during rotation and enabling the correct transmission of relative motion between components.

This precise modeling of mechanical interactions was essential to obtain relevant results in the dynamic and structural analysis of the end-effector. Additionally, the correct definition of kinematic joints contributed to an accurate representation of the mechanical constraints and load transfer points during the system's cyclic operation.

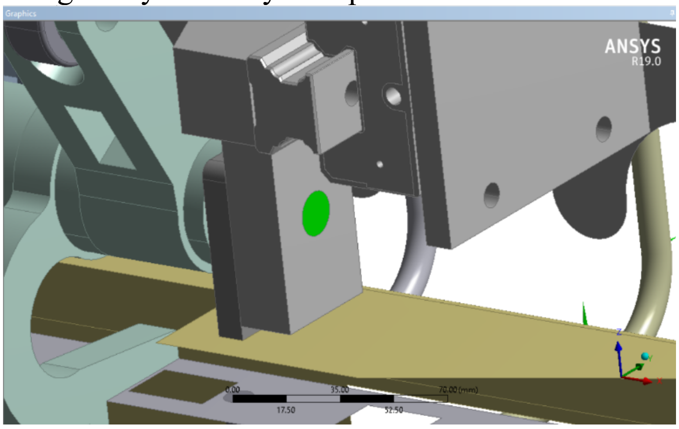

Fig. 7. Detailed modeling of the interaction between the system's moving components

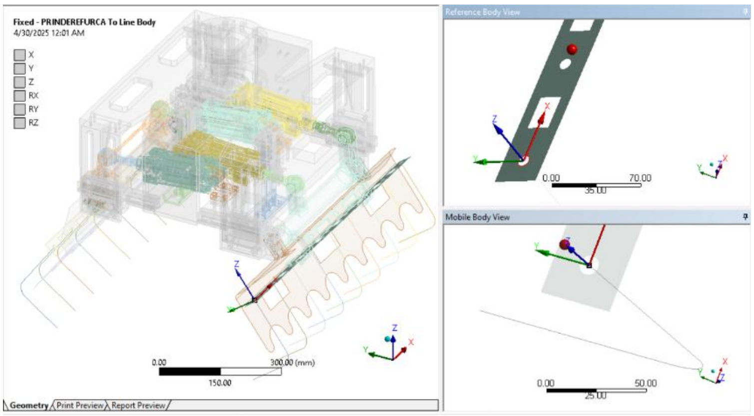

Fig. 8. Example of a fixed joint

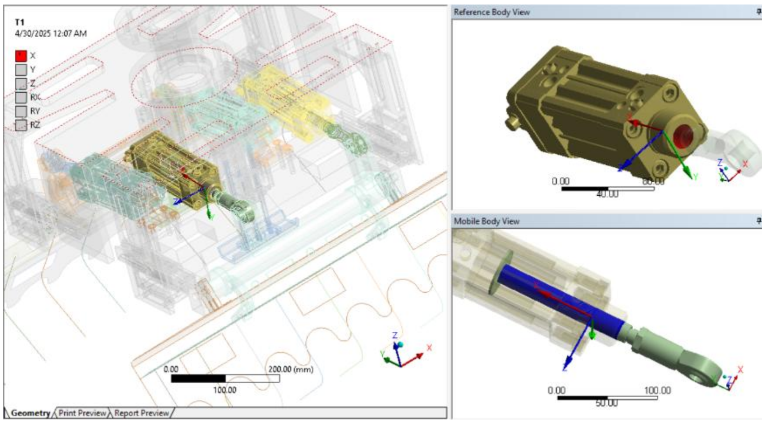

Fig. 9. Example of a translational joint

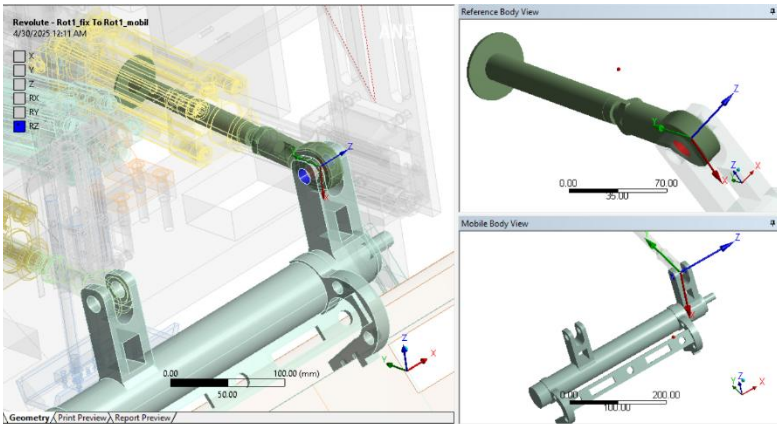

Fig. 10. Example of a revolute joint

For conducting the transient analysis, I defined the standard gravitational acceleration, a force applied to the claws representing the action of the rice bag on them, as well as the relative displacement of the pneumatic piston rods and the vertical translation of the end-effector, simulating its lifting after the claw assemblies close.

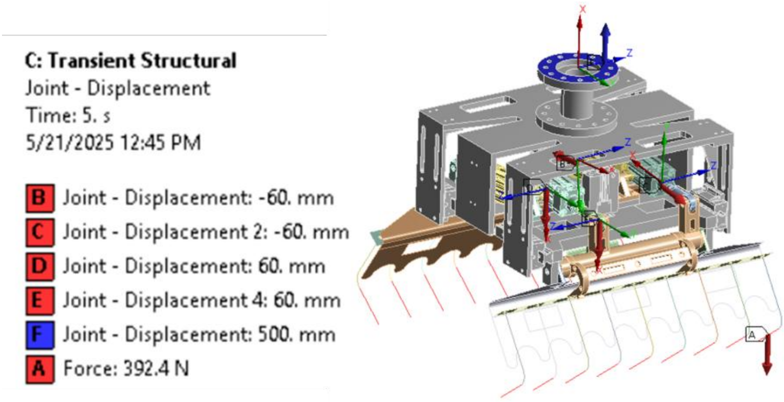

Fig. 11. Transient analysis setup

5. Solution

The maximum deformation is 15.202 mm, located at the tip of the claws, and results from the movements generated by the actuating elements. This deformation is sufficient for gripping and handling the object.

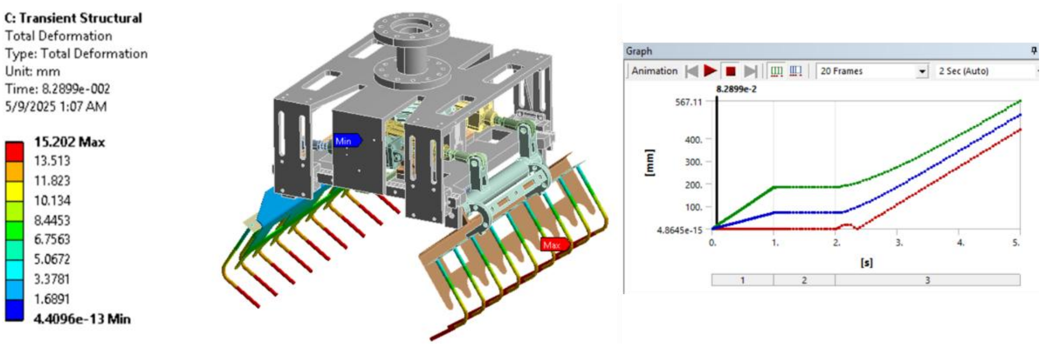

Fig. 12. Total Deformation

The maximum equivalent stress was recorded in the gripping area between the main lateral support plate of the claw assembly and the connecting elements with the rest of the end-effector. Its value of 1.7095 MPa indicates a safety factor greater than 10, considering the yield strength of the material is 280 MPa. Maximum stresses occur during the actuation of the subassemblies - specifically at moments of start, stop, and direction change.

Fig. 13. Equivalent Stress

The maximum direct stress is 0.286 MPa, indicating that the structure is subjected to a dynamic load over time and there are no signs of dangerous stress levels, as the value remains below 1 MPa.

From the results of the minimum and maximum combined stresses, a safety factor greater than 10 is obtained.

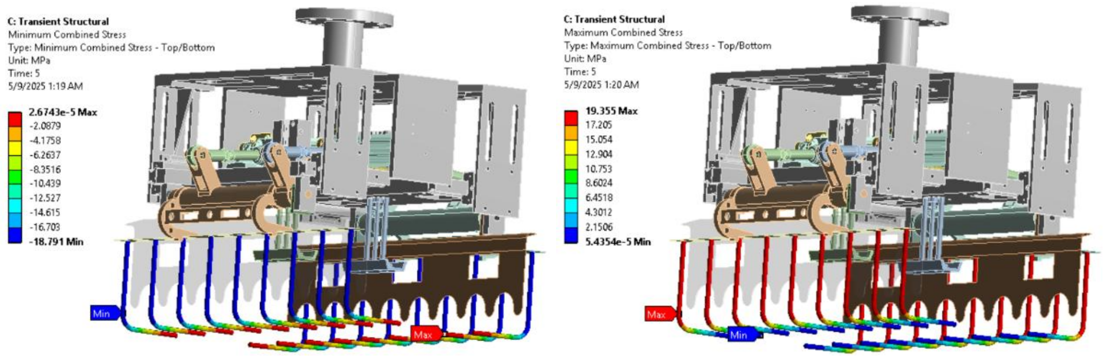

Fig. 14. Minimum and Maximum Combined Stress

6. Conclusions

From the perspective of safety factors, the structure can be considered safe, and the end-effector can be used in applications where the weight of the manipulated objects, stroke lengths, or speeds are greater than in this case.

The simulation results show small free vibrations that occur during start-up, stop, and direction change. These vibrations diminish within tenths of a second (six periods) and do not affect working precision or repeatability.

Original contributions of this work include:

- Accurate reproduction of the kinematic behavior of the assembly under real operating conditions;
- Transformation of the computational model from a full 3D structure to a combination of shell and beam elements, using 1D BEAM and 2D SHELL approaches, in order to optimize calculations;
- No similar applications or published articles have been found.

7. References

[1] Pupăză, C., Parpală, R.C. - Modelare şi analiză structurală cu ANSYS Workbench, Politehnica Press Publishing House, Bucharest, 2011

[2] Pupăză, C - Modelare CAD-FEM, Politehnica Press Publishing House, Bucharest, 2013

[3] User Manuals of CAE Software: Ansys Workbench, Nastran, SIMULIA - ABAQUS, LS-DYNA, etc.

[4] Written Materials for IAC1 and IAC2 courses, electronic format on Moodle Platform, 2024–2025

[5] MatWeb - Material Property Data. Available online at: https://www.matweb.com

TRANSIENT ANALYSIS (FEM) OF THE SLED IN THE GROUND TRANSLATION MODULE OF THE ROBOT

CODREA Valentin-Nicolae, Cristina PUPĂZĂ(Conducător științific)

Facultatea: Inginerie Industriala si Robotica, Specializarea:Robotica, Anul de studii:IV, e-mail: valentin.codrea@stud.fiir.upb.ro

The topic is the analysis of the dynamic behaviour of the ground translation module sled, an integral part of an articulated arm robot with seven degrees of freedom, used in a robotic cell designed for sheet bending operations.
The main objective of the research is to evaluate the dynamic parameters that influence the stability and performance of the sled during operation.
A very important aspect within the application is the positioning accuracy of the industrial robot (0.15mm- according to the catalogue [5]), accuracy that is in turn affected by the motions performed by the additional transaction axis under analysis and on which we monitor displacements and elastic deformations. The displacement must not exceed the robot positioning accuracy, or the limit imposed within the cell.

1. Introduction

In this paper, the dynamic behaviour of the sled, a component of the translation axis offered by ABB (ABB IRB Track motion 6006), an axis integrated in a robotic cell including an ABB IRB 6650s robot, is analysed. The cell is intended for bending sheets by cold plastic deformation. In this analysis, the aim is to validate the constructive solution of the translation axis in order to be integrated into the cell. In addition, it will be verified if by modifying the thickness of the supporting plate in the sled component, better results can be obtained regarding the stiffness of the assembly. For this purpose, the forces occurring in the axle actuator will be determined, as well as the deformations, and particularly the accuracy of the numerically controlled displacements.

As necessary data for the realization of the analysis are:
- Robot geometry and weight
- Movement diagram of the robot during operation - imported from the Process Simulate program
- The material used to realize the translation axis ABB IRB track motion 6006

The mass of the robot is taken from the technical manuals provided by ABB [5], being 2250 kg. In the study carried out in the ANSYS program, aluminium alloy was used as material for the industrial robot. After assigning the material for the geometric model, the weight is approximately equal to the weight presented in the technical catalogue, thus validating its

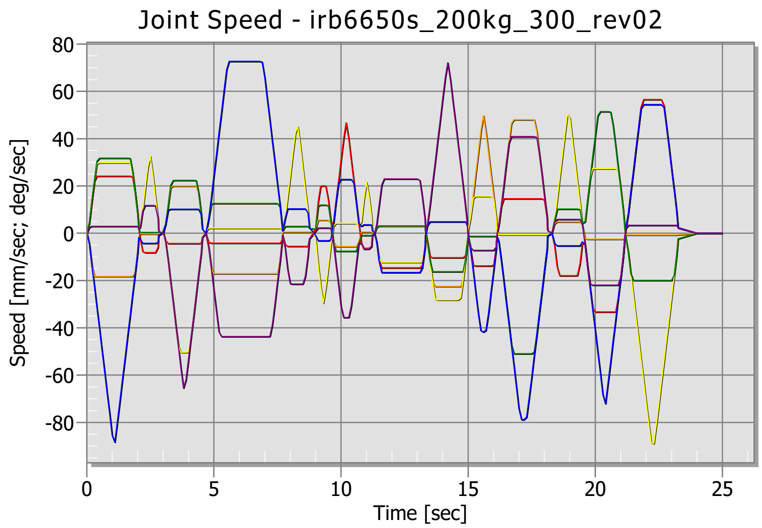

Figure 1

geometry and mass

The material used for the support plate between the industrial robot and the translation axis is a steel identified in the MatWeb database [6] as AISI 4000 Series Steel with the following properties:

Tabel 1. AISI 4000 Properties

Property	Value	Unit
Density	7850	Kgm^{-3}
Tensile Yield Strength	430	MPa
Compressive Yield Strength	250	MPa
Tensile Ultimate Strength	720	Mpa

A Rigid-Flexible Dynamics analysis was used as the research methodology for the dynamic analysis, this being preferred to the Transient Structural simulation, due to the functional characteristics of the investigated system, where the main components exhibit high stiffness and negligible deformability in relation to the overall motions.

It was aimed to faithfully model the kinematics and dynamic interactions between the components, without introducing additional complexities associated with elastic deformations, which in this case are very small.

By the choice made the computation time for 6 seconds of the cell duty cycle was reduced from 170 minutes (Transient Structural) to 12 minutes (Rigid Dynamics).

2. Theoretical foundations of the Finite Element Method (FEM)

Rigid Body Dynamics (RBD) refers to the study of the motion of mechanical assemblies during operation, assuming that all their components are perfectly rigid. The main goal of this analysis is to determine parameters such as velocity, acceleration, system energy, as well as reactions in kinematic couplings, over the entire duration of the mechanism's operation. If combined with the declaration of a single flexible component, the structural analysis of the flexible component can be performed simultaneously, maximizing the efficiency of the method. The RBD method gives the designer the possibility to identify critical moments in the operation of an assembly and to perform specific checks at the desired moments, without the need for a time-consuming full transient analysis. The RBD takes into account the applied forces, moments of inertia, as well as the positions of the centres of gravity of the components involved. It has a specialized solver - ANSYS Rigid Dynamics solver - which is very fast and solves the equations of motion using the Runge-Kutta method.

One of the main advantages of using ANSYS Workbench for kinematic analysis of robots is the possibility to calculate the kinematic characteristics of the system and evaluate static or dynamic behaviour under real operating conditions. The animated visualization of the results allows not only to analyse the motion, prevent collisions and obtain useful information from the design phase, but also to use these results for preliminary verification or validation of constructive solutions. The Runge-Kutta method of order 4 (RK4) calculates displacements step by step:

$$\frac{dy}{dt} = f(t, y) \tag{1}$$

$$k_4 = f(t_n + h, y_n + hk_3) \tag{2}$$

Rigid-flexible modeling has the following advantages:

- use of a FEM model reduced only to the component to be analyzed/verified in detail
- absence of free vibrations in the structural response
- reduced computation time and high accuracy of the results

In the present study a solution of the equations of motion by a 4th order numerical integration has been used, which ensures an optimal balance between accuracy of the results and computation time + FEM (on the condensed component) for the flexible element which is represented by the sled of the translation modulus.

3. The calculation model

Mathematical formulation of the problem, realization of the geometry and constraints

Geometry preparation was done by importing the CAD model with a neutral format into DesignModeler. Several simplifications of the geometric model have been made in order to obtain accurate results. These simplifications do not affect the accuracy of the results obtained, on the contrary, by simplifying the geometry it will be observed that the analysis works better. Unimportant elements in the simulation were deleted with **BODY DELETE** operations. For a better transfer of forces and displacements, the clamping area between the industrial robot base and the translation mode sled was designed and stamped, and the Mid Surface option was used to simplify the geometrical model of the sled to a plate model. To reduce the complexity, additional auxiliary operations were performed, elements not under analysis were removed and Boolean operations were performed to minimize the number of model components

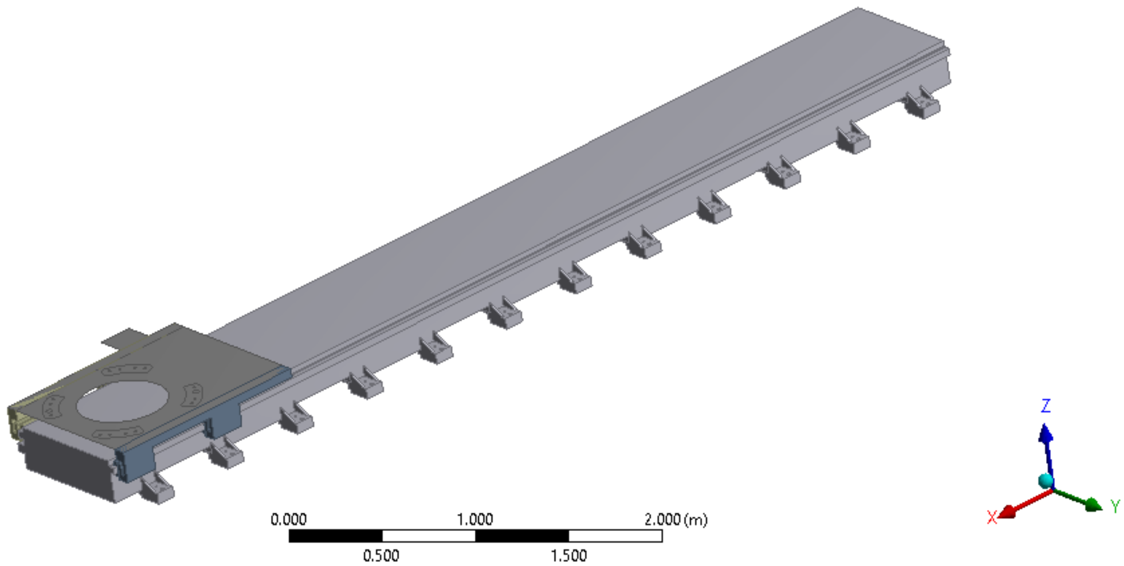

Figure 2

The complete definition of the kinematic torques and the drag conditions were realized in the Rogid Dynamics Module. The mounting base of the assembly was defined by a Body-Ground coupler. The Fix1_2 to Fix 1_1, respectively Fix2_1 to Fix2_2 couplings were defined for the connection between the system's cleats and the sled plate. Translation couplers were also used. The definitions of joint for the entire industrial robot are illustrated in figure 3. The electric actuating motors were attached to the robot structure by fixed couplings.

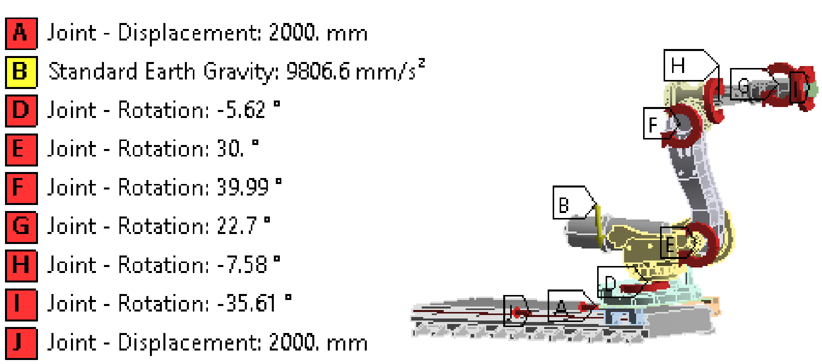

Figure 3

In the Rigid-Flexible analysis the discretization is performed on a single component, declared as a condensed part, in this case being the translation axis sled. The dynamic calculations were performed on 55 steps, following the table in Fig. 4

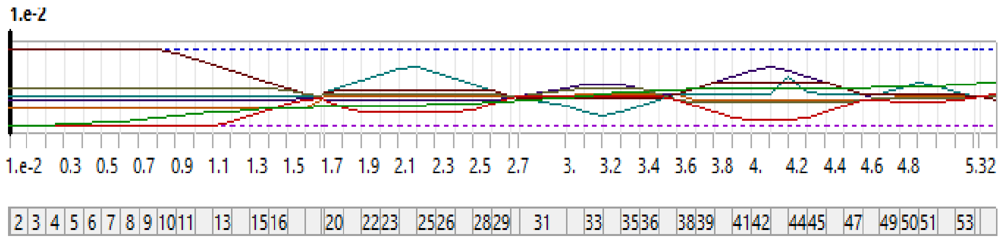

Figure 4

The motion on each couple was imported from the Process Simulate program, as shown in Fig. 1. The values were tabular extracted and entered into the ANSYS program.

The forces computed during simulation converge on each step, and the obtained results become stable as the simulation time is sampled. This indicates good training of the computational model and adequate discretization accuracy. Even though 471 iterations were performed, the computational time was exponentially reduced by choosing the Rigid-Flexible method over a Transient Structural analysis, and the accuracy of the results was higher.

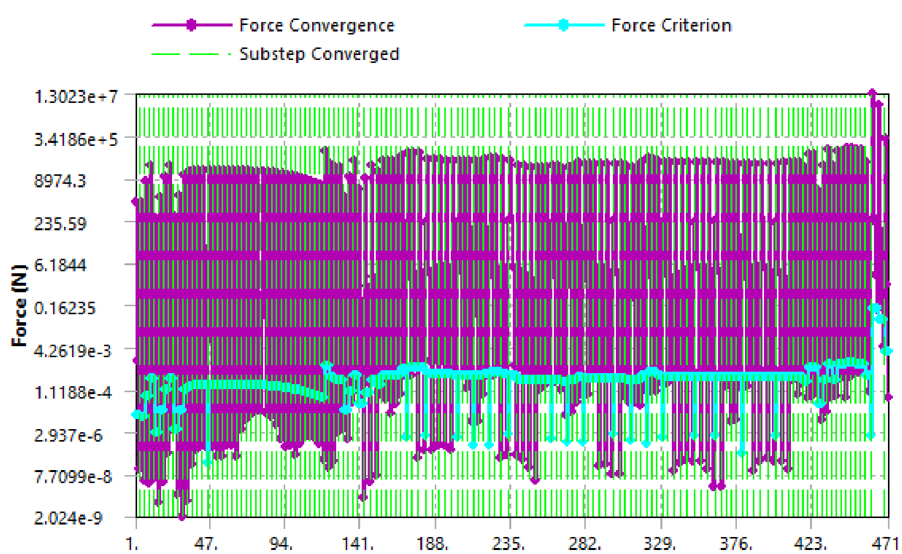

Figure 5

4. Analysis of result

The interpretation of the results is based on the impact of the forces, moments and initial conditions on the behavior of the analyzed system, evaluating the accuracy of the numerical simulation and the correlation with the computational model.

a) Specific deformations

The analysis shows that the elastic deformations (Strain) reach a maximum of 0.00097%, a value that can be considered negligible. Therefore, they do not influence the normal functioning of the assembly.

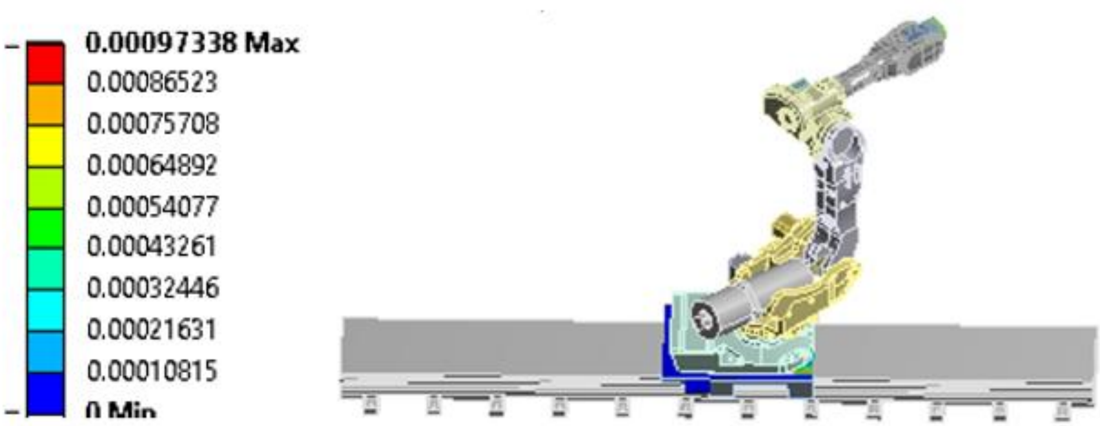

Figure 6

Total displacements:

The values obtained for the total displacements are within permissible limits and do not affect the proper functioning of the robot cell. These programmed displacements do not compromise the positioning accuracy (which is 0.14 mm) or the stability of the assembly.

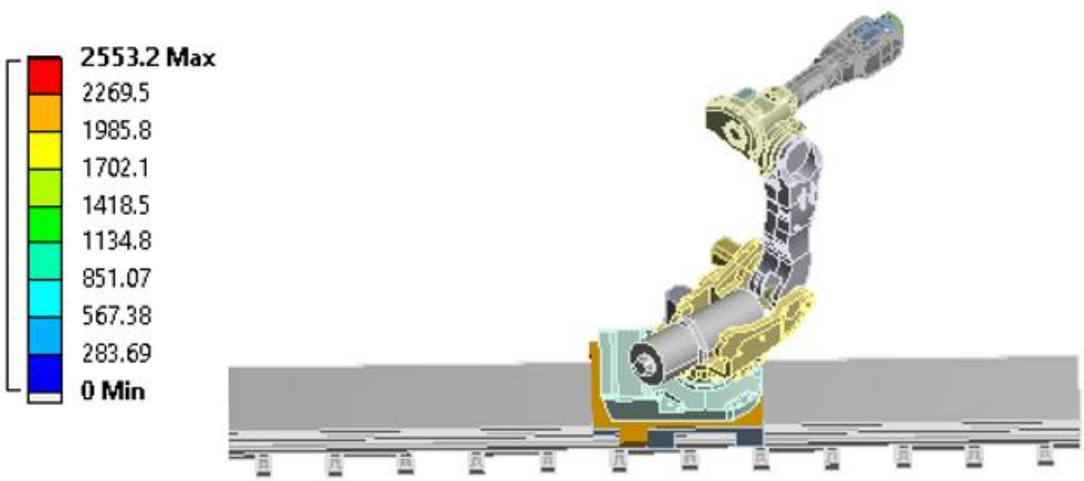

Figure 7

Equivalent stress according to the von-Mises criterion:

The variation of the stress during the working cycle and the identification of the moment at which the equivalent stress is maximum is illustrated in Fig. 7.

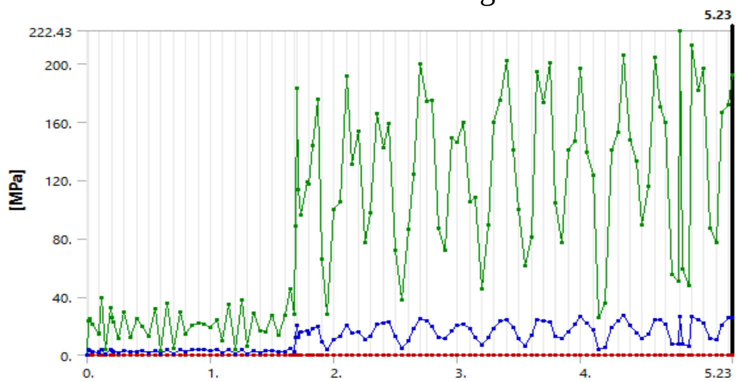

Figure 8

With the simulation, it can be seen that the maximum stress occurring after operation is 224.48 MPa (Fig. 14), which we will compare with the maximum allowable stress for the material used and to calculate the safety factor:

$$f = \frac{\sigma y}{\sigma VM} = \frac{430}{224.48} = 1.91 > 1.5 \qquad (1)$$

For robotic applications (excluding collaborative robots), the generally accepted safety factor is in the range of 1.5 to 2. This safety factor ensures that the robotic structure can withstand loads and forces beyond the expected operational limits, providing a margin of security against unexpected stresses or material fatigue. It acts as a buffer to accommodate variables such as manufacturing tolerances, material inconsistencies, dynamic loads, and potential misuse or unexpected interactions in the field.

In this case, the structural components have been evaluated under the expected operational conditions and have been found to remain within acceptable stress limits. The maximum stress levels observed during analysis or testing are well below the material's yield strength when adjusted for the selected safety factor range. This indicates that the structure not only performs reliably under normal usage but also retains sufficient durability under more extreme or transient loading scenarios.

It is important to note that for industrial or traditional robots (as opposed to collaborative robots, which operate in close proximity to humans and require additional safety measures), this safety factor is considered adequate based on industry standards and historical performance data. The chosen safety factor also reflects a balance between structural integrity, material usage, and overall cost-effectiveness of the design.

Therefore, with the applied safety factor and corresponding analysis, the structure confidently meets the operating conditions in terms of mechanical stress and load-bearing capability. This validates the design's compliance with the safety and reliability criteria necessary for typical robotic applications.

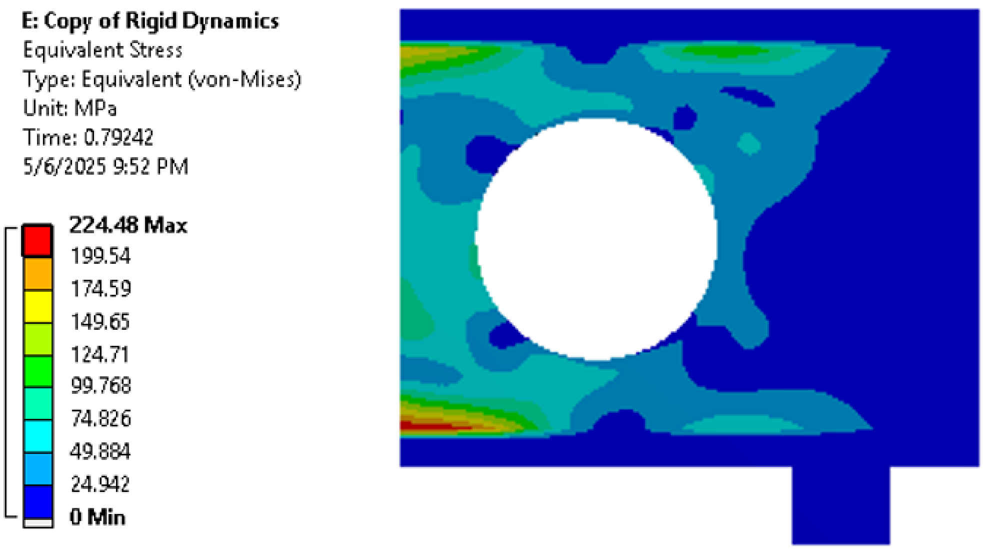

Figure 9

5. Final conclusions and originality of the study::

In order to investigate the dynamic behaviour of the sled of the ABB IRBT 6006 IRBT assembly, a complex kinematic simulation of the ABB IRB 6650S robot, including the translation module, was performed. The analysis was carried out over a time interval of 5.23 seconds, focusing on critical moments of operation, especially when the robot arm is fully extended, being at maximum distance from the centre of gravity - a situation with high potential for mechanical stress.

This simulation provided a detailed and rigorous evaluation of the essential kinematic parameters - displacements, velocities and accelerations of the sled and allowed the simultaneous optimization of hardware resource consumption, but also of the time required for numerical solution.

The analysis was carried out by means of the Rigid-Flexible Dynamics method, using an advanced mathematical model based on the Runge-Kutta-FEM combination through the Condensed Part technique, which allowed the acquisition of highly accurate results without the need to run a full Transient Structural analysis, known for its intensive consumption of computational resources. This hybrid approach effectively captures both the rigid body motion and the elastic deformation of flexible components, ensuring a more comprehensive understanding of the dynamic behaviour of the system. By integrating the Runge-Kutta numerical solver with the finite element method, it becomes possible to trace the system's response over time with improved precision and stability.

The Condensed Part technique further simplifies the model by reducing the number of degrees of freedom while preserving the essential dynamic characteristics of the flexible parts. This results in faster computation times and reduced memory requirements, making it particularly advantageous for iterative simulations or design optimizations. Additionally, the method facilitates the detection of transient phenomena such as vibrations, shock loads, and structural resonances that may impact the overall performance. The modelling process was validated through comparison with benchmark simulations and showed excellent agreement with expected theoretical outcomes. Overall, the chosen approach proved to be both efficient and robust, offering a high-fidelity simulation environment suitable for advanced robotic system development.

Upon evaluation of the results, it was found that the translation module fulfils the functional requirements and can be successfully integrated into most robot cells, especially in industrial applications such as sheet bending or pick and place operations, contributing to increased efficiency and flexibility of the production process. The module demonstrated consistent performance under varying load and speed conditions, confirming its reliability for high-cycle manufacturing tasks. Its compact design and ease of integration also minimize the need for extensive modifications to existing setups. Additionally, the module supports a range of motion profiles, allowing it to adapt to different workflow requirements with minimal reprogramming. This adaptability makes it a valuable component in automated production lines aiming for greater throughput and operational versatility.

6. Bibliography:

[1]. Pupăză, C., Parpală, R.C. - Modelare şi analiză structurală cu ANSYS Workbench, Editura Politehnica Press, București, 2011

[2]. Pupăză, C - Modelare CAD-FEM. Editura Politehnica Press, București, 2013

[3]. CAE programs manuals: Ansys Workbench, Nastran, SIMULIA - ABAQUS, LS-DYNA, etc.

[4]. CAE1 and CAE2 written support in electronic format on Moodle 2024-20255.

[5]. https://new.abb.com/products/robotics/robots/articulated-robots/irb-6650s.

[6]. https://www.ansys.com/academic/learning-resources.

OPTIMIZING PRODUCTION PROCESSES THROUGH IMPLEMENTING LEAN MANAGEMENT METHODOLOGY

ILIE Daniel Ștefan și TILINĂ Dana (Conducător Științific)

Facultatea: Inginerie Industrială și Robotică, Specializarea: Master Concepție și Management în Productică, Anul de studii: I, e-mail: daniel.ilie44@gmail.com

ABSTRACT: This paper presents the implementation of Lean Management as a strategic method for optimizing production processes in a manufacturing environment. The study focuses on identifying and eliminating non-value-added activities (waste or muda), improving workflow efficiency, and increasing customer value through systematic process improvement. Several Lean tools are applied, including 5S for workplace organization, Value Stream Mapping (VSM) for visualizing process inefficiencies, and Kaizen for fostering continuous improvement. Data were collected before and after implementation to evaluate performance indicators. The results indicate significant improvements in productivity, a reduction in lead times, better space utilization, and decreased material waste. The case study confirms that Lean principles, when correctly applied, can lead to measurable and sustainable operational gains, enhancing both process quality and employee involvement.

KEYWORDS: Lean, production, optimization, value stream, efficiency.

1. Introduction

In manufacturing companies, one of the most frequently identified problems is operational inefficiency generated by cumbersome, fragmented and non-optimized processes, which lead to significant waste of time, resources and energy. This reality translates into high production costs, long lead times, overstocks, quality defects and a low ability to adapt to market demands [1,2,3]. Especially in traditional industries, the lack of digitalization and advanced analytical tools contributes to maintaining these inefficiencies, undermining organizational competitiveness.

Most of the time, these problems are not obvious at first glance and are considered inherent to the production process. The lack of an organizational culture geared towards continuous improvement and the lack of standardized analysis tools lead to the perpetuation of these dysfunctions. Thus, organizations are faced with an imbalance between what they produce and what customers perceive as value [4,5]. In the absence of a Lean mindset and proactive management behaviour, system failures are often accepted as the norm.

The central research problem is to identify and reduce losses in the production process, as they are multiple, diverse and often hidden in the daily routine. Time wastage, overproduction, unnecessary transportation, unproductive movements, defects and excessive inventories are just some of the concrete manifestations of these losses [6,7,8]. In the absence of a clear methodology and a standardized framework for intervention, these problems not only persist but may become more pronounced over time, affecting the sustainability and operational resilience of enterprises.

In this sense, the research proposes a structured approach to answer the following key question: how can Lean Management methodology be implemented in a real production system to reduce losses and optimize the operational flow?

This question generates a number of specific sub-problems:

1. What are the main sources of waste in a concrete industrial process?
2. Which Lean tools are most effective for the type of process analysed?

3. How can improvements be measured, monitored and validated?

Solving this problem involves not only the application of theoretical concepts, but also a practical intervention, tailored to the particular context of the organization under analysis, with a focus on concrete and sustainable results.

The aim of the research is to formulate recommendations for the sustainable integration of Lean principles into the organizational culture of the enterprise.

The overall objective of the research is to optimize production processes by applying Lean Management methodology in order to reduce losses and improve operational performance. Starting from this general aim, the research proposes the following specific objectives:

1. Identification and classification of the main types of losses (Muda) in the analysed production process.
2. Application of relevant Lean tools (5S, Kaizen, VSM) to reorganize the workspace and improve operational flow.
3. Evaluation of the impact of the implemented measures on process performance, through key indicators such as cycle time, productivity level, space utilization and waste level.

To support the scientific approach, the research is built on the following working hypotheses:

1. The implementation of Lean tools contributes to a significant reduction of losses in the production process;
2. 5S workspace reorganization leads to improved productivity and reduced waiting and travel times;
3. The application of Value Stream Mapping allows a better understanding of the value stream and highlights areas with major potential for improvement;
4. The introduction of Kaizen-type practices stimulates employee involvement and contributes to increased standardization and process stability.

The research took place in a medium-sized industrial enterprise, using a practical and applied approach.

The company under analysis operates in the field of metalworking, specializing in the production of mechanical components for industrial equipment. The choice of this company was motivated by the nature of its repetitive and intensive processes, characteristics that make it relevant for the application of Lean methodology. The company also frequently faces problems with waiting times, intermediate inventories and inefficient use of space, making it a suitable setting for testing continuous improvement tools. Easy access to operational data, management's willingness to collaborate, and the organization's interest in process optimization were key factors in the selection of this facility as a case study.

The methodology was structured along several complementary strands. In the first phase, a diagnostic analysis was performed by collecting data on current processes, with a focus on identifying unproductive time and sources of waste, using direct observation, interviews and activity timing. This was followed by the application of specific Lean tools, including the 5S method for efficient workplace organization, Value Stream Mapping for the visual representation of the value stream and Kaizen as an approach for targeted improvement interventions.

The process continued with performance monitoring by measuring relevant indicators both before and after the implementation of Lean solutions, such as cycle time, defect rate or waste. The final step was to evaluate and validate the results obtained by benchmarking and interpreting the impact in order to draw clear conclusions.

Data were analysed quantitatively, and the implementation was rigorously documented to ensure the replicability of the research. Although the approach is exploratory, it has concrete applications and potential for scalability in other similar contexts.

In order to substantiate the research approach and to highlight the relevance of the topic, it is necessary to analyse the current state of knowledge in the literature on the application of Lean principles in the organizational environment.

2. State of play

Lean Management has become a central topic in the literature on industrial process improvement in recent decades. The origins of this methodology are closely linked to the Toyota Production System, developed in post-war Japan. The seminal work of Taiichi Ohno and his collaborators laid the foundations for a new vision of operational efficiency, in which the elimination of waste is considered essential for value creation. The concept was subsequently extended and refined in academia and practice, and is today a major reference in industrial engineering and operations management [9,10].

A number of authors define Lean Management as a systemic and integrated approach, aimed at identifying and eliminating activities that do not add value from the customer's perspective. Womack and Jones (2008), in their classic work "Lean Thinking", highlight five fundamental principles of Lean, namely value identification, value stream mapping, flow creation, flow establishment, print run establishment and perfection chasing [11]. Although these principles are widely accepted, the literature often criticizes their rigid application without adaptation to the cultural and organizational specificity of each enterprise [12,13].

Studies on Lean Management have been dominated by descriptive and normative research, focused on presenting the benefits of implementing different Lean tools such as 5S, Kaizen, Kanban or Value Stream Mapping. However, recent literature brings to the forefront a more critical approach, focusing on the limitations and difficulties encountered in applying these methods in practice. For example, Dinis-Carvalho et al. (2019) and Shahin et al. (2024) draw attention to the fact that many organizations treat Lean as a set of isolated techniques, without implementing the cultural changes required for a sustainable transformation [14,15].

Another critical issue highlighted in the literature is the complexity of measuring the actual impact of Lean on organizational performance. Although numerous case studies report cycle time reductions and productivity increases, the lack of a unitary evaluation framework makes it difficult to compare results across different industries or regions. Authors such as Dillinger et al. (2022) and Sasso et al. (2025). propose a more rigorous conceptualization of Lean practices and their degree of implementation, suggesting a direct relationship between Lean maturity level and the operational and financial performance of the enterprise [16,17].

At the same time, international literature is beginning to pay more and more attention to sustainability and social responsibility issues in the context of Lean Management. The traditional efficiency-centred approach is gradually being complemented by concerns for the environment, employee well-being and the social impact of operational decisions. In this sense, the concept of Lean Green or Green Lean has been introduced to integrate sustainability principles into the Lean model, emphasizing the synergies between reducing waste and reducing environmental impacts [18,19].

Studies carried out in the European and, more recently, in the Eastern European context highlight a significant gap between Lean theory and its practical implementation. Especially in small and medium sized enterprises, lack of resources, managerial training and cultural support are major barriers to full Lean adoption. Thus, researchers recommend gradual adaptation of the methodology, with a focus on continuous employee training, involvement of top management, and customization of Lean tools to the specifics of the organization [20,15,9].

From a critical perspective, the literature also points to the risks associated with a superficial or forced implementation of Lean principles. In the absence of a deep understanding of the Lean philosophy and a genuine commitment from management, the results may be temporary and side effects, such as employee overwork or excessive standardization, may negatively affect the organizational climate [8,14].

Therefore, the success of Lean implementation depends not only on the application of technical tools, but also on changing the organizational culture, involving all levels of the hierarchy and aligning strategic objectives with the real needs of customers and employees.

In order to assess the practical applicability of Lean principles and to test the hypotheses formulated, the research included an application phase carried out in a real organizational setting, the results of which are presented below.

3. Results

The application of Lean Management tools in the analysed company, active in the field of metal processing, generated a number of significant improvements in terms of operational efficiency, loss reduction and workflow optimization. The obtained results confirm the hypotheses formulated in the research and support the relevance of a structured approach in integrating Lean principles into the organizational culture of an industrial company.

As a first step, a thorough diagnostic analysis of the operational processes was carried out using qualitative and quantitative research methods such as direct observation, semi-structured interviews with key employees, analysis of process documents and timing of activities. The aim of this phase was to identify forms of waste according to the seven types of muda model. Among these, the most common wastage identified were: waiting time between operations, overproduction due to a lack of correlation between the pace of orders and production, unnecessary movements by operators to locate tools and materials, and excessive intermediate stocks, which took up valuable space and fragmented the flow.

The analysis revealed that many of these dysfunctions were not recognized by the employees as a natural part of daily work. The lack of a visual management system and clear space organization rules contributed to general disorder and previously unidentified losses. Against this backdrop, Lean intervention was instrumental in creating a more conscious and proactive organizational culture towards continuous improvement.

A first tool applied was the 5S method, a Japanese workplace organization system based on five essential steps: Sorting (Seiri), Systematization (Seiton), Shining (Seiso), Standardization (Seiketsu) and Support (Shitsuke). In the company, the implementation of 5S focused on reorganizing the production workshops, with an emphasis on eliminating unnecessary items, clearly labelling equipment and establishing dedicated areas for each type of resource.

The results obtained following the application of 5S have been remarkable. There has been a 24% increase in the efficient use of available space by freeing up unnecessarily occupied storage areas and reconfiguring workstations. Operators search and travel time was also reduced by 18%, which directly contributed to improved cycle time and reduced employee fatigue. In addition to the operational benefits, the 5S method also had a positive impact on employee morale, with employees perceiving the changes as a sign of professionalism and respect for their work.

In parallel, Value Stream Mapping (VSM), an essential tool to identify bottlenecks and non-value adding activities in the value chain, was implemented. By building a visual map of

the production flow, waiting times between steps, redundant processes and lack of synchronization between departments were highlighted. Based on this analysis, two non-productive activities that consumed resources without adding value were eliminated, and control and delivery points were repositioned to reduce the distances travelled by materials.
As a result of these interventions, the total cycle time was reduced by 21% and the level of intermediate inventory was reduced by 16%, which helped to smooth the workflow and reduce warehousing costs. Moreover, the visual representation provided by the VSM was an effective communication tool between the different hierarchical levels, facilitating decisions based on hard data rather than subjective perceptions.

Another pillar of the intervention was the application of Kaizen principles, focused on incremental and participative improvements. Within the company, brainstorming sessions were organized with the operational teams, where employees were encouraged to identify problems and propose simple but effective solutions. In this way, interventions were tailored to the real needs of the processes rather than imposed from above, which increased acceptance and involvement.

In order to assess the impact of Lean on operational performance, a number of key indicators were monitored before and after the implementation of improvement measures. The data collected reflect the changes resulting from workspace reorganization, optimization of production flows and process standardization, highlighting the effectiveness of the interventions implemented.

The results following the application of Kaizen have been visible at both process and organizational behaviour levels. Variations in the way tasks were performed were reduced by establishing standardized procedures, leading to a 28% increase in standardization. At the same time, there was an increase in the motivation of employees, who felt valued by being involved in the decision-making process. This participative attitude facilitated the consolidation of a culture of continuous improvement, based on learning and collaboration. Cumulatively, the implemented measures generated the following quantitative results (Table 1).

Table 1. Evolution of key operational performance indicators following Lean Management implementation

Indicator	Initial value	Final value	Improvement (%)
Total cycle time	108 min	85 min	-21%
Productivity level	78 units/day	96 units/day	+23%
Space utilization	65%	81%	+24%
Level of waste generated	8.4%	5.6%	-33%
Process standardization	54%	69%	+28%

According to Table 1, the data obtained from the application of Lean tools show significant improvements in several key areas of operational performance. The reduction in total cycle time from 108 minutes to 85 minutes indicates a smoother process and the elimination of non-productive activities, reflecting increased efficiency in the sequence of operations. The increase in productivity levels from 78 to 96 units per day confirms that the reorganization of space, standardization of work, and employee involvement in process improvement have resulted in a more sustained and consistent pace of production.

The degree of space utilization has increased considerably, from 65% to 81%, which denotes a better physical organization of the workplace, with a direct impact on search, access and travel times. The level of waste has decreased from 8.4% to 5.6%, reflecting a more careful management of resources, more rigorous quality control and a reduction in material losses. At the same time, the increase in process standardization from 54% to 69% indicates greater uniformity in the way we work, reducing variation and operational uncertainty.

Taking together, these indicators show that Lean interventions have produced consistent and measurable change, demonstrated the effectiveness of an integrated continuous improvement model and supporting a performance-oriented organizational culture.

These data validate the hypotheses formulated in the research and demonstrate that Lean tools can have a major impact on organizational efficiency and performance, even in medium-sized enterprises with limited resources. Moreover, Lean implementation is not just about applying technical methods, but also about changing the organizational mindset, promoting a culture of accountability and participation, and aligning operational and strategic objectives.

Therefore, the research results confirm that Lean Management is an effective framework for organizational transformation, provided that it is applied in a context-specific way, supported by leadership and accompanied by clear communication and active involvement of all stakeholders.

4. Conclusions

The application of Lean Management tools in the analyzed company generated a number of significant improvements in terms of operational efficiency, loss reduction and workflow optimization. The results obtained confirm the hypotheses formulated and support the relevance of a structured approach in integrating Lean principles into the organizational culture.

In the first stage, the diagnostic analysis identified and categorized losses according to the seven types of Muda. The most frequent forms of waste identified were: waiting time, overproduction, unnecessary movements and excess stocks. The use of direct observation and interviews revealed the existence of redundant activities, disorganized workspace and fragmented material flows, which contributed to low productivity.

Applying the 5S method has had a significant impact on workspace organization, leading to a 24% increase in efficient use of space and an 18% reduction in search and travel times. Through the steps of sorting, systematization and standardization, employees gained greater clarity in the use of equipment and materials, which led to a smoother flow of daily activities.

The Value Stream Mapping (VSM) tool enabled the visual representation of key processes and the identification of bottlenecks and delays. As a result of the VSM analysis, two non-productive activities were eliminated and control points were redefined, resulting in a 21% decrease in total cycle time and a 16% reduction in the level of intermediate inventory.

The implementation of Kaizen-type practices has been well received by the operational teams and has encouraged increased employee involvement in continuous improvement activities. Through regular brainstorming sessions and ad hoc interventions, clearer procedures were established, variations in the execution of tasks were reduced and the level of standardization increased by 28% compared to the initial phase.

The results demonstrate that the sustainable integration of Lean principles not only reduces losses, but also reinforces the culture of continuous improvement, supporting the organization's strategic goals. Also, the data obtained confirm the validity of the four research hypotheses and the relevance of applying Lean methodology in a way tailored to the specifics of the organization.

Although research has shown positive effects of applying Lean principles, it has limitations related to the unique context of a medium-sized enterprise and the relatively short implementation period, which does not allow for long-term impact assessment. The lack of a continuous monitoring system and the use of predominantly quantitative indicators limit the evaluation perspective. To deepen the understanding of the integration of Lean into the organizational culture, future research should benchmark other organizations in different industries, develop tools to measure Lean maturity and analyze the long-term effects on sustainability. Studies on the integration of digital technologies in Lean 4.0 and qualitative research capturing the role of employees in Kaizen processes are also needed. These directions can contribute to the development of an integrated implementation framework adapted to the challenges of modern manufacturing.

The original contributions of this research consist in demonstrating the integrated applicability of Lean tools (5S, Kaizen, VSM) in a metalworking enterprise, highlighting their quantifiable impact on operational efficiency. At the same time, the research proposes specific evaluation indicators that can guide Lean implementation in similar enterprises, strengthening the link between theory and practice.

5. Recommendations for sustainable integration of Lean principles into organizational culture

For Lean principles to have a sustainable and lasting impact on an organization's performance, it is essential that they are deeply embedded in the internal culture of the company, not applied in isolation as operational tools. A sustainable approach means, first and foremost, aligning organizational values and behaviors with the Lean philosophy, which focuses on continuous improvement, respect for people and eliminating waste.

An essential first step is clear and consistent top management commitment to Lean transformation. Leaders must become active drivers of change, model behaviors and encourage collaboration across all levels of the hierarchy. Lean integration into the organizational culture cannot happen without visible leadership that supports continuous learning and employee empowerment.

Another essential element is institutionalizing Lean practices through clear standards, visual rules and feedback systems. Creating a formal framework that supports 5S, Kaizen or Value Stream Mapping makes it easier to maintain consistent progress over time. Standardization should not be seen as a constraint, but as a foundation of stability on which further improvements can be built.

Promoting a culture of continuous improvement also involves recognizing employees' efforts and initiatives. Involving teams in identifying and solving problems needs to be accompanied by a transparent system for valuing their contributions, reinforcing internal motivation and ownership of the organization. In this way Lean becomes part of the collective identity, not an external obligation.

Last but not least, it is important that the organization adapts its performance measurement system to reflect not only quantitative results, but also progress in developing a Lean culture. Indicators such as the frequency of suggestions for improvement, the rate of implementation of internal ideas or the level of participation in Kaizen activities can provide a more complete picture of the cultural maturity of the organization.

8. Bibliography

[1]. Gama, M. D. S. B. and Bonamigo, A. (2024)."Sustainable lean manufacturing as long-term strategy: performance framework development and prioritization", Journal of Strategy and Management, 17(2), pp. 205-221.

[2]. Dillinger, F., Bernhard, O., and Reinhart, G. (2022) "Competence requirements in manufacturing companies in the context of lean 4.0", Procedia CIRP, 106, pp. 58-63.

[3]. Dieste, M., Panizzolo, R., and Garza-Reyes, J. A. (2020)."Evaluating the impact of lean practices on environmental performance: evidences from five manufacturing companies", Production Planning & Control, 31(9), pp. 739-756.

[4]. Ipinazar, A., Zarrabeitia, E., Rio Belver, R. M., and Martinez-de-Alegría, I. (2021)."Organizational culture transformation model: Towards a high performance organization", Journal of Industrial Engineering and Management (JIEM), 14(1), pp. 25-44.

[5]. Soltabgholi, F., Ardalan, M. R., Siroos, G. and Afzali, A. (2023) "The Role of Types of Organizational Culture on The Lean Behaviors of Principals Mediated By Coaching Leadership", School Administration, 11(1), pp. 157-189.

[6]. Dinis-Carvalho, J., Guimaraes, L., Sousa, R. M. and Leao, C. P. (2019)."Waste identification diagram and value stream mapping: a comparative analysis", International Journal of Lean Six Sigma, 10(3), pp. 767-783.

[7]. Mousavi, S. S., Khani Jazani, R., Cudney, E. A. and Trucco, P. (2020)."Quantifying the relationship between lean maturity and occupational health and safety: Antecedents and leading indicators", International Journal of Lean Six Sigma, 11(1), pp. 150-170.

[8]. Cusumano, M. A., Holweg, M., Howell, J., Netland, T., Shah, R., Shook, J., ... and Womack, J. (2021)."Commentaries on 'The lenses of lean'", Journal of Operations Management, 67(5), pp. 627-639.

[9]. Hopp, W. J. and Spearman, M. S. (2021)."The lenses of lean: envisioning the science and practice of efficiency", Journal of Operations Management, 67(5), pp. 610-626.

[10]. Womack, J. P. and Jones, D. T. (2008). lean thinking - szczupłe myślenie. ProdPress.com, Wrocław, ISBN 94.

[11] Laureani, A. and Antony, J. (2019)."Leadership and Lean Six Sigma: a systematic literature review", Total Quality Management & Business Excellence, 30(1-2), pp. 53-81.

[12]. Osman, A. A., Othman, A. A., and Rahim, M. K. I. A. (2019)."A review of lean application in manufacturing environment: definitions and terminologies", Journal of Technology and Operations Management, 14(2), pp. 28-45.

[13]. Dinis-Carvalho, J., Guimaraes, L., Sousa, R. M. and Leao, C. P. (2019)."Waste identification diagram and value stream mapping: a comparative analysis", International Journal of Lean Six Sigma, 10(3), pp. 767-783.

[14]. Shahin, M., Maghanaki, M., Hosseinzadeh, A., and Chen, F. F. (2024)."Improving operations through a lean AI paradigm: A view to an AI-aided lean manufacturing via versatile convolutional neural network", The International Journal of Advanced Manufacturing Technology, 133(11), pp. 5343-5419.

[15] Gutierrez, L., Lameijer, B. A., Anand, G., Antony, J., and Sunder M, V. (2022)."Beyond efficiency: the role of lean practices and cultures in developing dynamic capabilities microfoundations", International Journal of Operations & Production Management, 42(13), pp. 506-536.

[16]. Dillinger, F., Bernhard, O., and Reinhart, G. (2022) "Competence requirements in manufacturing companies in the context of lean 4.0", Procedia CIRP, 106, pp. 58-63.

[17]. Sasso, R. A., Filho, M. G. and Ganga, G. M. D. (2025)."Synergizing lean management and circular economy: pathways to sustainable manufacturing", Corporate Social Responsibility and Environmental Management, 32(1), pp. 543-562.

[18]. Gama, M. D. S. B. and Bonamigo, A. (2024)."Sustainable lean manufacturing as long-term strategy: performance framework development and prioritization", Journal of Strategy and Management, 17(2), pp. 205-221.

[19]. Ibrahim, A. F., Amartey-Jnr, E. B. and Sumaila, S. M. (2022)."Analyses of the Practice of Lean Business System in Textile Design and Production of Smocks in Northern Ghana for Sustainable Development", Management, 10(5), pp. 263-279.

[20]. Soltabgholi, F., Ardalan, M. R., Siroos, G. and Afzali, A. (2023) "The Role of Types of Organizational Culture on The Lean Behaviors of Principals Mediated By Coaching Leadership", School Administration, 11(1), pp. 157-189.

DEVELOPMENT OF A MINIATURE ECG DEVICE FOR HEALTH MONITORING OF OPERATORS IN SMART FACTORIES

ȘELARU Carmen Cristina Ioana, GHEORGHE-NĂFTĂILĂ Delia, ROTARIU Ștefan-Lucian,CAZACU Carmen-Cristiana(Conducător științific)

Faculty: Industrial Engineering and Robotics, Specialization: Robotics, Year: III,
e-mail: selaru.carmen.ioana@gmail.com

The project aims to develop a portable and intelligent device for monitoring the cardiac activity of industrial operators. The device is intended for modern work environments, where employee health is essential for productivity and safety. The system includes an analog ECG sensor (AD8232) that captures the heart's electrical signals and an optical sensor (GYMAX30102) that provides complementary measurements for heart rate and blood oxygen saturation (SpO_2). For real-time data transmission, a Plusivo ESP32 board is used. This board processes the data from the sensors and transmits it to a dedicated application. By collecting and analysing data in real time, the system enables the early detection of cardiac anomalies caused by stress or physical exertion, thus reducing the risk of medical incidents.

KEY WORDS: Safety, EKG, pulse, factory, operators.

1. Introduction

Smart factories, as part of the Industry 4.0 revolution, are based on digitalization and advanced automation. Beyond technological efficiency, monitoring employees' health status is needed to prevent accidents and support productivity. Thus, there is a need to integrate portable, non-invasive solutions for monitoring vital parameters such as heart rate and oxygen saturation.

2. Current state

Heart rate and its variability, as well as body temperature, are essential values for rapid diagnosis, whose continuous monitoring was, until recently, only possible in hospital settings. [1]. Over the years, several researchers have developed various systems to address issues such as distance, staff shortages, and high costs in providing medical services. [2]

One early example is a smartwatch that monitors multiple indicators, including ECG and PPG, which can be used to calculate pulse and heart rate. In addition, pulse transit time (PTT) can be determined by combining PPG and ECG signals—this is a key element in calculating blood pressure (BP). Environmental conditions (temperature, humidity, and atmospheric pressure) can also be detected and displayed on the screen. A motion state is used to activate the watch display. Meanwhile, all measured data could be transmitted to an Android smartphone via the Texas Instruments (TI) Bluetooth Low Energy CC2540 chip. PPG and ECG waveforms, heart rate, as well as systolic (SBP) and diastolic blood pressure (DBP) values could be displayed in real time on the Android client. [3]

Another developed smart system integrates not only biomedical sensors but also an MPU6050 accelerometer for fall detection, a GSM module for emergency communication via SMS, and a GPS module that transmits location details. Thus, in case of accidents, the system triggers an alert and sends an SMS containing the physical condition and location details of the injured person to a predefined emergency contact. [4]

Similarly, a non-invasive monitoring device for newborns is under development, aimed at fetal monitoring during the first 30–60 minutes after birth. The device tracks critical physiological parameters such as oxygenation, heart rate, and skin pH. The system integrates an ESP32 microcontroller and the MAX30102 sensor in a wearable sock-like format. Unlike traditional invasive neonatal monitors, this device provides continuous and real-time health assessment via wireless connectivity, including Bluetooth compatibility. [5]

Last but not least, a low-cost portable sleep monitor has been developed for home use. The system uses the Wemos D1 Mini microcontroller, the MAX30102 sensor for oxygen level measurement, the MPU6050 as an accelerometer, the DS18B20 for respiratory flow detection, and the MAX9814 as a microphone. Each sensor sends values to the microcontroller, which stores them in the cloud, and results are displayed on the user's device. The purpose of this system is to detect sleep disorders by analysing the data collected from sensors and to assess sleep quality, thus providing an early method of identifying symptoms before consulting specialists or doctors. [6]

3. Objective

The development of a miniature, wireless ECG device for monitoring the health of human operators in smart factories, aiming to prevent medical incidents and support safety and efficiency in the workplace.

3.1. Specific objectives

- **Acquisition of the ECG signal** using the analog AD8232 module, used at obtaining reliable information about the heart's electrical activity.
- **Implementation of an optical pulse and SpO_2 sensor** (MAX30102) to validate and complement data regarding the user's physiological state.
- **Integration of components into a compact hardware architecture** based on the ESP32 Plusivo, enabling local signal processing and real-time wireless transmission.
- **Ensuring energy autonomy** through a Li-Po battery power supply and charging via the TP4056 module, with integrated protection.
- **Transmission and storage of data** via Bluetooth Low Energy to a mobile application or web interface, for continuous visualization and analysis.
- **Creation of an ergonomic and wearable design** that allows comfortable use by operators during daily activities without affecting their mobility.
- **Testing and validation of the system's functionality** under real or simulated work conditions, to assess sensor accuracy and transmission reliability.

3.2. Future objectives

Transmission and storage of data via Bluetooth Low Energy to a mobile application or web interface, enabling continuous visualization and analysis. Data can be automatically stored in the cloud for historical access and longitudinal analysis, while the application may integrate additional features such as personalized alerts, AI-based automated interpretation, and report export to healthcare professionals.

To improve noise immunity in industrial environments, future versions of the device could integrate digital filtering techniques or machine learning-based artifact removal algorithms to ensure signal clarity.

4. Method

The project proposes the development of a miniature ECG device that can be integrated into the wearable equipment of operators in smart factories. Its primary goal is the real-time monitoring of cardiac activity and the detection of abnormalities that may arise during work hours, caused by stress, physical exertion, or challenging industrial conditions.
The device uses two types of sensors:

- **AD8232** for ECG signal acquisition, providing data on the heart's electrical activity.
- **GY-MAX30102** for complementary measurements of pulse and oxygen saturation (SpO_2), using optical technology.

The collected data is processed by an ESP32 microcontroller with Bluetooth Low Energy (BLE) support, which transmits the information to an application or analysis server. Power is supplied by a rechargeable Li-Po battery, managed by a TP4056 module with integrated protection.

To read the values, a web interface has been created and embedded directly into the device's firmware. This interface is lightweight—both in terms of code size and usability—and is built using HTML, CSS, and JavaScript. It displays:

- a real-time ECG graph,
- heart rate and blood oxygen values,
- electrode connection status, with a visible alert at the bottom of the page if the electrodes are not properly attached.

Given the prevalence of electromagnetic interference in factory settings, shielding techniques and PCB optimization are being considered to protect the integrity of sensor signals

For the user to access the website, both the ESP32 and the device being used to view the interface must be connected to the same network, when using smartphones, tablets, and laptops. For access from a desktop computer, the only requirement is using the same router.

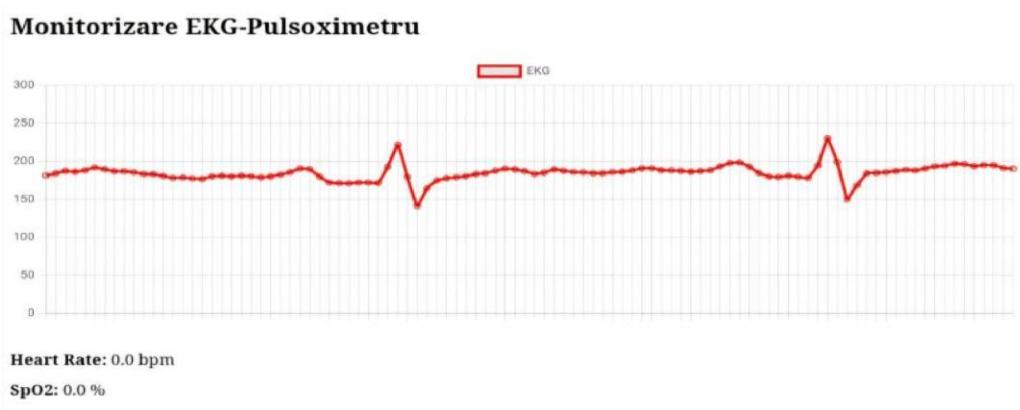

Fig. 1 Interface

The wearable system has been tested under simulated ergonomic stress conditions to assess comfort and skin contact stability during repetitive tasks.

5. Electronics

- The **AD8232 module** is an analog sensor used to monitor the electrical activity of the heart, specifically for measuring the ECG (electrocardiogram) signal.
- The **TP4056 module** is a linear charging module with integrated control for Li-Ion

batteries, equipped with overcharge, over-discharge, and short-circuit protection.

- The **GY-MAX30102** is an optical sensor for measuring pulse and blood oxygen saturation (SpO_2), using red and infrared LEDs for precise readings, ideal for portable medical applications.
- The **Plusivo E32** is a LoRa wireless communication module operating at 433 MHz, ideal for long-range data transmissions with low power consumption.
- The **LiPo battery** is rechargeable and supplies power to the circuit.

A modular architecture has been proposed to allow the easy addition of other biosensors such as galvanic skin response or temperature sensors.

The inclusion of haptic feedback or LED indicators on the device would allow operators to receive alerts even without direct access to a smartphone or display.

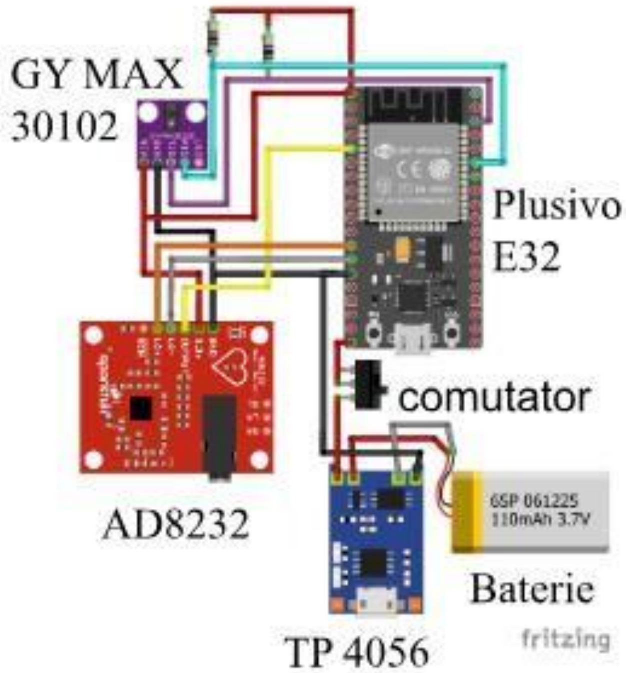

Fig. 2 - Electrical diagram of the circuit

6. Assembly

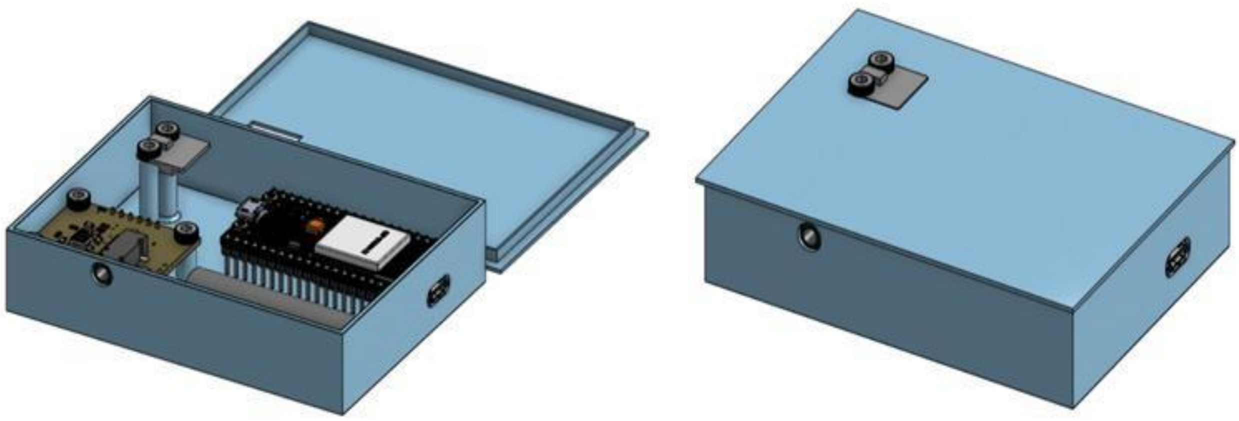

Fig. 3 - CAD of the device

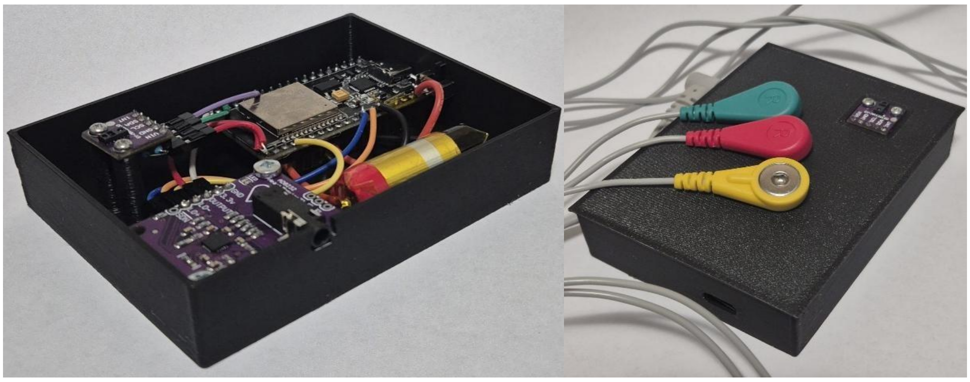

Fig. 4 - Assembled device

For the protection and assembly of the components, a 3D-printed case was designed specifically to fit the sensor, featuring an open window for direct skin contact. The printing material used was black, as it absorbs residual light and prevents reflections, thus supporting the optical pulse and SpO_2 sensor in acquiring more accurate data.

PLA Printing Parameters:
Nozzle Temperature: 200°C
Bed Temperature: 90°C
Print Speed: 100 mm/s
Cooling Fan Speed: 100%
Infill pattern: Gyroid

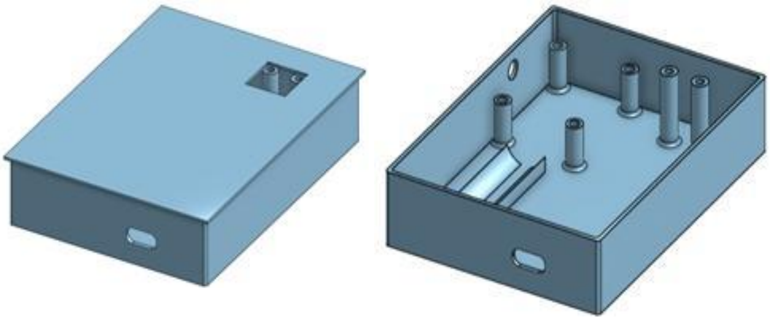

Fig. 5 - Isometric view of the cover

- The placement and assembly of the components inside the case was not only intended to meet their operational conditions but also to maintain the compact size of the case and ensure user comfort.
- Thus, the **AD8232 sensor** was positioned with its jack port facing the wall of the case, which has an appropriately sized opening. This ensures that the length of the connecting cable from the electrodes to the sensor, which impacts user comfort, remains unaffected. For mounting, the case was equipped with four standoffs for screws, with an inner diameter of 3 mm to match the module's mounting points, and an outer diameter of 5 mm to ensure strength and stability.
- The **MAX30100 sensor** is placed at the highest point of the case, with a cut-out in the cover corresponding to the module's size to ensure direct contact with the skin. It is fixed in place with two additional standoffs, each having an inner diameter of 2.5 mm (matching the module's mounting holes) and an outer diameter of 5 mm.

- The **battery power module** is also positioned so that the USB Type-C port is accessible from outside the case, with a dedicated opening for this purpose.
- To optimize space and maintain the compact nature of the device, the **Plusivo E32 development board** was placed above the battery power module.
- The **LiPo battery** is positioned near the charging module, supported by two holders shaped to fit it securely.

7. Conclusion

This project offers a practical and modern solution for ensuring the safety of employees in smart factories. The portable device monitors in real time the heart rate and blood oxygen levels, helping to quickly identify issues caused by stress or physical exertion. By using efficient and easily integrable technologies, the system contributes to a safer working environment that is more focused on the health of individuals.

Although there are numerous articles and research studies in the specialized literature that propose similar biometric monitoring solutions in industrial environments, the reality is that most of these projects remain at the prototype or feasibility study stage, without long-term practical application. Nevertheless, the need for such a system is becoming increasingly evident, considering the physical and psychological demands placed on operators. Implementing a stable and reliable real-time monitoring system would not only represent a technological advancement but also a necessary measure to prevent accidents.

A future objective includes interoperability with wearable platforms such as Apple HealthKit or Google Fit to broaden the utility of the collected data. Data collected can be anonymized and aggregated for broader health trend analysis across industrial sites. User feedback mechanisms, such as mobile app surveys or in-device gesture control, are under consideration for improving user acceptance and engagement.

8. Bibliography

[1] Taştan, M. (2018). *IoT Based Wearable Smart Health Monitoring System*. Celal Bayar University Journal of Science, 14(3), Article 3. https://doi.org/10.18466/cbayarfbe.451076

[2] Babalola, A.D., Akingbade, K.F, & Ubochi, B.C (2022): *The Performance of the STM32 Microcontroller and MAX30102 for Remote Health Monitoring Device Design.* Journal of Digital Innovations & Contemporary Research in Science, Engineering & Technology. Vol. 10, No. 3. Pp 51-68. dx.doi.org/10.22624/AIMS/DIGITAL/V10N1P4

[3] Fang, L., Chen, X., Fang, Z., Tong, K., Liu, J., He, Z., & Li, J. (2017). *Multi parameter health monitoring watch.* 19th International Conference on E-Health Networking, Applications and Services (Healthcom), 1–6. https://doi.org/10.1109/HealthCom.2017.8210807

[4] Raghunatha Rao, Prasanna Kumari, Hari Prasanna, R. Gurappa, Sai Kumar (2025). *IOT Based Health Monitoring and Location Tracking System*, International Journal Of Scientific Research In Engineering And Management 09(04):1-9, 10.55041/IJSREM43740

[5] Pinaaz Kiran Hode, Daniel Withers Gulick, Lawrence D. Devoe, Jennifer M Blain Christen, Mark Evans (2024): *Baby Sock to Monitor Newboms to Detect Risk for Neonatal Compromise.* Conference: 2024 IEEE 67th International Midwest

Symposium on Circuits and Systems (MWSCAS). 10.1109/MWSCAS60917.2024.10658791

[6] Pramudita Hanggara, Ade Septian Alfianto, Louis Putra Purnama, Ivan Tanra (2024): *Portable Low-Cost Home Sleep Monitor using Wemos D1 Mini.* Advance Sustainable Science, Engineering and Technology (ASSET) Vol. 6, No. 2, April 2024. ISSN: 2715-4211, DOI: https://doi.org/10.26877/asset.v6i2

INTELLIGENT TEMPERATURE MONITORING IN MULTI-ZONE INDUSTRIAL ENVIRONMENTS THROUGH IIOT SOLUTIONS

DRĂGHICEANU Armand Andrei, MIHALACHE Alexandra-Dimitria, IONESCU Robert Călin, CAZACU Carmen-Cristiana (Conducător științific)

Faculty: Industrial Engineering and Robotics, Specialization: Digital Manufacturing Systems, Year: II, email: da466204@gmail.com

ABSTRACT: This project presents a smart temperature monitoring system using IIoT technologies, which is designed for use in multi-zone environments. It uses the ThingWorx platform and three DHT11 temperature sensors, all integrated into a compact 3D-printed case, which was specifically customized to house them. The data collected is transmitted in real time to the ThingWorx platform, where it is displayed and monitored remotely. Alerts are made through the online interface, making it accessible from anywhere. This solution is cost-effective, easy to implement in real industrial settings and it demonstrates how IIoT can improve safety and optimize energy consumption. It has potential for future improvements such as predictive algorithms.

KEYWORDS: temperature monitoring, 3D printing, algorithms, 2D/3D design, CAD

1. Introduction

IIoT systems are a continuously evolving technology that aims to extend this concept beyond homes, into the industrial environment. It is about a fully wireless system for monitoring, control, and security of an industrial area, using simple devices and internet connection.[1] IIoT represents a global infrastructure for the information society, which enables the provision of advanced services by connecting objects, both physical and virtual, based on information exchange and communication technologies. [2]

In recent years, technologies in the IIoT field have experienced significant development, offering efficient solutions for real-time monitoring and control of industrial processes. One area where these technologies are applied is temperature monitoring, especially in large industrial environments where simultaneous surveillance of multiple areas is necessary. It helps with precise temperature control, which contributes to preventing equipment failures, reducing energy consumption, and maintaining optimal production conditions.

Traditional monitoring, based on manual readings or isolated systems, is often inefficient for modern industrial conditions. IIoT solutions allow the implementation of sensor systems that collect and transmit data in real time to a centralized platform, where the information is processed, displayed, and stored. Through sensor networks, these systems can quickly detect any temperature variation in different areas of the facility. A few examples can also be observed in large companies such as Carlsberg or Griffins Food Company, where production processes have seen major improvements following the implementation of IIoT systems, as efficiency increased and waste decreased drastically.

This project proposes the development of an intelligent real-time temperature monitoring system, using three sensors placed in the enclosure, which is located in a room. The collected information is transmitted to a processing system that displays the values in real time and can generate alerts if certain predefined thresholds are exceeded. This approach offers a practical application of IIoT concepts and can be easily expanded to cover a larger number of areas.

Through this paper, we analyse the benefits of IIoT technologies in the intelligent monitoring of industrial environments, while also providing a practical example (based on efficiency and scalability criteria). The proposed solution consists of integrating a robot head, which is built using 3D printing and placed in a specific area. The unit is equipped with temperature sensors and communication modules (the temperature sensors), which transmit the data to a centralized visualization and analysis platform called ThingWorx. The purpose of this project is to test whether the system works well and can be easily adapted and used in other industrial spaces, providing efficient monitoring of the surrounding temperature conditions.

2. State of the art

In the current industrial context, maintaining an optimal temperature is essential, both in terms of ensuring product quality and production processes, and in terms of equipment safety. In existing sensor networks, to ensure timely detection of reported temperature anomalies, the sensors must frequently measure the surrounding environment, which leads to high energy consumption. Moreover, if these sensor networks attempt to achieve better energy efficiency by extending sleep periods, they may not be able to detect the temperature anomaly in time, which can be unacceptable in certain applications. [4]

With the introduction of IIoT systems, this field has been revolutionized, allowing the integration of smart sensors that can be controlled remotely. However, many of the systems currently in use are not designed to monitor temperature in multiple areas, which makes them inefficient. Therefore, IIoT solutions are necessary as they can monitor multiple areas at the same time, provide a clear data interface, and can be controlled remotely. This evolution of systems brings real and visible benefits to the industrial field, significantly contributing to the optimization of processes carried out in factories. Automation through IIoT systems considerably reduces the need for manual interventions, which lowers the risk of operator errors and allows workers to focus on more important or creative tasks. At the same time, equipment coordination improves, and the use of available resources becomes more efficient.

Moreover, the integration of sensors into modern software platforms, such as ThingWorx, makes real-time monitoring possible, as well as the storage and long-term analysis of the collected data. This allows for the identification of patterns, evaluation of performance over time, and the making of better-informed decisions. Ultimately, these advantages lead to more efficient work, reduced costs, and a safer, autonomous operating system. It is proof that digitalization in industry has already become a real necessity, both for small and large companies.

3. Proof of Concept Design

To make the monitoring process more intuitive and relatable to an actual factory layout, we designed the enclosure to visually simulate a real industrial environment. The central box represents the core of the factory, while the three protruding sections, symbolize separate rooms or monitored zones. Each of these sections houses one sensor, allowing us to replicate a multi-zone monitoring setup, similar to what would be required in a real manufacturing factory. This analogy not only helps in visualizing the distribution of sensors in an industrial context but also proves that the model can be easily scaled and implemented in real life. The modular and compact design of the enclosure enables straightforward deployment across various locations in a factory, making the entire system both practical and scalable for actual industrial use. Thus, the project serves not only as a prototype but as a near-direct representation of how IIoT-based temperature monitoring can be applied in modern production systems.

In the enclosure design process, we aimed to choose a design that is as interesting and suggestive as possible, but also compact, so that it does not take up too much space and can be easily integrated into a room. In the first stage of the design, we determined the minimum dimensions that the head box could have so that the electronic components would fit without any issues, then proceeded to carry out the 3D design in the Onshape application.

The enclosure consists of 4 components: the box, which contains the parts that make up the temperature monitoring sensor, and the 3 separate sections (the side antennas and the one on the top) where the sensors are placed. The structure of the enclosure was designed with 3 openings through which the 3 separate sections are connected, specially created to fit the size of the temperature sensors, with 2 on the sides and 1 on the top.

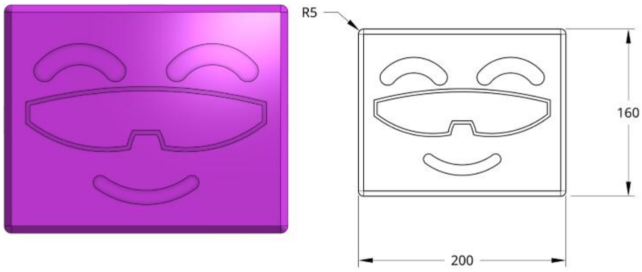

Fig. 1 The box dimensions in front view in 2D and 3D.

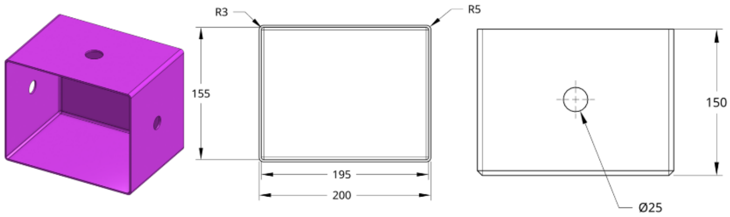

Fig. 2 Interior dimensions of the box in 2D and 3D.

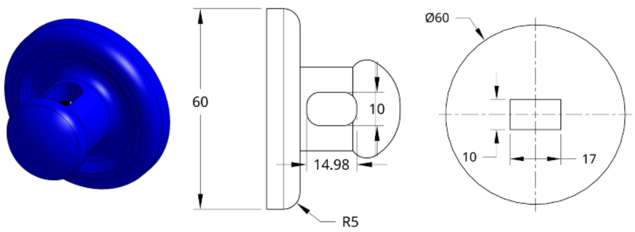

Fig. 3 The dimensions of the side sections in 2D and 3D.

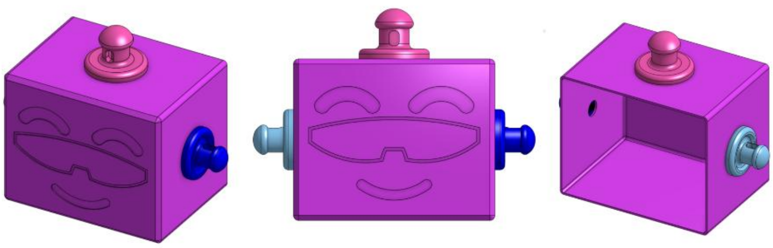

Fig. 4 The final 3D model of the enclosure.

2.1. Enclosure printing

For the creation of the enclosure and the side components, we used 3D printing, a fast and precise solution that allows for obtaining customized shapes, easily modifiable before the final version. In our project, the enclosure was designed to include three specially designed openings for the insertion of DHT11 temperature sensors.

The printing parameters: PLA Pro @ 220 grade C, Nozzle 0.8mm, Layer height 0.45 mm. The precision for the dimensional parts of PLA objects is high, as it shows less warping behavior compared to ABS filament. [3]

PLA Pro @ 220 grade C
Nozzle 0.8mm
Layer height 0.45 mm

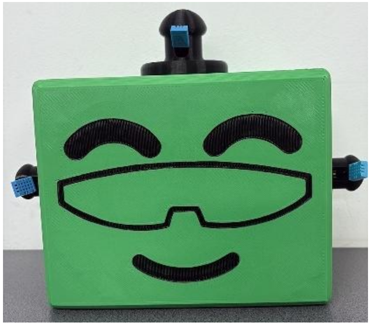

Fig. 5. The 3D printing model

2.2. Programming Raspberry Pi5

The code constantly reads the temperature from the sensors and transmits the information to the ThingWorx application. As for the DHT11 temperature monitoring sensors, they were connected to the Raspberry Pi 5 microcontroller using digital pins so that it can read the transmitted values.

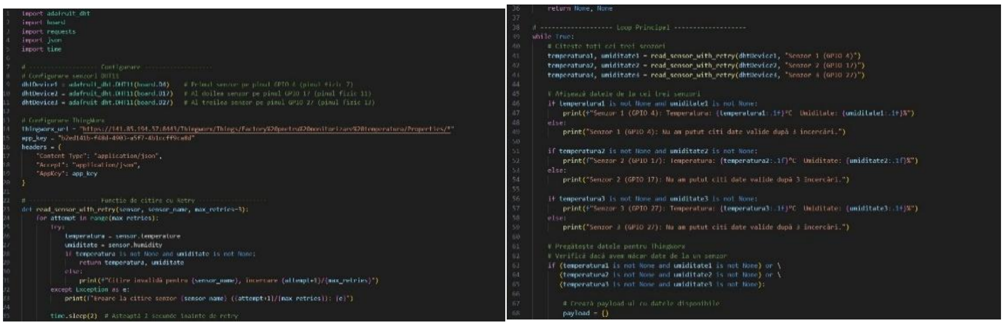

Fig. 6 The python code for the sensors.

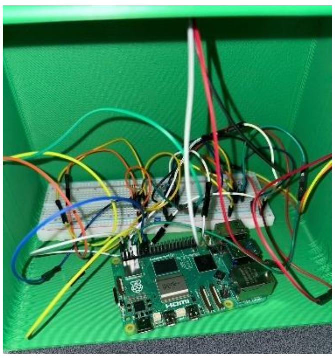

Fig. 7 Raspberry Pi Project with Breadboard and Jumper Wires in Enclosure .

2.3. Mashup in ThingWorx

The image below shows a ThingShape created in the ThingWorx platform. There are three ThingShapes created, corresponding to the three temperature sensors used in the project. Each ThingShape contains specific properties such as temperature, humidity, and the sensor's location, and for sensor 2, an additional timestamp property is defined. By activating the Alerts option, the system can automatically signal when predefined thresholds are exceeded, adding an extra layer of safety in industrial monitoring. These structures are later integrated into the Mashup visual interface, where the data is displayed in real time in an intuitive format. This type of organization allows for scalability and efficient control in industrial environments with multiple monitoring zones.

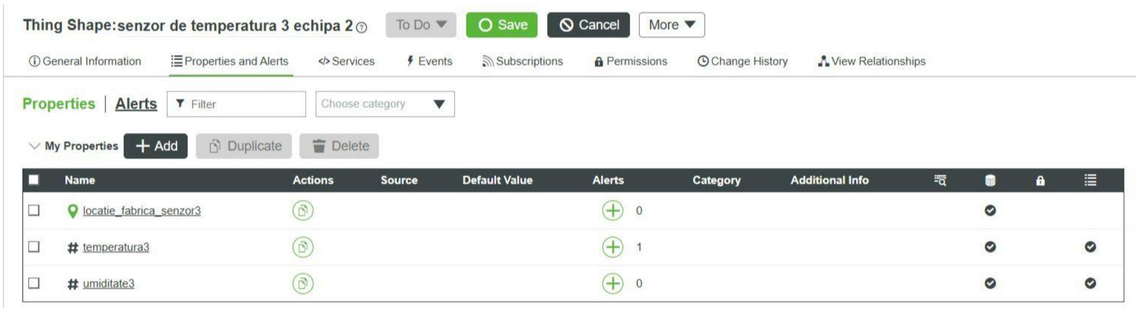

Fig. 8 ThingShape proprieties.

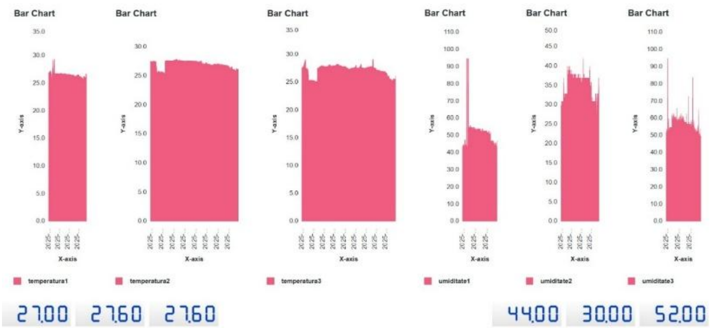

Fig. 9 The Mashup on ThingWorx

The ThingWorx platform is essential in the programming part, allowing the real-time display of the room temperature on a single screen, accessible from any device connected to the internet; this interface is also called a Mashup. Here, any deviations can be immediately observed, and an alarm is triggered if the thresholds are exceeded, which adds an important extra level of safety. The code constantly reads the temperature from the DHT11 sensors, which are connected to the Raspberry microcontroller, and displays it in the Mashup. In real time, the current temperature can be observed (in a gauge or numeric display widget), as well as the temperature evolution graph. All important values are transmitted to the ThingWorx application, where they are monitored in real time through the Mashup.

3. Conclusions

The development of this project enabled the successful implementation of a real-time temperature monitoring system, based on Industrial Internet of Things (IIoT) technologies. By integrating temperature sensors with a Raspberry Pi microcontroller and using the ThingWorx platform for data visualization and alerting, we achieved a functional and scalable solution applicable to real industrial environments.

Throughout the process, the team gained valuable interdisciplinary knowledge, both theoretical and practical. Key competencies acquired include 3D design using CAD tools, additive manufacturing through FDM 3D printing (PLA material), sensor integration and configuration, Python-based programming for data acquisition, and the development of a dynamic and interactive Mashup interface on the ThingWorx platform. These skills are essential in the context of Industry 4.0, where digitalization and intelligent automation are fundamental pillars.

Moreover, the physical model was conceptualized to simulate a simplified industrial environment with three monitoring zones, demonstrating that the proposed system can be easily adapted and scaled for use in actual factory settings. This reinforces the practical relevance of the project and its alignment with current industrial digital transformation trends.

In conclusion, the project not only validates a functional IIoT solution for smart temperature control but also provides solid learning experience across multiple domains, preparing the students for future challenges in modern engineering and industrial automation.

4. Bibliografie

[1]. Syeda Florence Madina, Md. Shahinur Islam, Fakir Mashque Alamgir, Mohammad Farhan Ferdous. (2022), "Industrial Internet of Things: Technologies, Design and Applications",SudanJha,9781003102267.
https://www.taylorfrancis.com/chapters/edit/10.1201/9781003102267-4/internet-things-iot-based-industrial-monitoring-system-syeda-florence-madina-md-shahinur-islam-fakir-mashque-alamgir-mohammad-farhan-ferdous

[2]. IGN Sangka, IGS Widharma, IN Sunaya, IM Sajayasa, IGP Arka. (2024), "Temperature Monitoring Efficiency With Internet of Things-Based Temperature Sensor Variations", 2720-9598.
https://www.researchgate.net/publication/382277305_Temperature_Monitoring_Efficiency_With_Internet_of_Things-Based_Temperature_Sensor_Variations

[3]. Eda Hazal Tumer, Husnu Yildirim Erbil. (2021), "Extrusion-Based 3D Printing Applications of PLA Composites: A Review".
https://www.mdpi.com/2079-6412/11/4/390

[4]. Shengbo Chen, Lanxue Zhang, Yuanmin Tang. (2020), "Indoor temperature monitoring using wireless sensor networks: A SMAC application in smart cities", volume 61, 102333.
https://www.sciencedirect.com/science/article/abs/pii/S2210670720305540

5. Notations

The following notations are used throughout the paper:
IIoT – Industrial Internet of Things
CAD - Computer Aided Design